

Electronic Thesis and Dissertation Repository

5-12-2010 12:00 AM

The Effect of Particle Size on Hydrolysis and Modeling of Anaerobic Digestion

Saad Aldin
The University of Western Ontario

Supervisor
Dr. George Nakhla
The University of Western Ontario Joint Supervisor
Dr. Madhumita B Ray
The University of Western Ontario

Graduate Program in Chemical and Biochemical Engineering
A thesis submitted in partial fulfillment of the requirements for the degree in Doctor of Philosophy
© Saad Aldin 2010

Follow this and additional works at: <https://ir.lib.uwo.ca/etd>

 Part of the [Biochemical and Biomolecular Engineering Commons](#), and the [Environmental Engineering Commons](#)

Recommended Citation

Aldin, Saad, "The Effect of Particle Size on Hydrolysis and Modeling of Anaerobic Digestion" (2010).
Electronic Thesis and Dissertation Repository. 60.
<https://ir.lib.uwo.ca/etd/60>

This Dissertation/Thesis is brought to you for free and open access by Scholarship@Western. It has been accepted for inclusion in Electronic Thesis and Dissertation Repository by an authorized administrator of Scholarship@Western. For more information, please contact wlsadmin@uwo.ca.

**THE EFFECT OF PARTICLE SIZE ON HYDROLYSIS AND MODELING OF
ANAEROBIC DIGESTION**

(Spine title: The Effect of Particle Size on Hydrolysis in Anaerobic Digestion)

(Thesis format: Integrated-Article)

The thesis by

Saad Aldin

Graduate Program
in
Engineering Science
Department of Chemical and Biochemical Engineering

A thesis submitted in partial fulfillment
of the requirements for the degree of
Doctor of Philosophy

School of Graduate and Postdoctoral Studies
The University of Western Ontario
London, Ontario, Canada

© Saad Aldin 2010

**THE UNIVERSITY OF WESTERN ONTARIO
SCHOOL OF GRADUATE AND POSTDOCTORAL STUDIES**

CERTIFICATE OF EXAMINATION

Joint-Supervisor

Dr. George Nakhla

Joint-Supervisor

Dr. Madhumita B Ray

Examiners

Dr. Argyrios Margaritis

Dr. Lars Rehmann

Dr. Gordon Southam

Dr. Nihar Biswas

The thesis by

Saad Aldin

entitled:

**THE EFFECT OF PARTICLE SIZE ON HYDROLYSIS AND THE MODELING OF
ANAEROBIC DIGESTION**

is accepted in partial fulfilment of the requirements for the degree of

DOCTOR OF PHILOSOPHY

Date _____

Chair of the Thesis Examination Board

ABSTRACT

Batch experiments were performed to investigate the effect of particulate protein particle size on the hydrolysis of casein in anaerobic degradation. While particle size did not affect the ultimate protein degradation efficiency, the hydrolysis rate coefficient increased from 0.034 to 0.298 d⁻¹ with the change in specific surface area from 0.01 to 0.192 m²/g. The maximum methane production rate was affected by the particle size change, although the ultimate amount of methane produced was approximately the same despite the change in specific surface area. A mathematical relationship between the hydrolysis rate coefficient and specific surface area was developed and a new hydrolysis equation was proposed and verified.

Ultrasound treatment of wastewater sludges prior to anaerobic digestion disrupts the flocs and causes lysis of the bacterial cells releasing both inter and intracellular materials. Primary (PS) and waste activated sludge (WAS) were treated with different ultrasonic intensities, varying sonication time and amplitude at a constant frequency. Results showed that gas production, volatile fatty acids, ratio of soluble chemical oxygen demand to total chemical oxygen demand and soluble protein increased, while particulate protein and particle size of the sludge decreased with sonication time. An empirical model was developed to determine the economic viability of ultrasound based on electrical energy input and energy obtained from enhanced methane production. Ultrasonic pretreatment is only economically viable for primary sludge at low sonication doses. The Anaerobic Digestion Model # 1 (ADM1) was applied to the batch anaerobic digestion for sonicated and non-sonicated sludge. The model successfully simulated the experimental trends.

The efficiency of ultrasound as a pretreatment method for hog manure prior to anaerobic digestion was also evaluated at specific energies of 250 to 30,000 kJ/kg total solids (TS). This

study confirmed that $COD_{\text{solubilisation}}$ from particulates correlated well with the more labor and time intensive degree of disintegration test. The particle size distribution for hog manure was bimodal (0.6 - 2500 μm), while ultrasound primarily impacting particles in the 0.6-60 μm range. Hog manure is more amenable to ultrasound than waste activated sludge, as it took only 3000 kJ/kgTS to cause 15% more solubilization as compared to 25000 kJ/kg TS for waste activated sludge. Bound protein degradation during sonication was 13.5% at 5000 kJ/kg TS and remained constant thereafter for higher energy input. Biomass cell rupture occurred at specific energy of 500 kJ/kg TS. An economic evaluation indicated that only a specific energy of 500 kJ/kg TS was economical, with a net energy output valued at \$ 4.1/ton of dry solids, due to a 28% increase in methane production.

Degradation of odorous compounds in sludge during anaerobic digestion was systematically studied and simulated using the Anaerobic Digestion Model # 1 (ADM1). The degradation of various protein fractions (particulate, soluble and bound), VFAs, lipids and amino acids of PS and WAS were monitored during anaerobic digestion. Degradation kinetics of the odorous compounds namely, protein, amino acids, lipid and volatile fatty acids (VFAs) were determined. Relationships between protein fractions and volatile suspended solid were established. A strong relationship between bound protein, a major odors precursor, and volatile suspended solid degradation was found, while no statistically significant difference in bound protein reduction was observed between PS and WAS. ADM1 successfully simulated the lab scale continuous anaerobic digestion; model results with optimized parameters showed good agreement with the experimental data for methane production and all other sludge parameters including odor precursors such as lipids, VFAs and proteins.

Keywords: Particle size, casein, anaerobic digestion, hydrolysis kinetics, specific surface area.

Pretreatment; Bound protein; Degree of disintegration; Ultrasound; hog manure, sludge pretreatment, gas production., odors precursors, cell protein, bound protein, ADM1 model.

CO-AUTHORSHIP

Chapter 3: Modeling the Influence of Particulate Protein Size on Hydrolysis in Anaerobic Digestion, Saad Aldin, George Nakhla, and Madhumita B. Ray. Saad Aldin was the principal author of this chapter, with 100% intellectual input, experimental conduction, data analysis, modeling and writing process. The manuscript was reviewed by Dr. George Nakhla and Dr. Madhumita B. Ray who provided additional recommendations for improvement. A version of this chapter has been submitted in *Bioresource Technology*, 2010,

Chapter 4: Modeling the Effect of Sonication on Biosolids Anaerobic Digestion, Saad Aldin, Elsayed Elbeshbishy, George Nakhla, and Madhumita B. Ray. Saad Aldin was the principal author of this chapter, with 100% intellectual input, 90% experimental conduction, 100% data analysis and modeling and 100% writing process. The manuscript was reviewed by Dr. George Nakhla and Dr. Madhumita B. Ray who provided additional recommendations for improvement. A version of this chapter has been published in the *Energy&Fuels*, 2010, 24 (9), pp 4703–4711

Chapter 5: Impact of Ultrasonication of Hog Manure on Anaerobic Digestability, Elsayed Elbeshbishy, Saad Aldin, Hisham Hafez, George Nakhla, Madhumita Ray. Saad Aldin was the second author of this chapter, with 80% intellectual input, 50% experimental conduction, 40% data analysis and 30% writing process. The manuscript was reviewed by Dr. George Nakhla and Dr. Madhumita B. Ray who provided additional recommendations for improvement. A version of this chapter has been published in the *Ultrasonics Sonochemistry*. 2010, 18, pp 164-171.

Chapter 6: Simulating the Degradation of Odors Precursors in Primary and Waste Activated Sludge during Anaerobic Digestion, Saad Aldin, Fuzhou Tu, George Nakhla and Madhumita B. Ray. Saad Aldin was the principal author of this chapter, with 90% intellectual input, 20% experimental conduction, 90% data analysis, 100% modeling and 95% writing process. The manuscript was reviewed by Dr. George Nakhla and Dr. Madhumita B. Ray who provided additional recommendations for improvement. A version of this chapter has been submitted in the *Journal of Hazardous Materials*. 2010,

Chapter 7: Development of Anaerobic Digestion Model Software, with 100% intellectual input, data analysis, modeling, and programming.

ACKNOWLEDGEMENTS

I would like to express my gratitude to Dr. George Nakhla and Dr. Madhumita B. Ray for being outstanding advisors and excellent professors, for their constructive criticisms and endless help throughout this study, for their utmost attention to my professional development and technical writing skills, and for their continuously challenging me to achieve higher goals. Their constant encouragement, support, and invaluable suggestions made this work possible and successful. I am also grateful to all of my colleagues for their invaluable support and perceptive comments.

I would like to express my appreciation to my managers at Trojan Technologies (Dr. Ted Mao, Dr. Linda Gowman, and Dr. Bill Cairns) for giving me the opportunity, time and funding to complete this work.

I am deeply and forever indebted to my wife Bushra and my three kids Ayman, Yousir, and Daniah for their love, support and encouragement throughout my study and my entire life, may God bless them all.

TABLE OF CONTENT

THE EFFECT OF PARTICLE SIZE ON HYDROLYSIS AND MODELING OF ANAEROBIC DIGESTION	i
CERTIFICATE OF EXAMINATION	ii
ABSTRACT.....	iii
CO-AUTHORSHIP	vi
ACKNOWLEDGEMENTS	viii
TABLE OF CONTENT	ix
LIST OF TABLES.....	xii
LIST OF FIGURES	xiv
LIST OF ABBREVIATIONS.....	xvi
CHAPTER ONE	1
1.1 Background.....	1
1.2 Synopsis of Literature	4
1.3 Research Objectives.....	5
1.4 Thesis Organization	7
1.5 Contribution of Thesis	9
1.6 References.....	11
CHAPTER TWO	15
2.1 Literature Review.....	15
2.1.1 Introduction.....	15
2.1.2 Anaerobic Digestion Modeling.....	18
2.1.3 Hydrolysis Modeling	25
2.1.4 Particle Size	34
2.1.5 Pre-treatment of Sludge for Anaerobic Digestion	40
2.1.5.1 Chemical Pre-treatment (Acids and Bases):	41
2.1.5.2 Ozone Pre-treatment	43
2.1.5.3 Mechanical Pre-treatment.....	43
2.1.5.4 Ultrasound Pre-treatment.....	45
2.1.5.5 Odor Precursors	50
2.2 Summary and Conclusions	54
2.3 References.....	57
CHAPTER THREE	72
Modeling the Influence of Particulate Protein Size on Hydrolysis in Anaerobic Digestion	72
3.1 Introduction:.....	72
3.2 Material and methods.....	78
3.2.1 Culture, Substrate and Media:.....	78
3.2.2 Batch Anaerobic Digestion:.....	78
3.2.3 Analytical Methods:.....	79
3.2.4 Modeling:.....	80
3.2.5 Statistical Analysis:.....	82
3.3 Results and discussion	82
3.3.1 Particulate Protein Degradation:.....	82
3.3.2 Biogas Production:.....	84
3.3.3 Effect of Particle Size on the Hydrolysis Coefficient:.....	87
3.3.4 Hydrolysis Equations and Verification:.....	91

3.4	Conclusions:	94
3.5	References	96
CHAPTER FOUR		99
Modeling the Effect of Sonication on Biosolids Anaerobic Digestion		99
4.1	Introduction	99
4.2	Materials and method	103
4.2.1	Experimental Set-up:	103
4.2.2	Analytical Methods:	103
4.2.3	Batch Anaerobic Digestion:	105
4.2.4	Specific Energy (SE) Input:	107
4.2.5	Anaerobic Modeling:	107
4.2.6	Statistical analysis:	108
4.3	Results and discussion	108
4.3.1	Chemical Oxygen Demand (COD):	108
4.3.2	Biological Oxygen Demand (BOD):	109
4.3.3	Proteins:	111
4.3.4	Volatile Fatty Acids (VFA):	115
4.3.5	Particle Size Distribution:	117
4.3.6	Methane Production:	118
4.3.7	Anaerobic Modeling:	121
4.3.8	Economic Viability of Ultrasound:	128
4.4	Conclusions	130
4.5	References	132
CHAPTER FIVE		137
Impact of Ultrasonication of Hog Manure on Anaerobic Digestability		137
5.1	Introduction	137
5.2	Material and methods	141
5.2.1	Analytical methods	141
5.2.2	Protein measurement	141
5.2.3	Experimental set-up	142
5.2.4	Batch anaerobic digestion	143
5.2.5	Specific energy input	143
5.2.6	Degree of disintegration (DD)	144
5.2.7	COD solubilization	144
5.2.8	TKN solubilization	144
5.3	Results and Discussion	145
5.3.1	Comparison of solubilisation and degree of disintegration	145
5.3.2	Particle size distribution	146
5.3.3	Solubilisation of hog manure	147
5.3.4	Proteins (particulate, bound and cell) solubilisation	151
5.3.5	Methane production and economics	152
5.4	Conclusions	155
5.5	References	157
CHAPTER SIX		160
Simulating the Degradation of Odors Precursors in Primary and Waste Activated Sludge during Anaerobic Digestion		160
6.1	Introduction:	160
6.2	Materials and methods:	163

6.2.1	Analytical methods:	164
6.2.2	Anaerobic digestion simulation:	165
6.2.3	Statistical analysis:	165
6.3	Results and discussion:	165
6.3.1	Performance of anaerobic digesters:	165
6.3.2	Odorous compounds and odours precursors:	168
6.3.2.1	Volatile Fatty Acids (VFA):	168
6.3.2.2	Proteins Fractions:	170
6.3.2.3	Lipid Degradation:	173
6.4	Simulation and kinetics for odor-causing constituent:	174
6.5	Conclusions:	180
6.6	References:	182
CHAPTER SEVEN		185
Anaerobic Digestion Model Software Implementation		185
7.1	Introduction:	185
7.2	Reaction System:	188
7.3	The Implementation of the ADM1 and Its Extension	192
7.3.1	Dynamic State Variables:	192
7.3.2	Liquid Phase Equations	194
7.3.3	Gas Phase Equations:	195
7.3.4	Liquid-Gas Transfer	196
7.3.5	Acid-Base Equilibria:	197
7.3.6	Determination of pH:	199
7.3.7	Inhibition:	200
7.4	Software Development:	201
7.5	Software Verification:	205
7.6	References	207
CHAPTER EIGHT		209
Conclusions and Recommendations		209
8.1	Conclusions	209
8.1.1	Impact of particulate size on hydrolysis:	209
8.1.2	The effect of sonication on biosolids particle size and anaerobic digestion:	210
8.1.3	Impact of sonication on high solids sludge (hog manure):	211
8.1.4	Degradation of odor precursors in primary and WAS during anaerobic digestion:	212
8.2	Recommendations for Future Research:	213
Appendix A: Anaerobic Digestion Model No.1		215
9.1	Biochemical process rates	215
9.2	Acid-base rates:	216
9.3	Gas transfer rates	216
9.4	Process inhibition	216
9.5	Water phase equations	217
9.6	Gas phase equations	221
9.7	Parameter Description:	222
9.8	Stoichiometric Matrix	225
10.1	Curriculum Vitae	226

LIST OF TABLES

Table 2.1 Hydrolysis rate models (adapted from Pin-Jing et al., 2006).	26
Table 2.2 Kinetic coefficients of the first-order rate of hydrolysis in literature.	32
Table 2.3 Size distribution of organic matter in municipal wastewater (adapted from Levine et al. [72]).	35
Table 2.4 Size of solids in raw sludge (primary sludge).	36
Table 2.5 Advantages and disadvantages of sludge pre-treatment for anaerobic digestion	41
Table 3.1 Size distribution of organic matter in municipal wastewater (adapted from Levine et al., 1991).	73
Table 3.2 Review of hydrolysis rate constants in literature.	74
Table 3.3 Hydrolysis rate models in literature (adapted from Pin-Jing et al., 2006).	75
Table 3.4 Gompertz (Lay et al., 1999) model coefficients, median $d(50)$ for the surface area, and specific surface area for different ranges of protein particle sizes.	84
Table 3.5 Hydrolysis rate and the amino acids uptake coefficients for different particle size ranges of protein.	89
Table 4. 1 Characteristics of the primary and WAS used in the experiment.	105
Table 4. 2 The median, 10%ile and 90%ile for the volume fraction of the primary and WAS.	117
Table 4. 3 Percentage of CH_4 increase in primary and waste activated sludge as a function of sonication time.	120
Table 4. 4 Primary and WAS sludge characterization for ADM1	122
Table 4. 5 Predicted and Measured Concentrations (average \pm Stdev) of acetic, butyric, propionic acids, and VFA after anaerobic digestion	125
Table 4. 6 Primary and WAS sludge model parameters at different sonication times.	127
Table 4.7 Specific energy, power and methane energy per ton of COD using the empirical model.	130
.....	
Table 5.1 Particle size and $COD_{solubilization}$ at different specific energy inputs	147
Table 5.2 $TKN_{solubilisation}$, ammonia and protein solubilisation at different specific energy inputs	150
Table 5.3 Ultrasonication and Methane Energy per ton of TS	153
Table 6.1 Performance of AD during PS and WAS runs	167
Table 6.2 Average concentrations, and reductions of various protein fractions in PS and WAS	170
Table 6.3 Default and optimized ADM kinetic parameters for both PS and WAS sludge.	177
Table 6.4 Experimental influent and effluent characterization with the ADM prediction for primary and WAS sludge.	179
Table 7.1. Units used in the ADM1 model	186
Table 7.2 Nomenclature, description of stoichiometric coefficients	186
Table 7.3 Nomenclature, description of equilibrium coefficients and constants.	186
Table 7.4 Nomenclature, description of kinetic constants and rates.	187
Table 7.5 Nomenclature, description of dynamic state variables, algebraic variables, and physical reactor parameters.	187
Table 7.6 Suggested stoichiometric parameters and qualitative sensitivity and variability [1]. ..	189
Table 7.7 Suggested parameter values and qualitative sensitivity and variability for mesophilic digestion [1].	190

Table 7.8 Soluble components of DAE system dynamic state variables.....	193
Table 7.9 particulate components of DAE system dynamic state variables.....	194
Table 7.10 Gas components.....	196
Table 7.11 Comparison between the output results of the ADM1-UWO, Batstone et al. [1] and Jeppsson at al. [9].....	206

LIST OF FIGURES

Figure 2.1 Flowchart showing the stages and pathway of anaerobic digestion [8].	16
Figure 3.1 Interrelated TCOD flow of Proteins in the Anaerobic Digestion Model No. 1 (ADM1)	81
Figure 3.2 Particulate protein degradation for different particles size versus time.	83
Figure 3.3 Methane production over digestion time using different protein particle sizes.	85
Figure 3.4 First-order hydrolysis rate coefficient as function of (a) surface weighted median diameter (μm) (b) specific surface area (m^2/g)	90
Figure 3.5 Amino acids variation with time for different protein particle sizes.	94
Figure 4.1 SCOD/TCOD ratio as a function of specific energy for primary and waste activated sludge.	109
Figure 4.2 SBOD/TCOD ratio as a function of specific energy for primary and waste activated sludge.	110
Figure 4.3 Particulate protein/TCOD as a function of specific energy for primary and waste activated sludge.	112
Figure 4.4 Bound protein/TCOD as a function of specific energy for primary and waste activated sludge.	112
Figure 4.5 Soluble protein/TCOD as a function of specific energy for primary and waste activated sludge.	112
Figure 4.6 Bound protein / mg VSS as a function of specific energy for primary sludge during anaerobic digestion.	113
Figure 4.7 Bound protein / mg VSS as a function of specific energy for waste activated sludge during anaerobic digestion.	113
Figure 4.8 Cell proteins released as a function of specific energy for primary and waste activated sludge.	115
Figure 4.9 VFA/TCOD as a function of specific energy for primary and waste activated sludge.	116
Figure 4.10 Specific surface area (m^2/g) as a function of specific energy.	118
Figure 4.11 Methane yield of the untreated and treated primary sludge over the digestion time	119
Figure 4.12 Methane yield of the untreated and treated waste activated sludge over the digestion time	119
Figure 4.13 Predicted and measured methane yields for the untreated and treated primary sludge.	123
Figure 4.14 Predicted and measured methane yields for the untreated and treated WAS sludge.	124
Figure 4.15. Increase in volume of methane produced in treated primary sludge	128
Figure 4.16 Increase in volume of methane produced in treated WAS.	129
Figure 5.1 Relationship between $\text{COD}_{\text{solubilisation}}$ and: (a) DDSCOD (%),	145
Figure 5.2 Particle size distribution for different specific energy inputs	146
Figure 5.3 Specific energy input for different TS at different degree of disintegrations.	148
Figure 5.4 Cumulative methane production at different specific energy inputs.	153
Figure 6.1 Reduction in PS and WAS in anaerobic digestion (a) TSS (b) VSS (c) TCOD (d) SCOD.	166
Figure 6.2 Average VFA in PS and WAS. (a) influent concentrations (b) reduction.	169
Figure 6.3 Relationship between VSS degradations and protein fractions during anaerobic digestion for PS and WAS (a) Particulate (b) Bound (c) Cell.	172

Figure 7.1 ADM1 Software interface	202
Figure 7.2 Percentage composition interface.....	203
Figure 7.3 Stoichiometric parameters interface.....	203
Figure 7.4 Kinetics coefficients interface	204
Figure 7.5 Initial (time = 0) state variables values.....	204

LIST OF ABBREVIATIONS

ADM1:	Anaerobic Digestion Model No. 1
DD:	Degree of Disintegration
AOP:	Advanced Oxidation Processes
HRT:	Hydraulic Retention Time
MWWT:	Municipal Wastewater Treatment
N:	Nitrogen
PS	Particle Size
PS	Primary sludge
PSD	Particle Size Distribution
Q:	Flow rate
SBOD:	Soluble Biological Oxygen Demand
SCOD:	Soluble Chemical Oxygen Demand
SS:	Suspended Solids
STKN:	Soluble TKN
TBOD:	Total Biological Oxygen Demand
TCOD:	Total Chemical Oxygen Demand
TKN:	Total Kjeldahl Nitrogen
TSS:	Total Suspended Solids
TS:	Total Suspended
V:	Volume
VFA:	Volatile Fatty Acid
VSS:	Volatile Suspended Solid
VS:	Volatile Suspended
WAS:	Waste Activated Sludge
WWT:	Wastewater Treatment
WWTP:	Wastewater Treatment Plant

CHAPTER ONE

1.1 Background

Municipal wastewater treatment is an important part of modern society as it reduces the amount of organic matter and the number of pathogens discharged to water streams. Unfortunately, wastewater treatment also generates large quantities of sludge. The treatment and disposal of sludge is recognized as the most expensive part of municipal wastewater treatment and the most complex problem facing the industry [1]. Sludge management includes pumping, grinding, screening blending, thickening, digestion, conditioning, dewatering and disposal.

Typically large-scale wastewater treatment plants employ conventional activated sludge (CAS) and generate two main types of sludge: primary and waste activated sludge (WAS). Primary sludge consists of settleable organic and inorganic matter, which has a very offensive odor and is readily biodegradable. WAS consists of the heterotrophic bacteria settled in secondary clarifier. It is difficult to degrade due to the large amount of energy required to rupture the bacteria cell envelope. Raw wastewater characteristics and particle removal efficiencies vary, resulting in a wide range of particle sizes in primary effluents [3].

Anaerobic digestion (AD) is the most popular sludge stabilization process. The advantage of this process includes the production of methane which can be used as an energy source, the low production of waste sludge and potentially high organic loading rates. AD is a complex biotechnological process capable of converting almost all types of organic materials into methane, carbon dioxide and stabilized sludge [4]. The physico-

chemical processes of AD are not biochemically mediated and include the ion association, dissociation, gas-liquid transfer, and mixing pattern [5, 6, 7]. The biochemical extracellular solubilization steps are divided into disintegration and hydrolysis, of which the first is a largely non-biological step that converts composite particulate substrate to individual components such as carbohydrates, proteins, lipids, and inerts. The second step is enzymatic hydrolysis of particulate carbohydrates, proteins and lipids to glucose, amino acids, and long chain fatty acids [7]. A separate group of acidogenic bacteria degrade glucose, amino acids, and long chain fatty acids to mixed organic acids, hydrogen, and carbon dioxide. The organic acids are subsequently converted to acetate, hydrogen, and carbon dioxide by acetogenic groups that utilize butyrate, valerate, and propionate. The hydrogen produced by these organisms is consumed by hydrogen-utilizing methanogenic bacteria, and the acetate by aceticlastic methanogenic bacteria.

Particle size and particle composition determine the rate and mechanism of hydrolysis and degradation in wastewater treatment [3]. Most of the biodegradable organic matter ranges from 10^{-3} to 100 μm . Microorganisms can directly take up particles that are smaller than 10^{-3} μm [8, 9]. It is also important to mention that the reaction rates vary widely based on the type of sludge or substrate used. Although the hydrolysis of particulate organic material has been considered the rate-limiting step in anaerobic digestion [10], some authors have emphasized that the hydrolytic process still remains as the least defined step [11, 12].

Rapid and complete stabilization of WAS via AD has not been fully achievable due to the rate-limiting hydrolysis of large organic molecules associated with microbial

cells. Recent studies have indicated that activated sludge has a more complex floc structure than first realized. It is comprised of different groups of microorganisms, organic and inorganic matter agglomerated together in a polymeric network formed by microbial extracellular polymeric substances (EPS) and cations [13, 14].

Improvement of biodegradability of sludge via AD depends on enhancement of the disintegration of the floc structure, thus increasing the accessibility to both intracellular (within the microbial cell) and extracellular (within the polymeric network) materials before sludge is sent to anaerobic digesters. Such pretreatment processes aim to disrupt the bacterial cell wall and breakdown the large particles, i.e., solubilization of particulate matter and consequentially increasing the amount of organic material available for digestion. Examples of pretreatment options that have been shown to enhance anaerobic digestion include chemical [15-17], mechanical [18, 19], and ultrasound pretreatment [20–24].

Mathematical models of biological sludge treatment systems are useful tools for simulation and design. Although simple models have been successfully applied to conventional systems, such as the activated sludge process, simple models are not satisfactory for describing the dynamic behavior of complex anaerobic systems [25]. It is necessary to apply more sophisticated structured models. Structured models consider the biomass and substrate to be divided into several components with each biomass mediating and transferring particular substrate. Structured models are very significant in the design and application of anaerobic treatment process. Because of the slow growth of anaerobic bacteria, experiments require a long time. However, a correctly constructed and calibrated structure model can rapidly predict system performance and simulate the

system response to operational changes. Models can be helpful in designing, explaining, and extrapolating experimental results. Also the development of a hydrolysis model that accounts for the impact of particle size is required to improve the understanding of the hydrolysis rate and subsequently for developing more efficient AD designs.

1.2 Synopsis of Literature

In the past few decades there have been many studies on AD, and the parameters that affect and enhance the process dynamics. Several approaches to mathematically model this complex process were investigated with various advantages and disadvantages.

Hydrolysis has been considered the rate-limiting step in AD, yet some authors have emphasized that the hydrolytic process still remains as the least defined step. Hydrolysis is well documented to be a function of specific surface area among other variables [26]. Studies on the effect of particle size on hydrolysis and its mathematical relationship are sparse, as most of the studies reported the hydrolysis rate coefficient as a single value and not a function of particle size. No study has addressed the effect of particle size distribution (full spectra distribution) on the hydrolysis rate coefficient.

The literature on odor production from anaerobically digested biosolids has been inadequate [27]. Although H_2S is considered to be the most prevalent odorous compound, there are typically other organic odorous compounds in AD, such as mercaptans and amines. Prior research has implicated volatile sulfur compounds (VSCs) including hydrogen sulfide (H_2S), methanethiol or methyl mercaptan (MT), dimethyl sulfide

(DMS), dimethyl disulfide (DMDS) and dimethyl trisulfide (DMTS) in odors from biosolids [28]. Laboratory tests have indicated that protein degradation and, especially the degradation of methionine, an amino acid, is the main source for the production of VSCs [28]. Literature on proteins during AD is both sparse and contradictory; in most studies total protein degradation was only reported under controlled conditions. No systematic study has been conducted on the degradation of various fractions of protein in conventional AD of sludge.

Various mechanical disintegration methods have been applied to the pretreatment of biosolids to enhance the rate and extent of AD. Sonication is a method for the break-up of microbial cells to extract intracellular material [29]. While most of the studies using ultrasound energy have focused on the dewaterability and solubilization of chemical oxygen demand (COD), there is a definite paucity on information related to the impact of sonication on other biosolids characteristics like odors precursors such as proteins as well as anaerobic biodegradability.

1.3 Research Objectives

Based on the above, the primary objective of this research is to develop a process model that integrates sonication pretreatment and anaerobic digestion incorporating the impact of sonication on particle size and subsequently the impact of particle size on biodegradation kinetics.

The proposed research will specifically examine the effect of particle size on the hydrolysis of municipal primary and secondary sludges and anaerobic sludge

biodegradability. The aim is to develop an integrated mathematical model that describes the effect of particle size on the anaerobic hydrolysis rate coefficient process, as well as its overall impact on the anaerobic digestion process. Primarily this can be done by the reduction of particle size through pretreatment which can alter the particle size distribution of the particulate substrates. More specifically, the objectives of this study and how they relate to the areas of further research identified above are:

1. Anaerobic modeling is complex and severely compromised with hydrolysis

modeling of single size particles: In this study, the following goals will be realized

- Assessment of particle size effect on hydrolysis rate coefficient
- Development of a mathematical/kinetic model of the hydrolysis phase of anaerobic digestion as a function of particle size.
- Application and validation of the developed model.

2. Relatively low digestion efficiency: This study aims at investigating sonication as a pretreatment technique in greater depth through the following;

- Assessment of sonication as a particle size reduction method for sludge.
- Evaluation of the effect of sonication on various characteristics of primary and secondary sludge, specifically the effect on solubilization, VFA and various fractions of proteins, and subsequent anaerobic biodegradability.

- Evaluation of the performance of batch anaerobic digesters using sonicated primary and waste activated sludge.

3. Inadequate information on odor and odor precursors: The goals of this study are:

- Investigation of the degradation of various odor precursors during conventional anaerobic digestion of primary and waste activated sludge.
- Investigation of the effect of sonication on odor precursors, primarily various fractions of proteins, both during sonication and anaerobic digestion.

1.4 Thesis Organization

This thesis comprises of eight chapters and conforms to the “integrated-article” format as outlined in the Thesis Regulation Guide by the School of Graduate and Postdoctoral Studies (SGPS) of the University of Western Ontario. A review of literature including background and a thorough assessment of information on anaerobic digestion models, hydrolysis models and pretreatment methods is presented in *Chapter 2*.

Chapter 3 demonstrates the effect of particulate protein particle size on anaerobic digestion and the influence of particulate size distribution on the anaerobic hydrolysis rate coefficients. Mathematical relationships that correlate the hydrolysis rate coefficient as a function of surface weighted median diameter and specific surface area are illustrated along with the development and verification of a more comprehensive hydrolysis kinetic model that takes particle size into consideration.

Chapter 4 presents the impact of ultrasound pretreatment on various protein fractions in primary sludge, waste activated sludge and hog manure and their anaerobic biodegradability. The effect of ultrasound on particle disintegration anaerobic digestion coefficients, and gas production was also determined and presented as well as an empirical model was developed to assess the economical viability of ultrasound based on electrical energy input versus energy obtained from additional methane gas produced.

Chapter 5 discusses the impact of ultrasound pretreatment on solubilisation and anaerobic biodegradability of hog manure with a much higher solid content and wider range of particle sizes than primary and waste activated sludge, with particular emphasis on the effect of ultrasound on proteins solubilisation, especially bound protein. Additionally, a correlation between standardized and easy-to-measure solubilization parameters and the laborious and expensive method of degree of disintegration was presented.

Chapter 6 presents the degradation of various protein fractions (particulate, soluble, and bound) of primary and secondary municipal sludge during anaerobic digestion, illustrate the relationship between various protein fractions and other sludge quality parameters, simulates the odors precursors (namely, protein, amino acids and volatile fatty acids) degradation, and estimates the anaerobic degradation kinetics,

Chapter 7 presents the development of the anaerobic digestion model software; model and code calibration; and software application.

Chapter 8 summarizes the major conclusions of this research and provides recommendations for future research directions based on the findings of this study.

1.5 Contribution of Thesis

Canada has over 700 mostly small and medium-sized water and wastewater firms with annual sales totaling \$1.4 billion, 40% of which is related to water and wastewater treatment. Currently, most medium and large size wastewater treatment plants employ anaerobic digestion of sludge to reduce pathogens, stabilize organic matter, and produce biogas. Unfortunately, despite extensive work on digester design, the efficiency of volatile solids destruction is limited to about 40-45% only.

The increasing quantity of municipal sewage sludge, the level of their treatment, and the requirements concerning the conditions of neutralization and their ultimate disposal are of serious concern in Canada and many parts of the world. For example, about seven million dry tons of wastewater solids are produced annually in the United States alone. With the implementation of stringent regulations on sludge disposal and closure of more landfills, sludge management is becoming a difficult task. A point in consideration is the on-going discussion over Toronto's garbage disposal to Carleton Farms landfill site in Port Huron, Michigan. Wastewater treatment plants are consequently forced to develop new and more effective sludge management strategies, and the proposed research is targeted towards this objective. The proposed work aims to enhance the anaerobic digestion efficiency by determining the effect of particle size on the rate-limiting step in the anaerobic digestion. In addition the study aims to reduce the volume of anaerobic digester; produce a greater amount of useful biogas, and lower the volume of sludge for final disposal by applying a feasible pre-treatment technique based on advanced oxidation processes (AOP). Moreover, another objective is to

mathematically verify the anaerobic digestion activity by applying a user-friendly anaerobic digestion model.

1.6 References

- [1] Metcalf and Eddy, Wastewater Engineering: Treatment Disposal Reuse, 2003, 4th ed. McGRAW-HILL
- [2] Tchobanoglous, G.; Burton, F.L.; Stensel, H.D. Wastewater Engineering, Treatment and Reuse, 4th Edition. McGraw-Hill, Inc., New York. 2003, 1819.
- [3] Morgenroth, E.; Kommedal, R.; Harremoës, P. Processes and modeling of hydrolysis of particulate organic matter in aerobic wastewater treatment – a review, Water Sci. Technol., 2002, 6, 25–40
- [4] Chynoweth, D.; Pullammanappallil, P. Anaerobic digestion of municipal solid waste in microbiology of solid waste. CRC Press, Boca Raton, FL. 1996, 71-113.
- [5] Vavilin, V.; Rytov, S.; Lokshina, L.; Rintala, J.; Lyberatos, G. Simplified hydrolysis models for the optimal design of two-stage anaerobic digestion. Water Research, 2001, 35 (17), 4247-4251.
- [6] Kalyuzhnyi, S. Modeling of anaerobic digestion. Water Sci. Technol. 2001, 624, 22-23.
- [7] Batstone, D. J.; Keller, J.; Angelidaki, I.; Kalyuzhnyi, S. V.; Pavlostathis, S. G.; Rozzi, A.; Sanders, W. T. M.; Siegrist, H.; Vavilin, V. A. Anaerobic Digestion Model No. 1, IWA Task Group for Mathematical Modelling of Anaerobic Digestion Processes, Water Sci. Technol. 2002, 10, 65–73.
- [8] Ferenci, T. The recognition of maltodextrins by *E.coli*. Eur. J. Biochem., 1980, 108, 631–636.

- [9] White, D. The physiology and biochemistry of prokaryotes, Second edition, Oxford University Press Inc., New York, 2000.
- [10] Pavlostathis, S.; Giraldo-Gomez, E. Kinetics of anaerobic treatment. *CRC Crit. Rev. Environ. Contr.*, 1991, 21, 411–490.
- [11] Miron, Y.; Zeeman, G.; van Lier, J.; Lettinga, G. The role of sludge retention time in the hydrolysis and acidification of lipids, carbohydrates and proteins during digestion of primary sludge in CSTR systems. *Water Research*. 2000, 34, 1705–1713.
- [12] Gavala, H.; Angelidaki, I.; Ahring, B.; Kinetics and modelling of anaerobic digestion process. *Adv. Biochem. Eng. Biotechnol*, 2003, 81, 57–93.
- [13] Li, A. and DiGiano, F. The availability of sorbed substrate for microbial degradation on granular activated carbon, paper presented at the 53rd Annual Water Pollution Control Federation Conference, Las Vegas, Nevada, 1980.
- [14] Higgins, M.; Glindemann, D.; Novak, J.; Murthy, S.; Gerwin, S.; Forbes, R. Standardized biosolids incubation, headspace odor measurement and odor production consumption cycles. *Proceedings Water Env. Federation and AWWA Odors and Air Emissions Conference*, Bellevue, Washington, 2004.
- [15] Lin J.G. and Chang C.N. Fenton process for treatment of desizing wastewater, *Water Research*. 1999, 31, 2050–2056.
- [16] Yasui, H.; Nakamura, K.; Sakuma, S.; Iwasaki, M.; Sakai, Y. A full scale operation of a novel activated sludge process without excess sludge production. *Water Sci. Technol*. 1996, 34, 395-40.

- [17] Tanaka, S. Effects of thermochemical pre-treatment on the anaerobic digestion of waste activated sludge. *Water Sci. Technol.* 1997, 35, 209-215.
- [18] Nah, I. W. Mechanical pre-treatment of waste activated sludge for anaerobic digestion process. *Water Research.* 2000, 34, 2362-2368.
- [19] Flint, E.B. and Suslick, K.S. The temperature of cavitation, *Water Science* 1991, 253, 1397–1399.
- [20] Suslick, K. Sonochemistry. The temperature of cavitations. *Science.* 1991, 253, 1397–1399.
- [21] Kuttruff, H. *Ultrasonics Fundamentals and Applications.* Essex, England.1991.
- [22] Wang, F.; Shan, L.; Ji, M. Components of released liquid from ultrasonic waste activated sludge disintegration, *Ultrason. Sonochem.* 2006, 13, 334–338.
- [23] Jeffrey, P.; Brown, P.; Hogan, F. Ultrasonic solids treatment yields better digestion. *WERF, Biosolids Technical Bulletin.* 2003
- [24] Gronroos, A.; Kyllonen, H.; Korpijarvi, K.; Pirkonen, P.; Paavola, T.; Jokela, J.; Rintala, J. Ultrasound assisted method to increase soluble chemical oxygen demand (SCOD) of sewage sludge for digestion, *Ultrason. Sonochem.* 2005, 12, 115–120.
- [25] Lyberatos, G. and Skiadas, I.V. Modelling of anaerobic digestion – A review. *Global Nest: the Int. J.* 1999, 2, 63-76
- [26] Sanders, W.; Geerink, M.; Zeeman, G.; Lettinga, G. Anaerobic hydrolysis kinetics of particulate substrates. *Water Sci. Technol.*, 2000, 41, pp17–24.

- [27] Higgins, M.; Adams, G.; Chen, Y.; Erdal, Z.; Forbes, R.; Glindemann, D.; Hargreaves, J. McEwen, D.; Murthy, S.; Novak, J.; Witherspoon, J. Role of protein, amino acids, and enzyme activity on odor production from anaerobically digested and dewatered biosolids, *Wat. Environ. Res.*, 2008, 80, 127.
- [28] Higgins, M.; Adams, G.; Chen, Y.; Erdal, Z.; Forbes, R.; Glindemann, D.; Hargreaves, J. McEwen, D.; Murthy, S.; Novak, J.; Witherspoon, J. Relationship between biochemical constituents and production of odor causing compounds from anaerobically digested biosolids, *WEF and AWWA Odors and Air Emissions 2004 Conference*, Washington, USA, 2004, 18-24.
- [29] Harrison, S.T.L., Bacterial cell disruption: a key unit operation in the recovery of intracellular products, *Biotechnol*, 1991, 9, 217–240.

CHAPTER TWO

2.1 Literature Review

2.1.1 Introduction

Anaerobic digestion (AD) is a complex biotechnology system capable of converting most organic materials into methane, carbon dioxide and stabilized sludge [1], which also reduces pollution and recovers fuel gas from municipal, industrial and agricultural wastes [1, 2, 3]. Different groups of microorganisms are responsible for conversion of organic carbon into its most reduced form (methane) and its most oxidized form (carbon dioxide) [4, 5]. During this conversion a variety of microorganisms grow and produce reduced end-products [6, 7]. AD involves series of metabolic interactions among various groups of microorganisms undergoing different biochemical processes as described in Figure 2.1 [8]. Biochemical processes are catalyzed by intracellular and extracellular enzymes. Disintegration and depolymerization of the waste are extracellular processes, and subsequent digestion of the soluble materials by the microbial consortia is an intracellular processes resulting in the growth and decay of the organisms [8]. Biochemical extracellular processes involved in extracellular solubilization steps are divided into disintegration and hydrolysis, of which the first is a largely non-biological step that converts composite particulate substrate to carbohydrates, proteins, and lipids, and inerts. The second step is enzymatic hydrolysis that hydrolyzes particulate carbohydrates, protein, and lipids to soluble forms glucose, amino acids and long chain fatty acids, respectively. Biochemical intracellular processes involve separate groups of acidogenic bacteria that degrade glucose, amino acids and long chain fatty acids to mixed organic acids, hydrogen, and carbon dioxide. The organic acids are subsequently

converted to acetate, hydrogen, and carbon dioxide by acetogenic bacteria groups that utilize butyrate and valerate, and propionate. The hydrogen produced by these organisms is consumed by hydrogen-utilizing methanogenic bacteria, and the acetate by aceticlastic methanogenic bacteria to produce methane and carbon dioxide. The physico-chemical processes of AD that are not biologically mediated include ion association, dissociation, gas-liquid transfer, and mixing [8, 9, 10, 11, 12, 13, 14, 15].

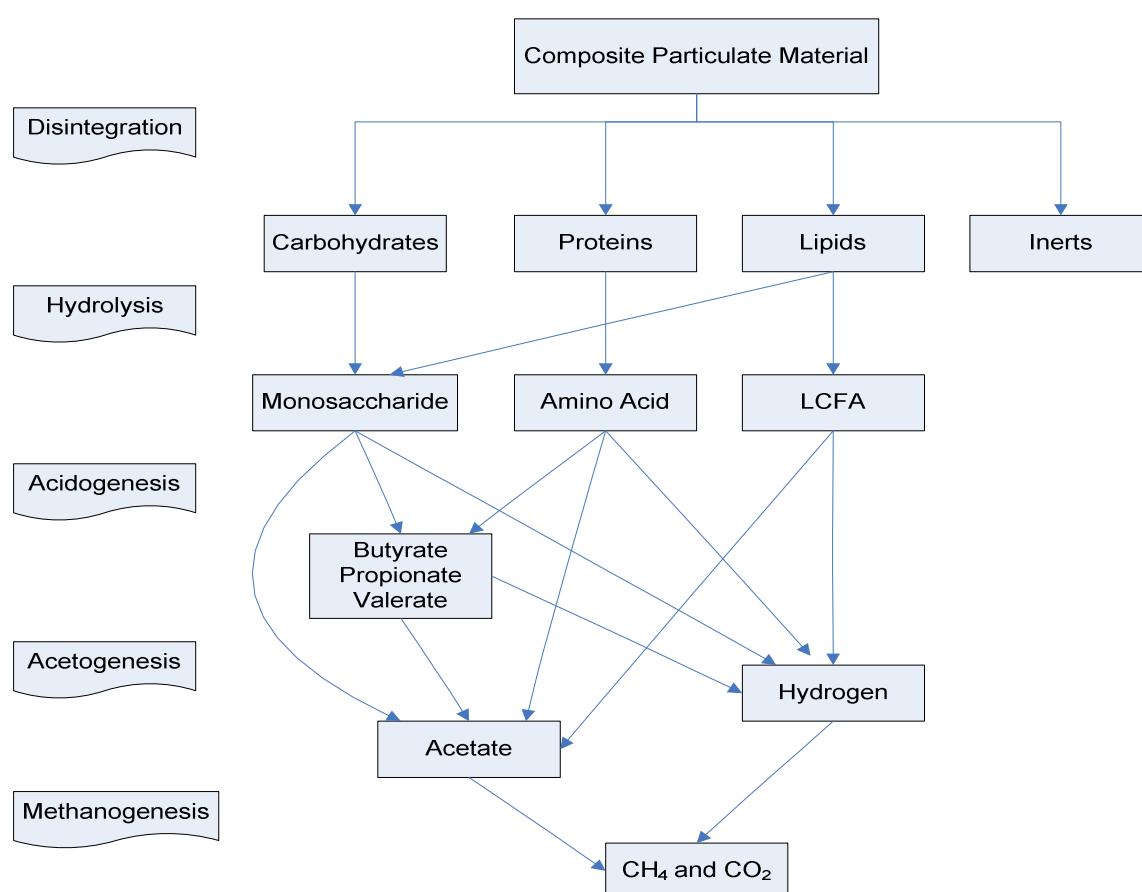


Figure 2.1 Flowchart showing the stages and pathway of anaerobic digestion [8].

Anaerobic sludge digestibility is strictly dependent on the origin of the sludge in the wastewater treatment plant. Waste activated sludge (WAS) is more difficult to digest than primary sludge due to the rate-limiting cell lysis step. The cell wall and the prokaryote membrane are composed of complex organic materials that are not readily biodegradable [16]. Consequently, the reduction of volatile solids is more pronounced in primary sludge digestion than in secondary sludge digestion [17]. One way of improving WAS hydrolysis and anaerobic digestion performance is to use cell lysing pre-treatments. Waste activated sludge disintegration can be defined as the modification of biomass structure by external forces in order to enhance the possibility of substrate release. Several disintegration pre-treatments such as mechanical, thermal, chemical, or biological exist; these forces can be physical, chemical, or biological in nature. The first effect is the disaggregation of the flocs, without disrupting the cells [17]. The separation of the sludge flocs is characterized by an intense particle size reduction, but the release of organic components into the sludge liquid phase is consequently poor [16]. Increasing energy input, the microorganism's cell walls are broken down, and the intracellular material is released [18]. Disintegration pre-treatment has been investigated over the last decade [19, 20, 21, 22, and 23].

In the following sections a comprehensive literature review on the topics of AD modeling, hydrolysis modeling, effect of particle size on AD, solids pre-treatment methods, and odor precursors will be illustrated and discussed.

2.1.2 Anaerobic Digestion Modeling

Several approaches have been developed for AD modeling. Each of these models has advantages and disadvantages. Their applicability is limited by time, expertise (knowledge of the process structure), and available data. The models developed are generally applicable for specific cases. The black box type models do not explain the processes and lack the robustness to model the complex digestion process property. The development of generic dynamic models based on the process dynamics and application as well as the extension of the models for different cases, such as different reactor types, environmental conditions, and organic waste types for AD is needed [3, 8].

The first dynamic model was developed by Andrews [24]. In this model, constant pH was assumed. This model consisted of a single substrate (un-ionized acetic acid) and single biomass (acetate utilizing methanogens). Nevertheless, it was the first model to incorporate the inhibitory effect of high un-ionized volatile acid concentration on the growth of methanogens. The general Monod type kinetic equation was used to express the growth of methanogens and was modified by including the inhibition function.

Hill and Barth [25] enhanced Andrews's model by adding the second bacterial group for acid formation and incorporated hydrolysis. They also added the carbonate equilibrium, nitrogen balance, cation exchange and inhibition of the methane formation by ammonia and volatile fatty acids (VFA). Their model considers three substrates and two kinds of microorganisms (acid formers and methanogens). The model includes the inhibitory effect of high concentration of volatile acids on both acid formers and methanogens, the inhibitory effect of high ammonia levels on the growth of methanogens, and decay of biomass.

Eastman and Ferguson [26] developed a model for sludge digestion, which considered the hydrolysis of particulate substrate rather than methanogenesis as the rate-controlling step. The system used in their study was a continuous stirred tank reactor (CSTR). Primary sewage sludge was the substrate used. In this model, the acidogenic phase included both the hydrolysis and digestion stages. The substrate pathway was described as the biodegradable solids hydrolyzed to smaller soluble molecules, then the soluble molecules are converted to digested products by the acid-forming bacteria. The main assumptions made in this model were: (1) cell decay contributes to the pool of digested products; (2) nitrate, and sulfate concentrations are negligible; and (3) electron acceptors consist solely of organics and carbon dioxide. Substrate was expressed as chemical oxygen demand (COD) to facilitate mass balance calculations. Hydrolysis kinetics under constant pH and temperature were expressed by the first-order equation with respect to the particulate biodegradable COD. Eastman and Ferguson [26] found that the hydrolysis constant to be 3 h^{-1} , growth yield coefficient to be $0.48 \text{ gCOD of VSS/gCOD}$, and decay coefficient to be 0.018 h^{-1} .

Mosey [27] developed an AD model with four different bacterial groups and included the hydrogen gas in the digestion of acetic, butyric and propionic acids in addition to the conversion of propionic and butyric acids to acetic acid [13]. This model was the first one that incorporates the dissolved hydrogen gas. Two years after the development of this model Rozzi et al. [28] modified Mosey's model by using hydrogen partial pressure instead of the dissolved hydrogen gas equations introduced by Mosey. Due to the complexity of the numerical integration problem, Rozzi et al. [28] kept pH

constant in the course of their simulation. Both the Morsey's and Rozzi's models were applied only to glucose as a soluble substrate.

Bryers [29] developed an anaerobic model that considers only one kind of methanogenic biomass but used two kinetic expressions for converting acetic acid and hydrogen respectively to methane. This model did consider the role of propionic acid utilizing bacteria by individually specifying the bacterial concentration, as the acid is an important intermediate and has a significant effect on the stability of that system.

Pavostanthis and Gossett [30] proposed a model where sludge composition is more detailed than the one illustrated by Eastman and Ferguson [26]. This model assumed that the biodegradable fractions of the activated sludge are all viable organisms. This biochemical oxygen demand (BOD) fraction is of two kinds soluble and particulate. Upon microbial death immediate release of the intracellular soluble BOD will occur. At the same time the dead cell particulate BOD is solubilized by extracellular hydrolysis induced by the active biomass in the digester, resulting in an increase in the soluble BOD for subsequent utilization by the acid-forming bacteria. The model takes into account the classical two-stage anaerobic pathway constituted by acidogenesis and methanogenesis. The proposed model is rather complex due to the large number of parameters to be assessed. One other issue in this model is that the two processes of biomass death and lysis are theoretically different in terms of final products. The authors reported unsuccessful attempts of measuring cell lysis rates, thus leading to combine of the two processes into a single death/lysis step and no lag phase between death and lysis on one hand and release of all intercellular on the other hand. A first-order empirical equation

was used for the hydrolysis process of the biodegradable particulate BOD. Cell decay constant was found to be 2 d^{-1} , while the hydrolysis constant was found to be 0.15 d^{-1} .

Shimizu et al. [31] proposed a model that considered the hydrolysis of intracellular biopolymers as the rate limiting step in the AD process. This model assumed that as hydrolysis of the cell walls and membrane proceeded, intracellular high biopolymers are released in the bulk phase. These compounds are then hydrolyzed by extracellular enzymes to volatile organic acids (acetic, propionic, butyric, valeric and caproic acids). Higher fatty acids are converted to acetic acid by the β -oxidation process [31]. In the final stage of the digestion process, acetic acid, hydrogen and carbon dioxide are converted to methane. In order to reduce model complexity, the aforementioned authors used the first-order kinetics for all reactions i.e, sludge solubilization, hydrolysis of intracellular polymers, conversion of higher fatty acids to acetic acid and H_2 , and methanogenesis.

Angelidaki et al. [32] developed a model where the substrate composition was defined by its organic (carbohydrates, lipids, and proteins), inorganic components (ammonium, phosphate, cations, and anions), and their degradation intermediates (volatile fatty acids). Carbohydrates are included in the model as particulate, soluble, and inert fractions; the particulate is hydrolyzed to soluble carbohydrates, which are then converted to volatile fatty acids by acidogenic bacteria. Lipids were expressed as glycerol trioleate which is converted to long chain fatty acids by acidogenic bacteria. The long chain fatty acids are then degraded to acetate and H_2 by acetogenic biomass. Proteins were modeled as gelatin and were considered to be composed of particulate, soluble, and inert fractions. The particulate components are hydrolyzed to amino acids that are

converted in the subsequent degradation step to acetate, propionate, butyrate, and valerate. The hydrolysis step was modeled by a first-order equation; the authors have used the first-order based on the results of previous studies [33, 34], which demonstrated that first-order kinetic model is the best for describing the complex chemical-biological interactions of the AD system. The first-order equation was also used to model the biomass decay. All of the biological processes (uptake and substrate degradation) are kinetically represented by a Monod equation, including a limiting term for ammonia nitrogen as nutrient for biomass growth. The effects of pH and temperature are taken into account in the process kinetics.

Vanvilin et al. [16] developed a multi-component, multi-species model called “METHANE” that takes the processes of hydrolysis, acidogenesis, acetogenesis and methanogenesis conducted by various groups of microorganisms as well as the gaseous phase into account. The model uses a system of differential equations for three groups of variables as suspended organic matter, soluble components and gaseous phase components. It also considers the four basic stages of the AD i.e. hydrolysis, acidogenesis, acetogenesis and methanogenesis together with lysis and hydrolysis of cell biomass. Additionally, substrate limitation and inhibition functions are taken into account in the model.

Siegrist et al. [9, 35] developed a model, for mesophilic and thermophilic digestion of sewage sludge based on the reaction proposed by Gujer and Zehnder [36]. The model considers the CSTR reactor and takes into account the variation in digested sludge and biogas composition. In addition to the biogas and hydrolysis of the particulate COD, six substrate processes are considered: amino acid digestion, sugar digestion,

LCFA, intermediates (propionic), acetotrophic methanogenesis, and hydrogenotrophic methanogenesis. The model also includes six processes of cell decay for the microbial groups catalyzing the bioconversion processes. Chemical equilibrium for the dissociation of bicarbonate, ammonium, acetic and propionic acids is taken into account in evaluating pH. Siegrist et al. [35] used the first-order equations for hydrolysis kinetics of particulate organic material and the biomass decay process. Other kinetics was expressed by a Monod type equation modified to take the inhibition into account.

Batstone et al. [8] introduced the Anaerobic Digestion Model Number 1 (ADM1). The aim of the model was to provide a tool that overcomes the limitation of the models developed over the last few decades that were basically attributed to their specificity. Due to this focus, some peculiar and specific aspects were not included in order to obtain an easy-to-use model. This model therefore can be taken as a platform for applications to specific processes [37]. This model classifies the complex system of the anaerobic conversion process into two main groups: (1) Biochemical reactions are governed by intracellular or extracellular enzymes that act on the organic substances. The disintegration of the particulate compounds, and their hydrolysis, which produces soluble monomers, are extracellular reactions. The degradation of the soluble substances is instead a process that occurs inside the bacterial cells and results in biomass growth, and (2) Chemical-physical reactions are not biologically catalyzed and include the processes of ionic association/dissociation, and gas-liquid mass transfer. Biochemical reactions are considered irreversible processes, while physical-chemical reactions are considered reversible systems. Biochemical equations are the heart of the model that represents the biological system. Physical-chemical reactions are considered to describe the effect of the

state variables (such as pH and gases concentration) on the anaerobic process. The complex substances are initially disintegrated to obtain particulate carbohydrates, lipids, proteins, and inert material. The model assumes inactive biomass derived from the cellular decay process increases the fraction of particulate composite substances. In the following hydrolysis stage, the particulate carbohydrates, lipids, and proteins are converted into their soluble forms of monosaccharides, long chain fatty acids and amino acids, respectively, which are metabolized by the acidogenic bacteria and converted to organic acids (propionate, valerate, butyrate and acetate) and hydrogen. The acetogenic bacteria will then metabolize the organic acids and convert them to acetic acid and hydrogen. The latter are further transformed by methanogenic bacteria to methane and carbon dioxide. A schematic representation of the metabolic pathways is shown earlier in Figure 2.1. The ADM1 model assumes all extracellular processes follow the first-order kinetics, the cellular decay processes are also described by the first-order kinetics equations that are dependent on the microbial concentration. The substrate utilization rates are expressed by Monod type kinetics, and they are expressed in terms of substrate consumption and not microbial growth, with the aim of simplifying the implementation of the inhibition functions. In addition to pH inhibition for all the bacterial groups, hydrogen inhibition for the acetogenic bacteria and free ammonia inhibition for the acetoclastic methanogens are also included in the model. The chemical-physical processes are important in modeling the anaerobic systems as they express the inhibiting factors for the biological reactions and quantify some variable parameters (gas flow rate, alkalinity, and pH). The gas phase in this model contains carbon dioxide, methane, and hydrogen. Henry's law is used to describe the gas-liquid equilibrium for the diluted

liquid phase. Carbon dioxide and ammonia are considered as acids and bases present in the free form. More details on the model parameters, dynamic variables, state variables, reaction equations, gas-phase equations, liquid-phase equation, acid-base equations, pH and inhibition equations, stoichiometric matrix and model development will be illustrated and discussed in chapter seven and appendix A.

2.1.3 Hydrolysis Modeling

The term hydrolysis means the solubilization of a defined particulate macromolecular substrate to its soluble monomers [8]. Hydrolysis is a slow process that depends on the nature of the particulate matter and size. Hydrolysis governs the rate of the whole anaerobic process and its lag time during start-up [26, 33, 36]. Although, methanogenic bacteria are highly sensitive to environmental conditions [38], previous studies [33, 39] on anaerobic sludge digestion found that methanogenesis is not always the rate-limiting step. The anaerobic degradation of complex substrates requires the viable fraction of the sludge to be first converted to suitable substrates for the anaerobic microorganisms. The hydrolysis of complex organics to soluble substrates, which provides the substrate for the acidogenic bacteria, also determines the availability of substrate for methanogens, as acidogenesis kinetics is one order of magnitude higher than methanogenesis. When a process is composed of a sequence of reactions, the overall rate is determined by the slowest reaction, named the rate-limiting step [25]. The rate-limiting step in anaerobic digestion with suspended organic matter is normally considered to be the hydrolysis of solids [40].

Simplified models for hydrolysis kinetics have been proposed including first-order, or saturation type kinetics [41]. Table 2.1 displays the various hydrolysis kinetic models available in the literature. Most of these models have been developed for specific situations with either very high or very low substrates to microorganism ratio.

Table 2.1 Hydrolysis rate models (adapted from Pin-Jing et al., 2006).

Name	Expression ($-dS/dt$)	References
Chemical first-order	$k_h S$	Eastman and Ferguson [26]
Biological first-order	$k_h SB$	Valentini et al. [42]
Half-order biomass kinetics	$k_h SB^{0.5}$	Rozzi and Verstraete [28]
A-order biomass kinetics	$k_h SB^A$	Valentini et al. [42]
Michaelis–Menten equation	$k_h SB/(K_s + S)$	Valentini et al. [42]
Monod equation	$\mu_{\max} SB/[Y(K_s + S)]$	Hobson [43]
Haldane equation	$\mu_{\max} B/[Y(1 + K_s/S + S/K_i)]$	Andrews and Graef [24]
Contois model	$k_h SB/(K_s B + S)$	Henze [2]
Chen–Hashimoto model	$k_h SB/[K_s(S_o - S) + S]$	Chen and Hashimoto [44]
Two phase model	$k_h SB/[(K_s + S)(K_B + B)]$	Vavilin et al. [45]
Step diffusion equation	$[v_{\max}^2 + k_h(S_o - S)]^{0.5}$	Cecchi et al. [46]
Shrinking core model	$3k_h S_o \phi^2 B$, $d\phi/dt = -k_h B$	Negri et al. [47]
Flux model	$k_h S_{surf} B \rho$	Terashima and Lin [26]
Surface based kinetics model	$k_h S_{surf}$	Sanders et al. [48]

where, A is the exponent in the A -order biomass kinetic equation;

B is the concentration of biomass or enzyme (mol/l);

K_B is the saturation constant for biomass or enzyme (mol/l);

k_h is the hydrolysis rate constant (h^{-1});

K_i is the inhibition constant for the i inhibitory agent (mol/l);

K_S is the saturation constant for the substrate (mol/l);

S is the substrate concentration (mol/l);

S_0 is the initial substrate concentration (mol/l);

S_{surf} is the surface area of the organic solid (cm^2);

v_{max} is the maximum hydrolysis rate (mol/ l h);

ϕ is the dimensionless particle radius, equal to the ratio of the radius of the particle at time t to the initial radius of the particle

Y is the growth yield coefficient;

μ_{max} is the maximum specific growth rate (h^{-1});

ρ is the density of the organic solid (g/cm^3);

t is time (h);

It is interesting to note that while they are fundamentally different, some of these models are sometimes equivalent to each other in terms of effectiveness [42, 45, 46]. For example, the chemical first-order kinetics is not directly coupled to the bacterial growth,

while the biological first-order, half-order biomass kinetics, and A-order biomass kinetics are models with similar structure as they contain the hydrolysis rate constant, substrate concentration, and biomass concentration. These models are more comprehensive than the chemical first-order kinetics model due to the consideration of biomass concentration. The Michaelis–Menten kinetic reaction is mainly applied for the hydrolysis of a soluble substrate.

Goel et al. [49] found that the hydrolysis of soluble starch follows the Michaelis–Menten kinetics model where the enzyme concentration was proportional to the substrate concentration. The Monod and Michaelis–Menten equations are considered to be similar when μ_{\max} and Y are constant. These models use the hydrolysis rate coefficient as a constant value which is not coupled to the physical characteristics of the particulates.

The surface-based kinetic model by Sanders et al. [48] was an attempt to correlate the hydrolysis equation to the physical characteristics of particulates, i.e., surface area. However this model did not take into account either the substrate or biomass concentration. Although the Flux model developed by Terashima and Lin [26], introduced the biomass concentration, surface area, and density of the substrate for hydrolysis rate calculation it still used the hydrolysis rate constant as a constant value.

Myint et al. [50] developed a two-phase leach-bed reactor system for dry digestion of cattle manure residues. The aim of their study was to optimize chemical oxygen demand (COD) generation by enhancing hydrolysis and acidogenesis and minimizing methanogenic activity by maintaining pH below 5.5 [26, 51] and heat treatment of seed sludge [52]. The authors developed a two-substrate, single-biomass model for the hydrolysis/acidogenesis phase. The developed model was based on the

premise that particulate hydrolysable fraction of cattle manure is composed of cellulose and hemicellulose that are hydrolyzed at different rates according to a surface-limiting reaction, and that the respective soluble products of hydrolysis are utilized by acidogens at different rates, according to a two-substrate, single-biomass model. Batch experiments were conducted and the results were used to identify the sensitive parameters and to calibrate and validate the model. The authors reported that the results predicted by the model agreed well with the experimentally measured data not used in the calibration process, with correlation coefficients exceeding 0.91. These results indicate that the most significant parameter in the hydrolysis–acidogenesis phase is the hydrolysis rate constant for the cellulose fraction.

Lu et al. [53] studied the effects of dosed ammonia (0–16 g NH₃) on hydrolysis rates of proteins and lipids from fish residues under mesophilic anaerobic incubation. An empirical kinetic model that describes the effects of ammonia on proteins and lipids hydrolysis rates was developed. The results showed that carbon hydrolysis was suppressed more by ammonium in the acidogenesis phase than in the acidogenesis/methanogenesis phase in a single-stage anaerobic digestion. Also it has been found that hydrolysis of compounds containing nitrogen was similarly suppressed by ammonia during acidogenesis and acidogenesis/methanogenesis phases of a single-stage anaerobic digestion. They also reported that the protein fraction of fish residues was entirely biodegradable. The aforementioned hydrolysis model fitting demonstrated that two fractions of lipid substrates exist, namely, easy and hard to biodegrade with hydrolysis rates that were affected differently by ammonia concentration.

Vavilin et al [54] compiled and reviewed the information available in the scientific literature relative to the kinetics of the hydrolysis process, highlighting the models in which hydrolysis is coupled to the growth of hydrolytic bacteria, as well as to substrate heterogeneity. In their study they compared the prediction of the first order, Michaelis–Menten, Monod, surface-based kinetic and Contois models against available experimental data. The concepts of rate-limiting step in anaerobic digestion and inhibition of hydrolysis at high loads of particulate substrates were also discussed. They reported that hydrolysis has mainly been modeled by first-order kinetics. For complex substrates, the first-order kinetics should be modified in order to take into account difficult-to-degrade material. They have shown that models in which hydrolysis are coupled to the growth of hydrolytic bacteria work well at high or at fluctuating organic loadings. In particular, the surface-related two-phase and the Contois models showed good fits to experimental data from a wide range of organic wastes. Both models converge to first-order kinetics at a high biomass to-waste ratio and, for this reason, they can be considered as more general models. They also reported that acetogenesis or methanogenesis might be the rate-limiting stages in complex wastes. In such cases, stimulation of hydrolysis (mechanically, chemically or biologically) may lead to a further inhibition of these stages, which ultimately affects hydrolysis as well. They also stated that since the hydrolysis process is characterized by surface and transport phenomena, new developments in spatially distributed models are considered fundamental to provide new insights in this complex process.

The first-order model is simple to use and has been reported to fit experimental data well [34, 36]. It has simplified the depolymerization rate of municipal solid waste

and solubilization rate of complex organics by first-order kinetic expressions, Pavlostathis et al. [40], reviewed the literature published up to 1990, and indicated that all of these works had used a first-order model to describe anaerobic hydrolysis of particulate wastes. In a recent study by Mohmoud et al. [55], a similar model has been adapted for anaerobic stabilization of primary sludge. Table 2.2 summarizes the typical values of rate coefficients for different substrates that can be found in the literature. A wide range of values of the first-order rate constant can be seen for composite and simpler organic materials including carbohydrates, lipids and proteins. This wide range of values can be explained by different experimental conditions, different hydrolytic biomass-to-substrate ratios and the lumped effect of disintegration and hydrolysis.

The first-order kinetic model has failed to predict the maximum biological activity when using a complex organics substrate [44]. Hobson [43] had confirmed that the hydrolysis is based not only on the concentration of the substrate, but also on the available surface area of the substrate. Sanders et al. [60] reported in their study that the first-order kinetics can only be applied when the rate-limiting factor is the surface of the particulate substrate, and bioavailability or biodegradability related phenomena do not interfere. Noykova et al. [61] have used the biological first-order model to describe the hydrolysis process in the digestion of fresh cow manure with total solid concentration ranging from 4.5 to 12.65 %.

Table 2.2 Kinetic coefficients of the first-order rate of hydrolysis in literature.

Sludge Type	Substrate	Hydrolysis constant (d ⁻¹)	References
Various types	Carbohydrates	0.041 - 0.13	Gujer and Zehnder [36]
Various types	Proteins	0.02 - 0.03	Gujer and Zehnder [36]
Various types	Lipids	0.08 - 0.4	Gujer and Zehnder [36]
Primary Sludge	Carbohydrates	0.21 - 1.94	O'Rourke et al. [56]
Primary Sludge	Proteins	0.0096 - 0.1	O'Rourke et al. [56]
Primary Sludge	Lipids	0.0096 - 0.17	O'Rourke et al. [56]
Sewage sludge	Carbohydrates	0.025 - 0.2	Christ et al. [57]
Sewage sludge	Proteins	0.015 - 0.075	Christ et al. [57]
Sewage sludge	Lipids	0.005 - 0.01	Christ et al. [57]
Various types	Carbohydrates	0.25 vary within (100%)	Batstone et al. [8]
Various types	Proteins	0.2 vary within (100%)	Batstone et al. [8]
Various types	Lipids	0.1 vary within (300%)	Batstone et al. [8]
Various types	Carbohydrates	0.5 - 2.0	Garcia-Heras [58]
Various types	Proteins	0.25 - 0.8	Garcia-Heras [58]
Various types	Lipids	0.1 - 0.7	Garcia-Heras [58]
Gelatin	Proteins	0.65	Flotats et al. [59]

Contois [62] proposed the Contois kinetic hydrolysis model that considers the bacterial specific growth rate, μ_m , as a function of cell mass concentration B, and limiting substrate.

$$\mu = \frac{\mu_m \cdot S}{K_s \cdot B + S} \quad \dots \quad (2.1)$$

$$\frac{dS}{dt} = -\frac{k_h \cdot B \cdot S}{K_s \cdot B + S} \quad \dots \quad (2.2)$$

Hashimoto et al. [63] have evaluated the Contois model, and found that it fitted well in swine waste fermentation and was acceptable for dairy manure digestion.

Negri et al. [47] proposed rates of depolymerization and solubilization of solid waste that are proportional to the fluid-solid surface area and enzyme concentration, assumed to be directly dependent on the concentration of acidogens. Using the Shrinking Core Model, the waste particles were assumed to be of spherical geometry, and the acidogens degrade the solid from the surface to the center. Hills and Nakano [65] used the same model and demonstrated a linear relationship between the gas production rate and the inverse of the particle diameter for tomato solid waste, with average particle diameters from 0.13 to 2.0 cm. Similar results were obtained by Sharma et al. [66] with agricultural and forest residues.

Vavilin et al. [67] used the A-order biomass kinetics model, assuming that the hydrolysis rate is limited by the contact area between spherically symmetrical particles of organic substrate and bacterial mass, and that the size of the hydrolyzed particle is much larger than the depth of the bacterial layer. Assuming also that the total number of particles per unit volume does not change but that the size of the particles decreases as a result of the hydrolysis, they proposed the A-Order biomass kinetics model. Valentini et al. [42] used the same approach and called it the power relationship between the rate constant of cellulose hydrolysis and the average particle diameter, where A is the degree index that equals to $2/3$, $1/2$ and 0 for spherical, cylinder and plate-form particles, respectively. Saravanane et al. [68] conducted an experiment where he divided the sago wastewater to three particle sizes with the following averages value: 400, 700, and 1100 μm . For each test, the experimental data were fitted using A-Order biomass kinetics

model. Results showed that the model allowed for more accurate mathematical representation of the hydrolysis process. A series of batch tests indicated that the best fit value of A was in the range of 0.43 to 0.62.

Sanders et al. [48] studied the influence of particle size on hydrolysis in anaerobic digestion, using surface-based kinetics where the rate of hydrolysis was proportional to the available surface area of the starch substrate. Assuming that the process of hydrolysis does not break apart particles but continuously reduces the particle diameter, then the surface area of similar size particles decreases proportionally with $(\text{soluble BOD})^{2/3}$. Dimock et al. [69] who studied the effect of small and large, surface area weighted mean diameters of 60 and 390 μm , respectively, of hard-boiled egg whites as artificial particles in activated sludge system. The hydrolysis rate constant was 0.038 - 0.24 d^{-1} and 0.019-0.98 d^{-1} for large and small particles, respectively. In this study Dimock used the surface based kinetic equation proposed by Sanders et al. [48].

2.1.4 Particle Size

Particulate organic matter is often removed in conventional primary clarification, which reduces about 50%-70% of suspended solids and 25%-40% of biochemical oxygen demands (BOD) [70]. Raw wastewater characteristics and particle removal efficiencies vary, resulting in a large range of particle sizes in primary effluents [41]. Munch et al. [71] reported on a primary effluent in which 28% of the particles were larger than 100 μm , while Levine et al. [72] found that only 7% of particulates in the primary effluent were larger than 12 μm and 49% of particulates in waste activated sludge were 12 μm ; an

overview of the particle size distribution for various waste streams is presented in Table 2.3.

Table 2.3 Size distribution of organic matter in municipal wastewater (adapted from Levine et al. [72]).

Waste type	Percent size distribution, μm				References
	< 0.001	0.001 – 1	1 – 100	>1 00	
Raw Influent wastewater	12	15	30	43	Munch et al., [71]
Primary effluent	9	48	15	28	Munch et al., [71]
Untreated Wastewater	38	13	19	30	Painter at el. [73]
Untreated Wastewater	29	13	31	27	Walter [74]
Untreated Wastewater	29	15	22	34	Walter [74]
	(< 0.1)	(0.1 - 1)	(1 – 12)	(> 12)	
Primary effluent	(51)	(8)	(34)	(7)	Levine et al., [75]
Waste activated sludge	(28)	(3)	(20)	(49)	Levine et al., [75]

Particle size and particle composition determine the rate and mechanism of hydrolysis and degradation in wastewater treatment [41]. Most of the biodegradable organic matter is in the range of 10^{-3} to $100 \mu\text{m}$. Microorganisms can directly take up particles that are smaller than $10^{-3} \mu\text{m}$ [76, 77]. It is also important to mention that the reaction rates vary widely based on the type of sludge or substrate used. The size of particles in municipal wastewater has been generally classified into four categories namely, settleable, supracolloidal, colloidal and dissolved.

Rudolf and Balmat [77] investigated various methods for the physical fractionation of wastewater. In their studies, they developed a separation procedure approximating the desired size limits. This separation procedure consists of settling and membrane filtration. Karr and Keinath in [78] modified Roudolfs's fractionation

procedure using a 100 μm fabric mesh, 1.0 μm , and 0.001 μm membrane filter. In this experimental procedure, the sludge is first screened through 100 μm mesh and the solids retained on the mesh are termed as rigid settleable solids. The filtrate from the 100 μm filter is flocculated for 15 min at 10 RPM and allowed to settle for 1 hr. These solids from the second procedure were termed fragile settleable solids. The supernatant from the second procedure is filtered through 1.0 μm and 0.001 μm filters to remove the supracolloidal and true colloidal solids, respectively from the dissolved solids. Their data presented in Table 2.4 shows only a small amount of colloidal and soluble matters present in the primary sludge. The large particulates (settleable and supracolloidal) cannot be consumed by bacteria unless they are first hydrolyzed.

Table 2.4 Size of solids in raw sludge (primary sludge)

Solids fraction	Size range (μm)	% of total	Solids (mg/L)
Settleable	> 100	66.5	6452
Supracolloidal	1 to 100	27.5	2675
Colloidal	0.001 to 1	0.5	45
Soluble	< 0.001	5.4	526

The significance of the size of particulate matter was pointed out by number of researchers [75-81]. They concluded that the rate of hydrolysis depends on particle size.

Levine et al. [75] observed that in his work related to the particle size in wastewater that the biological treatability could be enhanced by removing macrocolloidal and supracolloidal particles, or by modifying particulate organics since the treatability of

wastewater solids depends strongly on their size distribution. Moreover, rates of sedimentation, mass transfer, adsorption, diffusion, and biochemical reactions are all influenced by particle size.

Futakawa et al. [79] experimented with activated sludge and compared the rate of metabolism of suspended and soluble matter. They reported that the rate of metabolism of suspended matter decreased as the particle size increased. A similar result for anaerobic systems was reported by Koutsospyros [80] who used sonication as a method of particle size reduction. In the sonication pre-treatment step, the substrate kinetic coefficients are affected by sonication because the particles size decreases as sonication time increases. He stated that the utilization rate coefficient increases as sonication pre-treatment increases.

Andara et al. [81] in their work using pig manure as substrate established a relationship between the process of anaerobic digestion and the size variation of the different fractions of the influent, which were classified in several groups. They also studied the efficiency of a biological treatment process corresponding with the transformation of the organic substances and the size of the particles. They divided the substratum in 800 mL volume aliquots and each was introduced into a 2.5 L reactor. A batch process of anaerobic digestion was then applied using different hydraulic retention times (HRT), which ranged from 7 to 70 days. The temperature was set at approximately 35°C. Once the HRT was completed for every sample, a portion of the residue was classified under the Levine criterion (settleable, supracolloidal, colloidal and dissolved particles). The authors have reported a decrease of the soluble fraction and increase of the colloidal and supracolloidal fractions along the digestion. They also reported that the

prevalence of the soluble particles was observed during the maximum biogas yield. They stated that the described technique does not seem to be quite suitable, because the related errors during the filtration, due to the abundance of suspended solids necessitating high dilution.

Hu et al. [82] studied the effects of particle size on the hydrolysis and acidogenesis of cellulose with ruminal microbes, the optimum pH range for cellulose degradation, and the inhibitory effect of low pH to the artificial rumen degradation. The authors conducted batch experiments to investigate the influence of cellulose particle size and pH. They reported that at a particle size of 50 μm there was a higher hydrolysis and acidogenesis rate, and a reduced degradation time, than for 100 μm particles. Cellulose degradation increased with pH from 6.0 to 7.5, whereas at pH 5.5 there was no degradation. The inhibitory effect of low pH (5.5) on ruminal microbes was not completely remedied even when the pH of the medium was adjusted to a neutral range. In anaerobic cellulosic waste degradation with ruminal microbes, the fermentation system should therefore be maintained above pH 6.0. In all cases, volatile fatty acids were the major water-soluble products of cellulose degradation; acetate and propionate accounted for more than 90% of the total volatile fatty acids concentration.

Gea et al. [83] studied the influence of the bulking agent particle size and bulking agent:sludge volumetric ratio on the composting process of two different types of sewage sludge: dewatered raw sludge (RS) and dewatered anaerobically digested sludge (ADS). The results were analyzed using a full factorial experimental design in order to determine the optimal conditions for composting such sludges in terms of bulking agent particle size and bulking agent:sludge volumetric ratio, two of the key parameters to ensure an optimal

performance of the composting process. The objective function selected was simulated death kinetics of Salmonella, which was chosen as a model pathogen to represent the disinfection of the material. For both types of sludge, optimal values were found at bulking agent particle size of 5 μm and 1:1 bulking agent:sludge volumetric ratio when a Gaussian function was fitted to the experimental data.

Dimock and Morgenroth [69] evaluated the influence of particle size on hydrolysis rates of protein particles in batch, small and large, surface area weighted mean of diameters 60 and 390 μm , respectively, of hard-boiled egg whites as artificial particles in activated sludge system. It was found that the initial hydrolysis rates for large particles (390 μm), were low but increased over time, contradicting commonly used mathematical modeling approaches to describe hydrolysis. The hydrolysis results both in the release of readily biodegradable substrate, at the same time, breakup of larger aggregates resulting in an increase of the specific surface area available for hydrolysis. They reported that hydrolysis rate was 0.038 - 0.24 d^{-1} and 0.019-0.98 d^{-1} for large and small particles, respectively.

Mshandete et al. [84] studied the reduction of particle size as a pre-treatment method for increasing the biogas potential from Tanzanian sisal fibre waste. The treated sisal fibres were then tested in anaerobic batch experiments to determine the effect of the pre-treatment. Batch anaerobic digestion of sisal fibre waste was carried out in 1-l digesters with fibre sizes ranging from 2 to 100 μm , at an ambient temperature of 33°C. The researchers used sediment from a stabilisation pond at a sisal production plant as seed. Results reported that total fibre degradation increased from 31% to 70% for the 2 μm fibres, compared to untreated sisal fibres with a diameter of 100 μm . The results

confirmed that methane yield was inversely proportional to particle size. Methane yield increased by 23% when the fibres were cut to 2 μm size and was 0.22 $\text{m}^3 \text{CH}_4/\text{kg}$ volatile solids, compared to 0.18 $\text{m}^3 \text{CH}_4/\text{kg}$ volatile solids for untreated fibres. They reported that 148,000 tonne of waste sisal fibres generated annually in Tanzania could yield 22 million m^3 of methane and an additional 5 million m^3 of methane if reduced to size of 2 μm was applied.

The methods of particle size reduction methods can be classified into three groups; physical, chemical and biological methods. Since the biological and chemical size reduction methods interfere with the chemical and biological nature of the sludge, the physical size reduction methods are considered as the primary method. In the following section the pre-treatment methods will be briefly illustrated and discussed.

2.1.5 Pre-treatment of Sludge for Anaerobic Digestion

Over the past few decades, numerous experimental pre-treatment methods have been developed to enhance the anaerobic digestion of municipal sludge. The main goal is to reduce the size of the particles, which results in a greater surface area per unit volume available for degradation [85]. Another advantage is to disrupt the microorganisms in the sludge so that cell-bound substrate and intracellular material may be released from the cell into the bulk solution [86]. Table 2.5 displays the advantage and disadvantage of pre-treatment of sludge for anaerobic digestion [85] in addition to what has been illustrated above:

Table 2.5 Advantages and disadvantages of sludge pre-treatment for anaerobic digestion

Advantages of pre-treatment	Disadvantages of pre-treatment
<ul style="list-style-type: none"> - Enhance VS reduction, - Increase methane production, - Small reactor volume, - Lower disposal costs, - Improved disinfection in anaerobic digesters. 	<ul style="list-style-type: none"> - Increase polymer demand for dewatering, - Release of nitrogen in return wastewater - Increase ammonia concentration

In the following sections the numerous pre-treatment methods will be illustrated and discussed.

2.1.5.1 Chemical Pre-treatment (Acids and Bases):

Woodard and Wukasch [87] developed a hydrolysis, thickening, and filtration system to improve the solubilization of total suspended solids (TSS). Although this process was not established as a pre-treatment method for anaerobic digestion, the results of their solubilization study were interesting. Four grams of H_2SO_4 per g TSS were added to one L of WAS at 25, 40, 70 and 90°C. The highest TSS solubilization was reached at a temperature of 90°C, after 30 minutes of contact. The TSS solubilization had already reached 67% and reached a maximum of 69% after one hour. Another experiment investigated the effect of acid dose on WAS at room temperature for 30 seconds. With only 1 g H_2SO_4 per g TSS, the TSS solubilization reached 55% and increased linearly at

higher acid doses up to a value of 60% at a dose of 8 g H₂SO₄ per g TSS. During both studies the researcher observed that large quantities of carbon dioxide were being generated due to the acidification of bicarbonate ions and the associated dissolution of calcium carbonate salts [87]. The authors also reported that one serious drawback of this pre-treatment would be the large quantities of acids and bases required. Major gains in VS removal and methane production would be necessary to counterbalance this and to make it a viable pre-treatment technology.

Lin et al. [20] conducted a study in which WAS at 1 and 2% TS was pre-treated with sodium hydroxide at 20 and 40 mg/L for 24 hours at room temperature and under anoxic conditions. The untreated and pre-treated sludge was digested in 1-L semi-continuous anaerobic reactors at solids retention time (SRT) of 7.5, 10, 13, and 20 days. The highest solubilization was achieved in the 1% sludge treated with 40 mg/L of NaOH. For this sludge, the fraction of soluble to total COD was 38% as compared to 2% for the control. For all reactors digesting pre-treated sludge, the methane production was at least 19% greater than the control and at most 286% greater than control. The authors reported that pre-treatment with NaOH worsened the dewaterability of the digested WAS as it increased the capillary suction time by a factor of 4 to 11 as compared to the untreated digested WAS.

Tabaka et al. [21] compared the effect of chemical, thermal, and thermo-chemical pre-treatment on WAS. The sludge was mixed with different doses of NaOH in flasks and magnetically stirred for one hour. Increasing the dose of alkali from 0 to 0.6 g NaOH per g VSS improved the solubilization of the VSS linearly and reached a plateau at 15%

for greater alkali doses. On the other hand, methane production improved linearly with alkali dosage, reaching as high as 50% higher than the control at 1 g NaOH per g VSS.

2.1.5.2 Ozone Pre-treatment

Ozone is considered to be one of the strongest oxidizing agents, and has been found capable of solubilizing a significant portion of organics and converting part of the COD to carbon dioxide.

Weemaes et al. [22] investigated the effects of ozonation at doses of 0.05-0.2 g O₃ per g COD on mixture of primary and secondary sludge (ratio not specified). At a dose of 0.2 g O₃ per g COD the total COD was reduced from 7,900 to 4,900 mg/L, soluble COD increased from 60 to 2,300 mg/L, TSS decreased from 9,500 to 3,800 mg/L and VSS was reduced from 5,700 to 1,800 mg/L the authors had also reported a significant drop in pH, from 7.8 to 4.9.

Yeom et al. [88] studied a wide range of ozone doses, a 1.2 %TS sludge was ozonated at doses of 0.02 – 5 g O₃ per g TSS. The solubilization of the sludge particles improved from 0.8% for untreated sludge to 9.1%, 19.6%, 23.9% and 32.7% at doses of 0.02, 0.05, 0.1, and 0.2 g O₃ per g TSS, respectively, and decreased at higher doses, with the optimum dose of 0.2 g O₃ per g TSS, production of 165 mL CH₄ per g COD compared to 80 mL CH₄ per g COD for the control.

2.1.5.3 Mechanical Pre-treatment

The mechanical methods usually result in the rupture of the cell wall and the release of cell-bound substrate. The success of mechanical pre-treatment is typically

measured by comparing the soluble protein concentration before and after pre-treatment [84].

Choi et al. [18] applied 10, 30, and 50 bars pressure on WAS. The pressure of 50 bars achieved almost 90% VSS reduction. The mean particle size was found to be 69.1, 37, 21.6 and 18.7 μm for the untreated sludge, pre-treated with pressure of 10, 30, and 50 bars, respectively. The soluble COD increased by factors of 6.5 and 8 at pressures of 30 and 50 bars, respectively. The authors have also reported that both alkalinity and pH slightly increased as a result of pretreatment.

Nah [90] studied the effect of blending of raw sludge. Screened raw domestic sludge was blended for 5 minutes at 10,000 RPM with the temperature maintained between 25°C and 30°C by means of cold towels wrapped around the bowl of the blender. Their experiment showed a 10% increase in the colloidal soluble fraction. The comparative study of blending and sonication of primary sludge has been conducted by Koutsospyros [80]. Primary sludge samples of 250 mL were used to study the effect of both blending and sonication. Blending of the samples was performed by a Waring Blender and high speed homogenizer while an ultrasonic liquid processor was employed for sonication pre-treatment. Blending pretreatment time was 5 minutes, with ultrasonic pre-treatment time was of 5 minutes, 50% amplitudes, and 20 kHz frequency. pH was set to 5.5 for all samples. Solubilization is evident from the SCOD data. An increase of more than 1000 mg/L from (7979 to 6825 mg/L) in SCOD was observed in the sonicated samples, while the SCOD of blended samples was 200 mg/L (from 6825 to 7025 mg/L) higher than that of the untreated sample. It is apparent that total alkalinity, volatile acids and pH were not affected by the pre-treatment methods. On the other hand, excessive

foam production occurred during blending of the sample. These experiments probed that sonication is a superior method for solubilization to blending.

2.1.5.4 Ultrasound Pre-treatment

Ultrasound is a well-known method for the break-up of microbial cells to extract intracellular material [91]. When the ultrasound wave (>20 kHz) propagates in a medium such as sludge, it generates a repeated pattern of compressions and rarefactions in the medium. The rarefactions are regions of low pressure (excessively large negative pressure) in which liquid or slurry is torn apart. Micro-bubbles or cavitation bubbles are formed in the rarefaction regions. As the wave fronts propagate, micro-bubbles oscillate under the influence of positive pressure, thereby growing to an unstable size before they violently collapse. The collapsing of the bubbles often results in localized temperatures up to 5000 K and pressures up to 180 MPa [92, 93]. The sudden and violent collapse of huge numbers of micro-bubbles generates powerful hydro-mechanical shear forces in the bulk liquid surrounding the bubbles [94]. The collapsing bubbles disrupt adjacent bacterial cells by extreme shear forces, rupturing the cell wall and membranes. The localized high temperature and pressure could also assist in sludge disintegration. At high temperatures, lipids in the cytoplasmic membrane are decomposed, resulting in ruptures within the cell membrane, through which intracellular materials are released to the aqueous phase [91].

Ultrasound disintegration has been investigated at laboratory, pilot, and full-scale levels. Clear evidence exists of cell lysis [95] floc size reduction [92], increased volatile solids reduction [95, 96], and increased biogas production [95, 96, 97]. Batch and semi-

continuous digestion tests show that ultrasonically treated waste activated sludge produces more biogas, degrading more volatile solids with respect to untreated sludge, but the gain depends on the feed/inoculum ratio as well as on the organic loading rate [38]. A remarkable improvement of the biocatalysis of the hydrolytic reactions can be achieved with quite low ultrasound energy input [38, 98].

Tiehm et al. [17] observed an increase in SCOD concentration from 630 to 2,270 mg/L when a mixture of primary and waste activated sludge were irradiated for 64 seconds at a frequency of 31 kHz. This treatment also resulted in an increase of sludge temperature from 15 to nearly 45°C. The particle size distribution of the sludge with and without pre-treatment was also compared using laser light scanning. The median particle size of the untreated sludge was 165 µm and decreased to 135 and 85 µm after 29.5 and 96 seconds of sonication, respectively. Five 150 L semi-continuous anaerobic digesters were operated at HRTs of 22, 16, 12 and 8 days. In addition, a control reactor was run with a HRT of 22 days. On average, the control reactor achieved a 45.8% reduction in VS whereas the reactor digesting pretreated sludge at a HRT of 22 days removed 50.3% of the VS. The reactors operating at HRTs of 16 and 12 days removed more VS than the control reactor but the reactor operated with a HRT of 8 days could only destroy 44.3% of the VS. This showed that the pre-treatment of sludge with ultrasound could be used to reduce the size of anaerobic digesters and/or to increase the removal of VS.

Wang et al. [99], in their experimental work on the pre-treatment of WAS using ultrasound showed an increase in SCOD from 20 mg/L to 1,050 mg/L after 40 minutes of exposure to ultrasound at a frequency of 9 kHz. Digestion of a 3:1 ratio of seed sludge to pretreated WAS at 36°C yielded 350 mL methane per g VS whereas digestion of the

same ratio of seed sludge to untreated WAS only produced 205 mL methane per g VS. The concentration of VFAs in the reactor containing pretreated WAS increased sharply at the beginning of digestion to a value of 1,700 mg/L and then decreased linearly until completion of the batch test. The VFA profile in the reactor containing the control was similar but only peaked to a value of 1,100 mg/L a linear relationship with an R^2 of 0.994 was observed between cumulative methane generation (mL methane per g VS added) and solubilization ratio.

A wide range of ultrasound frequencies was explored by Tiehm et al. [101] Waste activated sludge (WAS) was sonicated at frequencies of 41, 207, 360, 616, 1068 and 3217 kHz for four hours by the use of an ultrasound reactor equipped with disk transducers. Both the lowest median particle size (17 μm) and highest degree of COD solubilization (81%) were reached at the lowest frequency tested. The degree of solubilization was defined as the increase in SCOD due to ultrasound pre-treatment divided by the increase in SCOD due to exposure to 0.5 mol/L NaOH for 22 hours. The next phase of the study involved the AD of sonicated WAS at a frequency of 41 kHz for 7.5, 30, 60 and 150 minutes. The digestion was carried out semi-continuously at an SRT of eight days at 37°C in 1 L reactors. The sludge sample sonicated for only 7.5 minutes did not show an increase in SCOD and actually produced less biogas than the control. However, the reactor holding this sample was characterized by a higher oxygen utilization rate and greater VS reduction. The exposure time that yielded the highest biogas production and VS degradation was 150 minutes. Despite this, after digestion, the supernatant of the sample sonicated for 150 minutes contained the highest soluble COD and ammonia concentrations. Thereafter, WAS samples were sonicated for 60 minutes at

frequencies of 41, 207, 360 and 1068 kHz. Once again, the best results were obtained at a frequency of 41 kHz as quantified by the degree of COD solubilization and VS removal during AD. A linear relationship could be fit to relate percent VS removal to the degree of COD solubilization with an R^2 of 0.94.

COD solubilization and oxidation-reduction potential (ORP) in WAS were monitored during ultrasonication and alkali addition by Chiu et al. [100]. Three pre-treatment schemes were tested on WAS: (1) exposure to sodium hydroxide for 24 hours in 1 L plastic bottles at room temperature at a dose of 40 meq/L. (2) some exposure to NaOH followed by 20-kHz sonication for 24 seconds per mL and (3) concurrent exposure to NaOH and sonication (14.4 seconds per mL) for 24 hours. The third scenario led to the fastest initial hydrolysis rate: 211.9 mg COD/L/min. The second and third schemes both yielded a SCOD of approximately 10,500 mg/L compared to only 4,880 mg/L for the first scenario. The ORP curve during the three pre-treatment scenarios behaved similarly during the first two hours. Indeed, the sharp decreases in ORP observed during this period accompanied by simultaneous increases in SCOD indicate that hydrolysis took place during the first two hours. The concentrations of VFA were also monitored during this experiment and the WAS pretreated simultaneously with NaOH and ultrasound yielded a TVFA/TCOD ratio of 84% after 21 hours compared with 10% for untreated sludge.

Wang et al. [95] examined the release in SCOD concentration at three different sonication times of 5, 15 and 20 min at TS content of 3%, frequency of 20 KHz, and ultrasonic density of 0.768 W/mL. The authors observed an increase in SCOD release from 2,581 to 7,509 mg/L, when the sonication time was increased from 5 to 15 min.

However, when the ultrasonic disintegration was continued for 20 min, the SCOD release slowed down significantly with final SCOD concentration of 8,912 mg/L.

Khanal et al. [10] studied the release of ammonia-N at different total solids (TS) contents and specific energy inputs (kJ/gTS) during ultrasonic disintegration of WAS. The results showed that the release of ammonia-N concentration increased with increase in specific energy inputs and TS contents. The ammonia-N concentration reached a fairly constant level at specific energy inputs of 20 kWs/gTS for 2.0%, 2.5%, and 3% TS contents, and 10 kWs/gTS for 1.5% TS content. The authors also investigated the effect of TS content and energy input on SCOD release, the study showed an increasing trend with increase in both TS and energy input.

Moonkhum [102] used ultrasonic to treat waste activated sludge for two anaerobic lab scale reactors, 'part stream' (50% sonicated and 50% nonsonicated) and 'full stream' (100% sonicated) reactors in addition to one control reactor, with 3% TS and 2 different SRT of 10 and 20 days. WAS samples were sonicated for 2.5 minutes with ultrasonic density of 1.9 W/mL, at sonication frequency of 20 kHz. Moonkhum reported that dissolved organic carbon (DOC) removal efficiency of the part stream and full stream reactor improved by 26% and 28% respectively, at 10 days SRT compared to the control reactor. Similarly, at 20 days SRT the efficiency of DOC removal of part stream and full stream reactor were enhanced by 20% and 23% respectively, compared to the control reactor.

Bunrith et al. [103] investigated ultrasonic disintegration of WAS sludge at frequency of 20 kHz using sonication times of 5, 10, 30, and 60 min, chemical (NaOH 10, 25, 50 and 75 mg NaOH/g TS) and the combination of chemical-ultrasonic pre-

treatment techniques. Results revealed that chemical–ultrasonic gave a better efficiency of sludge disintegration compared to individual chemical and ultrasonic techniques. The optimum condition of chemical-ultrasonic was found at 10 mg NaOH/g TS dose and 3.8 kJ/g TS specific energy input, whereas chemical dose of 50 mg NaOH/g TS and specific energy of 3.8 kJ/g TS were the optimum operating condition of individual chemical and ultrasonic pre-treatment, respectively.

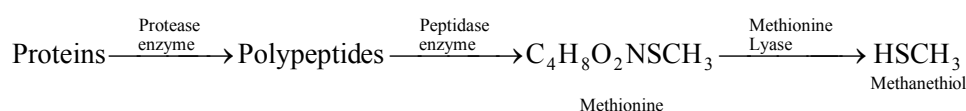
In summary, several studies performed on WAS have confirmed that the highest SCOD release and particle size reduction are the major goals of ultrasonic pretreatment. Khanal et al. [10] obtained SCOD of 16.2% at an energy input of 66,800 kJ/kgTS; whereas Bougrier et al. [17] achieved as much as twice that at an energy input of only 6,951 kJ/kg TS. In another study, SCOD of 40% was obtained at a specific energy input of 60,000 kJ/kg TS [96]; whereas Rai et al. [104] reported SCOD of 25% at energy input of 64,000 kJ/kg TS. Such variations might be attributed to the energy transfer efficiencies of ultrasonic equipment. Although many pre-treatment studies have been conducted to improve the digestion process, none of those studies presented detail cost analyses required for large scale application of these processes.

2.1.5.5 Odor Precursors

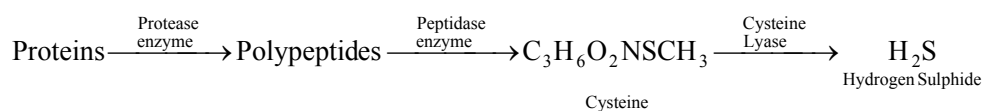
Study of odor production from anaerobically digested biosolids was inadequate until relatively recently [105]. Although H₂S is considered to be the most prevalent odor compound, there are typically other organic odorous compounds, such as mercaptans and amines, present in anaerobically digested sludges. Prior research has implicated volatile sulfur compounds (VSCs) including hydrogen sulfide (H₂S), methanethiol or methyl

mercaptan (MT), dimethyl sulfide (DMS), dimethyl disulfide (DMDS) and dimethyl trisulfide (DMTS) in odors from biosolids [106]. In addition to VSCs, ammonia, and volatile fatty acids (VFA), phenols are also implicated as possible odor causing compounds in the excretion of pigs [107].

Laboratory tests have indicated that protein degradation and, especially the degradation of methionine, an amino acid, is the main source for the production of VSCs [106]. Proteins are hydrolysed by extracellular enzymes (proteases) into their constituent polypeptides and amino acids. The pathway for the production of MT from methionine is described as [106]:



Hydrogen sulfide (H₂S) can be formed from the degradation of cysteine, sulfur containing amino acid, as shown below:



While the carbohydrate, lipid, and protein content of municipal biosolids often accounts for the majority (90%) of the organic load [8], in some industries, protein is the predominant part of the organic load. For example, the protein component of a dairy wastewater stream can account for more than 40%-60% of the total chemical oxygen demand [108]. Although the presence of proteins has been confirmed in the organic matter of treated municipal waste water and sludge [110], literature on protein degradation during anaerobic digestion is both sparse and contradictory.

In a pioneering work, Breure et al. [110] studied degradation of a model protein, gelatin, in controlled anaerobic digestion, and observed that it was converted at high rates and to a substantial extent to volatile fatty acids. Since, proteins, carbohydrates and lipid are almost always present simultaneously in biosolids, complete degradation of protein in the presence of carbohydrates may not be achieved as glucose and other easily fermentable substrates can repress the synthesis of exoproteases (a necessary enzyme) in pure cultures of bacteria [110], and the degradation of gelatin was retarded by increasing concentrations of carbohydrates present in the feed as a second substrate. In contrast, in a controlled study it was found that as much as 70% of the protein was broken down in the acidogenic reactor and inclusion of protein had no effect on the reaction pathway for lactose degradation [110]. Proteins in wastewater and sludge are generally divided into three fractions: soluble, bound/labile (loosely attached with the cells) and tightly bound fractions (within the bacterial cells) [161]. Labile proteins are thought to become readily bioavailable during dewatering giving rise to higher odor potential.

Morales et al. [111] reported the use of green fluorescent protein (GFP) as a probe protein to investigate the performance of proteins in wastewater sludge. They tested the suitability of the approach by monitoring GFP added to aerobic and anaerobic sludges. Under anaerobic conditions at 35°C, fluorescence signal due to GFP was reduced by 90% after only 6 h.

Lu et al. [112] suggested that the metabolic pathways to producing various acidogenic metabolites were inhibited differently by ammonia, resulting in different schemes of products distribution. For example, carbohydrate degradation efficiency was decreased to < 20% with increasing ammonia nitrogen loading rate; acidogenic bacteria

with an ability to utilize both carbohydrates and proteins grew by mainly utilizing proteins under the toxic ammonia concentration [113].

Higgins et al. [105] evaluated the role of proteins, amino acids, and enzyme activity on odor production from anaerobic digestion. their hypothesis on the concentration of bioavailable protein in different samples that would be related to the amount of odor-causing chemicals that are produced during the storage of biosolids. Also protein-degrading enzyme activity would be an indicator of VSC production, because these enzymes degrade protein to produce amino acids, which can be degraded to form VSCs. A large, collaborative research project was undertaken, supported by the Water Environment Research Foundation (Alexandria, Virginia) (WERF) and by 11 utilities across the United States and 1 utility in Canada. The study objectives of this research were, in part, to: (1) Determine the compounds produced by biosolids and their relationship to odors; (2) Determine the timeline for production of odorous compounds during storage; (3) Examine differences in odor constituents and odor-production profiles from different plants; (4) Determine the role of biochemical constituents, proteins, amino acids, and enzyme activity on the production of odorous compounds and the factors that affect the bioavailability and activity of these constituents and subsequent odorous compounds production; (5) Determine the effect of digestion parameters, such as temperature, solids retention time (SRT), volatile solids destruction, and residual biological activity, on odor production; (6) Determine the effect of upstream parameters, such as influent concentrations of different constituents, primary and secondary sludge storage time, fraction of primary sludge added to the digestion, and activated sludge SRT on subsequent odor production; and (7) Determine the role of dewatering equipment and

cake conveyance systems on odor production. These results showed that: (1) Protein concentration and, more specifically, the concentration of the sulfur-containing amino acid, methionine, were well correlated with the production of odorous VSCs; (2) Protein and amino acid content varied considerably for the 11 different plants; (3) Protein-degrading enzyme activity did not correlate well with the production of odorous VSCs; (4) The concentration of iron in the biosolids was negatively correlated with the extractable bound protein, meaning that more iron in the biosolids resulted in decreased extractable bound protein. As a result, iron addition could be a method to reduce odor production from biosolids.

These results suggest that odor control strategies could be aimed at reducing the amounts of bioavailable protein in the cake. Therefore, more complete degradation of protein during digestion would reduce the available substrate for odor production. For example, larger SRTs and pre-digestion enhancements, which aim to increase the digestibility of the solids, may aid in removing protein. Research is needed to explore these alternatives and their effect on odors from the final product.

2.2 Summary and Conclusions

In the earlier sections we have discussed the current AD modeling, illustrating the key areas, substrate pathways and structure of those models. The information available for anaerobic microorganisms degrading complex substrates as sewage sludge has large gaps regarding reliable kinetic and stoichiometric parameters required for accurate modeling [96]. More research efforts have to be made to achieve an accurate characterization of the substrate, at least in terms of the main components (carbohydrates,

proteins, and lipids) and not only in terms of “gross parameters” such as COD and VSS. For each component, specific parameters need to be determined with experiments reproducing the real system as far as possible. Moreover, information obtained from pure culture studies need to be supplemented with in situ characterization data directly evaluated in the mixed culture operating in the plants. At the same time, a more accurate monitoring and control of full-scale plants could provide valuable information of use in updating model parameters. This would help increase process knowledge and, at the same time, ensure greater process efficiency and stability.

Anaerobic hydrolysis is well documented to be a function of specific surface area among other variables [26]. Studies on the effect of particle size on hydrolysis and its mathematical relationship are sparse, as most of the studies reported the hydrolysis rate coefficient as a single value and not a function of particle size. Studies that address the effect of particle size distribution (full spectra distribution) on the hydrolysis rate coefficient are needed. Another key point in the biological sludge digestion process is the need to increase particulate hydrolysis kinetics, which represents the limiting step in the whole reaction chain. This may be done by pre-treating the influent stream in a thermal, ultrasonic, and/or chemical stage. (Ultrasonic pre-treatment is being widely investigated with promising results.) Nevertheless, the mechanisms of ultrasound disintegration/digestion are not fully understood, in spite of claimed reduction of digestion time and improvement of digestion efficiency by ultrasonic pre-treatment. Therefore, further investigations need to be carried out in this area, especially as far as the hydrolysis step is concerned. Accurate anaerobic hydrolysis modeling could prove

useful both for a reliable simulation of particulate matter degradation and for the design of anaerobic digesters.

In most of the above research reported degradation of total protein in controlled conditions was studied. However, proteins are usually divided into three types (total protein, bound protein, and soluble protein) [65]. The total protein is considered as the tightly bound fraction from flocs and is a of bacterial cell mass, the bound protein is the labile fraction loosely attached with solids, and the soluble protein is soluble fraction in the solution. No study has been found on degradation of these various fractions in conventional anaerobic sludge digesters, similarly systematic study of degradation of other odorous compounds such as volatile fatty acids is not available in literature.

2.3 References

- [1] Chynoweth, D.; Pullammanappallil, P. Anaerobic digestion of municipal solid waste in microbiology of solid waste. CRC Press, Boca Raton, FL. 1996, 71-113.
- [2] Henze, M. H.; Jonsen, J. C.; Arven E. Waste Water Treatment. Springer-Verlog, Berlin, Germany. 1997.
- [3] Chynoweth, D.; Owens, J. M. Anaerobic processing of piggery wastes: A review. Paper presented at the ASAE Meeting, Orlando, FL. 1998.
- [4] Lesisinger, T. Genetic and Molecular Biology of Anaerobic Bacteria. Springer-Verlog, B New York, NY. 1993, 1-12.
- [5] Ecke, H. L. Anaerobic digestion of putrescible refuse. Luella University of Technology, Luella, Sweden, 2001
- [6] Zinder, S. H. Methanogenesis. Encyclopedia of Microbiology. 1992, 3, 81-96.
- [7] Miyamoto, K. Renewable Biological Systems for Alternative Sustainable Energy Production. Food and Agriculture Organization of the UN. 1997, 128.
- [8] Batstone, D. J.; Keller, J.; Angelidaki, I.; Kalyuzhnyi, S. V.; Pavlostathis, S. G.; Rozzi, A.; Sanders, W. T. M.; Siegrist, H.; Vavilin, V. A. Anaerobic Digestion Model No. 1, IWA Task Group for Mathematical Modelling of Anaerobic Digestion Processes, Water Sci. Technol. 2002, 40, 65–73.
- [9] Siegrist, H.; Gujer, W. Mathematical modeling of anaerobic mesophilic sewage sludge treatment. Water Sci. Technol. 1993, 27, 25-36.

- [10] Khanal, S. K.; Grewell, D.; Sung, S.; Leeuwen, J.V. Ultrasound Applications in Wastewater Sludge Pretreatment: A Review, *Critical Reviews in Environmental Science and Technology*. 2007, 37, 277–313.
- [11] Marek, M, and Hans, J. Comparison of different models of substrate and product inhabitation in anaerobic digestion. *Water Research* .1999, 33, 2545-2554.
- [12] Lokshina, L. Kinetic Analysis of the key stages of low temperature methanogenesis. *Ecological Modeling*. 1999, 117, 285-303.
- [13] Masse, D. I.; Droste, R.L.; Comprehensive model of anaerobic digestion of swine manure slurry in a sequencing batch reactor. *Water Research*. 2000, 34, 3087-3106,
- [14] Alex, J. O. Modeling of Anaerobic Digestion as an Integral Part of the WWTP-first Experiences. *San Sebastian, Spine*. 2001, 624: p. 22-23.
- [15] Kalyuzhnyi S.; Veeken A.; Hamelers B. Two-particle model of anaerobic solid state fermentation. *Water Sci. Technol*. 2001, 41, 43-50.
- [16] Vavilin, V.A.; Rytov, S. V.; Lokshina, L. Y.; Rintala, J. A.; Lyberatos, G.. Simplified hydrolysis models for the optimal design of two-stage anaerobic digestion. *Water Research*, 2001, 35, 4247-4251.
- [17] Tiehm, A.; Nickel, K.; Neis, U. The use of ultrasound to accelerate the anaerobic digestion of sewage sludge. *Water Sci. Technol* 1997, 36, 121–128.
- [18] Bougrier, C.; Carrere, H.; Delgenes, J.P.; Solubilization of waste-activated sludge by ultrasonic treatment, *Chem. Eng. Journal*. 2005, 106, 163-169.

- [19] Choi, H. B.; Hwang, K. Y.; Shin, E. B. Effects on anaerobic digestion of sewage sludge pre-treatment. *Water Sci. Technol.* 1997, 35, 207-211.
- [20] Lin J.G. and Chang C.N. Fenton process for treatment of desizing wastewater, *Water Research.* 1999, 31, 2050–2056.
- [21] Yasui, H.; Nakamura, K.; Sakuma, S.; Iwasaki, M.; Sakai, Y. A full scale operation of a novel activated sludge process without excess sludge production. *Water Sci. Technol.* 1996, 34, 395-40.
- [22] Tanaka, S. Effects of thermochemical pre-treatment on the anaerobic digestion of waste activated sludge. *Water Sci. Technol.* 1997, 35, 209-215.
- [23] Weemaes, M.; Grootaerd, H.; Simoens, F.; Verstraete, W. Anaerobic digestion of ozonized biosolids, *Water Research* 2000, 34, 2330-2336.
- [24] Andrews, J. Dynamic Modeling and Simulation of the Anaerobic Digestion Process. *Anaerobic Biological Treatment Processes* 1971, 104.
- [25] Hill, D.T. and Barth, C.L. A dynamic model for simulation of animal waste digestion. *Journal WPCF*, 1977, 10, 2129-2143.
- [26] Eastman, J.A. and Ferguson, J.F. Solubilization of particulate organic carbon during the acid phase of anaerobic digestion. *Journal WPCF*, 1981, 53, 352–366.
- [27] Mosey, F. E. Mathematical Modeling of the Anaerobic Digestion Process: Regulatory Mechanisms for the formation of Short-Chain Volatile Acids from Glucose. *Water Sci. Technol.* 1983, 15, 209-232.

- [28] Rozzi, A.; Merlini, S.; Passino, R. Development of a four population model of the anaerobic degradation of carbohydrates. *Environmental Technology Letters*. 1985, 6, 610-619.
- [29] Bryers, J. D. Structured modeling of the anaerobic digestion of biomass particulates. *Biotechnology and Bioengineering*. 1985, 27, 638-649.
- [30] Pavlostathis, S.G.. and Gossett, J.M. A kinetic model for anaerobic digestion of biological sludge. *Biotechnol. Bioeng.* 1986, 28, 1519–1530.
- [31] Shimizu, T.; Kudo, K.; and Nasu, Y. Anaerobic waste-activated sludge digestion-a bioconversion mechanism and kinetic model. *Biotechnol. Bioeng.* 1993, 41, 1082–1091.
- [32] Angelidaki, I.; Ellegaard, L.; and Ahring, B.K. A comprehensive model of anaerobic bioconversion of complex substrates to biogas. *Biotech. Bioeng.*, 1999, 63(3), 363–372.
- [33] Noike, T.; Endo, G.; Chang, J.; and Matsumoto, J. Characteristics of carbohydrate degradation and the rate-limiting step in anaerobic digestion. *Biotechnol. Bioeng.* 1985, 27, 1482–1489.
- [34] Pavlostathis, S.G.; Miller, T.L.; Wolin, M.J. Kinetics of insoluble cellulose by continuous cultures of *Ruminococcus albus*. *Appl. Environ. Microbiol.* 1988, 54, 2600–2663.
- [35] Siegrist, H.; Gujer, W. Mathematical model for mesophilic thermophilic anaerobic sewage sludge digestion. *Environmental Science and Technology*. 2002, 36, 1113-1123.

- [36] Gujer, W. and Zehnder, A. J. B. Conversion processes in anaerobic digestion. *Water Sci. Technol.* 1983, 15, 127–167.
- [37] Yasui, H.; Sugimoto, M.; Komatsu, K.; Goel, R.; Li, Y.Y.; Noike, T. An approach for substrate mapping between ASM and ADM1 for sludge digestion. In: *Proc. First International Workshop on the IWA Anaerobic Digestion Model No.1.* Lyngby, Denmark, 2-4 September, 2006, 73–80.
- [38] Tomei, M.C.; Braguglia, C.M.; Mininni, G. Anaerobic degradation kinetics of particulate organic matter in untreated and sonicated sewage sludge: Role of the inoculum. *Biores. Technol.* 2007, 99, 6119–6126.
- [39] Gossett, J.M.; and Belser, R.L. Anaerobic digestion of waste activated sludge. *J. Environmental Eng. Division*, 1982, 1101–1120.
- [40] Pavlostathis, S. G. ; Giraldo-Gomez, E. Kinetics of anaerobic treatment: a critical review. *Critical Reviews in Environmental Control.* 1991, 21, 411-490.
- [41] Morgenroth, E.; Kommedal, R.; Harremoës, P. Processes and modeling of hydrolysis of particulate organic matter in aerobic wastewater treatment – a review, *Water Sci. Technol.*, 2002, 6, 45, 25–40
- [42] Valentini, A.; Garruti, G.; Rozzi, A.; Tilche, A. Anaerobic degradation kinetics of particulate organic matter: a new approach, *Water Sci. Technol.*, 1997, 36, 239–246.
- [43] Hobson, P.N., Wheatley, A., 1992. *Anaerobic Digestion: Modern Theory and Practice.* Elsevier, Amsterdam, The Netherlands, 1992.

- [44] Hashimoto, A.G.; Chen, Y.R.; Verel, V.H. Theoretical aspects of methane roduction: State of the art. In: Livestock waste: A renewable resources. Proceedings of the fourth international symposium of livestock wastes. Transaction of ASAE, USA, 1981, 86–91
- [45] Vavilin, V.A.; Rytov, S.V.; Lokshina, L.Y. A description of hydrolysis kinetics in anaerobic degradation of particulate organic matter. *Bioresource Technol.*, 1996, 56, 229–237.
- [46] Cecchi, F., Mata-Alvarez, J., Traverso, P. G., Medici, F., Fazzini, G. A, New Approach to the Kinetic Study of Anaerobic Degradation of the Organic Fraction of Municipal Solid Waste. *Biomass*. 1990, 23, 79-102
- [47] Negri, E. D.; Mata-Alvarez, J.; Sans, C.; Cecchi, F. A mathematical model of volatile fatty acids (VFA) production in a plug flow reactors treating the organic fraction of municipal solid waste (MSW). *Water Sci. Technol.* 1993, 27, 201-208.
- [48] Sanders, W.T.M.; Geerink, M.; Zeeman, G.; Lettinga, G. Anaerobic hydrolysis kinetics of particulate substrates. *Water Sci. Technol.*, 2000, 41, 17–24.
- [49] Goel, R.; Mino, T.; Satoh, H.; Matsuo, T. Comparison of Hydrolytic Enzyme Systems in Pure Culture and Activated Sludge under Different Electron Acceptor Conditions, *Water Sci. Technol.* 1988, 37, 335.
- [50] Myint, M. and Nirmalakhandan, N. Evaluation of first-order, second-order, and surface-limiting reactions in anaerobic hydrolysis of cattle manure, *Environ. Eng. Sci.* 2006, 23, 966–976.

- [51] Yu, H.Q.; Fang, H. Acidogenesis of gelatine-rich wastewater in an upflow anaerobic reactor: influence of pH and temperature. *Water Research*. 2003, 37, 55–66.
- [52] Oh, S.; Ginkel, S.V.; Logan, B.E. The relative effectiveness of pH control and heat treatment for enhancing biohydrogen gas production. *Environ. Sci. Technol.* 2003, 37, 5186–5190.
- [53] Lu, F.; He, P-J.; Shao, L.; Lee, D. Effects of ammonia on hydrolysis of proteins and lipids from fish residues *Appl Microbiol Biotechnol*, 2007, 75, 1201–1208
- [54] Vavilin, V.A.; Fernandez, B.; Palatsi, J.; Flotats, X. Hydrolysis kinetics in anaerobic degradation of particulate organic material: An overview *Waste Management* 2008, 28, 939–951
- [55] Mahmoud, N.; Zeeman, G.; Gijzen, H.; Lettinga, G.. Anaerobic stabilization and conversion of biopolymers in primary sludge-effect of temperature and sludge retention time. *Water Research*. 2004, 38, 983-991.
- [56] [] O'Rourke, J.R.. Kinetics of anaerobic treatment at reduced temperatures. Ph.D. Thesis, Stanford University, Stanford, CA, USA, 1968..
- [57] Christ, O., Wilderer, P.A., Angerhofer, R., Faulstich, M.,. Mathematical modelling of the hydrolysis of anaerobic processes. *Water Sci. Technol.* 2000, 41, 61–65.
- [58] Garcia-Heras, J.L. Reactor sizing, process kinetics and modelling of anaerobic digestion of complex wastes. In: Mata-Alvarez, J. (Ed.), *Biomethanization of the Organic Fraction of Municipal Solid Wastes*. IWA Publishing, TJ International Ltd., Padstow, Cornwall, UK, 2003, 21–62.

- [59] Flotats, X., Palatsi, J., Ahring, B.K., Angelidaki, I.,. Identifiability study of the proteins degradation model, based on ADM1, using simultaneous batch experiments. *Water Sci. Technol.* 2006, 54 (4), 31– 39.
- [60] Sanders, W.M.T.; Veeken, A.H.M.; Zeeman, G.; van Lier, J.B. Analysis and optimisation of the anaerobic digestion of the organic fraction of municipal solid waste. In: Mata-Alvarez, J. (Ed.), *Biomethanization of the Organic Fraction of Municipal Solid Wastes*. IWA Publishing Press, Cornwall, UK, 2003, 67–89.
- [61] Noykova, N. ; Muller, T. G.; Gylleberg, M.; Timmer, J. Quantitative analysis of anaerobic treatment processes: Identifiability and parameter estimation. *Biotechnology and Bioengineering*, 2002, 78, 89-102.
- [62] Contois, D. E. Kinetics of bacterial growth: relationship between population density and specific growth rate of continuous cultures. *Journal of General Microbiology*, 1959, 21, 40-50.
- [63] Hashimoto, A. G.; Chen, Y. R.; Varel, V. H. Anaerobic fermentation of beef cattle manure: final report. Roman L. Hruska U.S. Meat Animal Research Center, U.S. Department of Agriculture Clay Center. Nebraska. 1981.
- [64] Ray, B. T.; Huang, J. C.; Dempsey, B. A. Sludge digestion by anaerobic fluidized beds: kinetic model. *Journal of Environmental Engineering*. 1989, 115, 1156-1170.
- [66] Hills, D.J., Nakano, K., Effects of particle size on anaerobic digestion of tomato solid wastes. *Agr. Wastes*. 1984, 10, 285–295.

- [66] Sharma, S.K., Mishra, I.M., Sharma, M.P., Saini, J.S. Effect of particle size on biogas generation from biomass residues. *Biomass*. 1988, 17, 251–263.
- [67] Vavilin, V.A.; Rytow, S.V.; Lokshina, L.Y. Modelling hydrogen partial pressure change as a result of competition between the butyric and propionic groups of acidogenic bacteria. *Bioresour. Technol*, 1995, 54, 171–177.
- [68] Saravanane, R.; Murthy, D. V. S.; Krishnaiah, K. Anaerobic fluidized Bed degradation and the development of a kinetic model for a particulate organic matter enriched wastewater sludge *Water, Air, & Soil Pollution*. 2001, 127, 15-30.
- [69] Dimock, R.; Morgenroth, E. The influence of particle size on microbial hydrolysis of protein particles in activated sludge. *Water Research*. 2006, 40, 2064-2074.
- [70] Tchobanoglous, G., Burton, F.L., Stensel, H.D. *Wastewater Engineering, Treatment and Reuse*, 4th Edition. McGraw-Hill, Inc. New York. 2003.
- [71] Munch, R.; Hwang, C.P.; Lackie, T. H. Wastewater fractions add to total treatment picture. *Water Swage Wks*. 1980, 127, 49–54.
- [72] Levine, A. D. ; Tchobanoglous, G. ; Asano, T. Size distributions of particulate contaminants in wastewater and their impact on treatability. *Water Research*. 1991, 25, 911-922.
- [73] Painter H. A. and Viney M. Composition of a domestic sewage. *J. Biochem, microbiol. Technol*. 1959, 1, 143-162.
- [74] Walter L. (1961b) Composition of sewage and sewage effluents--Part 2. *Water Swage Wks* 108, 478-481.

- [75] Levine, A.D.; Tchobanoglous, G.; Asano, T. (1985). Characterization of the size distribution of contaminants in wastewater: treatment and reuse implications. *J. Wat. Pollut. Control Fed.* 1985, 57, 805–816.
- [76] Ferenci, T.. The recognition of maltodextrins by *E. coli*. *Eur. J. Biochem.* 1980,108, 631–636.
- [77] Rudolf, W.; Balmat, J. L. Colloids in sewage: separation of sewage colloids with the acid of the electron microscope. *Sewage and Ind. Wastes*, 1952, 24, 247.
- [78] Karr, P. B.; Keinath, T. M. Influence of particle size on sludge dewaterability. 1965, 50, 1911.
- [79] Futakawa, M.; Takahashi, H.; Inoue, G.; Fujioka, T. A review of industrial catalytic wet air oxidation processes. *Proc. IDA/WRPC World Conf. Desalin, Water Treat.* Yokohama. 1993, 1, 231.
- [80] Koutsospyros, A. Effect of Particle Size Reduction on Anaerobic Sludge Digestion. Ph.D thesis, Polytechnic Univ., Brooklyn, NY. 1990.
- [81] Andara, R.; Lomas, J.M. Transition of particle size fractions in anaerobic digestion of the solid fraction of piggery manure. *Biomass and Bioenergy.* 2002, 23, 229 – 235
- [82] Hu, Z.; Yu, H.; Zhu, R. Influence of particle size and pH on anaerobic degradation of cellulose by ruminal microbes. *International Biodeterioration & Biodegradation.* 2005, 55, 233–238

- [83] Gea, T.; Barrena, R.; Artola, A.; Sa'nchez, A. Optimal bulking agent particle size and usage for heat retention and disinfection in domestic wastewater sludge composting. *Waste Management*. 2007, 27, 1108–1116
- [84] Mshandete, A.; Bjornsson, L.; Kivaisia, A. K.; Rubindamayugi, M.S.T.; Mattiasson, B. Effect of particle size on biogas yield from sisal fibre waste. *Renewable Energy*. 2006, 31, 2385–2392.
- [85] Muller, J.; Winter, A.; Strunkmann, G.. Investigation and assessment of sludge pre-treatment processes. *Water Sci. Technol* 2004, 49, 97-104.
- [86] Lin, C.; Chen, C. Effect of Heavy Metals on the Methanogenic Granule. *Water Research*. 1999, 33, 409-416.
- [87] Woodard S. E. and Wukasz R. F. A hydrolysis/thickening/filtration process for the treatment of waste activated sludge, *Water Sci. Technol*. 1994, 30, 29-38.
- [88] Yeom, I. T. Effects of ozone treatment on the biodegradability of sludge from municipal wastewater treatment plants. *Water Sci. Technol*. 2002, 46, 421-425.
- [89] Hwang, K. Y.; Shin, E. B.; Choi H. B. A mechanical pre-treatment of waste activated sludge for improvement of anaerobic digestion system. *Water Sci. Technol*. 1997, 36, 111-116.
- [90] Nah, I. W. Mechanical pre-treatment of waste activated sludge for anaerobic digestion process. *Water Research*. 2000, 34, 2362-2368.

- [91] Harmand, J. M.; Pons, N.; Dagot, C. Evaluation of multiple modeling approaches for anaerobic digestion processes. *Optimal Management of Wastewater Systems*. 2001, 13-14.
- [92] Flint, E.B. and Suslick, K.S. The temperature of cavitation, *Water Science* 1991, 253, 1397–1399.
- [93] Suslick, K. Sonochemistry. The temperature of cavitations. *Science*. 1991, 253, 1397–1399.
- [94] Kuttruff, H. *Ultrasonics Fundamentals and Applications*. Essex, England. 1991.
- [95] Wang, F.; Shan, L.; Ji, M. Components of released liquid from ultrasonic waste activated sludge disintegration, *Ultrason. Sonochem.* 2006, 13, 334–338.
- [96] Jeffrey, P.; Brown, P.; Hogan, F. *Ultrasonic Solids Treatment Yields Better Digestion.. WERF, Biosolids Technical Bulletin*. 2003
- [97] Gronroos, A.; Kyllonen, H.; Korpijarvi, K.; Pirkonen, P.; Paavola, T.; Jokela, J.; Rintala, J. Ultrasound assisted method to increase soluble chemical oxygen demand (SCOD) of sewage sludge for digestion, *Ultrason. Sonochem.* 2005, 12, 115–120.
- [98] Yin, X.; Han P.; Lu X.; Wang Y. A review on the dewaterability of bio-sludge and ultrasound pretreatment, *Ultrason. Sonochem.* 2004, 11, 337-348.
- [99] Wang, Q.; Kuninobu, M.; Kakimoto, K.; Ogawa, H., Kata, Y. Upgrading of anaerobic digestion of waste activated sludge by ultrasonic pretreatment. *Bioresource Thecnology*. 1999, 68, 309-313.

- [100] Chiu, Y. ; Chang, C. ; Lin, J. ; Huang, S. Alkaline and ultrasonic pretreatment of sludge before anaerobic digestion. *Water Sci. Technol.* 1997, 36, 62-155.
- [101] Tiehm, A.; Nickel, K.; Zellhorn, M.M.; and Neis U. Ultrasound waste activated sludge disintegration for improving anaerobic stabilization, *Water Research.* 2001, 35, 2003–2009.
- [102] Moonkhum, M. Aerobic Digestion of Waste Activated Sludge With Ultrasonic Pretreatment. Master of Science in Environmental Engineering and Management Thesis. Prince of Songkla University., Surat Thani, Thailan, 2007
- [103] Bunrith, S. Anaerobic Digestibility of Ultrasound And Chemically Pretreated Waste Activated Sludge. Master of Science in Environmental Engineering and Management Thesis. Asian Institute of Technology School of Environment, Resources and Development, Thailand. 2008
- [104] Rai, C.; Struenkmann, G.; Mueller, J.; Rao, P. Influence of Ultrasonic Disintegration on Sludge Growth Reduction and Its Estimation by Respirometry. *Environ. Sci. Technol.*, 2004, 38 , 5779–5785
- [105] Higgins, M.; Adams, G.; Chen, Y.; Erdal, Z.; Forbes, R.; Glindemann, D.; Hargreaves, J. McEwen, D.; Murthy, S.; Novak, J.; Witherspoon, J. Role of Protein, Amino Acids, and Enzyme Activity on Odor Production from Anaerobically Digested and Dewatered Biosolids, *Wat. Environ. Res.*, 2008, 80, 127.
- [106] Higgins, M.; Adams, G.; Chen, Y.; Erdal, Z.; Forbes, R.; Glindemann, D.; Hargreaves, J. McEwen, D.; Murthy, S.; Novak, J.; Witherspoon, J. Relationship

between biochemical constituents and production of odor causing compounds from anaerobically digested biosolids, WEF and AWWA Odors and Air Emissions 2004 Conference, Washington, USA, 2004, 18-24.

- [107] Rideout T. C., Fan M. Z., Cant J. P., Wagner-Riddle C., and Stonehouse P. Excretion of major odor-causing and acidifying compounds in response to dietary supplementation of chicory inulin in growing pigs, *J. Anim. Sci.* 2004, 82, 1678-1684.
- [108] Barnett, J.W.; Kerridge, G.; Russell, J. Effluent treatment systems for the dairy industry. *Aus. Biotech.*, 1994, 4, 26-30.
- [109] Dignac, M. F.; Ginestet, M. P.; Rybacki, D.; Bruchet, A.; Urbain, V.; Scribe, P. Fate of wastewater organic pollution during activated sludge treatment: nature of residual organic matter, *Water Research*. 2000, 34, 4185-4194.
- [110] Breure, A. M.; Mooijman, K. A.; Van-Andel, J. G.. Protein degradation in anaerobic digestion: influence of volatile fatty acids and carbohydrates on hydrolysis and acidogenic fermentation of gelatin, *Appl. Microbiol. Biotechnol*, 1986, 24, 426-431.
- [111] Morales, B. ; Bindels, F. ; Corvini, P.; Gerin, P. Method for monitoring the fate of green fluorescent protein added to aerobic and anaerobic wastewater sludge, *Water Research* 2005, 39, 4933–4940.
- [112] Lu, M.C.; Lin, C.J.; Liao, C.H.; Ting, W.P.; Huang, R.Y. Influence of pH on the dewatering of activated sludge by Fenton's reagent, *Water Sci. Technol.* 2001, 44, 327–332.

- [113] Shigeki, F.; Takashi, M. I.; Yoshihiko, S.; Tatsuya, N. Volatile fatty acids (VFA) are dominant products from protein's acidogenesis, Proceedings of JSCE (Japan Society of Civil Engineers). 2001, 671, 71-78.

CHAPTER THREE

Modeling the Influence of Particulate Protein Size on Hydrolysis in Anaerobic Digestion ¹

3.1 Introduction:

A significant fraction of organic matter in municipal wastewater is in the form of particulates [1] which needs to be hydrolyzed before it can be utilized for bacterial metabolism [2]. Anaerobic digestion is the most commonly applied process for stabilization of biosolids. Mass reduction, methane production, and improved dewaterability of sludge are the most important advantages of anaerobic digestion. Anaerobic degradation of complex organic material has been described as a sequential process that involves the steps of hydrolysis, acidogenesis, acetogenesis and methanogenesis [3]. Furthermore, particulate organic matter that is hydrolyzed and used under anaerobic conditions is a valuable carbon source for biological nutrient removal from wastewater; a process that is often limited by the availability of readily biodegradable organic matter [4].

Particulate organic matter is often removed in conventional primary clarification, which removes about 50%-70% of suspended solids and 25%-40% of biochemical oxygen demands (BOD) [5]. Raw wastewater characteristics and particle removal efficiencies vary, resulting in a large range of particle sizes in the primary effluents [6]. Munch et al. [7] reported on a primary effluent in which 28% of the particles were larger than 100 μm ,

¹ A version of this chapter has been submitted to *Bioresource Technology*, 2010

while Levine et al. [2] found that only 7% of particulates in the primary effluent were larger than 12 μm and 49% of particulates in waste activated sludge were $> 12 \mu\text{m}$; an overview of the particle size distribution for various waste streams is presented in Table 3.1.

Table 3.1 Size distribution of organic matter in municipal wastewater (adapted from Levine et al., 1991).

Waste type	Percent size distribution, μm				References
	< 0.001	0.001 – 1	1 – 100	>1 00	
Raw Influent wastewater	12	15	30	43	Munch et al., (1980)
Primary effluent	9	48	15	28	Munch et al., (1980)
Untreated Wastewater	41	16	28	15	Blamat, (1957)
Untreated Wastewater	38	13	19	30	Painter et al. (1959)
Untreated Wastewater	29	13	31	27	Walter (1961a,b)
Untreated Wastewater	29	15	22	34	Walter (1961a,b)
	(< 0.1)	(0.1 - 1)	(1 – 12)	(> 12)	
Primary effluent	(51)	(8)	(34)	(7)	Levine et al., (1985)
Waste activated sludge	(28)	(3)	(20)	(49)	Levine et al., (1985)

Particle size and particle composition determine the rate and mechanism of hydrolysis and degradation in a wastewater treatment system [6]. Most of the biodegradable organic matter is in the range of 10^{-3} to $100 \mu\text{m}$, microorganisms can directly take up particles that are smaller than $10^{-3} \mu\text{m}$ [8, 9]. It is also important to mention that the reaction rates vary widely based on the type of sludge or substrate used. Table 3.2 displays the first-

order hydrolysis reaction rate coefficients for carbohydrate, lipid and protein obtained from the literature.

Table 3.2 Review of hydrolysis rate constants in literature.

Substrate	Hydrolysis constant (d⁻¹)	Sludge Type	References
Carbohydrates	0.041 - 0.13	Various types	Gujer and Zehnder (1983)
Proteins	0.02 - 0.03	Various types	Gujer and Zehnder (1983)
Lipids	0.08 - 0.4	Various types	Gujer and Zehnder (1983)
Carbohydrates	0.21 - 1.94	Primary Sludge	O'Rourke et al.(1968)
Proteins	0.0096 - 0.1	Primary Sludge	O'Rourke et al.(1968)
Lipids	0.0096 - 0.17	Primary Sludge	O'Rourke et al.(1968)
Carbohydrates	0.025 - 0.2	Sewage sludge	Christ et al. (2000)
Proteins	0.015 - 0.075	Sewage sludge	Christ et al. (2000)
Lipids	0.005 - 0.01	Sewage sludge	Christ et al. (2000)
Carbohydrates	0.25 vary within (100%)	Various types	Batstone et al. (2002)
Proteins	0.2 vary within (100%)	Various types	Batstone et al. (2002)
Lipids	0.1 vary within (300%)	Various types	Batstone et al. (2002)
Carbohydrates	0.5 -2.0	Various types	Garcia-Heras (2003)
Proteins	0.25 - 0.8	Various types	Garcia-Heras (2003)
Lipids	0.1 - 0.7	Various types	Garcia-Heras (2003)
Proteins	0.65	Gelatine	Flotats et al. (2006)

The wide variability in reaction rate coefficients, both in individual studies, as well as between studies is noteworthy so much so that the anaerobic digestion model # 1 (ADM1) allowed variability of 100%-300% for the kinetic parameters [3]. Although, the

hydrolysis of particulate organic material has been considered as the rate-limiting step in anaerobic digestion [10], some authors have emphasized that the hydrolytic process still remains as the least well defined step [11,12]. Simplified models for hydrolysis kinetics have been proposed including zero order, first-order, or saturation type kinetics [6]. Table 3.3 displays the various hydrolysis kinetic models available in the literature.

Table 3.3 Hydrolysis rate models in literature (adapted from Pin-Jing et al., 2006).

Name	Expression ($-dS/dt$)	References
Chemical first-order	$k_h S$	Eastman and Ferguson (1981)
Biological first-order	$k_h SB$	Valentini et al. (1997)
Half-order biomass kinetic	$k_h SB^{0.5}$	Rozzi and Verstraete (1981)
A-order biomass kinetic	$k_h SB^A$	Valentini et al. (1997)
Michaelis–Menten equation	$k_h SB / (K_s + S)$	Valentini et al. (1997)
Monod equation	$\mu_{\max} SB / [Y(K_s + S)]$	Hobson (1983)
Haldane equation	$\mu_{\max} B / [Y(1 + K_s / S + S / K_i)]$	Andrews and Graef (1971)
Contois model	$k_h SB / (K_s B + S)$	Henze (1995)
Chen–Hashimoto model	$k_h SB / [K_s (S_o - S) + S]$	Chen and Hashimoto (1980)
Two phase model	$k_h SB / [(K_s + S)(K_B + B)]$	Vavilin et al. (1996)
Step diffusion equation	$[V_{\max}^2 + k_h (S_o - S)]^{0.5}$	Cecchi et al. (1990)
Shrinking core model	$3k_h S_o \phi^2 B$, $d\phi/dt = -k_h B$	Negri et al. (1993)
Flux model	$k_h S_{surf} B \rho$	Terashima and Lin (2000)
Surface based kinetics model	$k_h S_{surf}$	Sanders et al. (2000)

where, A is the exponent in the A -order biomass kinetic equation; B is the concentration of biomass or enzyme (mol/l); K_B is the saturation constant for biomass or enzyme (mol/l); k_h is the hydrolysis rate constant (1/h); K_i is the inhibition constant for the i inhibitory agent (mol/l); K_S is the saturation constant for the substrate (mol/l); S is the substrate concentration (mol/l); S_0 is the initial substrate concentration (mol/l); S_{surf} is the surface area of the organic solid (cm^2); t is time (h); v_{max} is the maximal hydrolysis rate (mol/l-h); Y is the growth yield coefficient; μ_{max} is the maximum specific growth rate (1/h); ρ is the density of the organic solid (g/cm^3); \emptyset is the dimensionless particle radius, equal to the ratio of the radius of the particle at time t to the initial radius of the particle

Most of these models have been developed for specific situations with either very high or very low substrates to microorganism ratio. It is interesting to note that some of these models are sometimes equivalent to each other in terms of effectiveness [13, 14, 15], while they are fundamentally different. For example, the chemical first-order kinetics is not directly coupled to the bacterial growth, while the biological first-order, half-order biomass kinetics, and A -order biomass kinetics are models with similar structure as they contain the hydrolysis rate constant, substrate concentration, and biomass concentration. These models are more comprehensive than the chemical first-order kinetics model due to the involvement of biomass concentration. The Michaelis–Menten kinetic reaction is mainly applied for the hydrolysis of a soluble substrate. Goel et al. [16] found that the hydrolysis of soluble starch follows the Michaelis–Menten kinetics model where the enzyme concentration was proportional to the sludge concentration. The Monod and Michaelis–Menten equations are considered to be similar when μ_{max} and Y are constant.

These models use the hydrolysis rate coefficient as a constant value and are not coupled with the physical characteristics of particulates. The surface based kinetics model [17] was an attempt to correlate the hydrolysis equation to the physical characteristics of particulates, i.e., surface area, but it did not take into account either the substrate or biomass concentration. The Flux model, introduced the biomass concentration, surface area, and density of the substrate for hydrolysis rate, but it still used the hydrolysis rate constant as a constant value.

Over the last decade, significant research has been focused on various disintegration methods to enhance anaerobic digestion (AD) such as thermal, mechanical and chemical pre-treatments [18]. Therefore, the development of hydrolysis model that accounts for the impact of particle size is required for developing more efficient AD designs, and to improve our understanding of the hydrolysis rate. In a study to determine the substrate degradation pattern during acid-phase anaerobic digestion it was found that the changes in sludge retention time (SRT) influence protein dissimilation, whereas carbohydrate and lipid degradation patterns were not affected [19]. Therefore, it is worthwhile to characterize the effect of particle size on protein hydrolysis and its ultimate impact on SRT. In this study, the effect of particulate protein particle size on anaerobic digestion and the influence of particulate size distribution on the hydrolysis rate coefficients during anaerobic digestion were evaluated using casein as a model protein. Mathematical relationships that describe the hydrolysis rate constant as a function of surface weighted median (SWd_{50}) diameter and specific surface area (SSA) were established. In addition, a more comprehensive hydrolysis kinetic model that takes particle size into consideration was developed and verified.

3.2 Material and methods

3.2.1 Culture, Substrate and Media:

Casein protein (R25394, MP Biomedicals, LLC Ohio, US) was grinded using a cutting mill and then sieved using lab scale sieve (GilSonic UltraSiever, Gilson Company Inc., Ohio, US) with 500, 300, 200, 100, and 50 μm size meshes. The casein samples were seeded with anaerobic sludge (volatile suspended solid of 7 g/L) obtained from a full scale anaerobic digester at St. Marys, Water Pollution Control Plant (Ontario, Canada). The medium stock used in these experiments contained 280 g/L NH_4Cl , 250 g/L of K_2HPO_4 , 100 g/L of $\text{MgSO}_4 \cdot 7\text{H}_2\text{O}$, 10 g/L of $\text{CaCl}_2 \cdot 2\text{H}_2\text{O}$, 2 g/L of $\text{FeCl}_2 \cdot 4\text{H}_2\text{O}$, 0.05 g/L of H_3BO_3 , 0.05 g/L of ZnCl_2 , 0.03 g/L of CuCl_2 , 0.5 g/L of $\text{MnCl}_2 \cdot 4\text{H}_2\text{O}$, 0.05 g/L of $(\text{NH}_4)_6\text{Mo}_7\text{O}_{24}$, 0.05 g/L of AlCl_3 , 0.05 g/L of $\text{CoCl}_2 \cdot 6\text{H}_2\text{O}$, and 0.05 g/L of NiCl_2 . The initial pH value for the mixed solution was adjusted to 7 ± 0.2 using 1N NaOH and 2N HCl, and sodium bicarbonate (NaHCO_3) was used as buffer at concentration of 10 g/L.

3.2.2 Batch Anaerobic Digestion:

Batch anaerobic biodegradability tests were carried out in 250 mL serum bottles. The volumes of substrate (casein) and seed (anaerobic digested sludge) were determined based on food (as COD) to microorganism (as VSS) ratio of 4:1. The serum bottles were filled with 180 mL of seed or anaerobic culture, 1 mL of medium described above, and 5 g of casein, distilled water was used to make up the volume to 200 mL. Because the exact chemical formula of casein protein is unknown, the chemical oxygen demand concentration was measured experimentally, in triplicate, using six different casein

concentrations (0.5, 1, 3, 7, 14 and 20 g/L). A linear relationship between the protein concentration and COD value was observed. Six different particle sizes with surface weighted median diameter (SWd₅₀) of 628, 443, 229, 129, 61, 25 µm were tested. All bottles were capped and sealed with teflon septum after purging the headspace with nitrogen for 2 min to eliminate the presence of oxygen/air and create anaerobic conditions. Nine bottles were used for each particle size of casein in addition to nine for the blank (media and seed only); all samples were incubated in a rotary shaker (MaxQ 4000, Incubator and Refrigerated Shaker, Thermo Scientific, CA) at 37°C and 180 rpm. One bottle from each particle size was sacrificed each time for parameter analysis. The experiment was conducted two times to ensure reproducibility.

3.2.3 Analytical Methods:

Sludge parameters such as chemical oxygen demand (COD), total suspended solids (TSS), volatile suspended solid (VSS), volatile fatty acids (VFA), and proteins fractions (particulate and soluble) were measured with time in duplicate. All sludge parameters were analyzed according to the Standard Methods [20]. However, particulate and soluble proteins were analyzed using the method described by Lowry et al. [21] method. The concentrations of VFA in the filtered sludge (through 0.45 µm filter) were measured using a gas chromatograph (Varian 8500, Varian Inc., Toronto, Canada) with a flame ionization detector (FID) equipped with a fused silica column (30 m × 0.32 mm) with a 1 µm film thickness. Helium was used as the carrier gas at a flow rate of 5 mL/min. The temperatures of the column and detector were 110 and 250°C, respectively. The particle size distribution, surface weighted median diameter (SWd₅₀) and specific surface area

(SSA) were determined by Malvern Mastersizer 2000 (version 5.22) laser beam diffraction granulometer (Malvern Instruments Ltd, England). Total gas volume was measured by releasing the gas pressure in the bottles using appropriately sized glass syringes (Perfektum; Popper & Sons Inc., NY, USA) in the 5–100 mL range after equilibration with the ambient pressure as recommended by Owen et al. [22]. Biogas composition was determined by a gas chromatograph (Model 310, SRI Instruments, Torrance, CA) equipped with a thermal conductivity detector (TCD) and a molecular sieve column (Molesieve 5A, mesh 80/100, 182.88×0.3175 cm). The temperatures of the column and the TCD detector were 90 and 105°C, respectively. Argon was used as a carrier gas at a flow rate of 30 mL/min.

3.2.4 Modeling:

In this study, only the hydrolysis of protein, uptake of amino acids and microbial decay of amino acids degraders in anaerobic digestion were considered; inhibition due to pH, NH_3 , and H_2 were ignored for simplicity. The first-order kinetic model was used to describe the disintegration, hydrolysis and the decay reactions, while the Monod model was used for the biological uptake reactions [3]. Figure 3.1 shows the Total COD flow of proteins as described in the ADM1 [3].

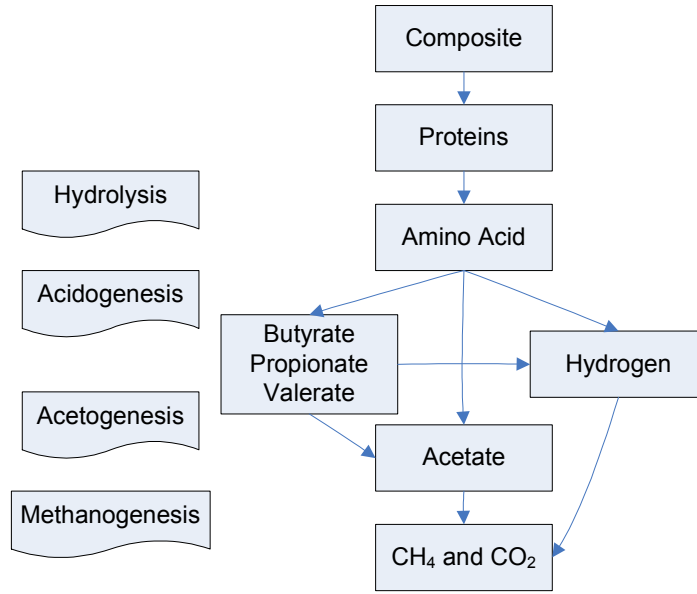


Figure 3.1 Interrelated TCOD flow of Proteins in the Anaerobic Digestion Model No. 1 (ADM1)

The following simplified model, henceforth referred to as the particulate protein model (PPrM) was used in this study:

$$\text{Disintegration: } \frac{dX_c}{dt} = k_{dec, X_{aa}} X_{aa} - k_{dis} X_c$$

In this study the concentration of X_c (kg COD m^{-3}) was set to zero due to the use of particle protein as the only substrate at the beginning, hence the disintegration equation

$$\text{can be expressed as follows } \frac{dX_c}{dt} = k_{dec, X_{aa}} X_{aa} \quad \dots \quad (1)$$

$$\text{Hydrolysis of protein: } \frac{dX_{pr}}{dt} = f_{pr, xc} k_{dis} X_c - k_{hyd, pr} X_{pr} \quad \dots \quad (2)$$

$$\text{Uptake of amino acids: } \frac{dS_{aa}}{dt} = k_{hyd, pr} X_{pr} - k_{m, aa} \frac{S_{aa}}{K_{S, aa} + S_{aa}} X_{aa} \quad \dots \quad (3)$$

Growth of amino acids degraders:

$$\frac{dX_{aa}}{dt} = Y_{aa} k_{m,aa} \frac{S_{aa}}{K_{S,aa} + S_{aa}} X_{aa} - k_{dec,Xaa} X_{aa} \quad \dots \quad (4)$$

Where, $k_{m,aa}$ is the Monod maximum specific uptake rate (d^{-1}) for amino acids, $K_{s,aa}$ is the Monod half saturation concentration ($kg\ COD\ m^{-3}$) for amino acids, k_{dis} , k_{hyd} and k_{dec} are the first-order coefficient rate (d^{-1}) for disintegration, hydrolysis, and decay, respectively. X_c , X_{pr} , and X_{aa} , are the particulate components ($kg\ COD\ m^{-3}$) for composite, protein, and amino acids degraders, S_{aa} is the soluble component ($kg\ COD\ m^{-3}$) for amino acids, $f_{pr,xc}$ is the yield of proteins from composites, Y_{aa} is the yield of biomass on substrate, and t is the time in day. AQUASIM 2.1 (Dübendorf, Switzerland) was used to solve the PPrM dynamic differential equation system.

3.2.5 Statistical Analysis:

The student t-test was used to test the hypothesis of equality at the 95% confidence level. The null hypothesis was defined as no difference between the two groups tested vs. the alternative hypothesis that there is a statistical difference between the two groups.

3.3 Results and discussion

3.3.1 Particulate Protein Degradation:

Figure 3.2 displays the anaerobic protein degradation versus digestion time for different particle sizes.

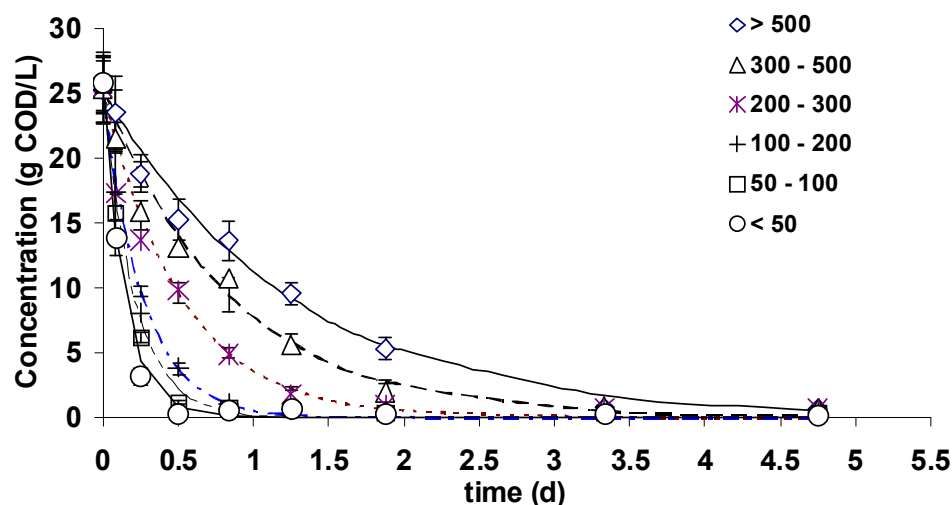


Figure 3.2 Particulate protein degradation for different particles size versus time.

Although final reduction in protein ($97\pm 1\%$) was achieved within 80 h for all particle sizes, initial degradation was significantly higher for the smaller size particles as shown in Figure 3.2. For example, for 80% particulate protein degradation, a residence time of 5 h is required for particle size $\leq 50 \mu\text{m}$, whereas ≈ 55 h is required for a size $\geq 500 \mu\text{m}$. This suggests that the reduction of particle size is beneficial to the hydrolysis rate of proteins during the anaerobic digestion, mainly due to the increase in specific surface area available for the microorganisms to adhere [17, 23] with decreasing particle size. Palmowski and Muller [24], who investigated the significance of the surface area in anaerobic degradation of various particulate substrates such as apple, rice, sunflower seeds, hay and maple leaves, found that the hydrolysis rate was mainly dependent on the specific surface area as opposed to increase in dissolved compounds due to cell rupture, alteration of the sample structure, and exposition of surface areas previously inaccessible for microbial degradation. Since hydrolysis of particulate protein occurs at the solid-

liquid interphase, it is only natural that overall rate increases with increasing surface area given enough biomass. The increase in surface area due to reduction in particle size is shown in Table 3.4.

Table 3.4 Gompertz (Lay et al., 1999) model coefficients, median $d(50)$ for the surface area, and specific surface area for different ranges of protein particle sizes.

PSR (μm)	λ	R_m	P	R^2	SW d_{50} (μm)	SSA (m^2/g)
> 500	21.12	6.14	333.31	0.99958	628	0.00999
300 - 500	18.72	6.97	334.83	0.99960	443	0.0129
200 - 300	16.00	8.35	329.29	0.99976	229	0.0201
100 - 200	13.58	9.61	319.98	0.99989	129	0.0469
50 - 100	12.98	11.78	323.84	0.99995	61	0.0985
< 50	10.56	13.47	323.13	0.99995	25	0.192

* PSR is the particle size range

3.3.2 Biogas Production:

Figure 6.3 shows the cumulative $\text{mLCH}_4/\text{gCOD}_{\text{added}}$ produced; the ultimate methane produced was approximately the same for all particle sizes because of the same initial COD concentration of 25 g/L. Overall, experimental CH_4 production ($1486 \pm 25 \text{ mL CH}_4$) was 14.7% lower than the theoretical methane production (1742 mL CH_4); theoretical methane was determined based on CH_4 equivalent COD of $0.395 \text{ L CH}_4/\text{gCOD}$ at 37°C (Metcalf and Eddy, 2003). However, the maximum rate of methane production increased from 6 to 14 $\text{mL CH}_4/\text{gCOD}_{\text{added-d}}$ with the decrease in SW d_{50} from 628 μm to 25 μm .

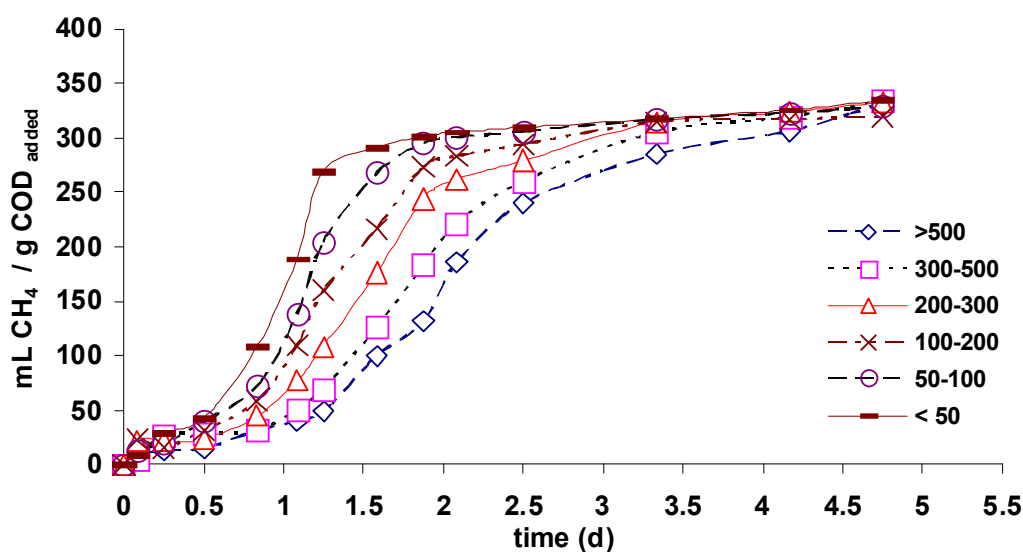


Figure 3.3 Methane production over digestion time using different protein particle sizes.

Interestingly, the effect of particle size on solubilization and gas production is not exactly the same; for example, 80% of the maximum gas production occurred at 30 h for particle size $\leq 50 \mu\text{m}$, whereas ≈ 80 h is required for a size $\geq 500 \mu\text{m}$. Therefore the benefit of smaller size on hydrolysis is not directly translated to the gas production. Overall, by decreasing particle size by 25 times, digestion time has been improved by 2.5 times. Similar trends have been observed by Hu et al. [25] who studied the effect of two different sizes of cellulose, $50 \mu\text{m}$ and $100 \mu\text{m}$, although the ultimate methane production in their study was lower in case of $50 \mu\text{m}$ than $100 \mu\text{m}$ due to the accumulation of VFAs. It is also important to note that a lag phase between 9 to 20 hours was observed in all protein sizes (Figure 3.3). Duration of the lag phase was found to be a function of particle size, as it increased with the increase in particle size.

To further elaborate on the effect of the particle size on the ultimate methane production, maximum methane rate and lag phase, the following modified Gompertz model [26] has been used to describe the cumulative gas production as:

$$CH_4 = P \cdot \exp\left\{-\exp\left[\frac{R_m}{P}(\lambda - t) + 1\right]\right\},$$

where CH_4 is the cumulative methane production per unit substrate (ml/g), P is the maximum methane production per unit substrate (ml/g), R_m is the maximum methane production rate (ml/g h), λ is the lag phase time (h), t is the digestion time (h).

The cumulative methane production per unit substrate data were fitted with Gompertz equation using the Newton-Raphson method for non-linear numerical estimation. The Newton's method was programmed using Visual Basic Application (VBA) language available in MSExcel 2003. Table 3.4 summarizes the results of the model coefficients. The correlation coefficient (R^2) over 0.99 for all the regressions confirms the applicability of the modified Gompertz model to fit the experimental data. Based on the model results, it is evident that as the particle size decreased from $\geq 500 \mu\text{m}$ to $\leq 50 \mu\text{m}$, the lag phase decreased from 21 h to 11 h, while the maximum methane production rate increased from 6 to 14 ml/g-h, respectively. More specifically, the lag phases for the 628, 443, 229, 129, 61, 25 μm SWd₅₀ were 21, 19, 16, 14, 13, and 11 h, and maximum methane production rates were 6, 7, 8, 10, 12, and 14 ml/g-h, respectively. It is also important to note that the model was able to predict the maximum methane production per unit substrate of 327 ± 6 ml/g successfully. The above results emphasize the significant impact of substrate particle size on gas production.

3.3.3 Effect of Particle Size on the Hydrolysis Coefficient:

Since hydrolysis is predominantly dependent on surface area rather than volume [27,28], Table 3.4 displays the, surface weighted median diameter (μm) and the specific surface area (m^2/g) as a function of particle size of the test protein. The structure of the model used in this study was obtained from the ADM1 model [3]. Due to the focus of this study on the protein hydrolysis, the ADM1 model was simplified with only particulate protein as the main substrate (Figure 3.1). The ADM1 model considers that all biochemical extracellular solubilization steps are divided into disintegration and hydrolysis, of which the first is a largely non-biological step that converts composite particulate substrate to carbohydrates, proteins, lipids, and inerts. As mentioned earlier, in this study the particulate protein was considered to be the only substrate. The second step is enzymatic hydrolysis of particulate proteins to amino acids. Disintegration is mainly included to describe degradation of dead biomass, while the hydrolysis steps are defined for pure substrates such as protein. Both disintegration and hydrolysis processes are represented by equation 1 and equation 2, respectively. The particulate protein will then be hydrolyzed to its soluble form of amino acids. A separate group of acidogenic bacteria degrade amino acids to mixed organic acids, hydrogen, and carbon dioxide, with the rate of degradation following Monod kinetics equation 3. The organic acids are subsequently converted to acetate, hydrogen, and carbon dioxide by acetogenic groups that utilize butyrate and valerate, and propionate. The hydrogen produced by these organisms is consumed by hydrogen-utilizing methanogenic bacteria, and the acetate by aceticlastic methanogenic bacteria. Due to the focus of this study on protein hydrolysis only, the acetogenic group was excluded from the model. Growth and death of biomass were

maintained in the anaerobic system as composite particulate material and was represented by equation 4. Inhibition due to pH, hydrogen and free ammonia was excluded for simplicity; pH was monitored and controlled by applying sodium bicarbonate NaHCO_3 as a buffer.

AQUASIM 2.1 (Swiss Federal Institute for Environmental, Switzerland) was used to solve the dynamic differential system of equations presented earlier as well as estimating the model coefficients, namely k_{hyd} , the hydrolysis rate constant (d^{-1}), $k_{\text{m, aa}}$ the maximum specific uptake rate (d^{-1}) for amino acids, and $K_{\text{s, aa}}$ the Monod half saturation constant (kgCOD/m^3). First-order decay rate k_{dec} (d^{-1}), first-order disintegration rate k_{dis} (d^{-1}), yield of proteins from composites $f_{\text{pr,xc}}$, and yield of biomass on substrate Y_{aa} were set to 0.5 d^{-1} , 0.02 d^{-1} , 0.2 , and 0.08 , respectively, based on the recommendation of the ADM1 model [3]. The amino acids components of biomass were set to $0.02 \text{ kg COD}/\text{m}^3$ following the recommendation of Jeong et al. [29] who evaluated the sensitivities of the kinetic and stoichiometric ADM parameters in predicting anaerobic glucose digestion and concluded that biomass concentration was closely associated with the Monod maximum specific uptake rate, that values could not be independently determined and verified.

Figure 3.2 shows the first-order hydrolysis kinetics fit of the experimental data for different particle sizes, while Table 3.5 displays the hydrolysis rate coefficients and the average percentage error (APE) of the hydrolysis model compared to the experimental data.

Table 3.5 Hydrolysis rate and the amino acids uptake coefficients for different particle size ranges of protein.

PSR (μm)	k_{hyd} (d^{-1})	APE (%)	$k_{\text{m, aa}}$ (d^{-1}),	$K_{\text{s, aa}}$ (kg COD m^{-3}), first-order 5.445	
				SWd ₅₀ KE	SSAKE
> 500	0.034	5	30	4.898	5.095
300 – 500	0.049	3	30	4.947	5.053
200 – 300	0.082	1	30	5.424	5.429
100 – 200	0.160	3	30	5.644	5.399
50 – 100	0.204	2	30	5.497	5.414
< 50	0.298	10	30	6.191	6.332

It is evident that the model equations (1-4) successfully fit the experimental data with APE between 1% and 10%, more specifically for SWd₅₀ of 628, 443, 229, 129, 61, and 25 μm the APE were 5, 3, 1, 3, 2, and 10 %, respectively. As the particle size decreased from ≥ 500 to ≤ 50 μm the hydrolysis rate coefficient increased from 0.034 to 0.298 d^{-1} , an enormous 776% increase. Similar results have been observed by Dimock et al. [30] who studied the effect of small and large, square-weighted mean chord lengths of 60 and 390 μm , respectively, of hard-boiled egg whites as artificial particles in activated sludge system. The hydrolysis rate was between 0.038 and 0.24 d^{-1} and 0.019 and 0.98 d^{-1} for large and small particles, respectively. Therefore, it is essential to note that using the first-order hydrolysis constant in the anaerobic digestion of particulate substrates without taking particle size into consideration would be both misleading and erroneous. The relationship between hydrolysis rate coefficients and both SWd₅₀ and SSA were mathematically evaluated and shown in Figures 6.4a and 6.4b, respectively.

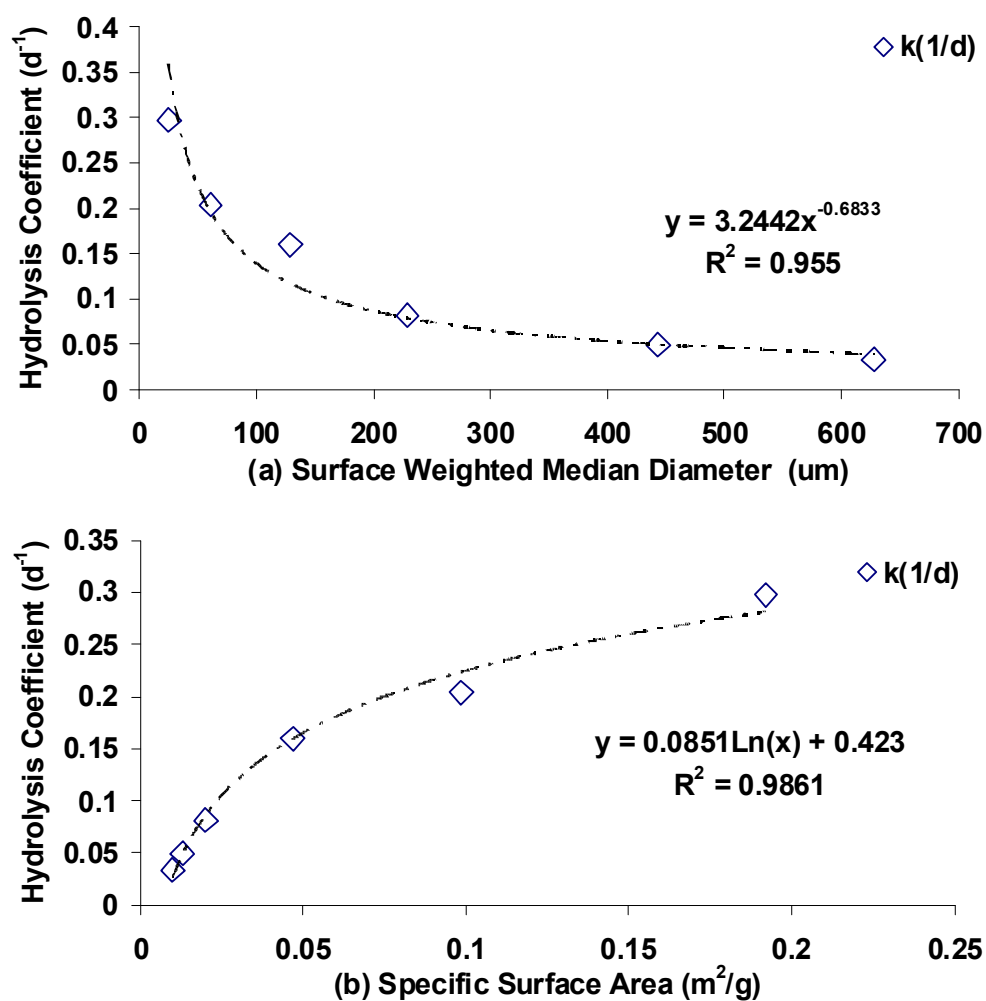


Figure 3.4 First-order hydrolysis rate coefficient as function of (a) surface weighted median diameter (μm) (b) specific surface area (m^2/g)

As evident from Figure 3.4, the hydrolysis rate coefficient was exponentially related to the SWd_{50} with R^2 of 96% while the relationship with SSA followed the power function with R^2 of 99% (as shown below in equations 5 and 6). It is clear that the developed equations based on SWd_{50} and SSA has good agreement with the first-order kinetics results with APE of 1% and 2% for SWd_{50} and SSA, respectively. Furthermore, the

spread of the data on both sides of the fitted curve confirms that the model does not systematically over-predict or under-predict the first-order results. Palmowski and Muller [24] have also concluded that surface area needs to be considered when describing the degradation kinetics of substrate containing particles solids, especially when investigating the significance of the surface area in anaerobic degradation of various particulate substrates.

3.3.4 Hydrolysis Equations and Verification:

To demonstrate the significance of the particle size in the anaerobic process, kinetic equations for anaerobic hydrolysis were proposed and presented below. The rationale behind the new hydrolysis equations were to overcome the limitation of the first-order hydrolysis model, which utilizes a constant hydrolysis rate coefficient that is independent of both particle size and surface areas (Table 3.3). The proposed equations were based on the relationship developed earlier (Figure 3.4) between SSA and the hydrolysis rate coefficients denoted as SSAKE (equation 5), as well as SWd₅₀ and the hydrolysis rate, denoted as SWd₅₀KE (equation 6).

$$\frac{dX_{pr}}{dt} = f_{pr,xc} k_{dis} X_c - [0.0851 \cdot \ln(SSA) + 0.423] \cdot X_{pr} \quad \dots \quad (5)$$

$$\frac{dX_{pr}}{dt} = f_{pr,xc} k_{dis} X_c - [3.244 \cdot (SWd_{50})^{-0.683}] \cdot X_{pr} \quad \dots \quad (6)$$

It should be noted that the proposed equations were developed for casein and thus might not be pertinent for other types of proteins or other particulates substrates like lipids and carbohydrates. In order to verify the two aforementioned proposed equations, first the

PPrM was applied to estimate the maximum specific uptake rate ($k_{m, aa}$) for amino acids and the Monod half saturation concentration ($K_{s, aa}$) using the first-order hydrolysis kinetic equation (equation 2) with experimentally determined hydrolysis rate coefficient 0.082 d^{-1} , correspond to the particle size 200-300 μm , the mid-range of the tested protein size (Table 3.5). The maximum specific uptake rate ($k_{m,aa}$) for amino acids and the Monod half saturation concentration ($K_{s,aa}$) were estimated using the Parameter Estimation feature available in AQUASIM 2.1 as 30 d^{-1} and $5.445 \text{ kg COD m}^{-3}$, respectively. The maximum specific uptake rate obtained in this study is similar to that reported by Ramsay [31] between 28 and 53 d^{-1} , however the Monod half saturation concentration observed was higher than the one reported by Ramsay, which is $1.027 - 1.198 \text{ kg COD m}^{-3}$ [3]. The proposed hydrolysis kinetic equations 5 and 6 were then used to simulate the experimental amino acid uptake, more specifically the maximum specific uptake rate ($k_{m, aa}$) for amino acids and the Monod half saturation concentration ($K_{s, aa}$). For these simulations, the hydrolysis equation (equation 2) presented in PPrM model was replaced by the newly developed SSAKE and then by the SWd₅₀KE (shown in Figures 6.4 a and b). Table 3.5 presents the fitted amino acids uptake coefficients for the two proposed hydrolysis models SSAKE and SWd₅₀KE. The result shows a slight change in the Monod half saturation concentration ($K_{s,aa}$) at different particle size. However this change was not statistically significant based on the t-test (null hypothesis was defined as no difference between the average $K_{s, aa}$ and 5.445) with a t-value of 0.06 and 0.05; and p-value of 0.96 and 0.97 at the 95% confidence level for SWd₅₀KE and SSAKE, respectively. The difference between the Monod half saturation concentration using SWd₅₀KE and SSAKE equations was also tested and was found to be statistically

insignificant at the 95% confidence interval, which implies that both models simulated the experimental data well. In other words, modified hydrolysis rate equations based on surface weighted median diameter and specific surface area of particulate protein performed equally well in predicting the experimental data. Figure 3.5 shows the experimental data for amino acids and the predictions by the three hydrolysis models (equations 2, 5, and 6) used in this study.

The amino acids concentration profile follows the typical consecutive reaction scheme, i.e., it is produced by the degradation of protein and concomitantly breaks down to volatile fatty acids. It is also interesting to note that the ' t_{\max} ' to produce the maximum amino acids (soluble protein) corresponds well with the hydrolysis rates shown in Figure 3.2, and the rate of degradation (acidogenesis phase) also depends on the particle size. It is also evident that the proposed hydrolysis models fit the experimental data better than the original first-order model at different particle sizes. Average percentage error between the experimental data and the models' prediction was between 9 to 22% in the case of SWd₅₀KE, and 9 to 25% in the case of SSAKE. More specifically for SWd₅₀ of 628, 443, 229, 129, 61, and 25 μm the APEs were 9, 20, 20, 20, 14, and 22 %, when applying SWd₅₀KE and 9, 17, 23, 25, 16, and 20 %, respectively, when applying SSAKE.

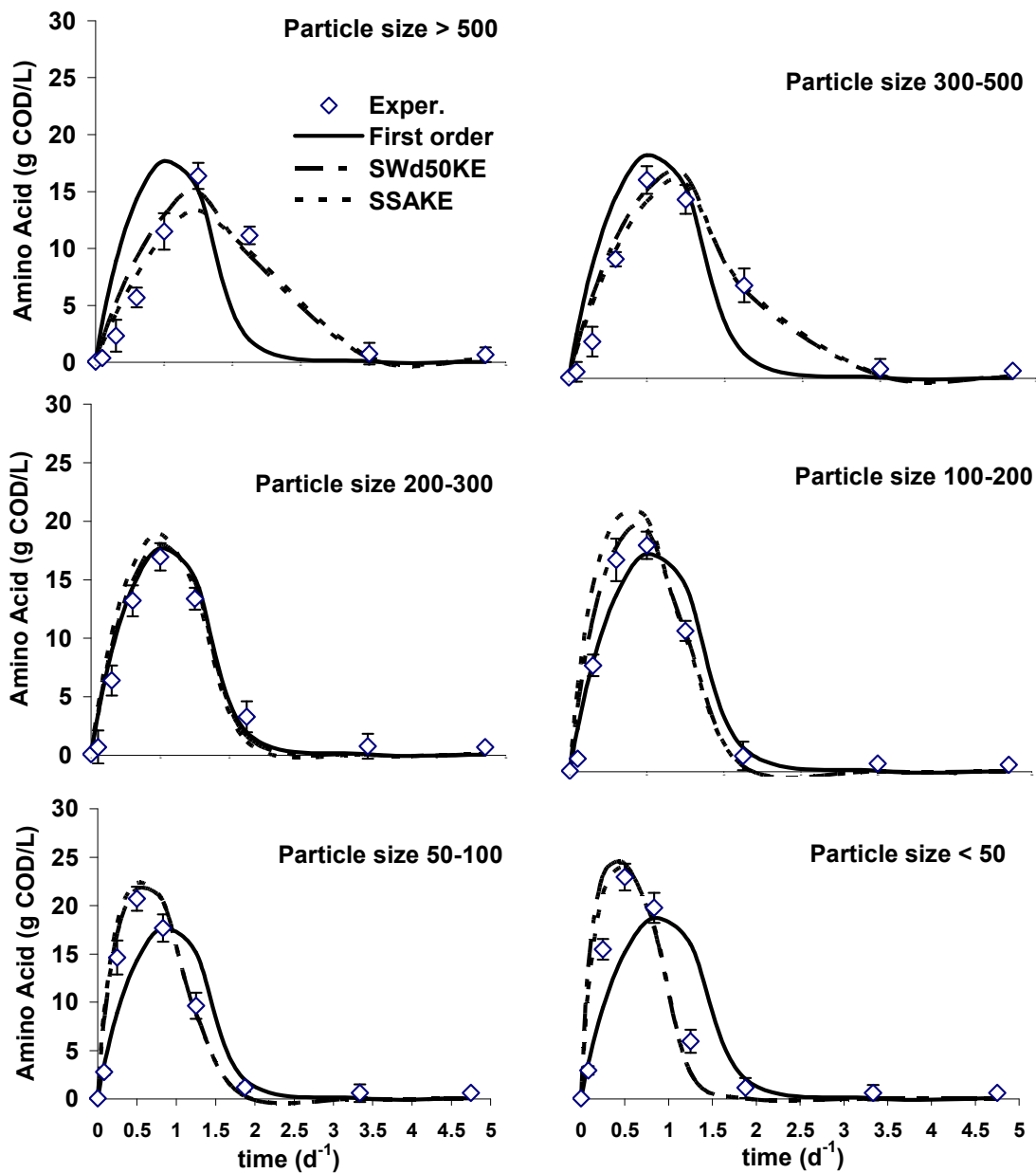


Figure 3. 5 Amino acids variation with time for different protein particle sizes.

3.4 Conclusions:

The effect of particle size on particulate protein degradation can be summarized as follows:

- Although casein degradation efficiency was $97\pm 1\%$ for all protein sizes within 80 h of digestion, the biodegradation rate increased significantly with decreasing particle size.
- The ultimate methane production of 8259 ± 139 mL was approximately the same for all protein sizes. However the maximum methane production rate increased from 5 to 15 ml/g-h, while the lag phase decreased from 21 to 11 h with the decrease in particle size from ≥ 500 μm to ≤ 50 μm .
- The hydrolysis rate coefficient increased by 786% from 0.034 to 0.298 d^{-1} with the decrease in particle size from ≥ 500 μm to ≤ 50 μm corresponding to increase in specific surface area from 0.01 to $0.19\text{ m}^2/\text{g}$.
- The hydrolysis rate coefficient of protein was experimentally related to median surface diameter and specific surface area.
- The new hydrolysis models, correlating the first-order hydrolysis rate coefficient to both median surface diameter and specific surface area were developed and verified using the experimental data.

3.5 References

- [1] Dimock, R.; Morgenroth, E. The influence of particle size on microbial hydrolysis of protein particles in activated sludge. *Water Research*. 2006, 10, 40, 2064-2074.
- [2] Levine, A. D.; Tchobanoglous, G.; Asano, T. Size distributions of particulate contaminants in wastewater and their impact on treatability. *Water Research*. 1991, 8, 25, 911-922.
- [3] Batstone, D. J.; Keller, J.; Angelidaki, I.; Kalyuzhnyi, S. V.; Pavlostathis, S. G.; Rozzi, A.; Sanders, W. T. M.; Siegrist, H.; Vavilin, V. A. Anaerobic Digestion Model No. 1, IWA Task Group for Mathematical Modelling of Anaerobic Digestion Processes, *Water Sci. Technol.* 2002, 40, 65–73.
- [4] Henze, M.; Mladenovski, C.; Hydrolysis of particulate substrate by activated sludge under aerobic, anoxic and anaerobic conditions, 1991, *Water Research*. 1991, 25, 61-64
- [5] Tchobanoglous, G.; Burton, F.L.; Stensel, H.D. *Wastewater Engineering, Treatment and Reuse*, 4th Edition. McGraw-Hill, Inc., New York. 2003, 1819.
- [6] Morgenroth, E.; Kommedal, R.; Harremoës, P. Processes and modeling of hydrolysis of particulate organic matter in aerobic wastewater treatment – a review, *Water Sci. Technol.*, 2002, 6, 45, 25–40
- [7] Munch, R., Hwang, C.P.; Lackie, T.H. Wastewater fractions add to total treatment picture, *Water Swage Wks.* 1980, 12, 127, 49–54.
- [8] Ferenci, T. The recognition of maltodextrins by *E. coli*. *Eur. J. Biochem.*, 1980, 108, 631–636.
- [9] White, D. *The physiology and biochemistry of prokaryotes*, Second edition, Oxford University Press Inc., New York, 2000
- [10] Pavlostathis, S.G.; Giraldo-Gomez, E. Kinetics of anaerobic treatment. *CRC Crit. Rev. Environ. Contr.* 1991, 21, 411–490.

- [11] Miron, Y.; Zeeman, G.; van Lier, J.B.; Lettinga, G. The role of sludge retention time in the hydrolysis and acidification of lipids, carbohydrates and proteins during digestion of primary sludge in CSTR systems. *Water Research*. 2000, 34, 1705–1713.
- [12] Gavala, H.N.; Angelidaki, I.; Ahring, B.K.; Kinetics and modelling of anaerobic digestion process. *Adv. Biochem. Eng. Biotechnol*, 2003, 81, 57–93.
- [13] Vavilin, V.A.; Rytov, S.V.; Lokshina, L.Y. A description of hydrolysis kinetics in anaerobic degradation of particulate organic matter. *Bioresource Technol.*, 1996, 56, 229–237.
- [14] Valentini, A.; Garruti, G.; Rozzi, A.; Tilche, A. Anaerobic degradation kinetics of particulate organic matter: a new approach, *Water Sci. Technol.*, 1997, 36, 239–246.
- [15] Cecchi, F.; Mata-Alvarez, J.; Traverso, P. G.; Medici, F.; Fazzini, G. A New Approach to the Kinetic Study of Anaerobic Degradation of the Organic Fraction of Municipal Solid Waste, *Biomass*, 1990, 2, 23, 79-102.
- [16] Goel, R.; Mino, T.; Satoh, H.; Matsuo, T. Comparison of Hydrolytic Enzyme Systems in Pure Culture and Activated Sludge under Different Electron Acceptor Conditions, *Water Sci. Technol.*, 1988, 37, 335
- [17] Sanders, W.T.M.; Geerink, M.; Zeeman, G.; Lettinga, G. Anaerobic hydrolysis kinetics of particulate substrates. *Water Sci. Technol.*, 2000, 41, 17–24.
- [18] Thibault, G. Effect of microwave irradiation on the characteristics and mesophilic anaerobic digestion of sequencing batch reactor sludge, MSc in Eng thesis, University of Ottawa, Ottawa, Canada, 2005
- [19] Elefsiniotis, P.; Oldham, W. K. Substrate degradation patterns in acid-phase anaerobic digestion of municipal primary sludge, *Enviro. Technol.*, 1994, 8, 15, 741–751
- [20] APHA. *Standard Methods for the Examination of Water and Wastewater*, Washington DC, APHA. 1998.
- [21] Lowry, O. H.; Rosebrough, N. J.; Fair, A. L.; Randall, R. J. Protein measurement with the folin-phenol reagent, *J. Biol. Chem*, 1951, 193, 265-275.

- [22] Owen, W.F.; Stuckey, D.C.; Healy, J.B.; Young, L.Y., McCarty, P.L. Bioassay for monitoring biochemical methane potential and anaerobic toxicity, *Water Research*, 1979, 6, 13, 485-492.
- [23] Mshandete, A; Bjojrnsseb, L.; Kivaisia, A. K., Rubindamayugia, M.S.T.; Mattiassonb, B. Effect of particle size on biogas yield from sisal fibre waste, *Renewable Energy*, 2006, 31, 2385–2392
- [24] Palmowski, L.M.; Muller, J. Influence of the size reduction of organic waste on their anaerobic digestion. *Water Sci. Technol.* 2000, 3, 41, 155–162.
- [25] Hu, Z; Yu, H.; Zhu, R. Influence of particle size and pH on anaerobic degradation of cellulose by ruminal microbes, *Inter. Biodeterioration & Biodegradation*, 2005, 55, 233–238
- [26] Lay, JJ; Lee, YJ; Noike, T. Feasibility of biological hydrogen production from organic fraction of municipal solid waste. *Water Research*. 1999, 33, 2579-25786.
- [27] Miller, W. P.; Baharuddin, M. K. Particle size of interrill-eroded sediments from highly weathered soils, *Soil Sci Soc Am.*1987 , 51, 1610-1615.
- [28] Vavilin, V.A.; Rytow, S.V.; Lokshina, L.Y. Modelling hydrogen partial pressure change as a result of competition between the butyric and propionic groups of acidogenic bacteria. *Bioresour. Technol*, 1995, 54, 171–177.
- [29] Jeong, H. S.; Chang-Won Suh; Jae-Lim Lim; Sang-Hyung Lee; Hang-Sik Shin. Analysis and application of ADM1 for anaerobic methane production. *Bioprocess Biosyst Eng.*, 2005, 27, 81–89.
- [30] Dimock, R.; Morgenrotha, E. The influence of particle size on microbial hydrolysis of protein particles in activated sludge, *Water Research*. 2006, 40, 2064 – 2074
- [31] Ramsay, I. R. Modelling and control of high-rate anaerobic wastewater treatment system, PhD thesis, University of Queensland, Brisbane, 1997

CHAPTER FOUR

Modeling the Effect of Sonication on Biosolids Anaerobic Digestion²

4.1 Introduction

Biosolids produced during wastewater treatment are one of the most abundant renewable energy resources [1]. Within the agricultural sector in the European Union only, about 1500 million tons of biosolids are produced each year [2]. Consumption of biosolids for energy production has increased significantly in recent years. Biosolids can be converted to energy either directly by combustion, where the main energy output is heat and electricity, or can be converted to an energy carrier that can be used as fuel for vehicles [3].

Energy from biosolids can be produced by biological (fermentation) or non-biological (thermo-chemical) processes [4]. Biological processes consume less energy than non-biological processes in the production of a variety of gaseous and liquid energy carriers [3]. Anaerobic digestion is the most commonly applied process for stabilization of biosolids. Mass reduction, methane production, and improved dewaterability of sludges are the most important advantages of anaerobic digestion. Due to carbon removal in the form of methane and carbon dioxide, the end product shows a substantially better biological stability than the unfermented material. A disadvantage of the fermentation process is the slow degradation rate of biosolids. Conventional residence times in anaerobic digesters are about 20-40 days, requiring large digesters. Sludge hydrolysis has been considered as the rate-limiting step of anaerobic digestion [5]. The biodegradability

² A version of this chapter has been published in *Energy&Fuels*, 2010, 24 (9), pp 4703–4711

of biosolids can be improved by sludge pretreatment methods that enhance solubilization of solids.

Various mechanical disintegration methods have been applied for the pretreatment of biosolids to enhance the rate and extent of anaerobic digestion. Sonication is a method for the break-up of microbial cells to extract intracellular material [6]. When the ultrasound wave (>20 kHz) propagates in an aqueous medium such as primary and waste activated sludge, it generates a repeating pattern of compressions and rarefactions in the medium. The rarefactions are regions of low pressure (excessively large negative pressure) in which liquid or slurry is torn apart. Micro-bubbles are formed in the rarefaction regions. As the wave fronts propagate, micro-bubbles oscillate under the influence of positive pressure, thereby growing to an unstable size before they violently collapse. The collapsing of the bubbles often results in localized temperatures up to 5000 K and pressures up to 180 MPa [7]. The sudden and violent collapse of huge numbers of micro-bubbles generates powerful hydro-mechanical shear forces and forms a high-speed liquid micro-jet that impacts the surfaces of the bulk liquid constituents surrounding the bubbles [8]. The collapsing bubbles, micro-jet of liquid, disrupt adjacent bacterial cells by extreme shear forces, rupturing the cell wall and membranes. Several studies have reported the benefits of ultrasound as a pretreatment method for sludge prior to anaerobic digestion such as improved dewaterability, solubilization, rapid hydrolysis rate, and enhanced biogas production [9, 11]. Ultrasound has also been tested for the enhancement of full-scale digesters [12].

Mathematical anaerobic digestion models (ADM) have been extensively investigated and developed during the last three decades [13]. As one of the most sophisticated and

complex ADM, the IWA Anaerobic Digestion Model No. 1 (ADM1) is the integrated anaerobic model developed by the IWA Task Group for modeling of Anaerobic Digestion Processes [14]. It consists of a number of processes to simulate all possible reactions occurring in anaerobic sludge digestion including not only biological reactions, such as disintegration and hydrolysis of suspended solids, uptake (growth) and decay of microorganisms, but also physico-chemical reactions, including ion association/dissociation and liquid-gas transfer. In total, 19 processes, 24 components, and 56 relative stoichiometric and kinetic parameters were assumed for biological processes, and also, additional processes and parameters were determined for physico-chemical processes. The steady-state Anaerobic Digestion Model #1 (ADM1) model had been used with good success for approximately two years on a wide range of full-scale wastewater treatment facilities [15, 17]. However, ADM1 has a critical disadvantage that many parameters are difficult or impossible to measure [18, 19]. Batstone et al. [15] used the ADM1 model to evaluate two industrial treatment applications. The first was the assessment of acid addition for pH decrease and avoidance of calcium carbonate (CaCO_3) precipitation in a paper mill fed UASB. The simulation work found, with a high degree of confidence, that acid dosing was neither economical for pH control nor had any real effect on the CaCO_3 levels present in the reactor. A specific calcium carbonate precipitation equation was added to the ADM1 to undertake this study. The second study was an assessment of the benefits of thermophilic (as opposed to mesophilic operation) for reduced ammonia inhibition, improved stability, and gas production in a solids digester at a gelatine production facility. Here, it was predicted that thermophilic operation could not attain either goal to a satisfactory extent. In addition to demonstrating

the application of the ADM1 to the two systems, they assessed the predictions generated in the case studies in terms of quality and utility. Johnson et al. [16] have reported in their study that a number of modifications were necessary to allow it to be used in the context of municipal wastewater treatment. It was found that the model's use was greatly simplified if used in conjunction with a larger plant simulator to assist in the feed fractionation. It was also found that a better fit to actual operating data was achieved if some of the slowly biodegradable particulate fraction was partitioned into ADM particulate fractions other than the composite fraction X_c . Blumensaat et al. [17] successfully implemented a process model to simulate the dynamic behaviour of a pilot-scale process for anaerobic two-stage (thermophilic / mesophilic) digestion of combined primary and WAS.

While most of the studies based on ultrasound energy have focused on the dewaterability and solubilization of chemical oxygen demand (COD), there is a definite paucity of information related to the impact of sonication on other biosolids characteristics like odors precursors such as proteins as well as anaerobic biodegradability. Furthermore a simplification of the complex ADM model and its application to simulate pretreated sludges enhances both process understanding and practical application. This study focuses on assessing the impact of sonication on various protein fractions and their anaerobic biodegradability as well as developing simple predictive empirical models that could be of significant practical use. The effect of ultrasound pretreatment on particle disintegration was also evaluated. Thereafter, the effect of sonication pretreatment on the anaerobic digestion coefficients and gas production was determined using ADM1. An

empirical model was developed to assess the economical viability of ultrasound based on electrical energy input vs. energy obtained from methane gas produced.

4.2 Materials and method

4.2.1 Experimental Set-up:

Lab-scale ultrasonic treatments were applied to primary sludge (PS) and waste activated sludge (WAS). Eight hundred (800) mL sludge samples from the Adelaide wastewater plant, London, Ontario, Canada were sonicated for 1, 5, 10, 20, 40, and 60 minutes. A 20 kHz 500 W ultrasonic generator (model VC-500 from Sonic and Materials, Connecticut, USA) with a standard probe (Titanium alloy Ti-6Al-4V, 1 inch in diameter, 5³/₄ inch length) was used for this purpose, with ³/₄ of the probe submerged in the sample during sonication. Amplitude was set to 100% and sonication pulse was set to 2 seconds on and 3 seconds off, whereas cooling water bath was used to control sludge temperature, which remained constant at 27°C ± 3°C during the experiments. All samples were placed on a magnetic stirrer with a speed of 350 ± 50 rpm during sonication.

4.2.2 Analytical Methods:

Sludge parameters such as chemical oxygen demand (COD), biological oxygen demand (BOD), total suspended solids (TSS), volatile suspended solid (VSS), volatile fatty acids (VFA), particle size distribution (PSD), lipids, ammonia and total, soluble and bound proteins were measured in triplicates for both primary sludge and WAS after each sonication time. All sludge parameters were analyzed according to the Standard Methods

(APHA, [20]). However, particulate, soluble and bound proteins were analyzed using Lowry et al. [21] Protein was determined by micro-bicinchoninic acid protein assay (Pierce, Rockford, USA), which was modified by Lowry et al. [21] method using a standard solution of bovine serum albumin. Cell protein was calculated as the difference between particulate and bound protein. 50 mL samples were centrifuged at 10,000 rpm for 15 minutes at 5 °C to separate the liquid and solids in the sample. The supernatant was filtered through a 1.5 µm glass microfiber filter (GLAS 934-AH 8.5cm, Whatman) and the filtrate was analyzed for the soluble protein fraction. Bound protein was extracted from the suspended solids by mild pH 8 phosphate buffers (50 µm), while particulate protein representing both the bound protein adsorbed on biomass and the protein within the biomass was extracted by an alkaline 1 N NaOH solution. The solids from the filter were re-suspended to a total volume of 50 mL with pH 8 phosphate buffer (50 µm) for measuring bound protein and 1 N NaOH for particulate protein. The solution was mixed using a magnetic stirrer at 1500 rpm for 10 minutes, and centrifuged at 10,000 rpm for 15 minutes at 5°C, with the centrate filtered through a 1.5 µm glass microfiber filter, prior to protein analysis. The concentrations of VFA were measured from the filtrate after passing the sludge through 0.45 µm filter using a gas chromatograph (Varian 8500, Varian Inc., Toronto, Canada) with a flame ionization detector (FID) equipped with a fused silica column (30 m × 0.32 mm) while a 1µm film thickness. Helium was used as carrier gas at a flow rate of 5 mL/min. The temperatures of the column and detector were 110 and 250 °C, respectively.

The particle size distribution and specific surface area (SSA) were determined by Malvern Mastersizer 2000 (version 5.22) laser beam diffraction granulometer (Malvern

Instruments Ltd, England). Table 4.1 displays the full characteristics of the sludges used in this study.

Table 4. 1 Characteristics of the primary and WAS used in the experiment.

Parameter (mg/L)	Primary Sludge	Waste Activated Sludge
TCOD	40760 ± 2250	22060 ± 1530
SCOD	2175 ± 140	720 ± 25
TSS	31500 ± 2002	22380 ± 1967
VSS	27840 ± 1876	15740 ± 1034
Lipid	4930 ± 193	1647 ± 98
VFA	1064 ± 72	1778 ± 180
Total Protein	2694 ± 187	1478 ± 79
Bound Protein	571 ± 34	350 ± 22
Soluble Protein	242 ± 18	121 ± 11
SBOD	450 ± 30	105 ± 17
Ammonia	436 ± 28	322 ± 18

4.2.3 Batch Anaerobic Digestion:

Batch anaerobic biodegradability studies were conducted to evaluate the effect of sonication on biodegradability and gas production. 90 mL of seed or anaerobic culture (VSS of 12,000 mg/L) obtained from a full scale anaerobic digester at St. Marys, Water Pollution Control Plant (Ontario, Canada) was mixed with 110 mL of primary sludge in 250 mL bottles capped with teflon septum and incubated in a rotary shaker (MaxQ 4000,

Incubator and Refrigerated Shaker, Thermo Scientific, CA) at 37°C and 180 rpm. Similarly, 140 mL of WAS and 60 mL of seed were added together in 250 mL bottles capped with teflon septum. All bottles were sealed after purging the headspace with nitrogen to eliminate the presence of oxygen/air. Twenty three bottles were used for each type of sludge, two bottles were set as blanks and the rest were used for sonicated and non-sonicated samples, three for each sonication time. The volumes of substrate (primary and waste activated sludge) and seed (anaerobic digester sludge) were determined based on food (as COD) to microorganism (as VSS) ratio of 4. For the blank, the substrate volume was replaced by distilled water.

The total gas volume was measured by releasing the gas pressure in the bottles using appropriately sized glass syringes (Perfektum; Popper & Sons Inc., NY, USA) in the 5–100 mL range and equilibrated with the ambient pressure as recommended by Owen et al. [22]. Biogas composition was determined by a gas chromatograph (Model 310, SRI Instruments, Torrance, CA) equipped with a thermal conductivity detector (TCD) and a molecular sieve column (Molesieve 5A, mesh 80/100, 182.88×0.3175 cm). The temperatures of the column and the TCD detector were 90 and 105 °C, respectively. Argon was used as a carrier gas at a flow rate of 30 mL/min. The experiment continued until the increase in methane over a period of one day was only one percent of the prior total volume.

4.2.4 Specific Energy (SE) Input:

SE is defined as the energy input per unit mass of sludge (as TSS) to achieve a certain degree of disintegration. The specific energy input is a function of ultrasonic power (P in kW), sonication time (t in seconds), volume of sonicated sludge (V in L) and TSS concentration (TSS in g/L), and can be calculated using the following equation [23]:

$$SE \text{ (kJ/g TSS)} = \frac{P \times t}{V \times \text{TSS}} \quad \dots \quad (4.1)$$

For primary sludge, sonication times of 1, 5, 10, 20, 40, and 60 minutes correspond to specific energy of 0.5, 2.3, 4.8, 9.1, 17.6, and 24.6 kJ/g TSS, while for WAS the sonication times of 1, 5, 10, 20, 40, and 60 minutes correspond to specific energy of 0.7, 3.2, 6.8, 12.2, 24.9, and 32.9 kJ/g TSS. Furthermore, the specific energy calculated is based on the actual power drawn by the device and does not reflect the efficiency of power transmission to the sludges.

4.2.5 Anaerobic Modeling:

As mentioned earlier, ADM1 is a complex model involving many input parameters which has been discussed in chapter 2. Inhibition and gas transfer are also complex steps in the model. In this study, inhibition due to pH, NH_3 , etc. was ignored for simplicity, and the simulation results were compared with the total methane production. The ADM1 stoichiometric matrix used was the one presented by Batstone et al. [14] and Galí et al. [25]. The stoichiometric matrix contains the components, stoichiometric coefficients and reaction rates [14] are presented in Appendix A.

4.2.6 Statistical analysis:

The student t-test was used to test the hypothesis of equality at the 95% confidence level. The null hypothesis was defined to be: no difference between the two groups tested vs. the alternative hypothesis of there is a statistical difference between the two groups.

4.3 Results and discussion

4.3.1 Chemical Oxygen Demand (COD):

Due to sonication, average SCOD increased from 2175 mg/L to 7405 mg/L and from 720 mg/L to 5070 mg/L after 60 minutes sonication (~25 KJ/g TSS for PS and ~33 KJ/g TSS for WAS) for primary and WAS, respectively. As expected TCOD remained constant with less than 10% variation during sonication and averaged 42180 ± 2629 and 21350 ± 1809 for primary and WAS, respectively. Figure 4.1 shows that the maximum SCOD/TCOD ratio for treated sludge increased from 5.3% to 18% and 3.3% to 27% after 60 minutes (~25 KJ/g TSS for PS and ~33 KJ/g TSS for WAS) of pretreatment for primary and waste activated sludge, respectively.

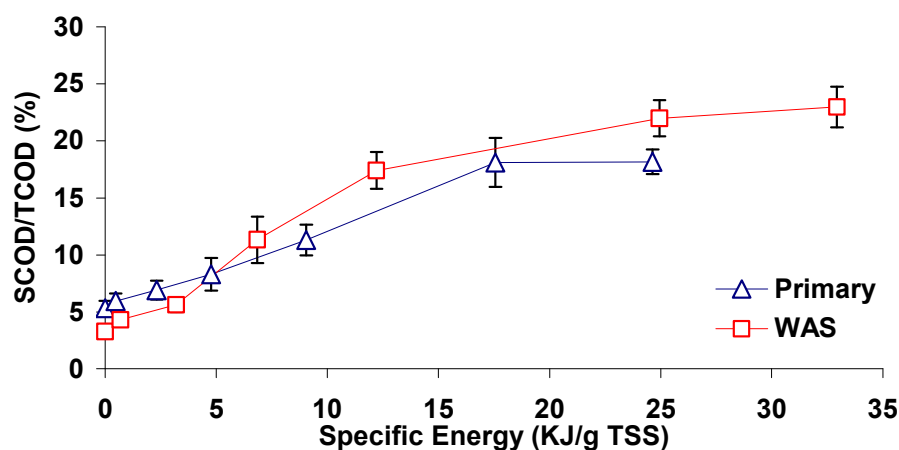


Figure 4.1 SCOD/TCOD ratio as a function of specific energy for primary and waste activated sludge.

It is important to mention that although the SCOD/TCOD ratios in primary and WAS were different, after 60 minutes sonication (12.7% and 23.7% for primary and WAS, respectively), the SCOD released were comparable at 5230 mg/L and 4350 mg/L for primary and WAS, respectively. The increase in SCOD/TCOD ratio is due to the release of extracellular polymeric substances (EPS), i.e., polysaccharides, proteins etc., which are embedded in the floc matrix [26], that is disintegrated due to sonication. This shows that sonication influences solubilization of particulate COD as the ratio increases with sonication, however the final SCOD/TCOD ratios suggest that the majority of the particulate matter was not solubilized.

4.3.2 Biological Oxygen Demand (BOD):

Due to sonication, soluble biological oxygen demand (SBOD) increased from 450 to 1032 mg/L and from 105 to 975 mg/L after 60 minutes sonication (~25 KJ/g TSS for PS

and ~ 33 KJ/g TSS for WAS), for primary and WAS, respectively. The initial rate of SBOD release of 207 mg/L per kJ/g TSS for WAS was higher than the 52 mg/L per kJ/g TSS observed for primary sludge. Figure 4.2 shows the ratio of SBOD to TCOD for both primary and WAS as a function of specific energy; SBOD/TCOD ratio increased due to sonication of the organic matters from 1.1% to 2.5% and 0.5% to 4.4% (582 mg SBOD/L) and (870 mg SBOD/L) after 60 minutes for primary and WAS, respectively.

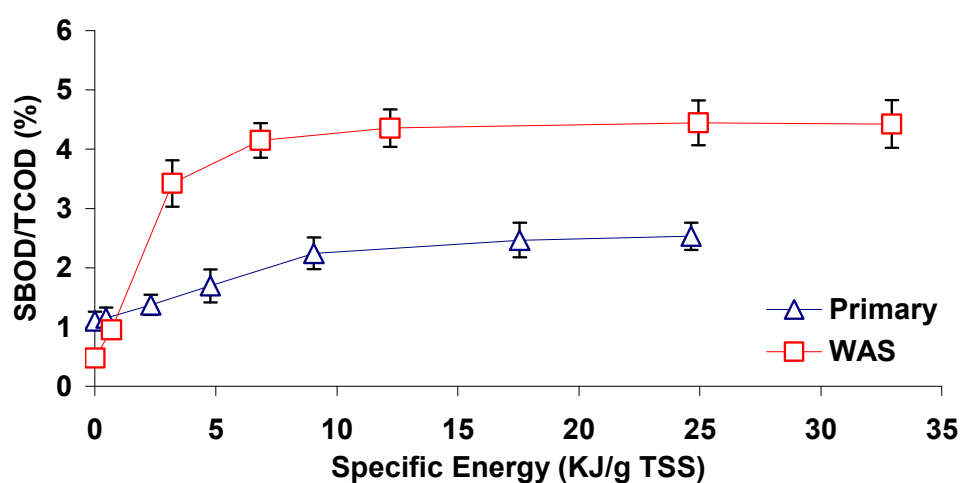


Figure 4.2 SBOD/TCOD ratio as a function of specific energy for primary and waste activated sludge.

Furthermore, it is noticeable that the SBOD/TCOD ratio almost reached a plateau after 20 minutes sonication (4.35% and 2.47% for WAS and primary, respectively). This increase in biodegradable organic matter is an indication of the potential enhancement of sludge digestion [10, 27, 29].

4.3.3 Proteins:

Dimock and Morgenroth [30], divided proteins in wastewater and sludge into three fractions: soluble, bound/labile (loosely attached with the cells) and tightly bound fractions (within the bacterial cells). Labile proteins are thought to become readily bioavailable giving rise to higher odor potential [31]. Particulate (cell + bound), soluble, and bound protein were monitored in this study.

An increase in soluble protein from 242 to 1335 and 121 to 956 mg/L was observed for primary and WAS, respectively, simultaneous with a decrease in particulate protein from 2694 to 884 and 1478 to 876 mg/L, and a decrease in bound protein from 571 to 452 and 350 to 163 mg/L during sonication. Particulate protein, which is the cellular and extracellular protein loosely bound to the cell, disintegrated and was mostly converted into soluble protein. It was observed that the overall protein (total protein + soluble protein) remained constant at 2476 ± 331 mg/L for specific energy in the range of 0 to 25 kJ/g TSS for primary and 1802 ± 117 for specific energy in the range of 0 to 33 kJ/g TSS for WAS. Figures 4.3, 4.4, and 4.5 show the variation of particulate, soluble, and bound protein per TCOD with specific energy, while Figures 4.6 and 4.7 depict the variation of bound protein per mg VSS with specific energy for primary sludge and WAS, respectively.

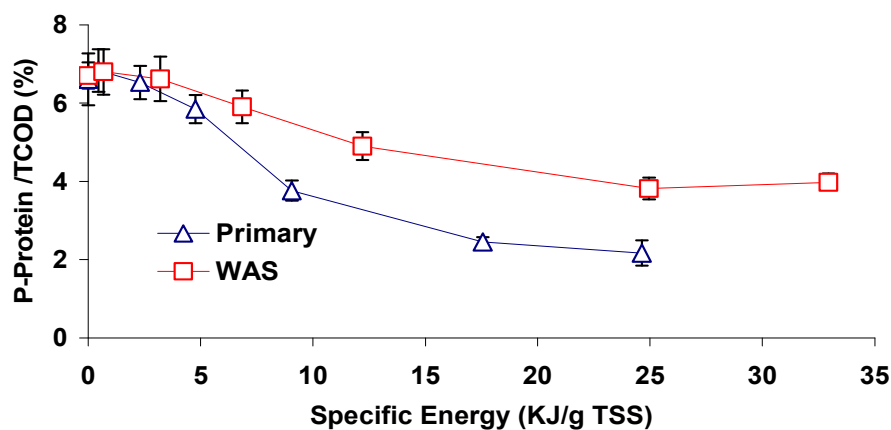


Figure 4.3 Particulate protein/TCOD as a function of specific energy for primary and waste activated sludge.

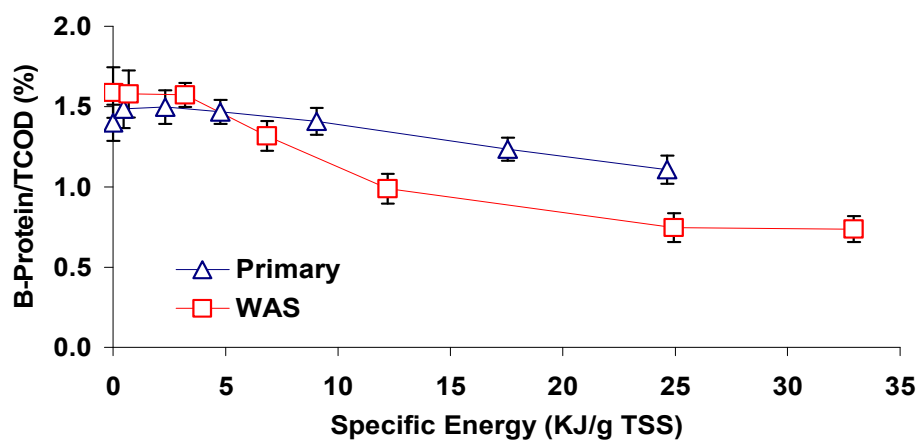


Figure 4.4 Bound protein/TCOD as a function of specific energy for primary and waste activated sludge.

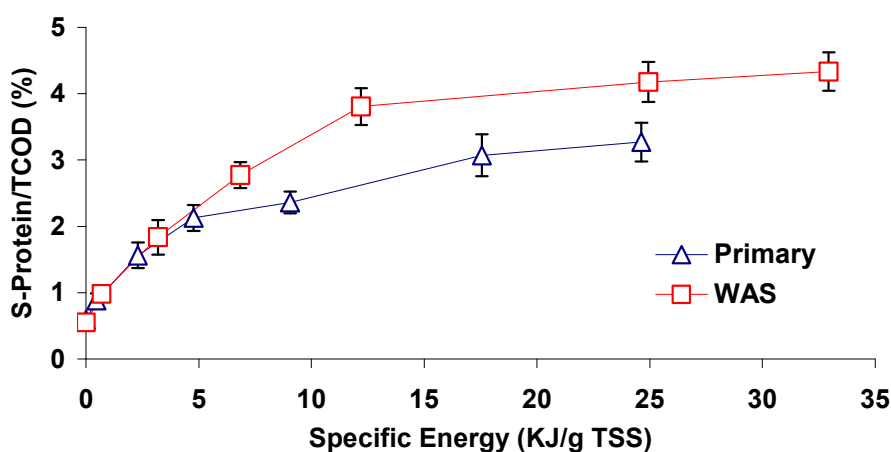


Figure 4.5 Soluble protein/TCOD as a function of specific energy for primary and waste activated sludge

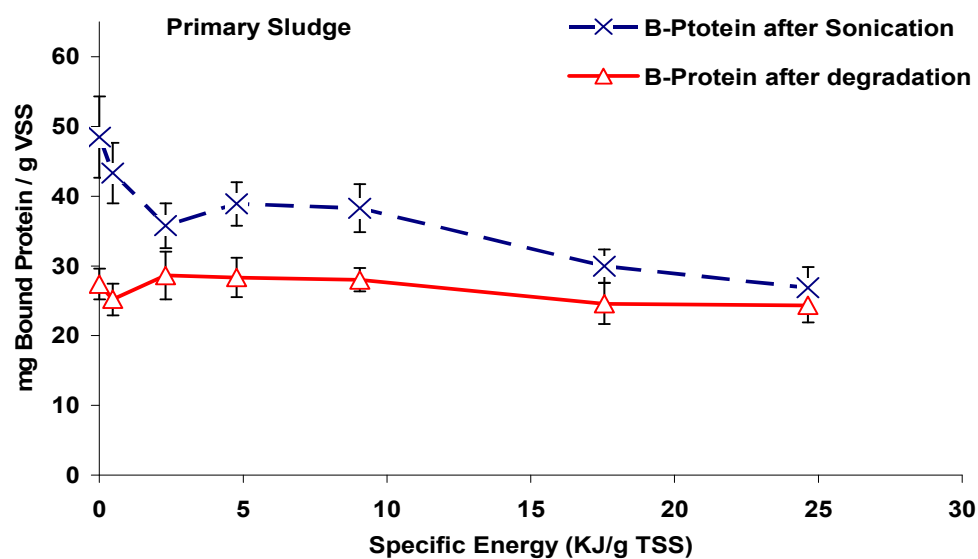


Figure 4.6 Bound protein / mg VSS as a function of specific energy for primary sludge during anaerobic digestion.

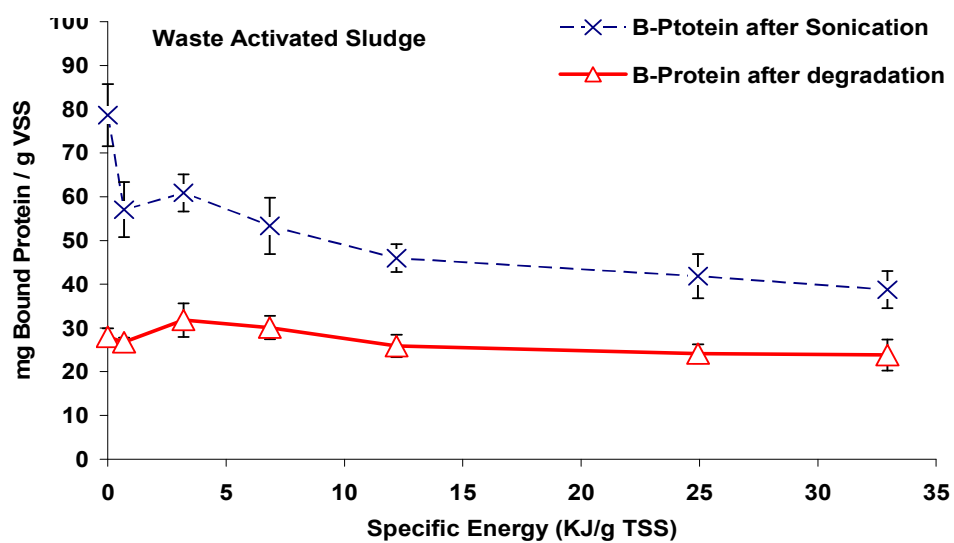


Figure 4.7 Bound protein / mg VSS as a function of specific energy for waste activated sludge during anaerobic digestion.

After 60 minutes of sonication the bound protein/TCOD decreased from 1.4% to 1.1% and 1.6% to 0.8%; particulate protein/TCOD decreased from 6.6% to 2.2% and 6.7% to 4%; and soluble protein/TCOD increased from 0.6% to 3.3% and 0.6% to 4.4% for primary and WAS, respectively. While this marginal decrease in bound protein may reflect the beneficial impact of ultrasound on the odor precursors in biosolids, there are two major concerns, namely the cost of energy and equally important is the anaerobic biodegradability. After anaerobic digestion, the percentage reductions in bound protein for sludges sonicated at 0, 1, 5, 10, 20, 40, and 60 minutes were 63%, 62%, 48%, 54%, 52%, 45%, and 40% for primary and 73%, 70%, 62%, 57%, 53%, 48%, and 44% for WAS, as depicted in Figures 4.6 and 4.7. The t-test method was conducted to compare the digested bound protein in both primary and WAS. The null hypothesis i.e, there are no differences between bound protein in both sludges, has been accepted based on the calculated t-value (2.23) and P-value of 0.68 at 95% confidence level. Thus, it can be concluded that there was no statistically significant difference in the digested bound proteins between primary and WAS samples, with the primary being in the range of 23.2-28.6 vs. 23.8-31.9 mg protein/ gVSS for the WAS. The results suggest that there is no enhancement in the final degradation of bound protein after digestion in both sludges due to sonication.

Figure 4.8 depicts the cell protein released, calculated as particulate protein less the bound protein, as a function of specific energy for both PS and WAS. It is clear from Figure 4.8 that low sonication times in the range of 0 to 5 minutes have no effect on the microbial cells as reflected by the initial lag-phase on the curves.

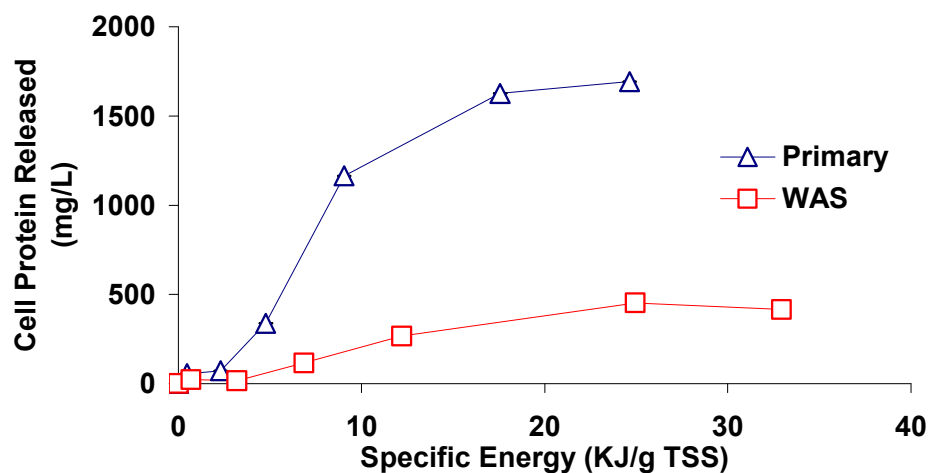


Figure 4.8 Cell proteins released as a function of specific energy for primary and waste activated sludge.

After 5 minutes of sonication (~ 2.3 KJ/g TSS for PS and 3.2 KJ/g TSS for WAS) a slow increase in WAS cell protein release relative to the fast increase in primary sludge was experienced, with WAS increasing from 20 to 415 mg/L vs. 70 to 1690 mg/L in the case of primary, clearly emphasizing that microbial cells in the WAS are harder to rupture than the microbial cells in primary sludge. Moreover, sonication energy of less than 5 kJ/g TSS appears to have no effect on microbial cells in both types of sludges.

4.3.4 Volatile Fatty Acids (VFA):

VFA increased from 1065 mg/L to 1795 mg/L and from 1778 mg/L to 2932 mg/L after 60 minutes of sonication, for primary and WAS, respectively. Figure 4.9 depicts that the VFA/TCOD ratio increases with increasing specific energy; the ratio distinctly increased in the case of waste activated sludge but not as much as in the case of primary sludge.

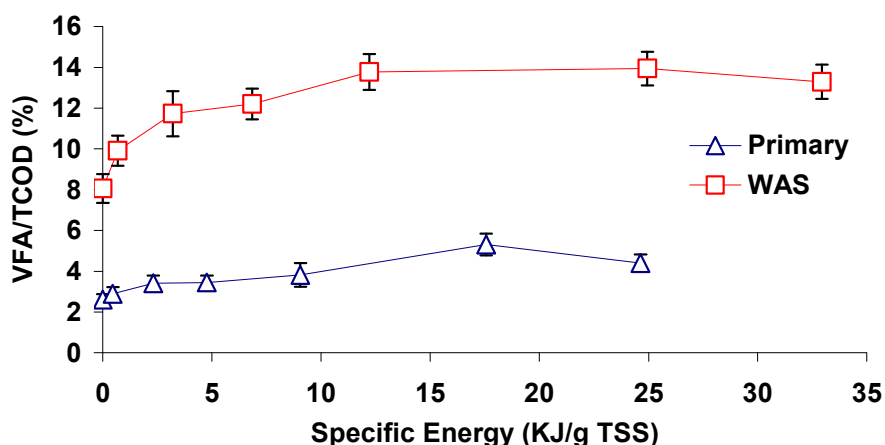


Figure 4.9 VFA/TCOD as a function of specific energy for primary and waste activated sludge.

VFA/TCOD ratio for treated sludge increased from 2.6% to 4.4% and from 8.1% to 13.3% after 60 minutes of pretreatment for primary and WAS, respectively. The observed increase in VFA is similar to the observation of Appels et al. [32], who sonicated WAS at 3.8% to 4.85 % solids (38.1 to 48.5 g dry solid/kg) at 1.25 kJ/g TS and observed an increase in VFA from 94.4 to 565 mg/L. The ratio of VFA released (730 and 1154 mg/L) to SCOD released (5230 and 4350 mg/L) was 14% and 27% for primary and WAS, respectively. The increase in VFA is probably due to oxidation of larger hydrocarbons by the hydroxyl radicals produced during the explosion of cavitation bubbles [32]. However, the observation that VFA increased by about 1150 mg/L in WAS and only 730 mg/L in primary sludge coupled with the much higher cell protein destruction in the primary sludge relative to the WAS (Figure 4.8) indicates that a possible microbial role can not be ruled out.

4.3.5 Particle Size Distribution:

The particle size distributions by volume fraction as a function of sonication time are shown in Table 4.2 for primary and WAS.

Table 4. 2 The median, 10%ile and 90%ile for the volume fraction of the primary and WAS.

	Spec. Energy. (KJ/g TSS)	d(10)	d(50)	d(90)
Primary Sludge	0	17.7	59.4	126.3
	0.5	8.1	26.2	79.8
	2.3	5.8	19.9	56.5
	4.8	5.5	20.9	79.8
	9.1	4.8	23.4	76.6
	17.6	1.5	18.5	-
	24.6	1.5	13.3	-
WAS	0.0	23.7	107.0	297.2
	0.7	9.8	40.5	135.3
	3.2	6.2	20.8	78.7
	6.8	6.1	16.1	37.3
	12.2	6.5	16.4	34.8
	24.9	6.4	15.9	32.1
	32.9	5.1	12.2	28.9

The results clearly show the change in particle size. In the case of primary sludge, the median (d_{50}) of the particle size decreased by 78% from 59.4 to 18.3 μm after 60 minutes of sonication and by 89% from 106.6 to 20.2 μm , in the case of WAS. Since hydrolysis is predominantly dependent on surface area rather than volume [33, 34], the hydrolysis rate decreased when the biomass concentration was high, as mass transfer limitations were observed due to limited surface area [35], and hence the impact of sonication on specific surface area (SSA) was examined. Figure 4.10 shows the specific surface area (m^2/g) as a function of specific energy.

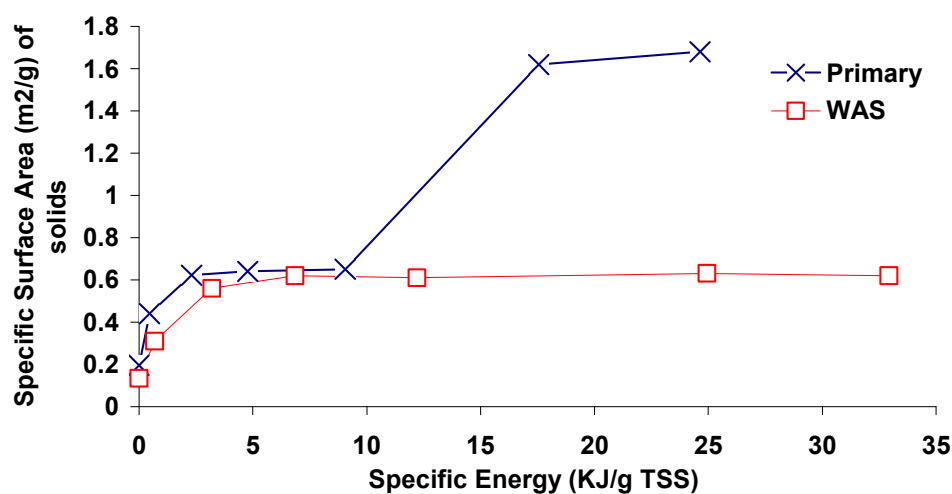


Figure 4.10 Specific surface area (m^2/g) as a function of specific energy.

It is interesting to note that no significant effect on SSA was experienced after 5 minutes (3.2 KJ/g TSS) sonication in the case of WAS as it reaches a plateau of $\sim 0.62 \text{ m}^2/\text{g}$. This finding suggested that with sonication pretreatment, particle size can only be reduced to a certain level in the case of WAS. The primary sludge, however, reaches the same SSA of $0.62 \text{ m}^2/\text{g}$ between 5 and 20 minutes of sonication, an increase (from 0.62 to $\sim 1.4 \text{ m}^2/\text{g}$) in SSA was experienced after 40 minutes sonication ($\sim 17 \text{ kJ/gTSS}$).

4.3.6 Methane Production:

Figures 4.11 and 4.12 show the cumulative $\text{mL CH}_4 / \text{g COD}_{\text{added}}$ produced from primary and WAS, respectively.

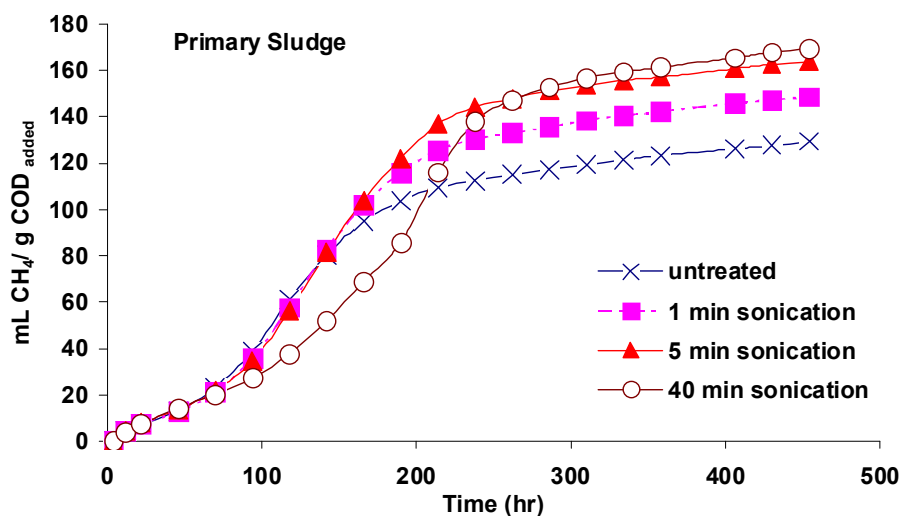


Figure 4.11 Methane yield of the untreated and treated primary sludge over the digestion time

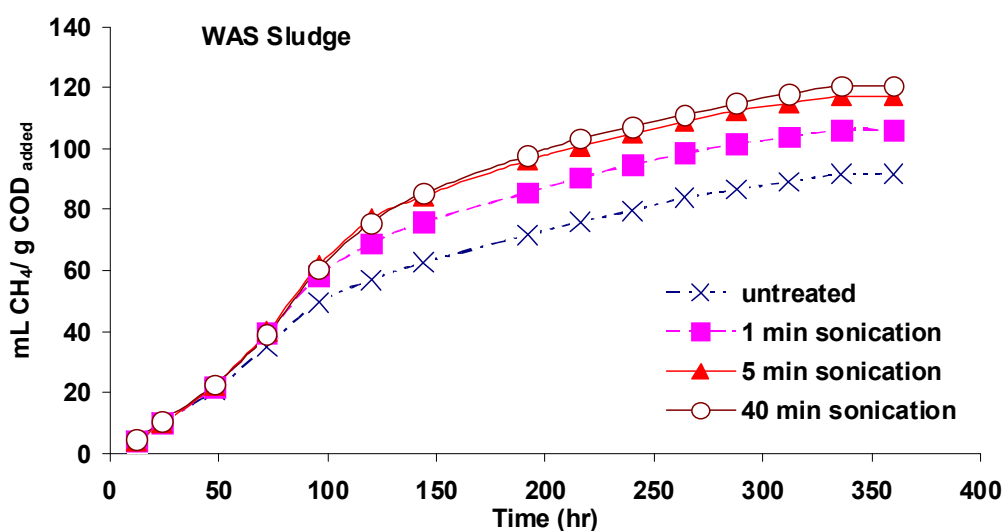


Figure 4.12 Methane yield of the untreated and treated waste activated sludge over the digestion time

The primary sludge results however exhibited an interesting pattern; the maximum rate of methane production remained constant at 3.65 ± 0.21 mL/h for low sonication times of 0 to 10 minutes, but decreased significantly with higher sonication time to 1.99 and 1.66

mL/h at 40 and 60 minutes. This decrease of maximum methane production rate at sonication times of 40 and 60 minutes corresponding to specific energies of 17.6 and 24.6 kJ/g TSS is consistent with the sharp decrease in biomass (as reflected by cell protein release) from 338 to 1691 mg/L after 10 minutes of sonication depicted in Figure 4.8. This pattern was not observed in the case of WAS, where the maximum rate of methane production increased from 1.66 mL/h in the untreated sample to 2.15, 2.28, 2.18, 2.08, and 2.12 mL/h for sonication times of 1, 5, 10, 20, 40, and 60, respectively. The results show that there is no significant change in the maximum rate after one minute sonication, as the average \pm standard deviation was 2.17 ± 0.07 . Table 4.3 displays the percentage increase in ultimate methane (CH₄) production in primary and WAS; 28% and 25% enhancement in methane production were observed after 5 minutes of sonication for primary and WAS, respectively.

Table 4. 3 Percentage of CH₄ increase in primary and waste activated sludge as a function of sonication time.

Sonication time (min)	Percent of CH ₄ increase (%)	
	Primary Sludge	Waste Activated Sludge
1	16	16
5	28	25
10	29	25
20	31	25
40	36	24
60	38	26

The methane production did not increase significantly with further increases in sonication time in the case of WAS, after 5 minutes the percentage increase in methane production varied randomly between 24% and 26%. However, the percentage increase in methane

production reached 38% in the case of primary at 60 minutes sonication due to higher COD solubilization.

4.3.7 Anaerobic Modeling:

In this study, based on the ADM1 steady-state model, equations were rearranged to simulate the anaerobic digestion in batch reactors. AQUASIM 2.1 was used to solve the dynamic differential and algebraic system of equations. Total protein, lipid, carbohydrate and VFAs were the model inputs with protein based on $C_6H_{14}O_2N_2$, lipid based on $C_{57}H_{104}O_6$ [36], carbohydrate (estimated from the particulate COD mass balance), acetate, propionate, and butyrate [14]. Table 4.4 presents the ADM1 input sludge characterization at different sonication times.

The model parameters (reaction coefficients) and degraders were set to the default values suggested by the ADM1 technical report [14]. The various components of biomass i.e. sugar degraders, amino acid degraders, long chain fatty acid degraders, valerate and butyrate degraders, propionate degraders, acetate degraders, and hydrogen degraders, were set at 200 mgCOD/L following the recommendation of Jeong et al. [37], who evaluated the sensitivities of the kinetic and stoichiometric ADM parameters in predicting anaerobic glucose digestion and concluded that biomass was closely associated with the Monod maximum specific uptake rate, that values could not be independently determined and verified.

Table 4. 4 Primary and WAS sludge characterization for ADM1

			Sonication time						
		Description	0	1	5	10	20	40	60
Primary (mg COD/L)	X_pr	Proteins	15858	16144	16138	14451	12557	10183	9770
	X_li	Lipids	14192	14200	13831	12060	11740	10852	10703
	X_ch	Carbohydrate	8824	9590	10800	10988	12102	12673	13170
	S_ac	Acetic acid	330	393	534	544	650	670	835
	S_pro	Propionic acid	237	272	323	340	377	382	384
	S_bu	Butyric acid	497	514	535	523	534	555	576
WAS (mg COD/L)	X_pr	Proteins	11689	11736	11729	10406	9219	8805	8024
	X_li	Lipids	4743	4805	4962	4617	4354	4299	3916
	X_ch	Carbohydrate	5281	5084	5371	4461	4546	4341	4141
	S_ac	Acetic acid	719	1085	1221	1346	1701	1778	1912
	S_pro	Propionic acid	498	547	701	681	673	633	688
	S_bu	Butyric acid	562	553	664	665	664	665	682

The typical variations of methane production with time at different sonication intensities obtained from the batch experiments were used to optimize the model parameters, namely, k_{m_c4} (valerate and butyrate) and k_{m_ac} (acetate) using the automated Parameter Estimation feature available in AQUASIM. The default value of k_{m_c4} and k_{m_ac} were changed based on the estimation results from 0.833 to 1.092 hr^{-1} and 0.333 to 1.154 hr^{-1} , respectively for primary sludge and from 0.333 to 0.526 hr^{-1} for k_{m_ac} in the case of WAS. It must be noted that the ADM1 report has indicated that variations of 30% and 300% in k_{m_c4} and k_{m_ac} from the default values are acceptable. Figures 4.13 and 4.14 show

comparison of the ADM predicted and measured methane yield, expressed in mLCH₄ per unit gram of COD added.

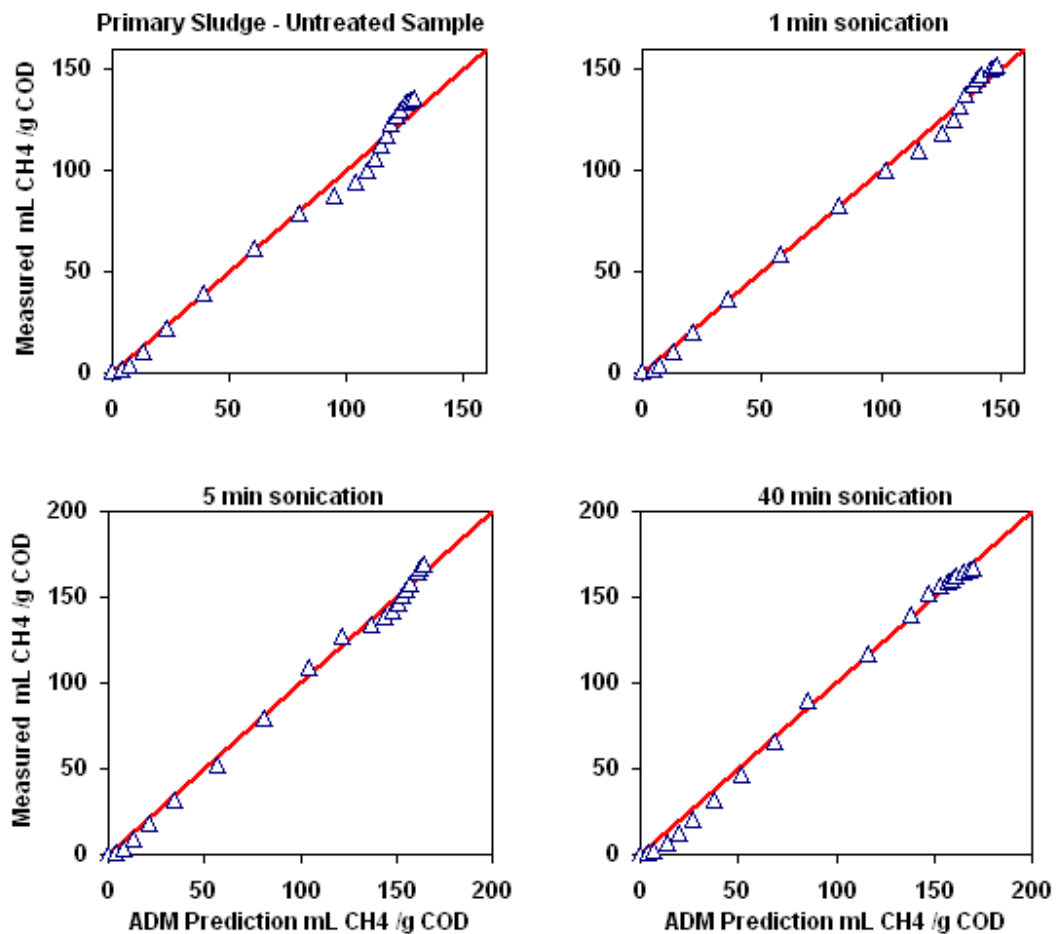


Figure 4.13 Predicted and measured methane yields for the untreated and treated primary sludge.

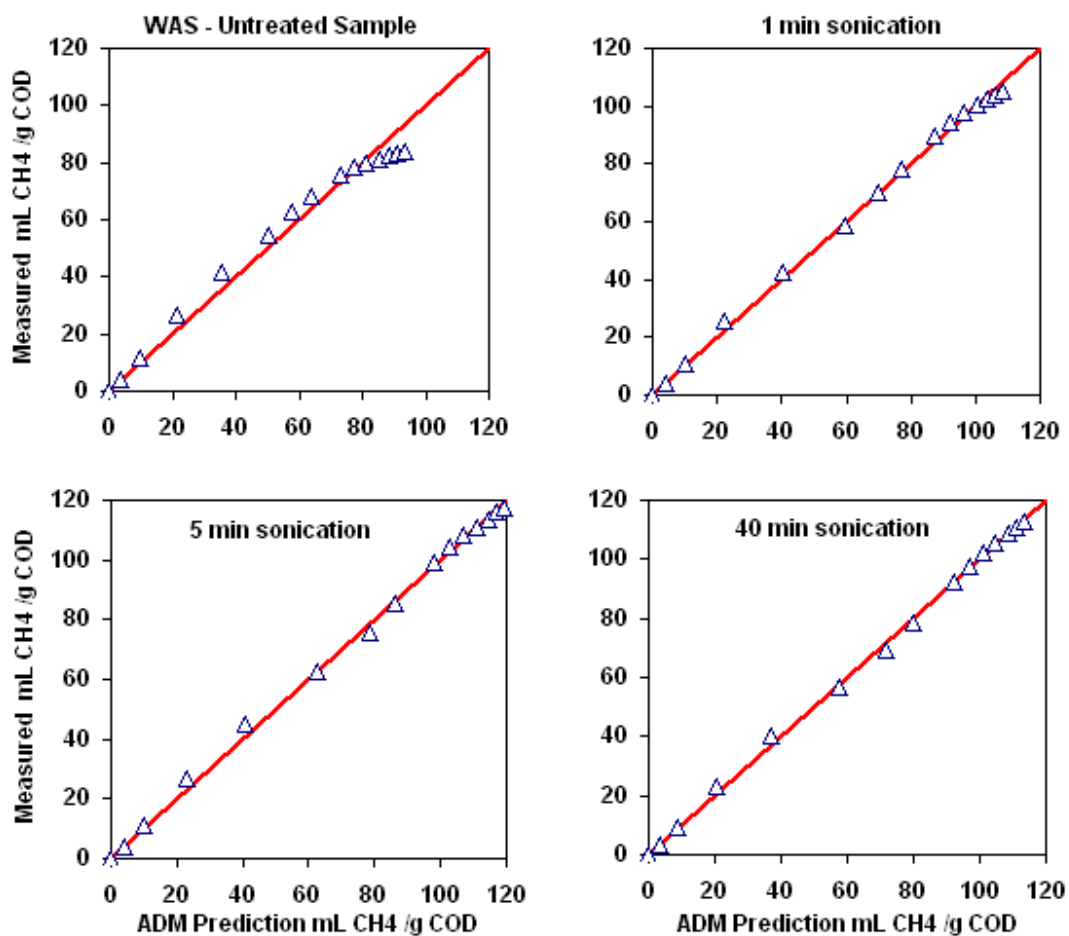


Figure 4.14 Predicted and measured methane yields for the untreated and treated WAS.

It is evident that the model results with optimized parameters showed good agreement with the experimental data for methane production with average percentage error defined as $(\text{measured} - \text{predicted}) / \text{measured} * 100\%$ of 13%, 11%, 15%, and 20% for primary and 9%, 3%, 4%, and 3% for WAS at sonication times of 0, 1, 5, and 40 minutes, respectively. Furthermore, the spread of the data on both sides of the diagonal line confirms that the ADM model does not systematically over-predict or under-predict the experimental data. Table 4.5 compares the model and measured concentrations of

volatile fatty acids for both primary and WAS. It is evident from Table 4.5 that in general the ADM model predictions for the individual volatile acids and the overall VFA are well within the range of experimental data i.e, average \pm standard deviation.

Table 4. 5 Predicted and Measured Concentrations (average \pm Stdev) of acetic, butyric, propionic acids, and VFA after anaerobic digestion

	SE (KJ/g TSS)	Acetic acid (mg COD/L)			Butyric acid (mg COD/L)		
		Input	Output Exp.	Output ADM	Input	Output Exp.	Output ADM
PS	0.0	330 \pm 29.7	13 \pm 1.3	11	237 \pm 28.5	43 \pm 4.3	42
	0.5	392 \pm 31.4	56 \pm 5.1	15	272 \pm 29.9	51 \pm 5.1	53
	2.3	533 \pm 37.3	47 \pm 3.3	42	323 \pm 42.0	124 \pm 11.2	111
	4.8	543 \pm 48.9	64 \pm 5.1	54	340 \pm 27.2	181 \pm 14.5	129
	9.1	649 \pm 51.8	67 \pm 6.7	63	377 \pm 26.4	278 \pm 22.3	289
	17.6	669 \pm 66.6	68 \pm 7.5	65	382 \pm 34.4	350 \pm 31.5	320
	24.6	835 \pm 91.7	73 \pm 6.5	0	384 \pm 42.3	352 \pm 24.7	323
WAS	0.0	719 \pm 71.8	205 \pm 20.5	175	562 \pm 50.6	505 \pm 60.6	498
	0.7	1085 \pm 79.7	487 \pm 48.7	428	553 \pm 44.3	488 \pm 53.6	467
	3.2	1221 \pm 85.5	548 \pm 49.3	502	664 \pm 46.5	647 \pm 84.1	621
	6.8	1346 \pm 107.7	567 \pm 45.4	594	665 \pm 59.8	643 \pm 51.4	628
	12.2	1701 \pm 177.8	966 \pm 77.3	987	664 \pm 53.1	589 \pm 41.2	577
	24.9	1778 \pm 195.5	987 \pm 89.3	1071	665 \pm 66.5	645 \pm 58.0	633
	32.9	1702 \pm 153.2	998 \pm 69.9	1010	612 \pm 67.3	544 \pm 59.9	588

	SE (KJ/g TSS)	Propionic acid (mg COD/L)			VFA_in (mg COD/L)		
		Input	Output Exp.	Output ADM	Input	Output Exp.	Output ADM
PS	0.0	497 ± 59.7	209 ± 20.9	198	1065 ± 127.8	265 ± 26.5	251
	0.5	514 ± 56.6	261 ± 26.1	277	1178 ± 129.6	369 ± 33.2	346
	2.3	535 ± 69.5	323 ± 29.0	323	1391 ± 180.8	493 ± 34.5	471
	4.8	523 ± 41.9	354 ± 28.3	340	1406 ± 112.5	599 ± 47.9	514
	9.1	534 ± 37.4	386 ± 30.9	377	1559 ± 109.1	731 ± 73.1	729
	17.6	555 ± 49.9	396 ± 35.6	380	1606 ± 144.5	814 ± 89.6	755
	24.6	576 ± 63.3	396 ± 27.7	340	1795 ± 197.4	821 ± 73.9	664
WAS	0.0	498 ± 49.8	473 ± 42.6	460	1778 ± 213.4	1183 ± 106.5	1133
	0.7	547 ± 49.2	450 ± 36.0	452	2185 ± 240.4	1425 ± 114.0	1347
	3.2	701 ± 49.1	599 ± 41.9	662	2586 ± 336.2	1794 ± 125.6	1785
	6.8	681 ± 54.5	625 ± 56.2	663	2692 ± 215.4	1835 ± 165.1	1885
	12.2	673 ± 67.3	659 ± 52.7	662	3038 ± 212.7	2214 ± 175.1	2226
	24.9	633 ± 69.6	594 ± 59.4	613	3076 ± 276.8	2225 ± 222.5	2317
	32.9	618 ± 55.6	591 ± 65.0	580	2932 ± 322.5	2133 ± 234.7	2178

Table 4.6 displays the ADM model parameters variations at different sonication times. As expected and described in the ADM1 technical report, the acetic acid is the most sensitive parameter in the dynamic system [14].

Table 4. 6 Primary and WAS sludge model parameters at different sonication times.

			Sonication time											
Parameter		0	1	5	10	20	40	60						
Primary Sludge	k_{hyd_CH}	Carbohydrate	0.25	No Change										
	k_{hyd_PR}	Proteins	0.2											
	k_{hyd_LI}	Lipids	0.1											
	k_{m_su}	Sugar	0.03											
	k_{m_aa}	Amino acid	0.05											
	k_{m_fa}	LCFA	0.006											
	k_{m_c4}	Butyric & Valeric acid	1.092	1.001	0.914	0.885	0.842	0.769	-					
	k_{m_pro}	Propionic acid	0.013	No Change										
	k_{m_ac}	Acetic acid	1.154	1.157	0.992	0.996	0.830	0.803	-					
	k_{m_h2}	Hydrogen	0.035	No Change										
WAS Sludge	k_{hyd_CH}	Carbohydrate	0.25	No Change										
	k_{hyd_PR}	Proteins	0.2											
	k_{hyd_LI}	Lipids	0.1											
	k_{m_su}	Sugar	0.03											
	k_{m_aa}	Amino acid	0.05											
	k_{m_fa}	LCFA	0.006											
	k_{m_c4}	Butyric & Valeric acid	0.833	No Change										
	k_{m_pro}	Propionic acid	0.013											
	k_{m_ac}	Acetic acid	0.526						0.428	0.422	0.401	0.356	0.354	0.34 4
	k_{m_h2}	Hydrogen	0.035						No Change					

As the acetic acid concentration increased with sonication time, the simulated reaction coefficient of the acetic acid decreased. This result is not intuitive as the reaction rates of the VFAs are influenced by both the reaction rate constant and the concentration of the VFAs in the sludge. As can be seen in Table 4.6, the acetic acid concentration increased with increasing sonication time for both primary sludge and WAS. However, the decrease in the rate constant is only about 30%-34% for both sludges, which also corresponds to the increased CH₄ yield in both the cases (about 26%-38%).

4.3.8 Economic Viability of Ultrasound:

An empirical model was developed to illustrate the relationship between CH₄ increase and specific energy for primary and waste activated sludge. The model was then used to verify the economical viability of ultrasonic pretreatment. Figures 3.15 and 3.16 show the empirical model for primary and waste activated sludge, respectively.

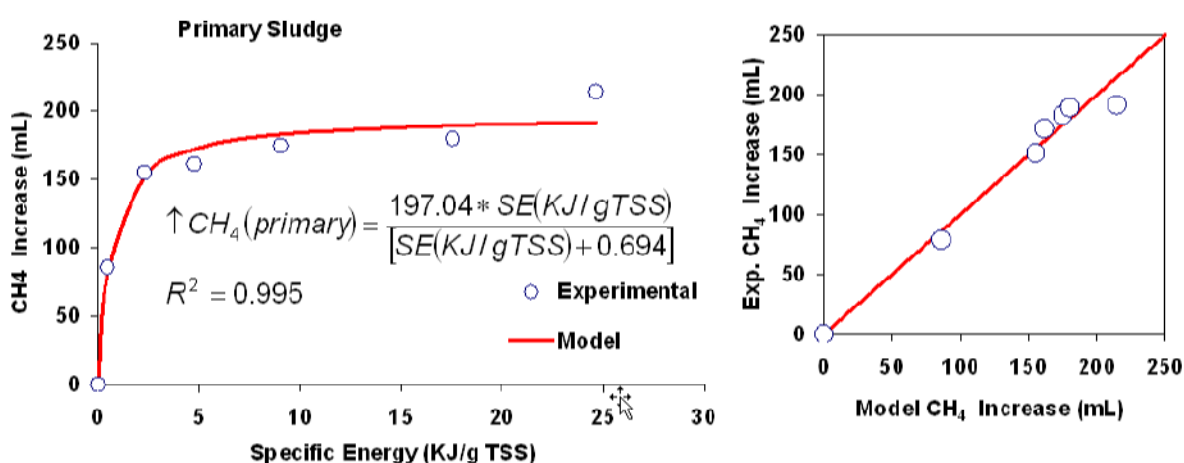


Figure 4.15. Increase in volume of methane produced in treated primary sludge

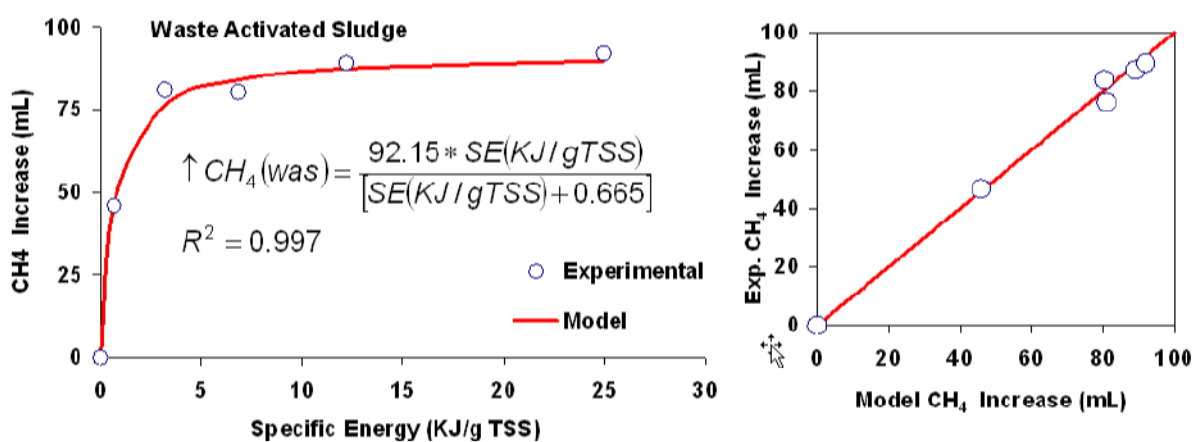


Figure 4.16 Increase in volume of methane produced in treated WAS.

The results are presented in Table 4.7, which shows the specific energy input per ton of TCOD, as well as the value of the methane produced based on power and natural gas costs of \$0.07/kWh and \$0.28/m³, respectively. The Power (\$)/ ton CODin was conducted using the formula shown below:

$$\text{Power (\$/ ton CODin)} = \text{power (kW.h)} / [\text{TCODin (ton)} * \text{volume (L)}] * \text{power cost (\$)}$$

It must be asserted that the sonication power used in the economic evaluation is the “real” power drawn by the sonicator and not the “actual” power transmitted to the liquid sludge since no information was available on the efficiency of the ultrasonic generator. It is evident that ultrasonic pretreatment is not economically viable for high specific energy. However, it is economically viable for primary sludge at low sonication doses of 0.1, 0.5, and 1 kJ/g TSS (values in bold). The empirical model can be used to estimate the increase in methane production for different sludges using different values of specific energy.

Table 4.7 Specific energy, power and methane energy per ton of COD using the empirical model.

SE (kJ/g TSS)	Per ton COD in			
	Primary Sludge TCOD = 40765 mg/L		WAS TCOD = 22058 mg/L	
	Power (\$)	CH ₄ (\$)	Power (\$)	CH ₄ (\$)
0.1	3.63	8.52	6.70	5.10
0.5	18.13	28.34	33.50	16.74
1	36.25	39.94	66.99	23.42
2	72.50	50.24	133.99	29.26
4	145.01	57.66	267.98	33.44
10	362.52	63.28	669.94	36.56
15	543.77	64.68	1,004.91	37.34

4.4 Conclusions

The effect of pretreatment of both primary and waste activated sludge using ultrasound can be summarized as follows:

- After 60 minutes of sonication corresponding to specific energy of ~25 kJ/g TSS for primary and ~33 kJ/g TSS for WAS, SCOD/TCOD ratio increased from 5.5% to 18% and 3.3% to 27%, SBOD/TCOD ratio increased from 1.1% to 2.5% and 0.5% to 4.4%, VFA/TCOD ratio increased from 2.6% to 4.4% and from 8.1% to 13.3%, bound protein/TCOD decreased from 1.4% to 1.1% and 1.6% to 0.8%; total protein/TCOD decreased from 6.6% to 2.2% and 6.7% to 4%; and soluble protein/TCOD increased from 0.6% to 3.3% and 0.6% to 4.3%, while total methane production increased by 28% and 25% after 5 minutes of sonication for primary and WAS, respectively.

- The effect of sonication on digested bound protein was not statistically significant for both primary and WAS samples at 95% confidence.
- Although, there is an increase in sludge surface area with sonication, no significant effect on specific surface area was found after 5 minutes of (3.2 KJ/g TSS) sonication in the case of WAS but for the primary sludge specific surface area increased by 8 times after 40 minutes of sonication (~17 kJ/gTSS).
- The Anaerobic Digestion Model #1 (ADM1) predicted well both the methane production and volatile fatty acids concentrations. The simulated rate constants for acetic acid and butyric acid uptake decreased by 30%-34% with sonication time.
- Ultrasound is neither economical for biogas enhancement despite the high solubilization of COD, nor effective in enhancing the biodegradability of bound proteins. However, at low sonication energy of 0.1, 0.5, and 1 kJ/g TSS, the process is economical for primary sludge only.

4.5 References

- [1] Karakashev, D.; Thomsen, A. B.; Angelidaki, I. Anaerobic biotechnological approaches for production of liquid energy carriers from biomass, *Biotechnology Letters*, 2007, 1005-1012.
- [2] Amon, B. A.; Boxberger, J.; Alt, C. Emissions of NH₃, N₂O and CH₄ from dairy cows housed in a farmyard manure tying stall (housing, manure storage, manure spreading). *Nutr Cycl Agroecosyst*. 2001, 60, 103-113.
- [3] Lens, P.; Westmann, P.; Haberbauer, M. and Moreno, A. *Biofuel for Fuel Cells* Tunbridge Wells. UK, IWA Publishing. 2005.
- [4] Claassen, P. A. M.; van Lier, J. B.; Lopez Contreras, A. M.; van Niel, E. W. J.; Sijtsma, L.; Stams, A. J. M.; de Vries, S. S.; Weusthuis, R. A. Utilisation of biomass for the supply of energy carriers. *Appl. Microbiol. Biotechnol.*, 1999. 52, 741–755.
- [5] Eastman, J. A.; Ferguson, J.F., Solubilization of particulate organic carbon during the acid phase of anaerobic digestion. *J. Water Pollut. Control Fed.* 1981, 53, 352–366.
- [6] Harrison, S.T.L., Bacterial cell disruption: a key unit operation in the recovery of intracellular products, *Biotechnol*, 1991, 9, 217–240.
- [7] Suslick, K. Sonochemistry. The temperature of cavitations. *Science*. 1991, 253, 1397–1399.
- [8] Kuttruff, H. Essex, England, *Ultrasonics Fundamentals and Applications*. Elsevier Science 1991.

- [9] Hwang, K. Y.U; Shin, E.B; Choi, H.B., A mechanical pretreatment of waste activated sludge for improvement of anaerobic digestion system, *Water Sci. Technol.* 1997, 36 , 213-220.
- [10] Tiehm, A.; Nickel, K.; Neis, U. The use of ultrasound to accelerate the anaerobic digestion of sewage sludge. *Water Sci. Technol.* 1997, 36, 121–128.
- [11] Cao, X. Q. Enhanced sludge decomposition by ultrasound. The R & D Centre for Sustainable Environmental Biotechnology, Beijing Inst. of Civil Engineering, 2004.
- [12] Brown, J. P., Ultrasonic solids treatment yields better digestion. WERF, Biosolids Technical Bulletin. 2004.
- [13] Gavala, H. N.; Angelidaki, I.; Ahring, B.K. Kinetics and modeling of anaerobic digestion process. *Adv. Biochem. Eng. Biotechnol.* 2003, 81, 57-93.
- [14] Batstone, D. J.; Keller, J.; Angelidaki, I.; Kalyuzhnyi, S.V.; Pavlostathis, S.G.; Rozzi. A.; Sanders, W.T.M.; Siegrist, H.; Vavilin, V.A., Anaerobic Digestion Model No. 1. IWA Task Group for Mathematical Modelling of Anaerobic Digestion Processes 1-77. *Water Sci. Technol.* 2002, 45, 65–73.
- [15] Batstone D.J.; Keller J., Industrial applications of the IWA anaerobic digestion model No. 1 (ADM1), *Water Sci. Technol.* 2003, 47, 199-206.
- [16] Johnson B.A.R.; Shang Y., Applications and limitations of ADM 1 in municipal wastewater solids treatment, *Water Sci. Technol* 2006, 54, 77–82.
- [17] Blumensaat, F.; Keller J.; Modelling of two-stage anaerobic digestion using the IWA Anaerobic Digestion Model No.1 (ADM1), *Water Research.* 2004, 39, 171–183.

- [18] Vanrolleghem, P.; Spanjers H, Britta P; Ginestet P, Takacs. Estimating (combination of) activated sludge model no. 1 parameters and components by respirometry. *Water Sci. Technol.* 1999, 39, 195–214.
- [19] Choi, D. Modeling for optimization of activated sludge process and parameter estimation using artificial intelligence. PhD thesis, Korea Advanced Institute of Science and Technology, Republic of Korea. 2000.
- [20] APHA. *Standard Methods for the Examination of Water and Wastewater.* Washington DC, American Public Health Association, 1998.
- [21] Lowry, O. H.; Rosebrough, N.J.; Farr, A.L.; Randall, R.J. Protein measurement with the folin phenol reagent. *J. Biol. Chem.* 1951, 193, 265–275.
- [22] Owen, W.F.; Stuckey, D.C.; Healy, J.B.; Young, L.Y.; McCarty, P.L., Bioassay for monitoring biochemical methane potential and anaerobic toxicity, *Water Research.* 1979, 13, 485–492.
- [23] Bougrier, C.; Carrere, H.; Delgenes, J.P.; Solubilization of waste-activated sludge by ultrasonic treatment, *Chem. Eng. Journal.* 2005, 106, 163-169.
- [24] Gujer, W.; Henze M; Mino T; Loosdrecht M., Activated sludge model no. 3. *Water Sci. Technol.* 1999, 39, 183–193.
- [25] Galí, A., Benabdallah, T.; Astals S.; Mata-Alvarez, J.. Modified version of ADM1 model for agro-waste application. *Bioresour. Technol.* 2009,100, 2783-2790.
- [26] Drews, A.; Vocksa, M.; Iversena, V.; Lesjean, B.; Kraume, M. Influence of unsteady membrane bioreactor operation on EPS formation and filtration resistance. *Desalination*, 2006, 192, 1-9.

- [27] Tiehm, A.; Nickel, K.; Zellhorn, M.; Neis, U. Ultrasonic waste activated sludge disintegration for improving anaerobic stabilization. *Water Research*. 2009, 35, 2003-2009.
- [28] Neis, U.; Nickel, K.; Tiehm, A. Enhancement of anaerobic sludge disintegration by ultrasonic disintegration. *Water Sci. Technol.* 2000, 42, 73-80.
- [29] Hogan, F.; Mormede, S.; Clark, P.; Crane, M. Ultrasonic sludge treatment for enhanced anaerobic digestion, *Water Sci. Technol.* 2004, 50, 25-32.
- [30] Dimock, R.; Morgenroth, E. The influence of particle size on microbial hydrolysis of protein particles in activated sludge. *Water Research*. 2006, 40, 2064-2074.
- [31] Higgins, M.; Glindemann, D.; Novak, J.T.; Murthy, S.N.; Gerwin, S.; Forbes, R. Standardized biosolids incubation, headspace odor measurement and odor production consumption cycles. *Proceedings Water Env. Federation and AWWA Odors and Air Emissions Conference, Bellevue, Washington, 2004.*
- [32] Appels, L; Dewil, R; Baeyens, J; Degeve J, Ultrasonically enhanced anaerobic digestion of waste activated sludge. *Int. J. Sustainable Eng.*, 2008, 94 -104.
- [33] Miller, W. P.; Baharuddin, M. K., Particle size of interrill-eroded sediments from highly weathered soils, *Soil Sci Soc Am.* 1987, 51, 1610-1615.
- [34] Vavilin, V.A.; Rytow, S.V.; Lokshina, L.Y. Modelling hydrogen partial pressure change as a result of competition between the butyric and propionic groups of acidogenic bacteria. *Bioresour. Technol*, 1995, 54, 171–177.
- [35] Munch, J. Keller; P. Lant; R. Newell, Mathematical modeling of prefermenters-I. Model development and verification, *Water Research*. 1999, 12, 2757–2768.

- [36] Jeppsson, Ulf. Investigation of anaerobic digestion alternatives for Henriksdal's WWTP" IEA, Lund University. 2007.
- [37] Jeong, H.-S.; Chang-Won Suh; Jae-Lim Lim; Sang-Hyung Lee; Hang-Sik Shin. Analysis and application of ADM1 for anaerobic methane production. *Bioprocess Biosyst Eng.*, 2005, 27, 81–89.

CHAPTER FIVE

Impact of Ultrasonication of Hog Manure on Anaerobic Digestability³

5.1 Introduction

Ultrasonication has been widely tested to improve the hydrolysis rate in anaerobic digestion of biosolids [1, 2]. Ultrasonication disrupts biosolids flocs and bacterial cells, releasing intracellular components, subsequently improving the rate of anaerobic degradation due to the solubilisation of the particulate matter, decreasing solid retention time (SRT) and improving the overall performance of anaerobic digestion [3]. The use of ultrasonication in the pretreatment of waste activated sludge (WAS) improved the operational reliability of anaerobic digesters, decreased odor generation and clogging problems, and enhanced sludge dewatering [4]. However, economical feasibility and durability due to erosion of the sonotrode as well as high energy inputs are major challenges that need to be resolved for the technology to be adopted [4]. Sludge characteristics such as type of sludge (primary solids, waste activated sludge or animal manure, etc.), total solids (TS) content and particle size could highly impact the disintegration efficiency and improve the overall economy of the process. Ultrasonication pretreatment studies found in the literature have focused mainly on WAS. While anaerobic digestion of hog manure is widely practiced, there has been sparse research on enhancing its hydrolysis. The main differences between hog manure and municipal biosolids, i.e primary and waste activated sludge are: solids concentration, composition and heterogeneity. In general, the limiting step for the anaerobic digestion is the first step,

³ A version of this chapter has been published in *Ultrasonics Sonochemistry*, 2010, 18, pp 164-171.

hydrolysis, wherein the cell wall is broken and particulate substrates are enzymatically hydrolyzed allowing the organic matter inside the cell to be available for biodegradation.

Hydrolysis is well documented to be a function of specific surface area among other variables [5]. Since hydrolysis is also a function of the ratio of biomass to particulate concentration (both of which are combined as volatile suspended solids), the rate of solubilisation depends on the nature and concentration of the particulates. Fibrous substrates such as those found in hog manure will likely hydrolyze slower than WAS and primary sludges due to differences in particle size and the ratio of biomass to particulate substrates. Thus, pretreatment is required in order to achieve the release of lignocellulosic material and thus accelerate the degradation process by means of waste solubilisation. In the literature, there is a contradiction about the effect of TS content on disintegration efficiency. Akin et al. [6] studied WAS disintegration efficiency at various TS contents (2, 4 and 6%), specific energy (SE) inputs (up to 40000 kJ/kgTS) and ultrasonic densities (from 0.44 to 3.22 W/mL), and found that at constant TS content, the soluble chemical oxygen demand (SCOD) release showed an increasing trend with the increase in both specific energy input and ultrasonic density at all TS contents. However, at constant specific energy, the SCOD release decreased with the increase in initial TS content. This finding contradicts other studies that reported significant improvement in SCOD release with WAS for TS concentration in the 0.8 to 2.5% range [7, 8].

It is well known that sludge viscosity increases with solids concentration, with the critical concentration around 25 g/L or 2.5% TS content [9]. Ultrasonication efficiency is expected to decline with increasing viscosity due to resistance to energy flow, and

theoretically increased TS concentrations are detrimental to ultrasonication, despite the lack of consensus on the critical solids concentrations.

Odor generation from biosolids is a significant global problem as it negatively affects natural environments. Laboratory tests have indicated that protein degradation, especially the bound protein, i.e, proteins that are physically adsorbed on the outer cell wall which can detach during high speed centrifugation, a very popular sludge dewatering technology, is the main precursor for the odor production in biosolids [10]. Proteins are hydrolysed by extracellular enzymes (proteases) into polypeptides their constituent and amino acids. Hydrogen sulfide (H_2S) can be formed from the degradation of the sulfur containing amino acid such as cysteine and methionine. The pathways for production of methyl mercaptan and hydrogen sulfide from protein are described by Higgins et al. [10]. Based on an extensive literature search, it can be concluded that the effect of ultrasonication on odor compounds precursors, especially bound protein needs more research since the very limited studies on protein solubilization focused primarily on total and soluble protein measurements with no information on the critical bound proteins from an odor perspective. For instance, Wang et al. [11] examined protein release using WAS (TS content of 3%) at different ultrasonication densities (from 0.528 to 1.44 W/mL) and different ultrasonication times (from 5 to 30 min). The aforementioned authors investigated the protein in EPS, total protein and cell protein (difference between total protein and protein in EPS). Akin et al. [6] studied the effect of ultrasonication on protein release at different TS content.

The evaluation of ultrasonication efficiency in the literature is mostly based on the degree of disintegration (DD), which is the ratio between SCOD releases by ultrasonication

divided by SCOD releases by chemical disintegration. It appears from the literature that there is no unique method for determining chemical disintegration. For instance, Kunz and Wagner [12] used 1 M NaOH in the ratio of 1:3.5 by volume at 20°C for 22 h, while Muller and Pelletier [13] used 1 M NaOH at a ratio of 1:2 by volume at 90°C for 10 min, and Bougrier et al. [14] used 1 M NaOH at room temperature for 24 h. Additionally, the used techniques are time consuming and expensive [15].

The extensive literature reviewed above highlighted the challenges of applying ultrasonication to hog manure vis-a-vis WAS and primary sludges due to its characteristics such as fibrous versus excess biomass, particulate to biomass ratios, total solids concentrations well above the 2% - 3% for WAS and primary sludge leading to increase viscosity, and heterogeneity. Furthermore, it is apparent that despite the few studies on protein solubilization, the bound protein fraction implicated in odor generation has not been investigated.

Therefore, the overall objective of this study is to evaluate the impact of ultrasonication on solubilisation and anaerobic biodegradability of hog manure with high solid content and wide ranges of particle sizes, with particular emphasis on the effect of ultrasonication on proteins solubilisation, especially bound protein. Additionally, in this work, correlations between standardized and easy to measure solubilization parameters and the laborious and expensive method of degree of disintegration will be presented.

5.2 Material and methods

5.2.1 Analytical methods

Samples were analyzed for total solids (TS), volatile solids (VS), volatile suspended solids (VSS), total Kjeldahl nitrogen (TKN), and soluble total Kjeldahl nitrogen (STKN) using standard methods [16]. Total and soluble chemical oxygen demand (TCOD, SCOD) and ammonia (NH₄-N) were measured using HACH methods and test kits (HACH Odyssey DR/2500). Soluble parameters were determined after filtering the samples through 0.45 µm filter paper. Particle size distribution was determined by Malvern Mastersizer 2000 (version 5.22) laser beam diffraction granulometer. The total gas volume was measured by releasing the gas pressure in the vials using appropriately sized glass syringes (Perfektum; Popper & Sons Inc., NY, USA) in the 5–100 mL range to equilibrate with the ambient pressure as recommended by Owen et al. [17]. Biogas composition was determined by a gas chromatograph (Model 310, SRI Instruments, Torrance, CA) equipped with a thermal conductivity detector (TCD) and a molecular sieve column (Molesieve 5A, mesh 80/100, 6 ft × 1/8 in). The temperatures of the column and the TCD detector were 90 and 105°C, respectively. Argon was used as carrier gas at a flow rate of 30 mL/min.

5.2.2 Protein measurement

Protein was determined by micro-bicinchoninic acid protein assay (Pierce, Rockford, USA) which was modified from Lowry et al. [18] using a standard solution of bovine serum albumin. Cell protein was calculated as the difference between particulate and bound protein. In order to measure proteins, 50 mL samples were centrifuged at 10000

rpm for 15 minutes at 5°C to separate the liquid and solids in the sample. The supernatant was filtered through a 1.5 µm glass microfiber filter and the filtrate was analyzed for the soluble protein fraction. Bound protein was extracted from the suspended solids by a mild pH 8 phosphate buffer (50 mM), while particulate protein representing both the bound protein adsorbed on biomass and the protein within the biomass was extracted by an alkaline 1 N Na OH solution [18]. The solids were resuspended to a total volume of 50 mL with pH 8 phosphate buffer (50 mM) for measuring bound protein and 1 N NaOH for particulate protein. The solution was mixed using a magnetic stirrer at 1500 rpm for 10 minutes, and centrifuged at 10000 rpm for 15 minutes at 5°C, with the centrate filtered through a 1.5 µm glass microfiber filter, prior to protein analysis.

5.2.3 Experimental set-up

A lab scale ultrasonic probe was used to treat hog manure obtained from local hog farm in Southwestern, Ontario, Canada. The average characteristics of the hog manure used in this study in (mg/L); TCOD: 144900, SCOD: 55800, TS: 93180, VS: 66980, particulate protein: 22862, bound protein: 15938, soluble protein: 9134, TKN: 16580, STKN: 96820 and ammonia: 7020. The ultrasonic probe was supplied by Sonic and Materials, Newtown, USA (model VC-500, 500 W, and 20 kHz). 200 mL of hog manure was sonicated for different sonication times corresponding to different specific energy inputs, with sonication pulses set to 2 seconds on and 2 seconds off. To control the temperature rise of the sludge, a cooling water bath was used, and the sludge temperature during the experiments did not exceed 30°C.

5.2.4 Batch anaerobic digestion

Anaerobic batch reactors were used to study the anaerobic biodegradability, and determine the ultimate methane potential and methane production rate for sonicated and unsonicated manure. The 250 mL serum flasks sealed with rubber septa on a screw-cap was placed on the shaker- incubator (MaxQ 4000, Incubated and Refrigerated Shaker, Thermo Scientific, CA) at 37°C and rpm of 180. Eighteen (18) flasks were used in this study, two of them were used as blank and the rest were used for sonicated and non-sonicated samples for different specific energy inputs, as described later. The volumes of substrate (hog manure) and seed (anaerobic digester sludge from St Marys plant, St Marys, Ontario, Canada) calculated based on food to microorganisms (F/M) ratio of 4 on COD to VSS basis. For the blank, the substrate volume was replaced by distilled water.

5.2.5 Specific energy input

The specific energy input is a function of ultrasonic power, ultrasonic duration, and volume of sonicated sludge and TS concentration, and can be calculated using the following equation [14]:

$$SE = \frac{P \times t}{V \times TS} \quad \dots \quad (1)$$

Where SE is the specific energy input in kW/kgTS (kJ/kgTS), P is the ultrasonic power in kW, t is the ultrasonic duration in seconds, V is the volume of sonicated sludge in litres, and TS is the total solids concentration in kg/L.

5.2.6 Degree of disintegration (DD)

In this study, the degree of disintegration was determined based on the equation of Muller and Pelletier [13]:

$$DD = \left[\frac{COD_{Ultrasound} - COD_{Original}}{COD_{NaOH} - COD_{Original}} \right] \times 100\% \quad \dots \quad (2)$$

Where $COD_{ultrasound}$ is the COD of supernatant of ultrasound treated sample (mg/L), $COD_{original}$ is the COD of supernatant of original (untreated) sample (mg/L), and COD_{NaOH} (mg/L) is the COD in the supernatant after addition of 1M NaOH for 24 h at room temperature.

5.2.7 COD solubilization

$COD_{solubilisation}$ was calculated using the SCOD released, which is the difference between SCOD at any time after ultrasonication ($SCOD_t$) and the initial SCOD ($SCOD_0$) divided by the initial particulate COD ($TCOD_i - SCOD_0$):

$$COD_{solubilisation} = \left[\frac{SCOD_t - SCOD_0}{TCOD_i - SCOD_0} \right] \times 100\% \quad \dots \quad (3)$$

Where $TCOD_i$ is the initial TCOD concentration.

5.2.8 TKN solubilization

$TKN_{solubilisation}$ was calculated using the STKN released which is the difference between STKN at any time after ultrasonication ($STKN_t$) and the initial STKN ($STKN_0$) divided by the initial particulate TKN ($TKN_i - STKN_0$):

$$TKN_{solubilisation} = \left[\frac{STKN_t - STKN_0}{TKN_i - STKN_0} \right] \times 100\% \quad \dots \quad (4)$$

Where TKN_i is the initial TKN concentration.

5.3 Results and Discussion

5.3.1 Comparison of solubilisation and degree of disintegration

Using $COD_{solubilisation}$ and plotting the results with respect to DD, $TKN_{solubilisation}$, % increase in soluble protein, and % decrease in particulate protein (Figure 5.1), a perfect linear relationship with an $R^2 = 1.0$ was obtained for the correlation between $COD_{solubilisation}$ and DD (Figure 5.1a). The linear relationship between $COD_{solubilisation}$ and $TKN_{solubilisation}$ emphasizes that the solubilisation of nitrogenous compounds followed the similar trend of COD solubilisation (Figure 5.1b). Figures 1c and 1d illustrating the relationship between $COD_{solubilisation}$ on one hand and % increase in soluble protein, and % decrease in particulate protein on the other hand emphasize that $COD_{solubilisation}$ is more strongly linearly related with % decrease of particulate protein than % increase in soluble protein. Thus, $COD_{solubilisation}$ from now on can be used to evaluate the solubilisation degree in lieu of the DD procedure, as it proved to be an accurate and easy measure.

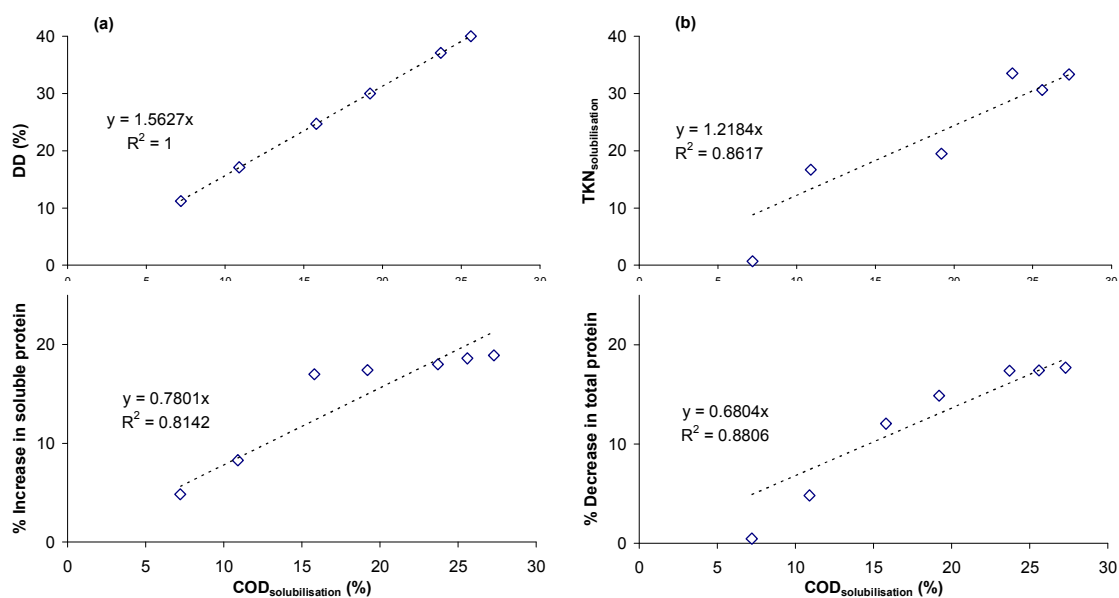


Figure 5.1 Relationship between COD solubilization and: (a) DDSCOD (%), (b) TKN solubilization, (c) % Increase in soluble protein, (d) % Decrease in total protein.

5.3.2 Particle size distribution

Particle size distribution is widely used as a qualitative measure for sludge disintegration. Anaerobic digestion of waste is governed by hydrolysis (solubilisation of particulates) that is highly affected by the particle size. Smaller particle sizes and the lower concentration of particulates, measured as VSS lead to higher degradation efficiency. As shown in Figure 5.2, the hog manure is characterized by a wide range of particle size ranging from 0.6 μm to 2500 μm , compared to a range of 0.4 μm to 1000 μm reported for WAS [14, 1]. As shown in Figure 5.2, the particle size distribution for the hog manure shows a bi-modal distribution, with two peaks, the first at 60 μm and the second at 1200 μm , respectively.

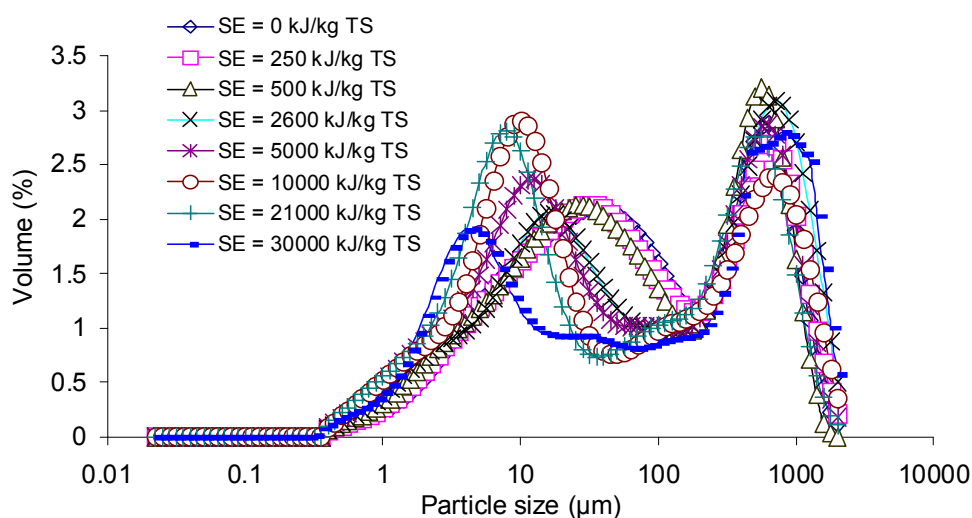


Figure 5.2 Particle size distribution for different specific energy inputs

Interestingly, the disintegration effect was more pronounced for the particles in the range of 0.6 μm to 60 μm ; while a minor effect was observed for particles $> 200 \mu\text{m}$. The mean particle size diameter (d_{50}) decreased from 59 μm in the raw hog manure to 21.9 μm with

the specific surface area (SSA) increasing from 0.523 to 1.2 $\mu\text{m}^2/\text{g}$ at a specific energy of 30000 kJ/kgTS (Table 5.1).

Table 5.1 Particle size and $\text{COD}_{\text{solubilization}}$ at different specific energy inputs

SE (kJ/kgTS)	0	250	500	2500	5000	10000	21000	30000
d_{50} (μm) [*]	59.0	56.0	53.9	47.3	39.7	33.3	27.4	21.9
SSA ($\mu\text{m}^2/\text{g}$)	0.52	0.56	0.59	0.63	0.78	0.8	0.91	1.2
% Reduction in VS	-	5	20	24	24	30	31	32
DD (%)	-	11	17	25	30	37	40	43
$\text{COD}_{\text{solub.}}$ (%)	-	7	11	16	19	24	26	27

* d_{50} : 50% of particles volume having a diameter lower than or equal to d_{50} .

Using WAS, Gonze et al. [1], Bougrier et al. [14] achieved decrease in mean particle size diameters from 320 to 18.1 μm and from 32 to 12.7 μm , at TS content of 1.2 to 3.2 gDS/L and 18.5 g/L, respectively. In another study, Akin et al. [6] achieved decrease in mean diameters from 209 to 18.1, from 217 to 38.2 and from 225 to 33.4 μm , at TS content of 2, 4 and 6% of WAS, respectively. Thus, it is evident that the effect of ultrasonication on particle size depends on the nature of the biomass and the TS content. For WAS the smallest particle size (18.1 μm) was achieved at lower TS content, 2% [6]. While for manure, the smallest particle size 21.9 μm was achieved at higher TS content, 9.3%.

5.3.3 Solubilisation of hog manure

Ultrasonic pretreatment solubilises extracellular matter and extracellular polymeric substances (EPS), increasing the SCOD. Thus, SCOD is mostly used to measure the sludge disintegration efficiency. The specific energies for various TS contents and DD from this study and two other studies are plotted in Figure 5.3.

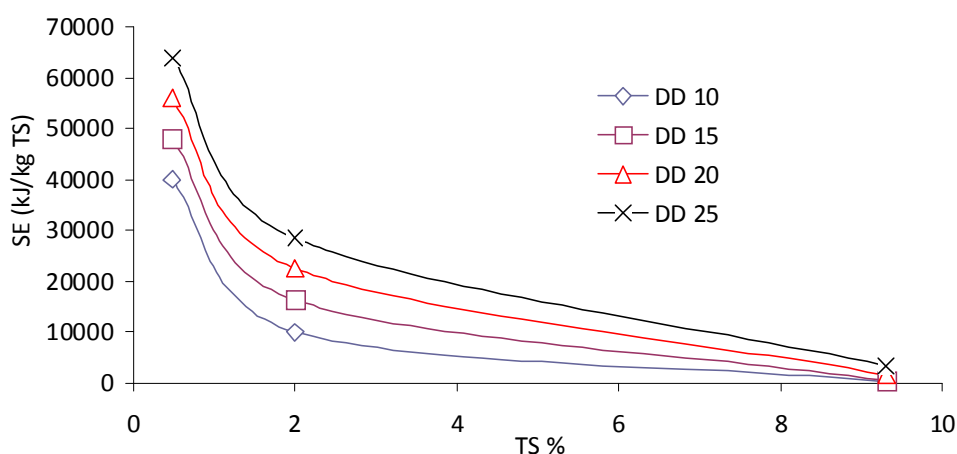


Figure 5.3 Specific energy input for different TS at different degree of disintegrations.

*Data in this graph from this study, Tiehm et al. (2001); Rai et al. 2004

A sharp decline in the required specific energy from 65000 kJ/kgTS to 10000 kJ/kgTS was observed when the TS increased from 0.5% to 2%. The slope of the curve then decreased drastically and the required specific energy to achieve a certain DD was almost constant regardless of the increase in TS. For hog manure with a TS content of 9.3%, only 3000 kJ/kgTS was required to increase the DD by 15% (from 10% to 25%), while for WAS, a specific energy of 20000 and 25000 kJ/kgTS is required to achieve the same increase in DD for WAS with TS content of 2% and 0.5%, respectively. Two other studies have been conducted on WAS with different TS content but they did not report the SE input, and therefore can not be compared. Gronroos et al. [7] studied WAS with dry solids (DS) content (0.8, 1.6 and 2.5%), different ultrasonic densities (50, 175 and 300 W/L), different frequencies (22 and 40 kHz) and treatment time (5, 17.5 and 30 min). The aforementioned authors observed that the largest SCOD increase was obtained with the highest power, highest DS and longest sonication time. Wang et al. [8], using WAS,

at two TS content (0.5% and 1%) studied different disintegration times (10, 20 and 30 min), different intensities (from 30 to 230 W/cm²) and different densities (0.25, 0.5, 1.0 and 1.5 W/mL), and found that the highest power, highest DS and longest treatment time resulted in highest SCOD increase consistent with Gronroos et al., (2005). Thus, the high solids content of hog manure of 9.3% versus the 0.5% to 2.5% for WAS in this case did not adversely impact solubilization. Comparing the 3000 kJ/kgTS required to achieve a 15% increase in DD for hog manure with the 20000 and 25000 kJ/kgTS for WAS implies that hog manure is about 6-8 times more amenable to ultrasonication than WAS.

The maximum solubilisation of hog manure measured as COD_{solubilisation} was 27.3% at 30000 kJ/kgTS, whereas Khanal et al. [19] and Bougrier et al. [14] using WAS, achieved 16.2% and 41.6% at specific energies of 66800 kJ/kgTS and 14547 kJ/kgTS, respectively. Applying ultrasonication of hog manure at different specific energy inputs achieved an increase of 1.35 mgSCOD/(kJ/kgTS) compared to 0.15, 0.12, 0.45 and 0.9 mgSCOD/(kJ/kgTS) calculated from data reported by Khanal et al. [19]; Gronroos et al. [7]; Navaneethan [2]; and Bunrith [20], respectively indicating greater pretreatment potential of hog manure by ultrasonication compared to WAS. On the other hand the average reduction in VS for hog manure was $22.5 \pm 2\%$ for the specific energy in the range of 500 to 5000 kJ/kgTS. While increasing the specific energy to 10000 kJ/kgTS raised the VS reduction percentage to 29.6%. Increasing the specific energy beyond 10000 kJ/kgTS did not improve the VS reduction significantly.

The TKN remained constant throughout the experiments, and thus no nitrogen mineralisation or volatilisation was observed. As shown in Table 5.2, ultrasonication of hog manure increased the STKN from 9682 mg/L to 11994 mg/L corresponding to a

TKN_{solubilisation} about 34% at a specific energy input of 10000 kJ/kgTS, after which the STKN remained constant, comparable to the nitrogen solubilisation of 40% at specific energy input of 10000 kJ/kgTS observed by Bougrier et al. [14] for WAS. The ammonia-nitrogen concentration increased from 7020 mg/L in the raw hog manure to 8380 mg/L after sonication, with increase in the ratio of NH₄-N/TKN of only 10% at 10000 kJ/kgTS (Table 5.2). The increase in ammonia concentration also indicates the hydrolysis of organic nitrogen due to ultrasonication.

Table 5.2 TKN_{solubilisation}, ammonia and protein solubilisation at different specific energy inputs

SE (kJ/kgTS)	STKN (mg/L)	TKN _{solub.} (%)	NH ₄ - N/TKN (%)	% Decrease in P-P	% Decrease in B-P	% Increase in S-P	% Decrease in Cell-P
0	9682	-	42	-	-	-	-
250	9731	0.7	48	0.4	8.0	4.8	0
500	10832	16.7	48	4.8	9.2	8.3	4.5
2600	10518	12.1	51	12.0	12.7	17	12.0
5000	11026	19.5	52	14.9	13.4	17.4	15.0
10000	11994	33.5	52	17.4	13.0	18.0	17.7
21000	11792	30.6	53	17.7	12.8	18.6	17.7
30000	11981	33.3	53	18.1	13.5	18.9	18.0

- % Decrease = [(initial value – value after ultrasonication)/ initial value]*100
- % Increase = [(value after ultrasonication - initial value)/ initial value]*100
- P-P = Particulate protein, B-P = Bound protein, S-P = Soluble protein, and Cell-P = cell protein

5.3.4 Proteins (particulate, bound and cell) solubilisation

Proteins are usually divided into three types; particulate protein, bound protein, and soluble protein [21]. The particulate protein was considered as the tightly bound protein in flocs and is composed of particles in the bacterial cell mass. Bound protein is the labile fraction loosely attached on biomass, while the soluble protein represents protein in solution. Bound protein is considered to be one of the main causes for odor in anaerobic digestion; and the effect of ultrasonication on the proteins needs to be characterized. The effect of ultrasonication on proteins is summarized in Table 5.2. While approximately a 17% decrease in the particulate proteins was achieved at a specific energy of 10000 kJ/kgTS, the soluble protein increased by 18%. It was observed that at specific energy inputs less than 500 kJ/kgTS, the reduction in particulate protein of up to 5% was attributed to the decrease in bound protein, while a 17.7% reduction in cell protein was observed for specific energy of 10000 kJ/kgTS, after which the solubilisation efficiency remained constant. In another study by Akin et al. [6] on ultrasonication of WAS, the protein release was significantly reduced at higher TS content. The maximum protein released was 73 mg/gTS at a TS content of 2% and SE of 10000 kJ/kgTS, but decreased to 40 and 22 mg/gTS at SE of 5000 kJ/kgTS for TS content of 4% and 6%, respectively. The soluble protein released in this work is about 17 mg/gTS at SE of 2600 kJ/kgTS in fact follows the same trend of decreasing protein solubilization with the decrease of SE. Comparing the protein per unit energy for hog manure with the WAS results of Akin et al. [6] reveals that for hog manure, protein solubilization of 17 mg/gTS at ultrasonication density of 234 MJ/m³ is identical to the 22 mg/gTS at ultrasonication density of 300 MJ/m³ since the 29% difference in protein released is commensurate with the 28% difference in ultrasonication density. Upon comparing the results of this study with Akin

et al. [6] with respect to the impact of TS content, it is readily discerned that for WAS, solubilization of proteins decreased with increasing TS content in the 2-6% range, while for hog manure even a 9.3% TS content did not negatively impact protein solubilization, reflecting the difference in the nature of hog manure.

It is interesting to note that a minimum of 500 kJ/kgTS specific energy input was required in order to rupture the cell wall and to release the cell protein, and it is more than an order of magnitude lower than 7700 kJ/kgTS required by Wang et al. [11] for WAS.

Data in Table 5.2 emphasizes that at low specific energy inputs (less than or equal to 2600 kJ/kgTS), up to 12.7% reduction in bound protein is achievable. The data for bound protein in Table 5.2 emphatically shows that ultrasonication has reduced bound protein by 8% to 13.5%, with the rate change diminishing rapidly at a specific energy higher than 2600 kJ/kgTS, at which a 12.5% reduction was achieved. Thus, it is evident that pretreatment by ultrasonication does significantly abate the potential for odor generation caused by bound proteins.

5.3.5 Methane production and economics

The biochemical methane potential (BMP) test was used to evaluate anaerobic biodegradability in batch reactors. Figure 5.4 shows the cumulative methane production over time at different sonication energy inputs, with the data summarized in Table 5.3.

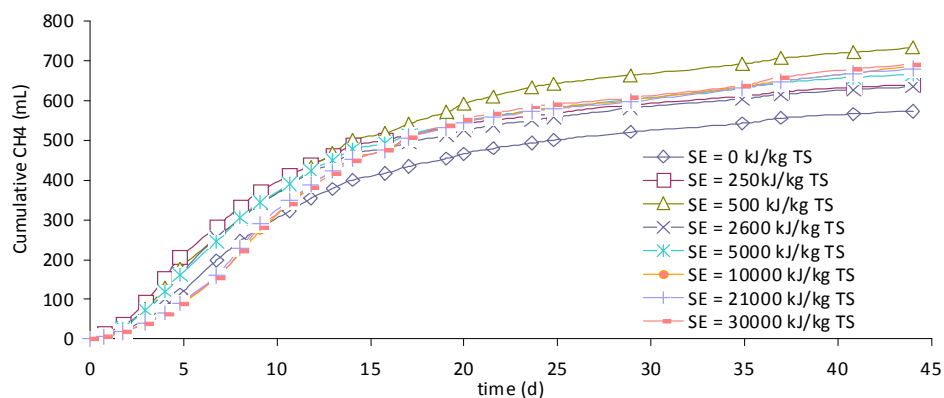


Figure 5.4 Cumulative methane production at different specific energy inputs.

Table 5.3 Ultrasonication and Methane Energy per ton of TS

SE (kJ/kgTS)	Methane		Power input		Methane out		
	% Increase in methane potential	% Increase in maximum methane production rate	kWh/ton TS _{in}	Price \$/ton TS _{in}	Increase of CH ₄ (mL)	CH ₄ m ³ /ton TS _{in}	Price \$/ton TS _{in}
0	-	-	0	-	-	-	-
250	11.7	33.7	69	4.9	67	17.2	4.8
500	28.0	61.3	139	9.7	160	50.4	14.1
2600	10.9	43.5	722	50.6	62	201.2	5.6
5000	16.3	35.5	1389	97.2	93	29.3	8.2
10000	19.9	46.6	2778	194.4	114	37.9	10.6
21000	18.7	75.4	5833	408.3	107	36.3	10.2
30000	20.7	80.6	8333	583.3	118	40.0	11.2

As shown in Figure 5.4, no lag phase was observed due to the sufficiency of soluble substrates. With respect to the results in Table 5.3, it is clearly observed that

ultrasonication of hog manure enhanced the biogas production at low energy inputs compared to unsonicated hog manure. Methane potential increased by 28% relative to the unsonicated hog manure for a specific energy input of 500 kJ/kgTS, while the increase at high energy inputs (30000 kJ/kgTS) was only 20.7%. While the % increase in methane production rate increased by increasing the energy input, maximum increase in methane production rate was 80.6% compared to unsonicated hog manure at a specific energy input of 30000 kJ/kgTS. The increase in methane production rate for specific energy input of 500 kJ/kgTS (high methane potential) was about 61.3%, and decreased for SE of 500 to 10000 kJ/kgTS before increasing again. Therefore, since ultrasonic pretreatment of hog manure with SE of 500 kJ/kgTS gave a comparable methane production enhancement in both rate and potential with SE of 21000-30000 kJ/kgTS, the 500 kJ/kgTS can be considered to be the optimum energy input for the pretreatment of ultrasonicated hog manure prior to anaerobic digestion. On the other hand, the reported optimum specific energy for ultrasonic pre-treatment of WAS in the literature was significantly higher at 11000 kJ/kgTS [11] and 12000 kJ/kgTS [2].

The COD mass balance for all the batches was computed considering the initial and final TCOD, and the equivalent COD of methane (0.395 LCH₄/gTCOD), which indicated a closure at 90–95%, thus emphasizing data reliability.

The maximum difference between the final VSS concentration in the sonicated and unsonicated hog manure after digestion was 14% of the unsonicated VSS at a SE of 10000 kJ/kgTS.

An economic analysis (the results are summarized in Table 5.3) was conducted based on power and natural gas costs of \$0.07/kWh and \$0.28/m³, respectively. As apparent from

Table 5.3, the specific energy of 500 kJ/kgTS can be considered to be the optimum energy input for anaerobic digestion of ultrasonic pretreated hog manure to be economically viable, as the value of the energy output exceeds that of the energy input by \$ 4.1/ton of dry solids.

5.4 Conclusions

Based on the finding of this study, the following conclusions can be drawn:

- The $COD_{\text{solubilisation}}$ correlated very well with the DD, the $TKN_{\text{solubilisation}}$ and the % decrease in particulate protein. Thus, $COD_{\text{solubilisation}}$ can be used to evaluate the degree of solubilisation in lieu of the labor and time intensive DD procedure, as it proved to be an accurate and easy to measure method.
- For hog manure, the disintegration of particles by ultrasonication was more pronounced for the smaller sizes, i.e., in the 0.6 to 60 μm range, as well as the reduction of VS by ultrasonication increased with increasing specific energy input in the 500-5000 kJ/kgTS and reached a plateau at 10000 kJ/kgTS.
- At solids content of 2%, the specific energy input increased from 10000 to about 30000 kJ/kgTS for an additional 15% increase in degree of disintegration, whereas at TS of about 9%, the specific energy input increased from 250 to about 3,300 kJ/kgTS to achieve the same increase in DD. Therefore, ultrasonication is more effective pretreatment process for hog manure with higher TS content than WAS and primary sludges.
- Upon comparing the results of this study with Akin et al. [6] with respect to the impact of TS content, it is readily discerned that for WAS, solubilization of proteins

decreased with increasing TS content in the 2-6% range, while for hog manure even a 9.3% TS content did not negatively impact protein solubilization, reflecting the effect of difference in the nature of sludge on the efficiency of pretreatment.

- Bound proteins decreased by 13.5% at specific energy of 5000 kJ/kgTS. Thus, the impact of ultrasonication on odor precursors such as bound proteins appears to be significant.
- The cell wall appeared to be ruptured at a minimum specific energy input of 500 kJ/kgTS, whereas the optimum specific energy was 10000 kJ/kgTS, affecting a 17.7% reduction in cell protein.
- The optimum specific energy input for methane production was 500 kJ/kgTS, and resulted in a 28% increase in methane production, and subsequently about \$ 4.1/ton of dry solids excess energy output.

5.5 References

- [1] Gonze, E.; Pillot, S.; Valette, E.; Gonthier, Y.; Bernis, A.; Ultrasonic treatment of an aerobic activated sludge in a batch reactor, *Chem. Eng. Process.* 2003, 42, 965–975.
- [2] Navaneethan, N. Anaerobic Digestion of Waste Activated Sludge with Ultrasonic Pretreatment, Master thesis, Asian Institute of Technology, Bangkok, Thailand, 2007.
- [3] Pavlostathis, S.G.; Gossett, J.M. A kinetic model for anaerobic digestion of biological sludge, *Biotechnol. Bioeng.* 1986, 27, 1519–30.
- [4] Pérez-Elvira, S. I.; Nieto Diez, P.; Fdz-Polanco, F. Sludge minimisation technologies, *Rev. Environ. Sci. Biotechnol.* 2006, 5, 375–398.
- [5] Sanders, W.T.M.; Geerink, M.; Zeeman, G.; Lettinga, G. Anaerobic hydrolysis kinetics of particulate substrates. *Water Sci. Technol.*, 2000, 41, 17–24.
- [6] Akin, B.; Khanal, S. K.; Sung, S.; Grewell, D.; Van Leeuwen, J. Ultrasound pre-treatment of waste activated sludge, *Water Sci. Technol. Water Supply.* 2006, 6, 35-42.
- [7] Gronroos, A.; Kyllonen, H.; Korpijarvi, K.; Pirkonen, P.; Paavola, T.; Jokela, J.; Rintala, J. Ultrasound assisted method to increase soluble chemical oxygen demand (SCOD) of sewage sludge for digestion, *Ultrason. Sonochem.* 2005, 12, 115–120.
- [8] Wang, F.; Wang, Y.; Ji, M. Mechanisms and kinetics models for ultrasonic waste activated sludge disintegration, *J. Hazard. Mater.* 2005, 145–150
- [9] Pham, T.; Brar, S.; Tyagi, R.; Surampalli, R. Influence of ultrasonication and Fenton oxidation pre-treatment on rheological characteristics of wastewater sludge, *Ultrason. Sonochem.* 2010, 17, 38-45.
- [10] Higgins, M.; Glindemann, D.; Novak, J.; Murthy, S.; Gerwin, S.; Forbes, R. Standardized biosolids incubation, headspace odor measurement and odor production consumption cycles. Proceedings Water Env. Federation and AWWA Odors and Air Emissions Conference, Bellevue, Washington, 2004.

- [11] Wang, F.; Lu, S.; Ji, M. Components of released liquid from ultrasonic waste activated sludge disintegration, *Ultrason. Sonochem.* 2006, 13, 334-338.
- [12] Kunz, P.; Wagner, S. Results and outlooks of investigations of sewage sludge disintegration, *Ergebnisse und Perspektiven aus Untersuchungen zur Klärschlamm-Disintegration*, awt_abwassertechnik, Heft 1, 1994. (From Schmitz, et al. [15])
- [13] Muller, J.; Pelletier, L. Désintégration mécanique des boues activées, *L'eau, l'industrie, les nuisances.* 1998, 217, 61–66. (From Schmitz, et al. [15])
- [14] Bougrier, C.; Carrère, H.; Delgenès, J. Solubilisation of waste-activated sludge by ultrasonic treatment, *Chem. Eng. J.* 2005, 106, 163-169.
- [15] Schmitz, U.; Berger, C.R.; Orth, H. Protein analysis as a simple method for the quantitative assessment of sewage sludge disintegration, *Water Research.* 2000, 34, 3682–3685.
- [16] APHA, *Standard Methods for the Examination of Water and Wastewater*, 20th ed.: American Public Health Association, Washington DC, USA, 1998.
- [17] Owen, W.F.; Stuckey, D.C.; Healy, J.B.; Young, L.Y.; McCarty, P.L. Bioassay for monitoring biochemical methane potential and anaerobic toxicity, *Water Research.* 1979, 13, 485–492.
- [18] Lowry, O. H.; Rosebrough, N. J.; Fair, A. L.; Randall, R. J. Protein measurement with the folin-phenol reagent, *J. Biol. Chem.* 1951, 193, 265-275.
- [19] Khanal, S.K.; Isik, H.; Sung, S.; Van Leeuwen, J. Ultrasound pretreatment of waste activated sludge: evaluation of sludge disintegration and aerobic digestion, In *CD-ROM Proceedings of IWA World Water Congress and Exhibition*, Sep 10-14, Beijing, China, 2006.
- [20] Bunrith, S. *Anaerobic Digestibility of Ultrasound and Chemically Pretreated Waste Activated Sludge*, Master thesis, Asian Institute of Technology, Bangkok, Thailand, 2008.

- [21] Dimock, R.; Morgenroth, E. The influence of particle size on microbial hydrolysis of protein particles in activated sludge. *Water Research*. 2006, 40, 2064-2074.

CHAPTER SIX

Simulating the Degradation of Odors Precursors in Primary and Waste Activated Sludge during Anaerobic Digestion⁴

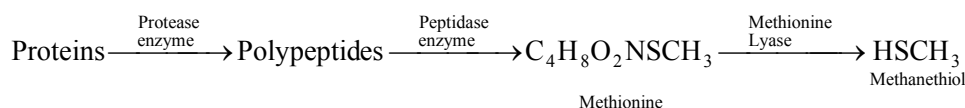
6.1 Introduction:

Anaerobic fermentation is the most commonly applied process for stabilization of biosolids. A disadvantage of the fermentation technique is the slow degradation rate of biosolids; usual residence times in anaerobic digesters are about 20-40 days, requiring large digesters. Noxious odor production during anaerobic digestion and from the stored biosolids is considered to be a significant disadvantage of this useful process [1]. Odor production from anaerobically digested biosolids has recently received interest due to increased load application of biosolids.[1]. Although H₂S is considered to be the most prevalent odor compound, there are typically other organic odorous compounds, such as mercaptans and amines, present in anaerobic digestion. Prior research has implicated volatile sulfur compounds (VSCs) including hydrogen sulfide (H₂S), methanethiol or methyl mercaptan (MT), dimethyl sulfide (DMS), dimethyl disulfide (DMDS) and dimethyl trisulfide (DMTS) in odors from biosolids [2]. In addition to VSCs, ammonia and volatile fatty acids (VFA), phenols are also implicated as possible odor causing compounds in the excretion of pigs [3].

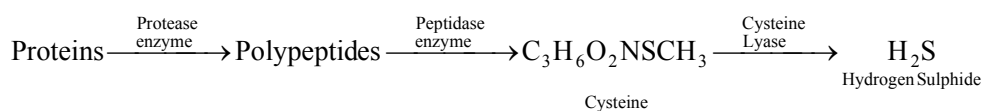
Laboratory tests have indicated that protein degradation and, especially the degradation of methionine, an amino acid, is the main source for the production of VSCs [2]. Proteins

⁴ A version of this chapter has been submitted to *Journal of Hazardous Materials*, 2010

are hydrolysed by extracellular enzymes (proteases) into their constituent polypeptides and amino acids. The pathway for the production of MT from methionine is described as [2]:



Hydrogen sulfide (H₂S) can be formed from the degradation of cysteine, sulfur containing amino acid, as shown below:



While the carbohydrate, lipid, and protein content of municipal biosolids often accounts for the majority (90%) of the organic load [4], in some industries, protein is the predominant part of the organic load. For example, the protein component of a dairy wastewater stream can account for more than 40%-60% of the total chemical oxygen demand [5]. Although the presence of proteins has been confirmed in the organic matter of treated municipal waste water and sludge [6], literature on protein degradation during anaerobic digestion is both sparse and contradictory. In a pioneering work, Breure et al. [7] studied degradation of a model protein, gelatin, in controlled anaerobic digestion, and observed that it was converted at high rates and to a substantial extent to volatile fatty acids. Since, proteins, carbohydrates and lipid are almost always present simultaneously in biosolids, complete degradation of protein in the presence of carbohydrates may not be achieved as glucose and other easily fermentable substrates can repress the synthesis of exoproteases (a necessary enzyme) in pure cultures of bacteria [7], and the degradation of gelatin was retarded by increasing concentrations of carbohydrates present in the feed as

a second substrate. In contrast, in a controlled study it was found that as much as 70% of the protein was broken down in the acidogenic reactor and inclusion of protein had no effect on the reaction pathway for lactose degradation [8]. Proteins in wastewater and sludge are generally divided into three fractions: soluble, bound/labile (loosely attached with the cells) and tightly bound fractions (within the bacterial cells) [2]. Labile proteins are thought to become readily bioavailable during dewatering giving rise to higher odor potential.

Mathematical anaerobic digestion models (ADM) have been extensively investigated and developed during the last three decades [9]. As one of the most sophisticated and complex ADM, the IWA Anaerobic Digestion Model No. 1 (ADM1) is the integrated anaerobic model developed by the IWA Task Group for modeling of Anaerobic Digestion Processes [4]. It consists of a number of processes to simulate all possible reactions occurring in anaerobic sludge digestion including not only biological reactions, such as disintegration and hydrolysis of suspended solids, uptake (growth) and decay of microorganisms, but also physico-chemical reactions, including ion association/dissociation and liquid–gas transfer. In total, 19 processes, 24 components, and 56 relative stoichiometric and kinetic parameters are assumed for biological processes. One of the significant limitations of this model is the absence of phosphorus modeling and the fate of sulfur compounds. This includes the generation of H₂S in the digester gas and the fate of sulfur species in the digested sludge, as a predictor of odor-generating potential [10]. Although Higgins et al. [2] studied the fate of odor precursors (such as protein) in anaerobic digestion, systematic research on odor precursors in anaerobic digestion of municipal biosolids is very limited [1]. The objectives of this work were to monitor the

degradation of various protein fractions (particulate, soluble, and bound) of primary and secondary municipal sludge during anaerobic digestion; determine the relationship between various protein fractions and other sludge quality parameters; simulate the odors precursors degradation; and estimate the odors precursors reaction kinetics, namely, protein, amino acids and volatile fatty acids (VFAs) using the state of the art anaerobic digestion model (ADM1). Modeling of the odors precursors is beneficial as it allows users to mathematically predict degradation of those compounds for different types of sludges with known characteristics.

6.2 Materials and methods:

Primary sludge (PS), waste activated sludge (WAS), and anaerobic sludge (seed sludge) were obtained from a full scale anaerobic digester at St. Marys, Water Pollution Control Plant (Ontario, Canada) twice a week. The sludges were then stored in a cool room at 4°C. Four 4-L reactors were used as anaerobic bioreactors, with a working volume of 3.5 L and hydraulic retention time (HRT) of 14 days. The working volume in all reactors was filled with anaerobic sludge at the beginning. Subsequently, two reactors (duplicates) were fed with 250 mL/d of primary sludge and the other two (duplicates) were fed with 250 mL/d of waste activated sludge. The reactor contents were continuously mixed using the WU-50007-30 Cole-Parmer[®] Stir-Pak[®] mixer. A temperature of 38°C was maintained by using hot water recycled from a water bath, and pH was controlled in a narrow range of 6.5-7.5 during the experiments. Both influent and effluent of the reactors were analyzed once a week over the entire duration of experiments. The reactors' biogas was measured using a Wet-Tip gas meter (Gas Meters for Laboratories, Nashville, TN). All

four reactors were operated continuously over a period of seventy days and served to maintain constant inoculums for the experiments described. All the experiments and analysis were conducted in duplicates.

6.2.1 Analytical methods:

Standard methods [11] were used to determine total chemical oxygen demand (TCOD), soluble chemical oxygen demand (SCOD), biological oxygen demand (BOD), total suspended solids (TSS), volatile suspended solid (VSS), alkalinity, lipid, total nitrogen (TN), total phosphorus (TP), and H₂S content of the biogas (iodometric method). For volatile fatty acids (VFA) 50 mL samples were centrifuged at 3,000 x g for 15 minutes at 5°C to separate the liquid and solids in the sample. The centrate was filtered with a 0.45- μ m membrane and the filtrate was used to measure the VFA concentrations using a gas chromatograph (Varian 8500, Varian Inc., Toronto, Canada) with a flame ionization detector (FID) equipped with a fused silica column (30 m \times 0.32 mm). Helium was used as carrier gas at a flow rate of 5 mL/min. The temperatures of the column and detector were 110 and 250 °C, respectively. Protein was determined by micro-bicinchoninic acid protein assay (Pierce, Rockford, USA), which was modified by Lowry et al. [12]. The biogas composition was determined by a gas chromatograph (Model 310, SRI Instruments, Torrance, CA) equipped with a thermal conductivity detector (TCD) and a molecular sieve column (Molesieve 5A, mesh 80/100, 182.88 \times 0.3175 cm).

6.2.2 Anaerobic digestion simulation:

ADM1 is a complex model involving many input parameters; for example, the decay of microorganisms and the regeneration cycle are strongly interrelated and the COD content assumed in ADM1 is rather complex [13]. The decay processes of all microorganisms result in the production of carbohydrates, proteins and lipids, which can be used as substrates after disintegration and hydrolysis. The regeneration of organic matter from biomass decay makes the model more complex [13]. Inhibition and gas transfer are also complex steps in the model. The default stoichiometric matrix and rate of reactions equations described by the ADM1 technical report [4] were used. MATLAB 2008 (The MathWorks, Inc. Natick, US) ODE23S ordinary dynamic equation solver was used to solve the dynamic differential and algebraic system of equations.

6.2.3 Statistical analysis:

The student t-test was used to test the hypothesis of equality at the 95% confidence level. The null hypothesis was defined as no difference between the two groups tested vs. the alternative hypothesis that there is a statistical difference between the two groups.

6.3 Results and discussion:

6.3.1 Performance of anaerobic digesters:

The biodegradability of waste components in anaerobic digestion varies widely [14] depending on many factors, such as the concentration and components of sludge, types and amount of anaerobic bacteria, organic loading rate, hydraulic residence time,

temperature, and pH. The reductions of total suspended solids (TSS), volatile suspended solids (VSS), total chemical oxygen demand (TCOD), soluble chemical oxygen demand (SCOD), and biological oxygen demand (BOD_5) are usually used to evaluate the removal efficiency of waste substances in anaerobic digestion. Steady-state data collection was after 30 days of operation corresponding to two turnovers of the mean SRT, and steady state reductions of TSS, VSS, TCOD, SCOD in both PS and WAS are shown in Figure 6.1 (a, b, c, and d), respectively. A summary of the steady-state performance data for the digesters is also shown in Table 6.1.

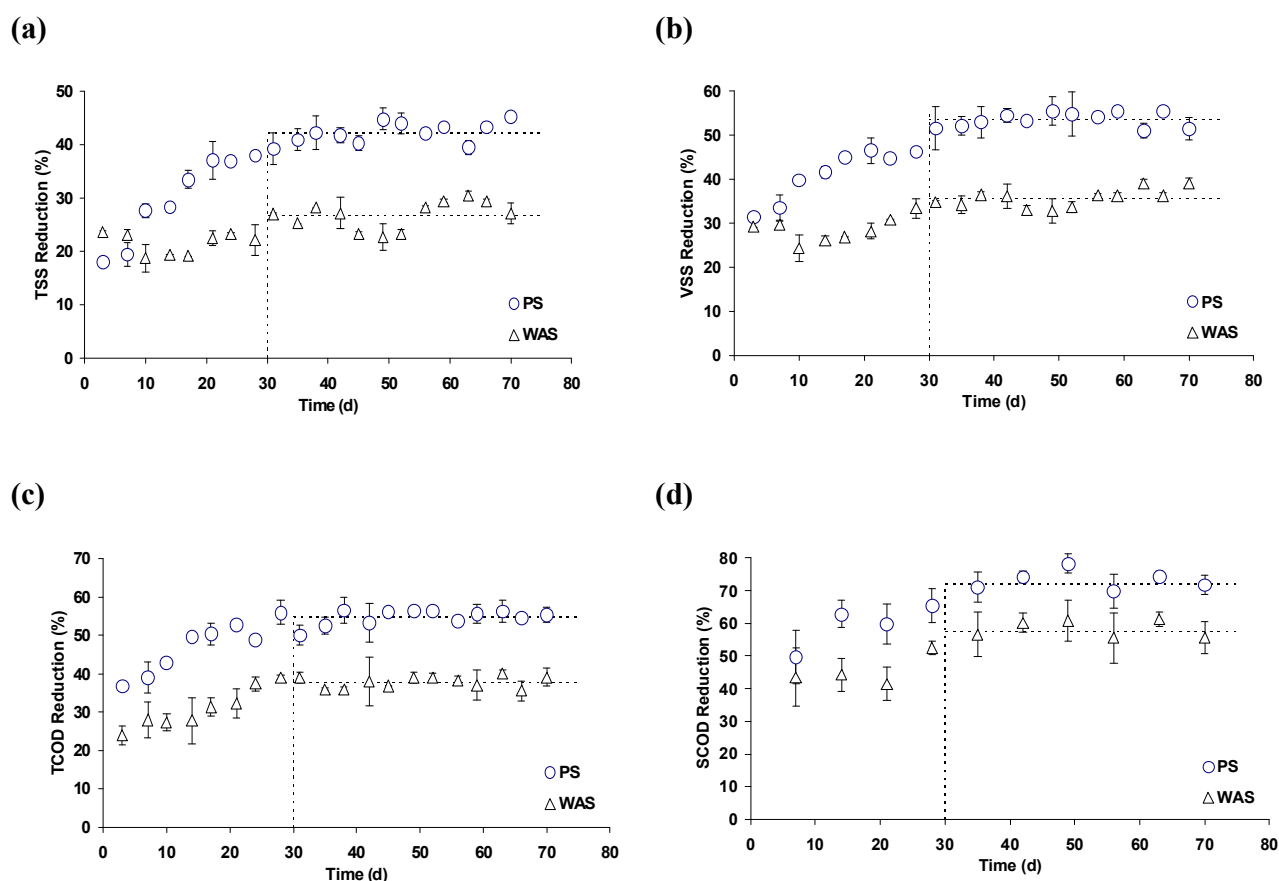


Figure 6.1 Reduction in PS and WAS in anaerobic digestion (a) TSS (b) VSS (c) TCOD (d) SCOD.

Table 6.1 Performance of AD during PS and WAS runs

Param.	Steady-state Performance [AVG \pm SD (n)]					
	Primary Sludge (mg/L)		Waste Activated Sludge (mg/L)		Ave. Red. (%)	
	Influent	Effluent	Influent	Effluent	PS	WAS
TSS	20521 \pm 768(12)	11843 \pm 627(24)	17914 \pm 721(12)	13138 \pm 412(24)	42.3	26.5
VSS	15729 \pm 1364(12)	7990 \pm 679(24)	12728 \pm 397(12)	8485 \pm 611(24)	53.7	35.7
TCOD	30827 \pm 1223(12)	13931 \pm 1010(24)	23402 \pm 1069(12)	14288 \pm 477(24)	54.8	38.6
SCOD	3078 \pm 61(12)	878 \pm 77(24)	2092 \pm 212(12)	852 \pm 69(24)	71.4	58.5
TBOD₅	7532 \pm 542(6)	1690 \pm 434(12)	7345 \pm 798(6)	2886 \pm 463(12)	77.6	60.7
CH₄ (%)	54.0 \pm 3.0		62.0 \pm 3.0			
CO₂ (%)	44.5 \pm 5.0		36.2 \pm 4.0			
H₂S (%)	1.06 \pm 0.4		1.62 \pm 0.5			

Average TSS reduction of 42 \pm 5% and 27 \pm 3%, VSS reduction of 54 \pm 1.7% and 36 \pm 2%, TCOD reduction of 55 \pm 1.2% and 39 \pm 2.3%, and SCOD reduction of 71 \pm 3.9% and 59 \pm 3% for PS and WAS, respectively are in consistent with the literature [14, 15, 16]. Average TBOD₅ reduction was 78 \pm 5% and 61 \pm 3.7% for PS and WAS, respectively, on the other hand, total nitrogen (TN) and total phosphorus (TP) removal in both systems were insignificant (practically zero) as expected and not identifiable within the analytical accuracy. In both PS and WAS, the order of reductions was: TBOD₅ > SCOD > TCOD > VSS > TSS. The above results indicate that WAS is more difficult to be degraded than PS as widely reported in the literature. The accumulation of methane from PS was greater than that in WAS as the total experimental methane was 84 \pm 1.6 L and 49 \pm 0.1 L vs. theoretical methane of 89 \pm 1.3 mL and 41 \pm 0.5 mL, respectively. Experimental methane production rates were 1.2 and 0.7 L/d vs. theoretical production rate of 1.3 and 0.6 L/d

for PS and WA, respectively. Theoretical methane was determined based on CH₄ equivalent COD of 0.395L CH₄/gCOD at 37°C [17]. It is necessary to note that in the case of PS the theoretical values of CH₄ were 6% higher than the experimental values, while the opposite (19% lower) was observed in the case of WAS. Nonetheless, based on the results obtained from the t-test analysis we can conclude that there is no statistically significant difference between experimental and theoretical methane for both PS and WAS at the 95% confidence level. The composition of bio-gas in both systems is shown in Table 6.1. Although the WAS digester exhibited lower VSS and COD destruction efficiencies, higher methane content was observed at 62% versus 54% in the PS digester. The above results indicated that both PS and WAS digestion reactors were working well and produced expected results.

6.3.2 Odorous compounds and odours precursors:

6.3.2.1 Volatile Fatty Acids (VFA):

Figure 6.2a shows the influent concentrations of the volatile fatty acid components in PS and WAS. The concentration of VFA in PS (1855±58 mg/L) was much higher than that of WAS (506±17 mg/L). For PS, acetic acid (482±59 mg/L), propionic acid (481±46 mg/L), and butyric acid (540±79 mg/L) were the predominant VFA, while in WAS only acetic and propionic acid concentrations were high at 226±26 mg/L and 171±15 mg/L, respectively. The ratio of VFA in PS to WAS was around 3.7. The average VFA/SCOD ratios were 2.2% and 0.6% for PS and WAS, respectively. Higher concentrations of the organic acid in PS may indicate septicity of the sludge [18]. In addition, higher concentrations of VFAs after anaerobic digestion in PS indicate greater odor potential for

this sludge. Figure 6.2b presents the average reduction of each VFA for both systems. The removal efficiencies are very high for all volatile acids. The average VFA reduction reached $97\pm 1\%$ for PS and $92\pm 5\%$ for WAS.

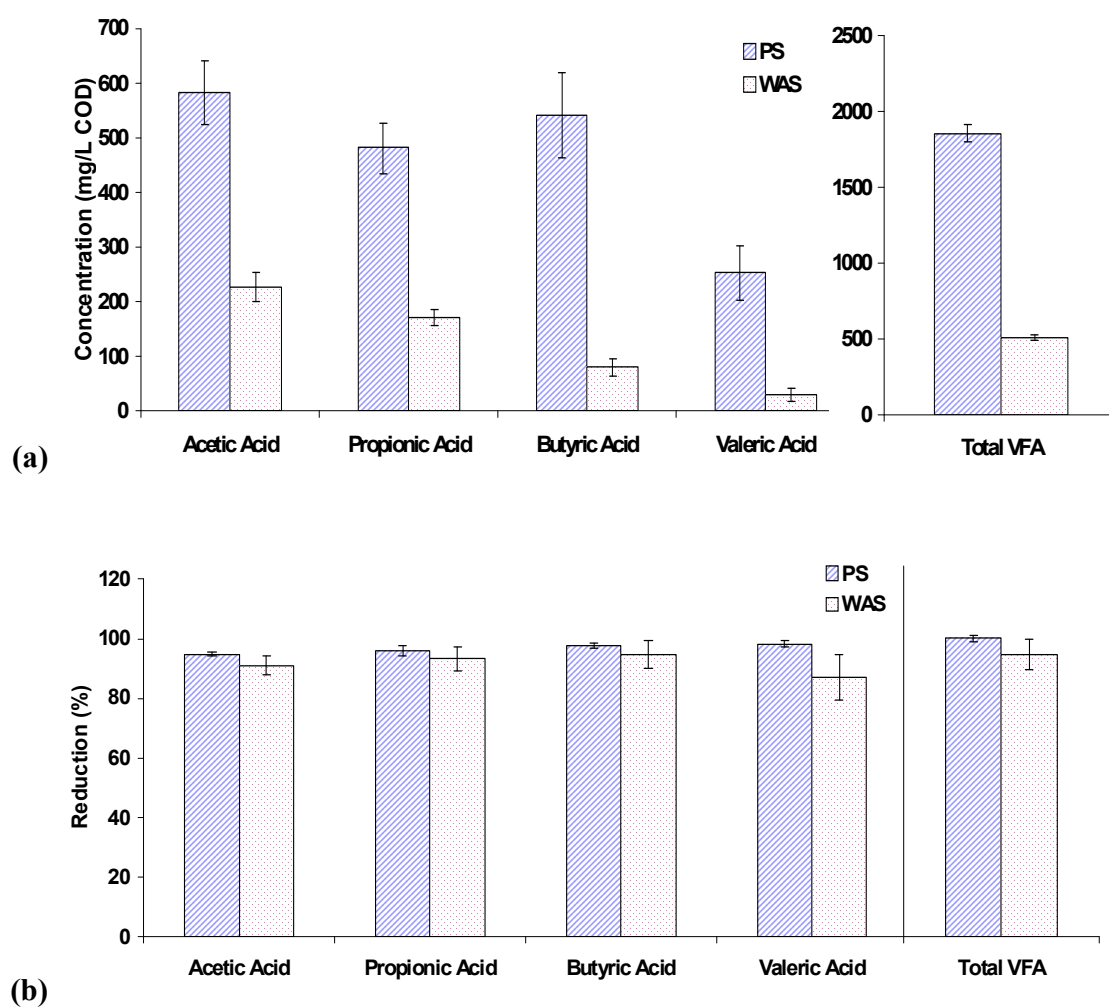


Figure 6.2 Average VFA in PS and WAS. (a) influent concentrations (b) reduction.

6.3.2.2 Proteins Fractions:

Table 6.2 displays the average influent concentrations of various protein fractions in PS and WAS. Soluble protein was 12% and 10% of the SCOD for PS and WAS, respectively, while the particulate protein was 9% and 12% of the particulate COD.

Table 6.2 Average concentrations, and reductions of various protein fractions in PS and WAS

Proteins	Primary Sludge (mg/L)			Waste Activated Sludge (mg/L)		
	Influent	Effluent	Red. (%)	Influent	Effluent	Red. (%)
Soluble protein (mg/L)	387 ± 98			230 ± 77		
Particulate protein (mg/L)	2158 ± 119			2531 ± 87		
Bound protein (mg/L)	380 ± 37	158 ± 16	61.4 ± 4.8	702 ± 33	294 ± 28	58.5 ± 3.2
Cell protein (mg/L)	1777 ± 92	1204 ± 82	31.2 ± 5.0	1828 ± 64	1481 ± 71	18.0 ± 5.5
Particulate Protein (g/gVSS)	0.133	0.171		0.199	0.211	
Bound Protein (g/gVSS)	0.024	0.020		0.055	0.036	
Cell Protein (g/gVSS)	0.110	0.151		0.143	0.174	

The labile and particulate protein fractions of the PS were lower than those of WAS, whereas higher soluble protein was observed in the PS compared to WAS. The relatively higher labile and particulate protein concentrations in WAS relative to PS are reasonable since labile and particulate proteins are associated with bacterial cell mass and the WAS is primarily biomass. As seen above, average reduction of soluble protein and particulate

protein in PS was $67\pm 3.4\%$ and $40\pm 2.5\%$, respectively, which is slightly higher than that of WAS' $61\pm 3.2\%$, and $31\pm 3\%$, respectively. Figure 6.3a shows that particulate protein reduction correlated well with the VSS reduction in both PS and WAS with R^2 of 85% and 82%, respectively. Since particulate protein is composed of the cellular protein and bound protein (loosely attached with the cell), it is also considered as a component of VSS, and the correlation of its degradation with that of VSS is reasonable. As indicated earlier, odor potential is directly related to the labile/bound protein content in sludge/biosolids [2, 19] and its removal can substantively reduce the malodor of sludge. The average reduction of bound or labile protein for both PS and WAS were $61\pm 4.8\%$ and $59\pm 3\%$, respectively. It is also noticeable that there is no statistically significant difference between the bound protein reductions in both PS and WAS at the 95% confidence level. Figure 6.3b shows the relationship between bound protein reduction and VSS reduction; bound protein reduction increases from 45% to 68% with VSS reduction from 28% to 37% in the case of PS. For WAS bound protein reduction increased from 51% to 67% with VSS reduction changed from 31% to 50%; bound protein or the labile fraction of proteins reduction are also positively correlated with VSS reduction.

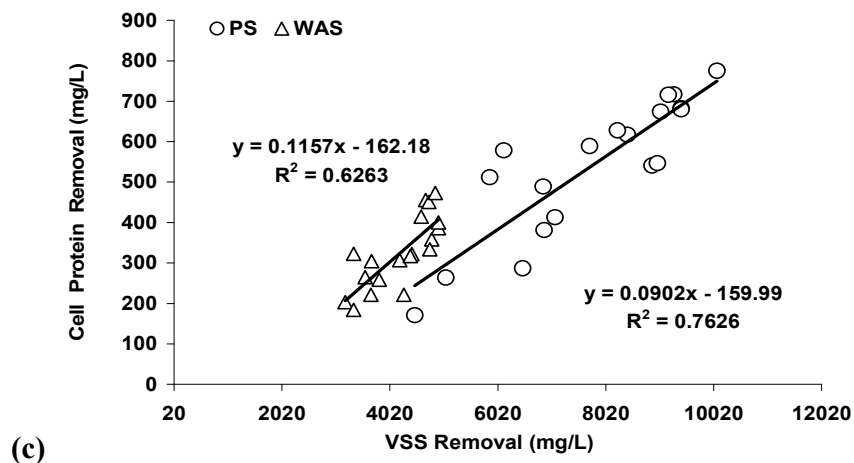
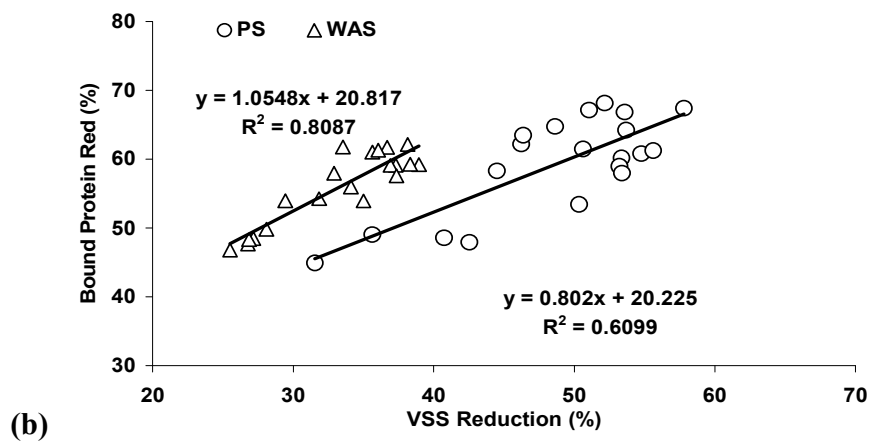
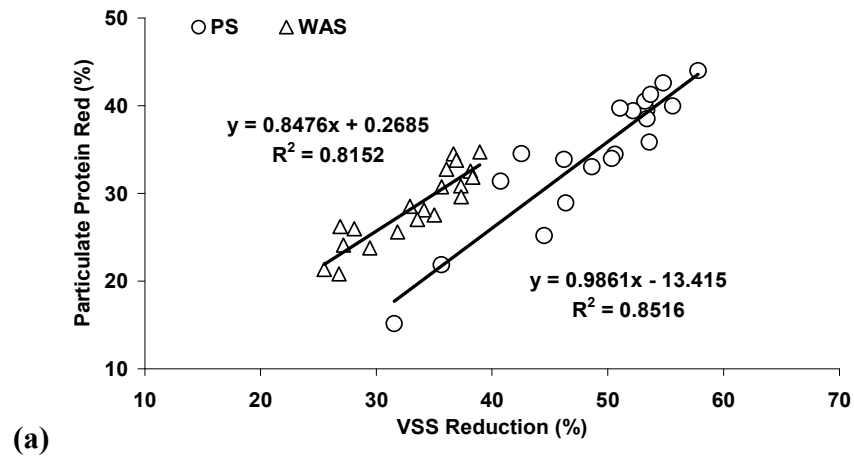


Figure 6.3 Relationship between VSS degradations and protein fractions during anaerobic digestion for PS and WAS (a) Particulate (b) Bound (c) Cell.

Further analysis was conducted using the particulate protein data. The difference between particulate and bound protein is the cellular protein of the bacterial mass, degradations of bound and cell protein in both PS and WAS are compared in Table 6.2. Although, bound protein removals in both sludges were comparable, the cellular protein removal was slightly higher in PS than WAS consistent with the relatively higher VSS destruction in PS. Cell protein removal was reasonably correlated with VSS removal (Figure 6.3c). Bound protein removal was better than cell protein in both sludges reflecting the biodegradability of bound protein [13]. The particulate protein content was normalized with respect to VSS content and is presented in Table 6.2 for the raw and digested sludges. As expected, WAS has more particulate protein than PS, due to the fact that WAS is predominantly biomass and both bound and cell protein are parts of the biomass in WAS. Data in Table 6.2 confirm that bound protein per unit mass of VSS in primary sludge and WAS decreased by about 17% and 33%, respectively implying that odor generation potential downstream of anaerobic digestion is mitigated not only as a result of anaerobic VSS reduction, but also by a reduction in bound/labile protein per unit mass, as bound protein is also a constituent of VSS. In this study, cell protein removal was only about 7% - 8% of the VSS removal.

6.3.2.3 Lipid Degradation:

Lipids are also a source of odor in biosolids storage. The average concentrations of lipids in raw PS and WAS were 1486 ± 423 mg/L and 367 ± 144 mg/L, respectively. Compared to other constituents, lipid reduction for both types of sludges exhibited greater variability, as reflected by the steady state averages of 64 ± 6.8 % and 38 ± 4.7 % for PS and WAS,

respectively. The higher lipid reduction in PS is intriguing as fats and greases, which predominate in PS are generally less biodegradable than oils [20].

6.4 Simulation and kinetics for odor-causing constituent:

The steady-state Anaerobic Digestion Model #1 (ADM1) had been used with good success for approximately two years on a wide range of full-scale wastewater treatment facilities [10, 21, 22]. All biochemical extracellular solubilization steps are divided into disintegration and hydrolysis, of which the first is a largely non-biological step and converts composite particulate substrate to inerts, particulate carbohydrates, protein and lipids. The second is enzymatic hydrolysis of particulate carbohydrates, proteins and lipids to monosaccharides, amino acids and long chain fatty acids (LCFA), respectively. Disintegration is mainly included to describe degradation of composite particulate material with lumped characteristics (such as primary or waste-activated sludge), while the hydrolysis steps are to describe well defined, relatively pure substrates (such as cellulose, starch and protein feeds). All disintegration and hydrolysis processes are represented by first order kinetics. Two separate groups of acidogens degrade monosaccharide and amino acids to mixed organic acids, hydrogen and carbon dioxide. The organic acids are subsequently converted to acetate, hydrogen and carbon dioxide by acetogenic groups that utilize LCFA, butyrate and valerate (one group for the two substrates), and propionate. The hydrogen produced by these organisms is consumed by hydrogen-utilizing methanogenic bacteria, and the acetate by aceticlastic methanogenic bacteria. Death of biomass is represented by first order kinetics, and dead biomass is maintained in the system as composite particulate material. Inhibition functions include

pH (all groups), hydrogen (acetogenic groups) and free ammonia (aceticlastic methanogens). pH inhibition is implemented as one of two empirical equations, while hydrogen and free ammonia inhibition are represented by non-competitive functions. The other uptake-regulating functions are secondary Monod kinetics for inorganic nitrogen (ammonia and ammonium), to prevent growth when nitrogen is limited, and competitive uptake of butyrate and valerate by the single group that utilizes these two organic acids.

Total protein, lipids, carbohydrate, inert particulates as well as soluble components that include amino acids, long chain fatty acids, sugars and VFAs were the model inputs with protein (measured) based on $C_6H_{14}O_2N_2$, lipid (measured) based on $C_{57}H_{104}O_6$, [23], inert particulates (measured as TS minus VS), carbohydrate (estimated from the particulate COD mass balance), long chain fatty acids (measured), amino acids (measured as soluble protein), sugars (estimated from the soluble COD balance), acetate (measured), propionate (measured), and butyrate (measured). The various components of biomass, i.e., sugar, amino acid, long chain fatty acids, valerate and butyrate, propionate, acetate, and hydrogen degraders, all were set to zero following the recommendation of Batstone et al. [4]. The input values of ADM parameters as percentages of PCOD (particulate chemical oxygen demand) were 10% protein, 15% lipids, and 57% carbohydrate with sugars, amino acids, long chain fatty and VFA's contributing 2%, 8%, 5%, and 60% of the SCOD respectively in the case of PS, while in the case of WAS the corresponding contribution of protein, lipid and carbohydrate to PCOD were 6%, 5%, and 55% with sugars, amino acids, long chain fatty and VFA's contributing, 13%, 7%, 27% and 24% of the SCOD. It is evident that PS contained higher percentage of lipids and VFAs than WAS, while the sugars and long chain fatty acids were higher in WAS than PS. The

kinetics, stoichiometric and physico-chemical parameters used in this simulation are the recommended/default values reported in the ADM1 technical report [4], whereas the modified (optimized) kinetics parameters were determined after calibration of the ADM1 simulations with the experimental data of the anaerobic reactors used in this work. It is important to mention that the reaction rates (kinetics) vary widely based on the type of sludge or substrate used, Christ et al. reported the hydrolysis rate coefficient (k) were in the range of $0.025-0.2d^{-1}$, $0.015-0.075d^{-1}$, and $0.005-0.01d^{-1}$ for carbohydrates, proteins and lipids in sewage sludge, respectively [13], Gujer and Zehnder reported that the k were in the range of $0.041-0.13d^{-1}$, $0.02-0.03d^{-1}$, and $0.08-0.4d^{-1}$ [4], O'Rourke et al. found them to be $0.21-1.94d^{-1}$, $0.0096-0.1d^{-1}$, and $0.0096-0.17d^{-1}$ in PS [4], while Batstone et al. reported that k was $0.25d^{-1} \pm 100\%$, $0.2d^{-1} \pm 100\%$, and $0.1d^{-1} \pm 300\%$ [4].

The first step was to set the initial (default) values for all model parameters. Subsequently the simulation was undertaken to fit the model output to the experimental data. Based on the simulation outcome the kinetics values were optimized. Initial parameter values, percent variation, estimated parameter values for PS and WAS that better fit the experimental data are given in Table 6.3.

Table 6.3 Default and optimized ADM kinetic parameters for both PS and WAS sludge

				ADM*	Varies within*	Estimated PS	Estimated WAS
Hydrolysis	carbohydrate	K_hyd_ch	d ⁻¹	0.25	100%	0.3	0.1
	protein	K_hyd_pr	d ⁻¹	0.2	100%	0.05	0.03
	lipids	K_hyd_li	d ⁻¹	0.1	300%	0.09	0.05
Maximum uptake rate	sugars	km_su	d ⁻¹	30	100%	30	30
	amino acids	km_aa	d ⁻¹	50	100%	4	5
	long chain fatty acids	km_fa	d ⁻¹	6	300%	6	6
	Propionic acid	km_pro	d ⁻¹	13	100%	15	20
	Acetic acid	km_ac	d ⁻¹	8	100%	8	11
	Valeric acid + Butyric acid	km_c4	d ⁻¹	20	100%	20	30
Half saturation constant	sugars	Ks_su	kgCOD/m ³	0.5	100%	0.5	0.5
	amino acids	Ks_aa	kgCOD/m ³	0.3	30%	0.3	0.3
	long chain fatty acids	Ks_fa	kgCOD/m ³	0.4	300%	0.4	0.4
	Propionic acid	Ks_pro	kgCOD/m ³	0.1	100%	0.1	0.1
	Acetic acid	Ks_ac	kgCOD/m ³	0.15	100%	0.1	0.1
	Valeric acid + Butyric acid	Ks_c4	kgCOD/m ³	0.3	300%	0.1	0.1

* (Batstone et al., 2002)

To better describe the process, the initial values of the carbohydrate, lipid and protein hydrolysis rate coefficients, for example, were set based on the technical report [4] $k_{\text{hyd_ch}} = 0.25 \text{ d}^{-1}$, $k_{\text{hyd_pr}} = 0.2 \text{ d}^{-1}$, and $k_{\text{hyd_li}} = 0.1 \text{ d}^{-1}$ respectively, then ADM1 model was

applied and its outcomes were compared to experimental data, based on the comparison the kinetics were optimized to $k_{\text{hyd_ch}} = 0.3 \text{ d}^{-1}$, $k_{\text{hyd_pr}} = 0.05 \text{ d}^{-1}$, and $k_{\text{hyd_li}} = 0.09 \text{ d}^{-1}$ in the case of PS and $k_{\text{hyd_ch}} = 0.1 \text{ d}^{-1}$, $k_{\text{hyd_pr}} = 0.03 \text{ d}^{-1}$, and $k_{\text{hyd_li}} = 0.05 \text{ d}^{-1}$ in the case of WAS. As expected, the hydrolysis kinetic parameters were higher in PS than WAS, since primary sludge contains more particulate substrates such as lipids, carbohydrates and proteins than the WAS, which is predominantly biomass with large biopolymers that are more difficult to degrade. The relative ease of biodegradability of PS as compared to WAS is well documented in the literature [15]. Table 6.4 displays the influent and effluent sludge characteristics as well as the methane production along with the ADM predictions for both PS and WAS, respectively.

It is evident that the model results with optimized parameters showed good agreement with the experimental data for methane production with average percentage error of 3% and 5% for primary and WAS, respectively. Similar agreement was observed in case of odor precursors, namely, protein, VFAs, lipids and amino acid as the percentage error were 6%, 4%, 1%, and 5% for PS and 3%, 11%, 6%, and 0.1% in the case of WAS, respectively. Maximum deviation in the fitted parameter values from the default values occurred for hydrolysis rate constant for protein and maximum uptake rate for amino acids.

Table 6.4 Experimental influent and effluent characterization with the ADM prediction for primary and WAS sludge.

		Exp.	ADM			
Primary Sludge	Gas (L/d)	1.2	1.24			
		Influent	Effluent	ADM	Reduction Exp.	Reduction ADM
	SCOD (mg/L)	3078	878	961	71%	69%
	TCOD (mg/L)	30827	13931	14627	55%	53%
	Lipid (mg/L)	1485.0	665	657.4	55%	56%
	P Protein (mg/L)	2158.0	1367	1281.5	37%	41%
	Amino acid (mg/L)	193.5	81.5	85.2	58%	56%
	Propionate (mg/L)	481	19	20.8	96%	96%
	Butyrate (mg/L)	540	12	10.7	98%	98%
	Valerate (mg/L)	252	4	4.9	98%	98%
	Acetate (mg/L)	582	30	31.1	95%	95%
VFA (mg/L)	1855.0	65.0	67.6	96%	96%	
Waste Activated Sludge	Gas (L/d)	0.68	0.65			
		Influent	Effluent	ADM	Reduction Exp	Reduction ADM
	SCOD (mg/L)	2092	852	788	59%	62%
	TCOD (mg/L)	23402	14288	14993	39%	36%
	Lipid (mg/L)	367	215	228.3	41%	38%
	P Protein (mg/L)	2529	1828	1774.3	28%	30%
	Amino acid (mg/L)	115	56	56.4	51%	51%
	Propionate (mg/L)	171	11	13.6	94%	92%
	Butyrate (mg/L)	80	5	6.3	94%	92%
	Valerate (mg/L)	29	3	2.9	90%	90%
	Acetate (mg/L)	226	19	19.5	92%	91%
VFA (mg/L)	506.0	38.0	42.2	92%	92%	

6.5 Conclusions:

Degradation of odorous compounds such as VFA, lipid and bound protein in sludge during anaerobic digestion was systematically monitored and modeled using the ADM1.

Below are the highlights of the major findings of this study:

- In general, anaerobic digestion efficiency for all sludge primary parameters such as TSS, VSS, TCOD, SCOD and TBOD₅ for primary sludge was higher than waste activated sludge.
- The concentration of VFA in the raw PS of 1855 ± 58 mg/L was considerably higher than the raw WAS of 506 ± 17 mg/L, with average removal efficiencies during anaerobic digestion of $97 \pm 1\%$, and $92 \pm 5\%$, respectively. The average concentrations of lipids in the raw PS and WAS were 1486 ± 423 mg/L and 367 ± 144 mg/L, respectively, and the removal of lipid varied during anaerobic digestion varied.
- Average reductions of various protein fractions were $40 \pm 2.5\%$ and $31 \pm 3\%$ for particulate protein, $67 \pm 3.4\%$ and $61 \pm 3.2\%$ for soluble protein, and $61 \pm 4.8\%$ and $59 \pm 3\%$ for bound or labile protein for PS and WAS, respectively. Reduction of bound protein or the labile protein, which is implicated in odor production in sludge, was positively correlated with VSS reduction for both sludges. No statistically significant difference was observed between the bound protein reductions in both PS and WAS. A 17% and 37% reduction in bound protein per unit VSS, indicates a possible reduction in odor generation potential not only associated with stabilization of VSS, but also due to bound protein degradation.

- The steady-state Anaerobic Digestion Model #1 (ADM1) was used to simulate the steady state lab scale anaerobic digester. The model predicted both the methane production and odor precursors. The model results with optimized parameters showed good agreement with the experimental data for methane production with average percentage errors of 3% and 5% for primary and WAS, respectively. Good agreement was also observed for the odor precursors, namely, protein, VFAs, lipids and amino acids as reflected by percentage errors of 6%, 4%, 1%, and 5% in the case of PS and 3%, 11%, 6%, and 0.1% in the case of WAS, respectively.

6.6 References:

- [1] Higgins, M.; Adams, G.; Chen, Y.; Erdal, Z.; Forbes, R.; Glindemann, D.; Hargreaves, J. McEwen, D.; Murthy, S.; Novak, J.; Witherspoon, J. Role of Protein, Amino Acids, and Enzyme Activity on Odor Production from Anaerobically Digested and Dewatered Biosolids, *Wat. Environ. Res.*, 2008, 80, 127.
- [2] Higgins, M.; Adams, G.; Chen, Y.; Erdal, Z.; Forbes, R.; Glindemann, D.; Hargreaves, J. McEwen, D.; Murthy, S.; Novak, J.; Witherspoon, J. Relationship between biochemical constituents and production of odor causing compounds from anaerobically digested biosolids, *WEF and AWWA Odors and Air Emissions 2004 Conference*, Washington, USA, 2004, 18-24.
- [3] Rideout, T. C.; Fan, M. Z.; Cant, J. P.; Wagner-Riddle, C.; Stonehouse, P. Excretion of major odor-causing and acidifying compounds in response to dietary supplementation of chicory inulin in growing pigs, *J. Anim. Sci.* 2004, 82, 1678-1684.
- [4] Batstone, D. J.; Keller, J.; Angelidaki, I.; Kalyuzhnyi, S. V.; Pavlostathis, S. G.; Rozzi, A.; Sanders, W. T. M.; Siegrist, H.; Vavilin, V. A. Anaerobic Digestion Model No. 1, IWA Task Group for Mathematical Modelling of Anaerobic Digestion Processes, *Water Sci. Technol.* 2002, 10, 65–73.
- [5] Barnett, J.W.; Kerridge, G.J.; Russell, J. M. Effluent treatment systems for the dairy industry. *Aus. Biotech.* 1994, 4, 26-30.
- [6] Dignac, M. F.; Ginestet, M. P.; Rybacki, D.; Bruchet, A.; Urbain, V.; Scribe, P.; Fate of wastewater organic pollution during activated sludge treatment: nature of residual organic matter, *Water Research.* 2000, 34, 4185-4194.
- [7] Breure, A. M.; Mooijman, K. A.; Van-Andel, J. G. Protein degradation in anaerobic digestion: influence of volatile fatty acids and carbohydrates on hydrolysis and acidogenic fermentation of gelatin, *Appl. Microbiol. Biotechnol.* 1986, 24, 426-431.
- [8] Kisaalita, W. S. ; Lo, K. V.; Pinder, K. L. Influence of whey protein on continuous acidogenic degradation of lactose, *Biotechnol. Bioeng.* 1990, 36, 642-646.

- [9] Gavala, H. N.; Angelidaki, I.; Ahring, B. K. Kinetics and modeling of anaerobic digestion process. *Adv. Biochem. Eng. Biotechnol.* 2003, 81, 57-93.
- [9] Johnson, B. A and Shang, Y. Applications and limitations of ADM 1 in municipal wastewater solids treatment, *Water Sci. Technol.* 2006, 54, 77–82.
- [10] APHA. *Standard Methods for the Examination of Water and Wastewater*, Washington DC, APHA, 1998.
- [11] Lowry, O. H.; Rosebrough, N. J.; Fair, A. L.; Randall, R. J. Protein measurement with the folin-phenol reagent, *J. Biol. Chem.* 1951, 193, 265-275.
- [12] Gujer, W.; Henze, M.; Mino, T.; Loosdrecht, M. Activated sludge model no. 3, *Water Sci. Technol.* 1999, 39, 183–193.
- [13] Mata-Alvarez, J.; Macé, S.; Llabrés, P.; Anaerobic digestion of organic solid wastes. an overview of research achievements and perspectives. *Bioresour. Technol.* 2000, 74, 3-16.
- [14] Roš, M.; Zupančič, G. D. Thermophilic anaerobic digestion of waste activated sludge. *Acta Chim. Slov.* 2002, 50, 59-74.
- [15] Park, C.; Lee, C.; Kim, S.; Chen, Y.; Chase, H. Upgrading of anaerobic digestion by incorporating two different hydrolysis processes *J. Biosci. Bioeng.* 2005, 100, 164-167.
- [16] Metcalf and Eddy, *Wastewater Engineering: Treatment Disposal Reuse*, 2003, 4th ed. McGraw-Hill
- [17] Richard, M. Activated sludge microbiology problems and their control. 20th Annual USEPA National Operator Trainers Conference. Buffalo, NY, June 8, 2003.
- [18] Subramanian, R.; Novak, J. T.; Murthy, S.; North, J. Investigating the role of process conditions in wastewater sludge odor generation, *WEFTEC 2005*, Washington, D.C., USA. 2005.
- [19] Cirne, D. G.; Paloumet, X.; Björnsson, L.; Alves, M.; Mattiasson, B. Anaerobic digestion of lipid-rich waste-effects of lipid concentration. *Ren. Ene.* 2007, 32, 965-975.

- [20] D. J. Batstone and J. Keller, Industrial applications of the IWA anaerobic digestion model No. 1 (ADM1), *Water Sci. Technol.* 47 (12), 2003, pp199-206.
- [21] Blumensaat, F.; Keller, J. Modelling of two-stage anaerobic digestion using the IWA Anaerobic Digestion Model No.1 (ADM1), *Wat. Res.* 2004, 39, 171–183.
- [22] Jeppsson, U. Investigation of anaerobic digestion alternatives for Henriksdal's WWTP IEA, Lund University. 2007.

CHAPTER SEVEN

Anaerobic Digestion Model Software Implementation

7.1 Introduction:

The Anaerobic Digestion Model No. 1 (ADM1) concept, parameters, implementation specifics are presented and discussed in this chapter. The ADM1 is a structured knowledge model which takes biochemical and physicochemical processes of the AD into account. It was developed by the IWA task group for Mathematical Modeling of Anaerobic Digestion Processes [1] and carried the following benefits:

- 1- Model application for full-scale plant design, operation and optimization.
- 2- Process optimization and control, aimed at direct implementation in full-scale plants as a further development work.
- 3- Forming the common basis for further model development and validation studies to make outcomes more comparable and compatible.
- 4- Technology transfer from research to industry.

The ADM1 model expresses the state variables concentration in kgCOD/m^3 , the molar concentration kmole/m^3 was used for components that have no COD content. The overall units used throughout the model are given in Table 7.1. Tables 7.2 to 7.5 display the model parameters for stoichiometric coefficients, equilibrium coefficients and constants, kinetic reaction coefficients and rates and dynamic state variables and algebraic variables.

Table 7.1. Units used in the ADM1 model

Discretion	Units
Concentration	kgCOD/m ³
Concentration (carbon non-COD)	kmole C/m ³
Concentration (nitrogen non-COD)	kmole N/m ³
Concentration (cations and anions)	kmole/m ³
Pressure	bar
Temperature	K
Volume	m ³
Time	d

Table 7. 2 Nomenclature, description of stoichiometric coefficients

Symbol	Discretion	Units
C _i	Carbon content of component i	kmole C/kg COD
N _i	Nitrogen content of component i	kmole N/kg COD
v _{ij}	Stoichiometric coefficients for component i and process j	kgCOD/m ³
f _{product, substrate}	Yield of product on substrate	kgCOD/kg COD
Y _{substrate}	Yield of biomass on substrate	kgCOD/kg COD

Table 7.3 Nomenclature, description of equilibrium coefficients and constants

Symbol	Discretion	Units
K _{a,acid}	Acid-base equilibrium constant	M (kmole/m ³)
K _h	Henry's law coefficient	M bar ⁻¹
pK _a	-log ₁₀ [K _a]	
R	Gas law constant (8.314 x 10 ⁻²)	bar M ⁻¹ .K ^{o-1}

Table 7. 4 Nomenclature, description of kinetic constants and rates

Symbol	Discretion	Units
$K_{A/Bi}$	Acid-base kinetic constant	1/d
$K_{dec,acid}$	First order decay rate	1/d
$I_{inhibitor, process}$	Inhibition function	
$k_{process}$	First order constant	1/d
k_{La}	Gas-liquid transfer coefficient	1/d
$K_{I,inhibit,substrate}$	Inhibitory concentration	kgCOD/m ³
$k_{m, process}$	Monod maximum specific uptake rate	kgCOD subs/ kg COD biomass d ⁻¹
$k_{s, process}$	Half saturation constant	kgCOD subs /m ³
μ_{max}	Monod maximum specific growth rate	1/d

Table 7.5 Nomenclature, description of dynamic state variables, algebraic variables, and physical reactor parameters

Symbol	Discretion	Units
pH	$-\log_{10}[H^+]$	
$P_{gas,i}$	Partial pressure of gas i	bar
P_{gas}	Total gas pressure (1.013 bar)	bar
S_i	Soluble component i	kgCOD/m ³
T	Temperature	K ^o
V	Volume	m ³
X_i	Particulate component i	kgCOD/m ³

7.2 Reaction System:

Two main types of reactions were considered in the ADM1 [1] and they are: biochemical reactions and physicochemical reactions.

The model includes three overall biological intracellular steps and they are; acidogenesis, acetogenesis and methanogenesis as well as an extracellular disintegration (non-biological) step. In the biochemical processes, total input COD are separated since a considerable fraction of the input COD may not be anaerobically biodegradable [1, 2]. Physicochemical conversions aside from the biochemical equations are to describe the physico-chemical state effects, such as the effect of pH and gas concentration on biochemical reactions.

ADM1 assumes that complex particulate waste (total input COD) will first disintegrate to carbohydrate, protein and lipid particulate substrate, as well as particulate and soluble inert material. The disintegration occurs before the depolymerizations, since the primary substrate is represented by lumped kinetic and biodegradability parameters [1, 2, 3]. The particulate waste is also used as a pre-lysis repository of decayed biomass. The disintegration step is assumed to include lysis, non-enzymatic decay, phase separation, and physical breakdown.

All biochemical extracellular steps were assumed to be first order, which is a simplification based on empiricism reflecting the cumulative effect of a multi-step process [1, 2]. The cellular processes were defined by uptake, growth, and decay expressions. Substrate uptake is chosen as a key rate equation to decouple the growth from uptake and to allow variable yields. The uptake is based on Monod-type kinetics. The substrate uptake includes the biomass growth implicitly. The process rate and

stoichiometry matrix for biochemical reactions are given in Appendix A, together with the physico-chemical rate equations. Suggested parameters and qualitative sensitivity and variability are given in Table 7.6 and 7.7.

Table 7. 6 Suggested stoichiometric parameters and qualitative sensitivity and variability

[1].

Parameter (dimensionless)	Description	Value	Var	Notes
$f_{si, xc}$	Soluble inerts from composites	0.1	2	1
$f_{xi, xc}$	Particulate inerts from composites	0.25	2	1
$f_{ch, xc}$	Carbohydrates from composites	0.20	2	1
$f_{pr, xc}$	Proteins from composites	0.20	2	1
$f_{li, xc}$	Lipids from composites	0.25	2	1
N_{xc}, N_i	Nitrogen content of composites and inerts	0.002	2	1
$f_{fa, li}$	Fatty acids from lipids	0.95	1	2
$f_{h2, su}$	Hydrogen from sugars	0.19	3	3
$f_{bu, su}$	Butyrate from sugars	0.13	3	3
$f_{pro, su}$	Propionate from sugars	0.27	3	3
$f_{ac, su}$	Acetate from sugars	0.41	3	3
$f_{h2, aa}$	Hydrogen from amino acids	0.06	2	3
N_{aa}	Nitrogen in amino acids	0.007	2	3
$f_{va, aa}$	Valerate from amino acids	0.23	2	3
$f_{bu, aa}$	Butyrate from amino acids	0.26	2	3
$f_{pro, aa}$	Propionate from amino acids	0.05	2	3
$f_{ac, aa}$	Acetate from amino acids	0.40	2	3

Var = Variability of parameter, 1 = varies very little between processes; 2 = varies between processes and substrates; 3 = varies dynamically within process.

Notes:

1 = Varies widely

2 = Based on palmitate triglyceride

3 = Calculated from sugar and amino acid values

Table 7. 7 Suggested parameter values and qualitative sensitivity and variability for mesophilic digestion [1].

Parameter	Mesophilic high-rate (nom.35°C)	Mesophilic solids (nom, 35°C)	S	Var	Notes
$k_{dis}(1/d)$	0.40	0.50	3	3	1
$k_{hyd_CH}(1/d)$	0.25	10	3	2	2
$k_{hyd_PR}(1/d)$	0.2	10	2	3	2
$k_{hyd_LI}(1/d)$	0.1	10	2	3	2
$t_{res, x}(d)$	40	0	3	2	2
$k_{dec_all}(1/d)$	0.02	0.02	2	2	3
$k_{S_NH3_all}(1/d)$	1×10^{-4}	1×10^{-4}	1	1	
pH _{UL} acet/acid	5.5	5.5	1	2	4
pH _{LL} acet/acid	4	4	1	2	4
$k_{m_su}(CODCOD/d)$	30	30	1	2	
$k_{S_su}(kgCOD/d)$	0.50	0.50	1	2	
$Y_{su}(COD/COD)$	0.10	0.10	1	1	
$k_{m_aa}(CODCOD/d)$	50	50	1	2	
$k_{S_aa}(kgCOD/m^3)$	0.30	0.30	1	1	
$Y_{aa}(COD/COD)$	0.08	0.08	1	1	
$k_{m_fa}(CODCOD/d)$	6	6	1	3	
$k_{S_fa}(kgCOD/m^3)$	0.40	0.40	1	3	
$Y_{fa}(COD/COD)$	0.06	0.06	1	1	
$K_{I,H2_fa}(kgCOD/m^3)$	5×10^{-6}	5×10^{-6}	1	1	
$k_{m_c4+}(CODCOD/d)$	20	20	1	2	
$k_{S_c4+}(kgCOD/m^3)$	0.30	0.30	1	3	
$Y_{c4+}(COD/COD)$	0.06	0.06	1	1	
$K_{I,H2_c4+}(kgCOD/m^3)$	1×10^{-5}	1×10^{-5}	1	1	
$k_{m_pro}(CODCOD/d)$	13	13	2	2	
$k_{S_pro}(kgCOD/m^3)$	0.30	0.30	2	2	

Y_{pro} (COD/COD)	0.04	0.04	1	1	
$K_{I,H2_pro}$ (kgCOD/m ³)	3.5×10^{-5}	3.5×10^{-5}	2	1	
k_{m_ac} (CODCOD/d)	8	8	3	2	
k_{S_ac} (kgCOD/m ³)	0.15	0.15	3	2	
Y_{ac} (COD/COD)	0.05	0.05	1	1	
pH _{UL ac}	7	7	3	1	5
pH _{LL ac}	6	6	2	1	5
$K_{I,NH3}$ (M)	0.0018	0.0018	2	1	
k_{m_h2} (CODCOD/d)	35	35	1	2	
k_{S_h2} (kgCOD/m ³)	2.5×10^{-5}	2.5×10^{-5}	1	1	
Y_{h2} (COD/COD)	0.06	0.06	2	2	5

S = Sensitivity of important output to parameter at average parameter values.

1 = low or no sensitivity of all outputs to parameter

2 = some sensitivity or significant sensitivity under dynamic conditions

3 = Significant sensitivity under steady-state conditions and critical sensitivity under dynamic conditions.

Var = Variability of parameter

1 = varies within 30%

2 = varies within 100%

3 = varies within 300%

Notes:

1 = mainly of importance in solids digester

2 = mainly of importance for pure or semi-separated solid substrates. When used with activated sludge fed digesters, k_{dis} is rate limiting

3 = decay rate can be set the same for all variables as a first guess. In many cases, a k_{dec} double the given values can be used for certain groups, such as acidogens and acetoclastic methanogens.

4 = pH_{acet/acid} inhibition factors for all acidogenic and acetogenic bacteria

5 = Notes as for (4) except values are methanogens-specific.

7.3 The Implementation of the ADM1 and Its Extension

Anaerobic digestion could be implemented as a Dynamic and Algebraic Equation (DAE) System [1, 4]. MatLab software provides ordinary dynamic equation solver system. Some of these solvers are explained below [4, 5]:

Ode23: This solver is an implementation of an explicit Runge-Kutta formula. It is a one-step solver and could be more difficult to converge than *Ode45* in cases of crude tolerances and moderate stiffness.

Ode45: this solver is based on an explicit Runge-Kutta formula. It is a one-step solver and it could be considered as the best function to apply for a “first try” for most problems.

Ode15s: this solver is a variable order solver based on the numerical differentiation formulas (backward differential formation, BDF, also known as Gear’s method) that are usually less efficient. It is a multi-step solve and can be considered as good for stiffness problems or when solving a differential-algebraic problem.

Ode23s: this solver is based on an extended Rosen Brock formula. It is a one-step solver, therefore, could be more efficient than *Ode15s* at crude tolerances and is used for the solution of specific type of stiffness problems where *Ode15s* are not efficient.

7.3.1 Dynamic State Variables:

There are 32 dynamic state variables, 19 biochemical process rates, and 3 liquid-gas transfer processes in the ADM1 dynamic system, in addition to six acid-base kinetic processes. ADM1 takes into account 6 more dynamic state variables due to the acid-base

dissociation. Table 7.8 and Table 7.9 display the ADM1 variables for soluble and particulate components, respectively.

Table 7. 8 Soluble components of DAE system dynamic state variables

State number	Name	Description	Units
1	S _{su}	Sugars	kgCOD/m ³
2	S _{aa}	Amino acids	kgCOD/m ³
3	S _{fa}	Long chain fatty acids	kgCOD/m ³
4	S _{hva}	Valeric acid	kgCOD/m ³
5	S _{va-}	Valerate	kgCOD/m ³
6	S _{hbu}	Butyric acid	kgCOD/m ³
7	S _{bu-}	Butyrate	kgCOD/m ³
8	S _{hpro}	Propionic acid	kgCOD/m ³
9	S _{pro-}	Propionate	kgCOD/m ³
10	S _{hac}	Acetic acid	kgCOD/m ³
11	S _{ac}	Acetate	kgCOD/m ³
12	S _{h2}	Dissolved hydrogen	kgCOD/m ³
13	S _{CH4}	Dissolved methane	kgCOD/m ³
14	S _{CO2}	Dissolved carbon dioxide	kgCOD/m ³
15	S _{HCO3}	Dissolved bicarbonate	kgCOD/m ³
16	S _{NH4+}	Ammonium	kgCOD/m ³
17	S _{NH3}	Ammonia	kgCOD/m ³
18	S _I	Soluble inerts	kgCOD/m ³
31	S _{cat}	Cations	kmol/m ³
32	S _{an}	Anions	kmol/m ³

Table 7. 9 Particulate components of DAE system dynamic state variables

State number	Name	Description	Units
19	X _c	Composites	kgCOD/m ³
20	X _{ch}	Carbohydrates	kgCOD/m ³
21	X _{pr}	Proteins	kgCOD/m ³
22	X _{li}	Lipids	kgCOD/m ³
23	X _{su}	Sugar degraders	kgCOD/m ³
24	X _{aa}	Amino acid degraders	kgCOD/m ³
25	X _{fa}	LCFA degraders	kgCOD/m ³
26	X _{C4}	C4 degraders	kgCOD/m ³
27	X _{pro}	Propionate degraders	kgCOD/m ³
28	X _{ac}	Acetate degraders	kgCOD/m ³
29	X _{h2}	Hydrogen degraders	kgCOD/m ³
30	X _I	Particulate inerts	kgCOD/m ³

7.3.2 Liquid Phase Equations

The general mass balance equation neglecting the diffusion terms and interfacial mass transfer for a CSTR reactor is given below [6].

$$[\text{Accumulation of mass}] = [\text{input}] - [\text{Output}] + [\text{Production}]$$

For each state component the mass balance equation can be written as [1]:

$$\frac{dV S_{liq,i}}{dt} = q_{in} S_{in,i} - q_{out} S_{liq,i} + V_{liq} \sum_{j=1-19} r_j v_{i,j} \quad \dots (7.1)$$

where $S_{liq,i}$ = liquid volume specific concentration variable

q_{in} = flow in

q_{out} = flow out

V = liquid volume

$\sum r_i v_{i,j}$ = summation of the specific kinetic rates for process j multiplied by rate coefficient, v_{ij} .

Assuming constant volume, $q = q_{in} = q_{out}$, equations can be further refined to:

$$\frac{dS_{liq,i}}{dt} = \frac{q \cdot S_{in,i}}{V_{liq}} - \frac{q \cdot S_{liq,i}}{V_{liq}} + \sum_{j=1-19} r_i v_{i,j} \dots (7.2)$$

and for varying retention time in the case of particulate substrates:

$$\frac{dX_{liq,i}}{dt} = \frac{q \cdot X_{in,i}}{V_{liq}} - \frac{X_{liq,i}}{t_{res,x} + \frac{V_{liq}}{q}} + \sum_{j=1-19} r_i v_{i,j} \dots (7.3)$$

where: $t_{res,x}$ = Retention time of solids components above hydraulic retention time used to simulate the separation solids retention.

7.3.3 Gas Phase Equations:

The model assumes constant reaction volume and integrating the gas state variables into the system of dynamic state variables, the gas phase differential equation can be stressed as follows:

$$\frac{dS_{gas,i}}{dt} = -\frac{q_{gas} S_{gas,i}}{V_{gas}} + r_{T,i} \frac{V_{liq}}{V_{gas}} \dots (7.4)$$

where $S_{gas,i}$ = Gas volume specific concentration variable

q_{gas} = overall dry gas flow (water corrected)

V_{gas} = Headspace volume

V_{liq} = Bulk reactor volume

$r_{T,i}$ = Liquid volume specific gas transfer rate, and i stands for one of the three gas components.

Table 7. 10 displays the dynamic state variables for gas composition

Table 7. 10 Gas components

State variables number	Name	Description	Unit
33	H ₂	Hydrogen	kgCOD/m ³
34	CH ₄	Methane	kgCOD/m ³
35	CO ₂	Carbon Dioxide	kgCOD/m ³

7.3.4 Liquid-Gas Transfer

The liquid-gas transfer rate equation is given below:

$$r_{T,j} = k_L a (S_{liq,i} - K_{H,i} p_{gas,i}) \quad \dots (7.5)$$

where $r_{T,j}$ = specific mass transfer rate of gas i

$k_L a$ = Overall mass transfer coefficient

$S_{liq,i}$ = Concentration of gas component i in the bulk

$K_{H,i}$ = Henry's law coefficient for gas i

$p_{gas,i}$ = Partial pressure of gas i in the headspace

Partial gas pressure, $p_{gas,i}$ for each gas component was calculated using ideal gas law pressure as:

$$P_{gas,i} = S_{gas,i} RT_{op} \quad \dots (7.6)$$

$S_{gas,i}$ = Concentration of gas i in the head space

R = Universal gas constant (0.08134 bar/M.K)

T = Operation temperature in Kelvin K°

$S_{gas,i}$ was divided by 16 and 64 for hydrogen and methane, respectively, to account for the COD equivalent of the gas.

The overall gas flow corrected for water vapor is found as:

$$q_{gas} = \frac{RT}{P_{gas} - P_{gas,H_2O}} V_{liq} \left(\frac{r_{T,H_2}}{16} + \frac{r_{T,CH_4}}{64} + r_{T,CO_2} \right) \quad \dots (7.7)$$

where P_{gas} = Total gas pressure generally could be fixed to 1.013 bar

P_{gas,H_2O} = Gas pressure of water at headspace corrected for operating temperature T_{op}

using the following formula:

$$P_{gas,H_2O} = 0.0313 \text{ Exp} \left(5290 \left(\frac{1}{298} - \frac{1}{T_{op}} \right) \right) \quad \dots (7.8)$$

The total head pressure of 1.013 bar was assumed for the case where the gas volume is frequently exchanged with the environment and direct connection to normal pressure conditions in the environment is provided.

7.3.5 Acid-Base Equilibria:

Six more state variables were added to represent the acid-base equilibrium [4]. The acid-base equilibrium equation is given below:

$$r_{A/B,i} = k_{A/B,i} (S_{liq,i-} (K_{a,i} + S_{H^+}) - K_{a,i} S_{liq,i}) \quad \dots (7.9)$$

$r_{A/B,i}$ = Production rate of acid from the base

$k_{A/B,i}$ = Acid-base kinetic constant

$S_{liq,i}$ = Total concentration of free form of organic acid, dissolved carbon dioxide or ammonium

$S_{liq,i-}$ = Concentration of ionic form of acid

S_{H^+} = Concentration of hydrogen ions in the bulk

$K_{a,i}$ = Acid-base equilibrium coefficient

Acid-base kinetic constant, $k_{A/B,i}$ is generally set to one order of magnitude higher than the highest biochemical rate since physicochemical reactions run faster than the biochemical ones. $k_{A/B,i}$ of 10^8 is applied for all acid-base equilibrium and 10^{12} applied to the IN and IC (CO₂) results in model performance with best numerical stability. Acid-base rates for VFA and IC applied as follows [7]:

$$\frac{dS_{liq,i}}{dt} = \frac{q_{in} S_{in,i}}{V_{liq}} - \frac{q_{out} S_{liq,i}}{V_{liq}} \quad \dots (7.10)$$

Where: $S_{in,i}$ = total concentration of organic acid in incoming waste

$S_{liq,i}$ = Total concentration of free form of organic acid, dissolved carbon dioxide or ammonium, and for ionic components:

$$\frac{dS_{i-}}{dt} = -r_{A/B,i} \quad \dots (7.11)$$

Where i is the total concentration and i^- is the ionic concentration form of the organic acids.

7.3.6 Determination of pH:

The pH is computed using the following equation:

$$\sum S_{C^+} - \sum S_{A^-} = 0 \quad \dots (7.12)$$

where S_{C^+} = the cationic equivalent concentrations

S_{A^-} = is anionic equivalent concentrations

Charge balance equation as implemented in ADM1 is given below:

$$S_{Cat^+} + S_{NH_4^+} + S_{H^+} - S_{HCO_3^-} - \frac{S_{Ac^-}}{64} - \frac{S_{pr^-}}{112} - \frac{S_{Bu^-}}{160} - \frac{S_{va^-}}{208} - S_{OH^-} - S_{An^-} = 0 \quad \dots (7.13)$$

$$\text{For } S_{OH^-} = \frac{K_w}{S_{H^+}} \quad \dots (7.14)$$

The S_{H^+} is computed from the quadratic equation (algebraic equation) by substituting equation 7.13 into the equation 7.12 [4, 7]:

The equation obtained by this substitution is given below:

$$S_{H^+} = -\frac{v + \sqrt{(-v)^2 + 4K_w}}{2} \quad \dots (7.15)$$

$$\text{Where } v = S_{Cat^+} + S_{NH_4^+} - S_{HCO_3^-} - \frac{S_{Ac^-}}{64} - \frac{S_{pr^-}}{112} - \frac{S_{Bu^-}}{160} - \frac{S_{va^-}}{208} - S_{An^-}$$

K_w = ionic product of water corrected for particular operational temperature.

This equation gives only one physical solution and the pH value is obtained from the following:

$$pH = -\log(S_{H^+}) \quad \dots (7.16)$$

7.3.7 Inhibition:

The following inhibition forms are assumed in the implementation:

- 1- Free ammonia and hydrogen inhibition: Inhibition due to the free ammonia is applied for the group of acetoclastic methanogens. Inhibition due to the high hydrogen level is applied to long chain fatty acids, C4 (butyrate, valerate) and propionate degrading bacteria, the inhibition is expressed as a non-competitive function:

$$I = \frac{1}{1 + \frac{S_I}{K_I}} \quad \dots (7.17)$$

where I = free ammonia and hydrogen inhibition, S_I = inhibitor concentration, K_I = inhibitor parameter ($K_{I, H_2, pro}$, $K_{I, H_2, c4}$, $K_{I, H_2, ac}$, K_{I, NH_3})

- 2- pH inhibition: this inhibition is applied to all degrading bacteria with specific limits for acetoclastic methanogens and hydrogen-utilizing methanogens. No inhibition is assumed above a pH of 7 (i.e., $I_n = 1$).

$$I = \exp\left(-3 \cdot \left(\frac{pH - pH_{UL}}{pH_{UL} - pH_{LL}}\right)^2\right) \quad \dots (7.18)$$

where the PH_{UL} and PH_{LL} are the upper and lower limits

3- Nitrogen limitation: this is included as a growth limitation due to the lack of nitrogen, using the following term:

$$I = \frac{1}{1 + \frac{S_I}{K_I}} \dots (7.19)$$

7.4 Software Development:

Batstone et al. [1], Johnson et al. [8] and Jeppsson et al. [9] have implemented and successfully applied the ADM1 model using AQUASIM, MATLAB/Simulink, MS EXCEL and FORTRAN, but their implementations were by no means close to the commercializing level or even user-friendly with enough documentation, which made the use of the ADM1 rather complex. The objective of this work was to develop a user-friendly software for ADM1.

Based on the work implemented by Batstone et al. [1] and Jeppsson et al. [9], the MATLAB 2008 (The MathWorks, Inc. Natick, US) ODE23S ordinary dynamic equation solver was used to solve the dynamic differential and algebraic system of equations, MS Visual Basic 6.0 was used to develop the user-interface, while MS Access was used to host the stoichiometric coefficients, equilibrium coefficients and constants, and reaction kinetic coefficients.

Figure 7.1 displays the ADM1 software developed in this work (ADM1-UWO) and shows the required field for input parameters.

The ADM1-UWO allows users to choose between two methods to load the required information:

- 1- Concentration method: in the method the users have to input all the required parameters illustrated in Figure 7.1.
- 2- Fraction method: users can set the percent of COD fractions based on their experience and knowledge, this can be done by entering the percentages for each of the component on the interface illustrated in Figure 7.2. In this method the user is required to enter TCOD, SCOD, TSS and VSS only and then click on the “%” button to activate the preset COD fractionation.

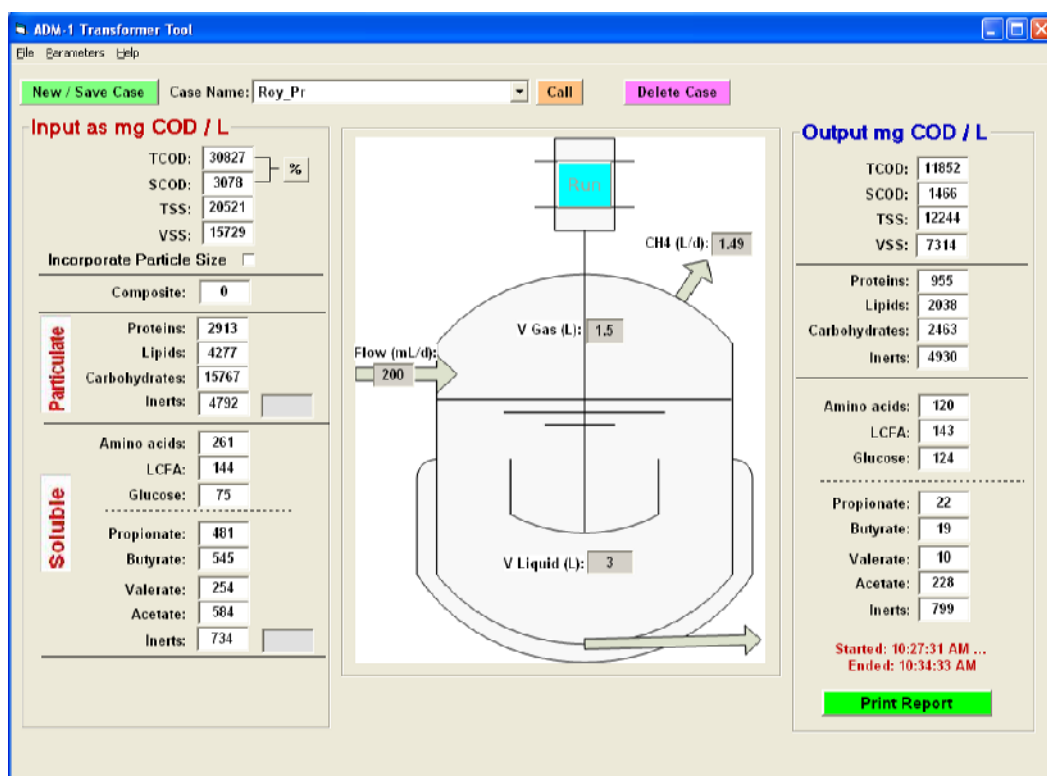


Figure 7. 1 ADM1 Software interface

SCOD (mg/L):	
Proteins (mg/L):	30
Lipids (mg/L):	30
Carbohydrates (mg/L):	30
Inerts (mg/L):	10
Amino acids (mg/L):	15
LCFA (mg/L):	15
Glucose (mg/L):	15
Propionate (mg/L):	10
Butyrate (mg/L):	5
Valerate (mg/L):	5
Acetate (mg/L):	15
Inerts (mg/L):	20

Figure 7. 2 Percentage composition interface

The software also allow users to change and modify the reaction kinetic coefficients, stoichiometric coefficients and initial (time = 0) state variables values. Figures 7.3 to 7.5 display the forms whereby the coefficients can be modified.

f_sl_xc:	0.1	f_h2_aa:	0.06	Y_su:	0.1	K_H_h2o_base:	0.0313
f_xl_x:	0.2	f_va_aa:	0.23	Y_aa:	0.08	K_H_co2_base:	0.035
f_ch_xc:	0.2	f_bu_aa:	0.26	Y_fa:	0.06	K_H_ch4_base:	0.0014
f_pr_xc:	0.2	f_pro_aa:	0.05	Y_c4:	0.06	K_H_h2_base:	7.8e-4
f_li_xc:	0.3	f_ac_aa:	0.4	Y_pro:	0.04	k_A_Bva:	1.0e10
f_fa_li:	0.95	T_op:	308.15	Y_ac:	0.05	k_A_Bbu:	1.0e10
f_h2_su:	0.19055	R:	0.08314	Y_h2:	0.06	k_A_Bpro:	1.0e10
f_bu_su:	0.13280	P_atm:	1.013			k_A_Bac:	1.0e10
f_pro_su:	0.26910	k_La:	200.0			k_A_Bco2:	1.0e10
f_ac_su:	0.40755					k_A_BIN:	1.0e10

Figure 7. 3 Stoichiometric parameters interface

Kinetics

k_dis (1/d):	0.5	k_dec_Xsu (1/d):	0.02
k_hyd_ch (1/d):	10	k_dec_Xaa (1/d):	0.02
k_hyd_pr (1/d):	10	k_dec_Xfa (1/d):	0.02
k_hyd_li (1/d):	10	k_dec_Xc4 (1/d):	0.02
km_su (1/d):	30	k_dec_Xpro (1/d):	0.02
KS_su (kgCOD/m3):	0.5	k_dec_Xac (1/d):	0.02
km_aa (1/d):	50	k_dec_Xh2 (1/d):	0.02
KS_aa (kgCOD/m3):	0.5		
km_fa (1/d):	6		
KS_fa (kgCOD/m3):	0.4		
km_pro (1/d):	13		
KS_pro (kgCOD/m3):	0.1		
km_ac (1/d):	8		
KS_ac (kgCOD/m3):	0.15		
km_c4 (1/d):	20		
KS_c4 (kgCOD/m3):	0.2		
km_h2 (1/d):	35		
KS_h2 (kgCOD/m3):	7e-6		

k	first-order coefficient rate
km	maximum specific uptake rate
KS	half saturation concentration
dis	Disintegration
hyd	hydrolysis
dec	decay
ch	Carbohydrates
pr	Proteins
li	Lipids
su	Sugars
aa	Amino acids
fa	Long chain fatty acids
pro	Propionic acid
ac	Acetic acid
c4	Valeric acid + Butyric acid
h2	hydrogen
X	Biomass

Default Save

Figure 7. 4 Kinetic coefficients interface

Initial Values (at t=0)

Sugars (kgCOD/m3):	0.012	Composites (kgCOD/m3):	0.31
Amino acids (kgCOD/m3):	0.0053	Carbohydrates (kgCOD/m3):	0.028
Long chain fatty acids (kgCOD/m3):	0.099	Proteins (kgCOD/m3):	0.01
Valeric acid (kgCOD/m3):	0.012	Lipids (kgCOD/m3):	0.029
Butyric acid (kgCOD/m3):	0.013	Sugar degraders (kgCOD/m3):	0.42
Propionic acid (kgCOD/m3):	0.016	Amino acid degraders (kgCOD/m3):	1.18
Acetic acid (kgCOD/m3):	0.2	LCFA degraders (kgCOD/m3):	0.24
Dissolved hydrogen (kgCOD/m3):	2.3E-07	C4 degraders (kgCOD/m3):	0.43
Dissolved methane (kgCOD/m3):	0.055	Propionate defrauders (kgCOD/m3):	0.14
Inorganic carbon (kmole C/m3):	0.15	Acetate degraders (kgCOD/m3):	0.76
Inorganic nitrogen (kmole N/m3):	0.13	Hydrogen degraders (kgCOD/m3):	0.32
Soluble inerts (kgCOD/m3):	0.33	Particulate inerts (kgCOD/m3):	25.6
		Cations (kmole/m3):	0.04
		Anions kmole/m3):	0.03

Default Save

Figure 7. 5 Initial (time = 0) state variables values

7.5 Software Verification:

The ADM1-UWO was programmed in MATLAB 2008 and linked to a MS Visual Basic interface to provide user-friendly interface. The MATLAB code was tested and compared to the example provided by Batstone et al. [1] as well as the case study done by Jeppsson et al. [9]. Table 7.11 displays the comparison between the ADM1-UWO software and the output of the two aforementioned examples [1, 9].

The paired t-test method was conducted to compare the ADM1-UWO results to both Batstone et al. [1] and Jeppsson et al. [9] ADM1 results. The null hypothesis i.e. there are no differences between the ADM1-UWO results and the results obtained from both of the studies mentioned above, have been accepted based on the calculated t-value (0.11 and 0.43) and P-value of 0.91 and 0.67 at the 95% confidence level, respectively. Thus, it can be concluded that ADM1-UWO compares, well to the output presented by Batstone et al. [1] and Jeppsson et al. [9].

Table 7. 11 Comparison between the output results of the ADM1-UWO, Batstone et al. [1] and Jeppsson et al. [9].

State Parameter	Input KgCOD/m ³	Output KgCOD/m ³		
		UWO	Jeppsson at al. [9]	Batstone et al. [1]
Flow rate	1.5	1.5	1.5	1.5
temperature	35	35	35	35
V _{gas}	5	5	5	5
V _{liq}	28	28	28	28
Ssu = monosacharides	2.8	0.013	0.013	0.013
Saa = amino acids	4.2	0.006	0.006	0.006
Sfa = long chain fatty acids (LCFA)	6.3	0.110	0.110	0.110
Sva = total valerate	0	0.011	0.117	0.012
Sbu = total butyrate	0	0.015	0.015	0.015
Spro = total propionate	0	0.018	0.018	0.018
Sac = total acetate	0	0.045	0.051	0.049
Sh ₂ = hydrogen gas	0	0.000	0.000	0.000
Sch ₄ = methane gas	0	0.052	0.055	0.054
Sic = inorganic carbon	0.005	0.050	0.075	0.075
Sin = inorganic nitrogen	0.003571	0.037	0.033	0.032
Si = soluble inerts	0.7	1.618	1.671	1.671
Xc = composites	10	1.041	1.040	1.040
Xch = carbohydrates	0	0.010	0.010	0.010
Xpr = proteins	0	0.010	0.010	0.010
Xli = lipids	0	0.016	0.016	0.016
Xsu = sugar degraders	0	0.355	0.354	0.354
Xaa = amino acid degraders	0	0.367	0.357	0.357
Xfa = LCFA degraders	0	0.389	0.391	0.391
Xc ₄ = valerate and butyrate degraders	0	0.149	0.144	0.145
Xpro = propionate degraders	0	0.062	0.061	0.061
Xac = acetate degraders	0	0.475	0.470	0.470
Xh ₂ = hydrogen degraders	0	0.225	0.224	0.224
Xi = particulate inerts	18	20.171	19.941	19.941
scat ₊ = cations (metallic ions, strong base)	0.04	0.040	0.040	0.040
san ₋ = anions (metallic ions, strong acid)	0.003571	0.035	0.004	0.004
Sgas,h ₂ = hydrogen concentration		0.000	0.000	0.000
Sgas,ch ₄ = methane concentration		1.580	1.708	1.670
Sgas,co ₂ = carbon dioxide concentration		0.013	0.011	0.011

7.6 References

- [1] Batstone, D. J.; Keller, J.; Angelidaki, I.; Kalyuzhnyi, S. V.; Pavlostathis, S. G.; Rozzi, A.; Sanders, W. T. M.; Siegrist, H.; Vavilin, V. A. Anaerobic Digestion Model No. 1, IWA Task Group for Mathematical Modelling of Anaerobic Digestion Processes, *Water Sci. Technol.* 2002, 40, 65–73.
- [2] Masse, D.; Droste, R. I. Microbial interaction during the anaerobic treatment of swine manure slurry in a sequencing batch reactor. *Canadian Journal of Agricultural Engineering*, 1997, 39, 35-41
- [3] Siegrist, H.; Gujer, W. Mathematical modeling of anaerobic mesophilic sewage sludge treatment. *Water Sci. Technol* 1993, 27, 25-36.
- [4] Rosen, C.; Jeppson, U. Anaerobic COST benchmark model description (report), San Sebastian, Spain. 2002
- [5] Copp, J. B.; Alex, J.; Beteau, J-F. ; Dudley, J.; Dupont, R.; Gillot, S.; Jeppsson, U.; Lelann, J-M.; Pons, M-N.; Vanrolleghem, P. A. the COST simulation benchmark, office of official publication of the European communities, Luxemburg. 2002
- [6] Chynoweth, D.; Pullammanappallil, P. Anaerobic digestion of municipal solid waste in microbiology of solid waste. CRC Press, Boca Raton, FL. 1996, 71-113.
- [7] Stumm, W.; Morgan, J. J. Anaerobic chemistry: chemical equilibria and rates in natural water (3ed edition), John Wiley and Sons New York, N.Y. 1996
- [8] Johnson B.A.R.; Shang Y., Applications and limitations of ADM 1 in municipal wastewater solids treatment, *Water Sci. Technol.* 2006, 54, 77–82.

- [9] Jeppsson, Ulf. Investigation of anaerobic digestion alternatives for Henriksdal's WWTP" IEA, Lund University. 2007.

CHAPTER EIGHT

Conclusions and Recommendations

8.1 Conclusions

The following findings summarize the major outcomes of this research.

8.1.1 Impact of particulate size on hydrolysis:

- Although casein degradation efficiency was $97\pm 1\%$ for all protein sizes within 80 h of digestion, the biodegradation rate increased significantly with decreasing particle size.
- The ultimate methane production of 8259 ± 139 mL was approximately the same for all protein sizes. However the maximum methane production rate increased from 5 to 15 ml/g-h, while the lag phase decreased from 21 to 11 h with the decrease in particle size from ≥ 500 μm to ≤ 50 μm .
- The hydrolysis rate coefficient increased by 776% from 0.034 to 0.298 d^{-1} with the decrease in particle size from ≥ 500 μm to ≤ 50 μm corresponding to an increase in specific surface area from 0.01 to $0.19\text{ m}^2/\text{g}$ (1800% increase).
- The hydrolysis rate coefficient of protein was experimentally related to median surface diameter and specific surface area.
- The newly developed hydrolysis models, correlating the first-order hydrolysis rate coefficient to both median surface diameter and specific surface area were superior to the constant first-order rate model in fitting the experimental data.

8.1.2 The effect of sonication on biosolids particle size and anaerobic digestion:

- After 60 minutes of sonication corresponding to specific energy of ~25 kJ/g TSS for primary and ~33 kJ/g TSS for WAS, SCOD/TCOD ratio increased from 5.5% to 18% and 3.3% to 27%, SBOD/TCOD ratio increased from 1.1% to 2.5% and 0.5% to 4.4%, VFA/TCOD ratio increased from 2.6% to 4.4% and from 8.1% to 13.3%, bound protein/TCOD decreased from 1.4% to 1.1% and 1.6% to 0.8%; total protein/TCOD decreased from 6.6% to 2.2% and 6.7% to 4%; and soluble protein/TCOD increased from 0.6% to 3.3% and 0.6% to 4.3%, while total methane production increased by 28% and 25% after 5 minutes of sonication for primary and WAS, respectively.
- The effect of sonication on digested bound protein was not statistically significant for both primary and WAS samples at the 95% confidence level.
- Although, there is an increase in sludge surface area with sonication, no significant effect on specific surface area was found after 5 minutes of (3.2 KJ/g TSS) sonication in the case of WAS but for the primary sludge specific surface area increased by 8 times after 40 minutes of sonication (~17 kJ/gTSS).
- The Anaerobic Digestion Model #1 (ADM1) predicted well both the methane production and volatile fatty acids concentrations. The simulated rate constants for acetic acid and butyric acid uptake decreased by 30%-34% with sonication.
- Ultrasound is generally neither economical for biogas enhancement despite the high solubilization of COD, nor effective in enhancing the biodegradability of

bound proteins. However, at low sonication energy of 0.1, 0.5, and 1 kJ/g TSS, the process is economical for primary sludge only.

8.1.3 Impact of sonication on high solids sludge (hog manure):

- The $COD_{\text{solubilisation}}$ correlated very well with the DD, the $TKN_{\text{solubilisation}}$ and the % decrease in particulate protein. Thus, $COD_{\text{solubilisation}}$ can be used to evaluate the degree of solubilisation in lieu of the labor and time intensive DD procedure, as it proved to be an accurate and easy to measure method.
- For hog manure, the disintegration of particles by ultrasonication was more pronounced for the smaller sizes, i.e., in the 0.6 to 60 μm range, as well as the reduction of VS by ultrasonication increased with increasing specific energy input in the 500-5000 kJ/kgTS and reached a plateau at 10000 kJ/kgTS.
- At a solids content of 2%, the specific energy input increased from 10000 to about 30000 kJ/kgTS for an additional 15% increase in degree of disintegration, whereas at TS of about 9%, the specific energy input increased from 250 to about 3,300 kJ/kgTS to achieve the same increase in DD. Therefore, ultrasonication is more effective pretreatment process for hog manure with higher TS content than WAS and primary sludges.
- Bound proteins decreased by 13.5% at specific energy of 5000 kJ/kgTS. Thus, the impact of ultrasonication on odor precursors such as bound proteins appears to be significant.
- The cell wall appeared to be ruptured at a minimum specific energy input of 500 kJ/kgTS, whereas the optimum specific energy was 10000 kJ/kgTS, affecting a 17.7% reduction in cell protein.

- The optimum specific energy input for methane production was 500 kJ/kgTS, and resulted in a 28% increase in methane production, and subsequently about \$ 4.1/ton of dry solids excess energy output.

8.1.4 Degradation of odor precursors in primary and WAS during anaerobic digestion:

- In general, anaerobic digestion efficiency for all sludge primary parameters such as TSS, VSS, TCOD, SCOD and TBOD₅ for primary sludge was higher than waste activated sludge.
- The concentration of VFA in the raw PS of 1855±58 mg/L was considerably higher than the raw WAS of 506±17 mg/L, with average removal efficiencies during anaerobic digestion of 97±1%, and 92±5%, respectively. The average concentrations of lipids in the raw PS and WAS were 1486±423 mg/L and 367±144 mg/L, respectively, and the removal of lipid varied during anaerobic digestion varied.
- Average reductions of various protein fractions were 40±2.5% and 31±3% for particulate protein, 67±3.4% and 61±3.2% for soluble protein, and 61±4.8 % and 59±3 % for bound or labile protein for PS and WAS, respectively. Reduction of bound protein or the labile protein, which is implicated in odor production in sludge, was positively correlated with VSS reduction for both sludges. No statistically significant difference was observed between the bound protein reductions in both PS and WAS. A 17% and 37% reduction in bound protein per

unit VSS, indicates a possible reduction in odor generation potential not only associated with stabilization of VSS, but also due to bound protein degradation.

- The steady-state Anaerobic Digestion Model #1 (ADM1) was used to simulate the steady state lab scale anaerobic digester. The model predicted well both the methane production and odor precursors. The model results with optimized parameters showed good agreement with the experimental data for methane production with average percentage errors of 3% and 5% for primary and WAS, respectively. Good agreement was also observed for the odor precursors, namely, protein, VFAs, lipids and amino acids as reflected by percentage errors of 6%, 4%, 1%, and 5% in the case of PS and 3%, 11%, 6%, and 0.1% in the case of WAS, respectively.

8.2 Recommendations for Future Research:

Based on the work conducted and literature reviewed, the following are the list of recommendations for future work

- The information available for anaerobic microorganisms degrading complex substrates such as sewage sludge as well as the anaerobic degraders contains large gaps regarding reliable kinetic and stoichiometric parameters required for accurate modeling.
- More research efforts are needed to achieve an accurate characterization of the substrate, at least in terms of the main components (carbohydrates, proteins, and lipids) and not only in terms of “gross parameters” such as COD and VSS.

- At the same time, a more accurate monitoring and control of full-scale plants could provide valuable information of use in updating model parameters. This would help increase process knowledge and, at the same time, ensure greater process efficiency and stability.
- The ADM1 model needs to capture phosphorus for all the relevant fractions, and needs to include the handling of inorganic reactions such as struvite precipitation and metal phosphate/metal hydroxide precipitation. Activity effects on chemical equilibria are significant when considering phosphorus. Also of importance in wastewater treatment is the fate of sulfur compounds. This includes the generation of H₂S in the digester gas and the fate of the sulfur species in the digested sludge (as a predictor of odour-generating potential).
- Based upon the ADM1 model applications, it was apparent that for accurate model simulations the influent sludge must be well characterized in terms of biodegradable and recalcitrant COD.

Appendix A: Anaerobic Digestion Model No.1

9.1 Biochemical process rates

$$r_1 = k_{dis} \cdot X_c$$

$$r_2 = k_{hyd,ch} \cdot X_{ch}$$

$$r_3 = k_{hyd,pr} \cdot X_{pr}$$

$$r_4 = k_{hyd,li} \cdot X_{li}$$

$$r_5 = k_{m,su} \cdot \frac{S_{su}}{K_{S,su} + S_{su}} \cdot X_{su} \cdot I_5$$

$$r_6 = k_{m,aa} \cdot \frac{S_{aa}}{K_{S,aa} + S_{aa}} \cdot X_{aa} \cdot I_6$$

$$r_7 = k_{m,fa} \cdot \frac{S_{fa}}{K_{S,fa} + S_{fa}} \cdot X_{fa} \cdot I_7$$

$$r_8 = k_{m,c4} \cdot \frac{S_{va}}{K_{S,c4} + S_{va}} \cdot X_{c4} \cdot \frac{S_{va}}{S_{bu} + S_{va}} \cdot I_8$$

$$r_9 = k_{m,c4} \cdot \frac{S_{ba}}{K_{S,c4} + S_{ba}} \cdot X_{c4} \cdot \frac{S_{ba}}{S_{va} + S_{bu}} \cdot I_9$$

$$r_{10} = k_{m,pr} \cdot \frac{S_{pro}}{K_{S,pro} + S_{pro}} \cdot X_{pro} \cdot I_{10}$$

$$r_{11} = k_{m,ac} \cdot \frac{S_{ac}}{K_{S,ac} + S_{ac}} \cdot X_{ac} \cdot I_{11}$$

$$r_{12} = k_{m,h2} \cdot \frac{S_{h2}}{K_{S,h2} + S_{h2}} \cdot X_{h2} \cdot I_{12}$$

$$r_{13} = k_{dec,Xsu} \cdot X_{su}$$

$$r_{14} = k_{dec,Xaa} \cdot X_{aa}$$

$$r_{15} = k_{dec,Xfa} \cdot X_{fa}$$

$$r_{16} = k_{dec,Xc4} \cdot X_{c4}$$

$$r_{17} = k_{dec,Xpro} \cdot X_{pro}$$

$$r_{18} = k_{dec,Xac} \cdot X_{ac}$$

$$r_{19} = k_{dec,Xh2} \cdot X_{h2}$$

9.2 Acid-base rates:

$$\begin{aligned}
 r_{A,4} &= k_{A,Bva} (S_{va} - (K_{a,va} + S_{H^+}) - K_{a,va} S_{va}) \\
 r_{A,5} &= k_{A,Bbu} (S_{bu} - (K_{a,bu} + S_{H^+}) - K_{a,bu} S_{bu}) \\
 r_{A,6} &= k_{A,Bpro} (S_{pro} - (K_{a,pro} + S_{H^+}) - K_{a,pro} S_{pro}) \\
 r_{A,7} &= k_{A,Bac} (S_{ac} - (K_{a,ac} + S_{H^+}) - K_{a,ac} S_{ac}) \\
 r_{A,10} &= k_{A,Bco2} (S_{hco2} - (K_{a,co2} + S_{H^+}) - K_{a,co2} S_{IC}) \\
 r_{A,11} &= k_{A,BIN} (S_{nh3} - (K_{a,IN} + S_{H^+}) - K_{a,IN} S_{IN})
 \end{aligned}$$

9.3 Gas transfer rates

$$\begin{aligned}
 r_{T,8} &= k_{La} (S_{h2} - 16 \cdot K_{H,h2} p_{gas,h2}) \\
 r_{T,9} &= k_{La} (S_{ch4} - 46 \cdot K_{H,ch4} p_{gas,ch4}) \\
 r_{T,10} &= k_{La} (S_{co2} - 16 \cdot K_{H,co2} p_{gas,co2})
 \end{aligned}$$

9.4 Process inhibition

$$I_{5,6} = I_{pH,aa} \cdot I_{IN,lim}$$

$$I_7 = I_{pH,aa} \cdot I_{IN,lim} \cdot I_{h2,fa}$$

$$I_{8,9} = I_{pH,aa} \cdot I_{IN,lim} \cdot I_{h2,c4}$$

$$I_{10} = I_{pH,aa} \cdot I_{IN,lim} \cdot I_{h2,pro}$$

$$I_{11} = I_{pH,ac} \cdot I_{IN,lim} \cdot I_{nh3}$$

$$I_{12} = I_{pH,h2} \cdot I_{IN,lim}$$

$$I_{pH,aa} = \begin{cases} \exp\left(-3\left(\frac{pH - pH_{UL,aa}}{pH_{UL,aa} - pH_{LL,aa}}\right)^2\right) & pH < pH_{UL,aa} \\ 1 & pH > pH_{UL,aa} \end{cases}$$

$$I_{pH,ac} = \begin{cases} \exp\left(-3\left(\frac{pH - pH_{UL,ac}}{pH_{UL,ac} - pH_{LL,ac}}\right)^2\right) & pH < pH_{UL,ac} \\ 1 & pH > pH_{UL,ac} \end{cases}$$

$$I_{pH,h2} = \begin{cases} \exp\left(-3\left(\frac{pH - pH_{UL,h2}}{pH_{UL,h2} - pH_{LL,h2}}\right)^2\right) & pH < pH_{UL,h2} \\ 1 & pH > pH_{UL,h2} \end{cases}$$

$$I_{IN,lim} = \frac{1}{1 + \frac{K_{S,IN}}{S_{IN}}}$$

$$I_{h2,fa} = \frac{1}{1 + \frac{S_{h2}}{K_{I,h2,fa}}}$$

$$I_{h2,c4} = \frac{1}{1 + \frac{S_{h2}}{K_{I,h2,c4}}}$$

$$I_{h2,pro} = \frac{1}{1 + \frac{S_{h2}}{K_{I,h2,pro}}}$$

$$I_{nh3} = \frac{1}{1 + \frac{S_{nh3}}{K_{I,nh3}}}$$

$$pH = -\log(S_{H^+})$$

9.5 Water phase equations

Differential equations 1-4, soluble matter

$$\frac{dS_{su}}{dt} = \frac{Q_{in}}{V_{lip}} (S_{su,in} - S_{su}) + r_2 + (1 - f_{fa,li})r_4 - r_5$$

$$\frac{dS_{aa}}{dt} = \frac{Q_{in}}{V_{lip}} (S_{aa,in} - S_{aa}) + r_3 - r_6$$

$$\frac{dS_{fa}}{dt} = \frac{Q_{in}}{V_{lip}} (S_{fa,in} - S_{fa}) + f_{fa,li} \cdot r_4 - r_7$$

$$\frac{dS_{va}}{dt} = \frac{Q_{in}}{V_{lip}} (S_{va,in} - S_{va}) + (1 - Y_{aa}) \cdot f_{va,aa} \cdot r_6 - r_8$$

Differential equations 5-8, soluble matter:

$$\frac{dS_{bu}}{dt} = \frac{Q_{in}}{V_{lip}} (S_{bu,in} - S_{bu}) + (1 - Y_{su}) \cdot f_{bu,su} \cdot r_5 + (1 - Y_{aa}) \cdot f_{bu,aa} \cdot r_6 - r_9$$

$$\frac{dS_{pro}}{dt} = \frac{Q_{in}}{V_{lip}} (S_{pro,in} - S_{pro}) + (1 - Y_{su}) \cdot f_{pro,su} \cdot r_5 + (1 - Y_{aa}) \cdot f_{pro,aa} \cdot r_6 + (1 - Y_{c4}) \cdot 0.54 \cdot r_8 - r_{10}$$

$$\begin{aligned} \frac{dS_{ac}}{dt} = & \frac{Q_{in}}{V_{lip}} (S_{ac,in} - S_{ac}) + (1 - Y_{su}) \cdot f_{ac,su} \cdot r_5 + (1 - Y_{aa}) \cdot f_{ac,aa} \cdot r_6 + (1 - Y_{fa}) \cdot 0.7 \cdot r_7 + (1 - Y_{c4}) \cdot 0.31 \cdot r_8 + \\ & (1 - Y_{c4}) \cdot 0.8 \cdot r_9 + (1 - Y_{pro}) \cdot 0.57 \cdot r_{10} - r_{11} \end{aligned}$$

$$\begin{aligned} \frac{dS_{h2}}{dt} = & \frac{Q_{in}}{V_{lip}} (S_{h2,in} - S_{h2}) + (1 - Y_{su}) \cdot f_{h2,su} \cdot r_5 + (1 - Y_{aa}) \cdot f_{h2,aa} \cdot r_6 + (1 - Y_{fa}) \cdot 0.3 \cdot r_7 + (1 - Y_{c4}) \cdot 0.15 \cdot r_8 + \\ & (1 - Y_{c4}) \cdot 0.2 \cdot r_9 + (1 - Y_{pro}) \cdot 0.43 \cdot r_{10} - r_{11} - r_{T,8} \end{aligned}$$

Differential equations 9-12, soluble matter:

$$\frac{dS_{ch4}}{dt} = \frac{Q_{in}}{V_{lip}} (S_{ch4,in} - S_{ch4}) + (1 - Y_{ac}) \cdot r_{11} + (1 - Y_{h2}) \cdot r_{12} - r_{T,9}$$

$$\frac{dS_{IC}}{dt} = \frac{Q_{in}}{V_{lip}} (S_{IC,in} - S_{IC}) - \sum_{j=1}^{19} \left(\sum_{i=1}^{24 \exists 10} C_i \nu_i r_j \right) - r_{T,10}$$

$$\begin{aligned} \frac{dS_{IN}}{dt} = & \frac{Q_{in}}{V_{lip}} (S_{IN,in} - S_{IN}) + Y_{su} N_{bac} r_5 + (N_{aa} - Y_{aa} N_{bac}) r_6 - Y_{fa} N_{bac} r_7 - Y_{c4} N_{bac} r_8 - \\ & Y_{c4} N_{bac} r_9 - Y_{pro} N_{bac} r_{10} - Y_{ac} N_{bac} r_{11} - Y_{h2} N_{bac} r_{12} + (N_{bac} - N_{xc}) \sum_{i=13}^{19} r_i + \\ & (N_{xc} - f_{x1,xc} N_I - f_{s1,xc} N_I - f_{pr,xc} N_{aa}) \cdot r_1 \end{aligned}$$

$$\frac{dS_I}{dt} = \frac{Q_{in}}{V_{lip}} (S_{I,in} - S_I) + f_{s1,xc} \cdot r_1$$

$$\sum_{j=1}^{19} \left(\sum_{i=1}^{24 \div 10} C_i V_i r_j \right) = \sum_{k=1}^{12} S_k r_k + S_{13} (r_{13} + r_{14} + r_{15} + r_{16} + r_{17} + r_{18} + r_{19})$$

where

$$S_1 = -C_{xc} + f_{s1,xc} C_{sl} + f_{ch,xc} + f_{pr,xc} C_{pr} + f_{li,xc} C_{li} + f_{xl,xc} C_{xl}$$

$$S_2 = -C_{ch} + C_{su}$$

$$S_3 = -C_{pr} + C_{aa}$$

$$S_4 = -C_{li} + (1 - f_{fa,li}) C_{su} + f_{fa,li} C_{fa}$$

$$S_5 = -C_{su} + (1 - Y_{su}) (f_{bu,su} C_{bu} + f_{pro,su} C_{pro} + f_{ac,su} C_{ac}) + Y_{su} C_{bac}$$

$$S_6 = -C_{aa} + (1 - Y_{aa}) (f_{va,aa} C_{va} + f_{bu,aa} C_{bu} + f_{pro,aa} C_{pro} + f_{ac,aa} C_{ac}) + Y_{aa} C_{bac}$$

$$S_7 = -C_{fa} + (1 - Y_{fa}) 0.7 C_{ac} + Y_{fa} C_{bac}$$

$$S_8 = -C_{va} + (1 - Y_{c4}) 0.54 C_{pro} + (1 - Y_{c4}) 0.31 C_{ac} + Y_{c4} C_{bac}$$

$$S_9 = -C_{bu} + (1 - Y_{c4}) 0.8 C_{ac} + Y_{c4} C_{bac}$$

$$S_{10} = -C_{pro} + (1 - Y_{pro}) 0.57 C_{ac} + Y_{pro} C_{bac}$$

$$S_{11} = -C_{ac} + (1 - Y_{ac}) 0.54 C_{ch4} + Y_{ac} C_{bac}$$

$$S_{12} = (1 - Y_{h2}) C_{ch4} + Y_{h2} C_{bac}$$

$$S_{13} = -C_{bac} + C_{xc}$$

Differential equations 13-16, particulate matter:

$$\frac{dX_c}{dt} = \frac{Q_{in}}{V_{lip}} (X_{c,in} - X_c) - r_1 + \sum_{i=13}^{19} r_i$$

$$\frac{dX_{ch}}{dt} = \frac{Q_{in}}{V_{lip}} (X_{ch,in} - X_{ch}) + f_{ch,xc} r_1 - r_2$$

$$\frac{dX_{pr}}{dt} = \frac{Q_{in}}{V_{lip}} (X_{pr,in} - X_{pr}) + f_{pr,xc} r_1 - r_3$$

$$\frac{dX_{li}}{dt} = \frac{Q_{in}}{V_{lip}} (X_{li,in} - X_{li}) + f_{li,xc} r_1 - r_4$$

Differential equations 17-20, particulate matter:

$$\frac{dX_{su}}{dt} = \frac{Q_{in}}{V_{lip}} (X_{su,in} - X_{su}) + Y_{su} r_5 - r_{13}$$

$$\frac{dX_{aa}}{dt} = \frac{Q_{in}}{V_{lip}} (X_{aa,in} - X_{aa}) + Y_{aa} r_6 - r_{14}$$

$$\frac{dX_{fa}}{dt} = \frac{Q_{in}}{V_{lip}} (X_{fa,in} - X_{fa}) + Y_{fa} r_7 - r_{15}$$

$$\frac{dX_{c4}}{dt} = \frac{Q_{in}}{V_{lip}} (X_{c4,in} - X_{c4}) + Y_{c4} r_8 + Y_{c4} r_9 - r_{16}$$

Differential equations 21-24, particulate matter:

$$\frac{dX_{pro}}{dt} = \frac{Q_{in}}{V_{lip}} (X_{pro,in} - X_{pro}) + Y_{pro} r_{10} - r_{17}$$

$$\frac{dX_{ac}}{dt} = \frac{Q_{in}}{V_{lip}} (X_{ac,in} - X_{ac}) + Y_{ca} r_{11} - r_{18}$$

$$\frac{dX_{h2}}{dt} = \frac{Q_{in}}{V_{lip}} (X_{h2,in} - X_{h2}) + Y_{h2} r_{12} - r_{19}$$

$$\frac{dX_I}{dt} = \frac{Q_{in}}{V_{lip}} (X_{I,in} - X_I) + f_{xl,xc} r_1$$

Differential equations 25-26, cations and anions:

$$\frac{dS_{cat^+}}{dt} = \frac{Q_{in}}{V_{lip}} (S_{cat^+,in} - S_{cat^+})$$

$$\frac{dS_{an^-}}{dt} = \frac{Q_{in}}{V_{lip}} (S_{an^-,in} - S_{an^-})$$

Differential equations 27-32, ion states:

$$\frac{dS_{va^-}}{dt} = -r_{A,4}$$

$$\frac{dS_{bu^-}}{dt} = -r_{A,5}$$

$$\frac{dS_{pro^-}}{dt} = -r_{A,6}$$

$$\frac{dS_{ac^-}}{dt} = -r_{A,7}$$

$$\frac{dS_{hco3^-}}{dt} = -r_{A,10}$$

$$\frac{dS_{nh3}}{dt} = -r_{A,11}$$

Algebraic equation:

$$S_{H^+} = -\frac{\theta}{2} + \frac{\sqrt{\theta^2 + 4K_w}}{2}$$

$$\theta = S_{cat^+} + S_{nh4^+} - S_{hco3^-} - \frac{S_{ac^-}}{64} - \frac{S_{pro^-}}{112} - \frac{S_{bu^-}}{160} - \frac{S_{va^-}}{208} - S_{an^-}$$

$$S_{nh4^+} = S_{IN} - S_{nh3}$$

$$S_{co2} = S_{IC} - S_{hco3^-}$$

9.6 Gas phase equations

Differential equations:

$$\frac{dS_{gas,h2}}{dt} = -\frac{S_{gas,h2}Q_{gas}}{V_{gas}} + r_{T,8} \cdot \frac{V_{liq}}{V_{gas}}$$

$$\frac{dS_{gas,ch4}}{dt} = -\frac{S_{gas,ch4}Q_{gas}}{V_{gas}} + r_{T,9} \cdot \frac{V_{liq}}{V_{gas}}$$

$$\frac{dS_{gas,co2}}{dt} = -\frac{S_{gas,co2}Q_{gas}}{V_{gas}} + r_{T,10} \cdot \frac{V_{liq}}{V_{gas}}$$

Algebraic equations:

$$p_{gas,h2} = S_{gas,h2} \frac{RT_{op}}{16}$$

$$p_{gas,ch4} = S_{gas,ch4} \frac{RT_{op}}{64}$$

$$p_{gas,co2} = S_{gas,co2} RT_{op}$$

$$Q_{gas} = \frac{RT_{op}}{P_{atm} - p_{gas,H2O}} \cdot V_{liq} \left(\frac{r_{T,8}}{16} + \frac{r_{T,9}}{64} + r_{T,10} \right)$$

9.7 Parameter Description:

Parameter	Description	Unit	Suggested value at time zero
S_{su}	monosacharides	(kg COD/m3)	0.012
S_{aa}	amino acids	(kg COD/m3)	0.0053
S_{fa}	long chain fatty acids (LCFA)	(kg COD/m3)	0.099
S_{va}	total valerate	(kg COD/m3)	0.012
S_{bu}	total butyrate	(kg COD/m3)	0.013
S_{pro}	total propionate	(kg COD/m3)	0.016
S_{ac}	total acetate	(kg COD/m3)	0.20
S_{h2}	hydrogen gas	(kg COD/m3)	2.3e-007
S_{ch4}	methane gas	(kg COD/m3)	0.055
S_{ic}	inorganic carbon	(kmole C/m3)	0.15
S_{in}	inorganic nitrogen	(kmole N/m3)	0.13
S_i	soluble inerts	(kg COD/m3)	0.33
X_c	composites	(kg COD/m3)	0.31
X_{ch}	carbohydrates	(kg COD/m3)	0.028
X_{pr}	proteins	(kg COD/m3)	0.10
X_{Li}	lipids	(kg COD/m3)	0.029

X_{su}	sugar degraders	(kg COD/m ³)	0.42
X_{aa}	amino acid degraders	(kg COD/m ³)	1.18
X_{fa}	LCFA degraders	(kg COD/m ³)	0.24
X_{c4}	valerate and butyrate degraders	(kg COD/m ³)	0.43
X_{pro}	propionate degraders	(kg COD/m ³)	0.14
X_{ac}	acetate degraders	(kg COD/m ³)	0.76
X_{h2}	hydrogen degraders	(kg COD/m ³)	0.32
X_i	particulate inerts	(kg COD/m ³)	25.6
pH	pH within AD system		
S_{H^-}	protons	(kmole/m ³)	
S_{va^-}	valerate	(kg COD/m ³)	0.011
S_{bu^-}	butyrate	(kg COD/m ³)	0.013
S_{pro^-}	propionate	(kg COD/m ³)	0.016
S_{ac^-}	acetate	(kg COD/m ³)	0.2
S_{hco3^-}	bicarbonate	(kmole C/m ³)	0.14
S_{co2}	carbon dioxide	(kmole C/m ³)	
S_{nh3}	ammonia	(kmole C/m ³)	0.0041
S_{nh4^+}	ammonium	(kmole C/m ³)	
$S_{gas,h2}$	hydrogen concentration in gas phase	(kg COD/m ³)	1.02e-005
$S_{gas,ch4}$	methane concentration in gas phase	(kg COD/m ³)	1.63
$S_{gas,co2}$	carbon dioxide concentration in gas phase	(kmole C/m ³)	0.014
$p_{gas,h2}$	partial pressure of hydrogen gas	(bar)	
$p_{gas,ch4}$	partial pressure of methane gas	(bar)	
$p_{gas,co2}$	partial pressure of carbon dioxide gas	(bar)	
$p_{gas,total}$	total head space pressure (H ₂ +CO ₂ +CH ₄ +H ₂ O)	(bar)	
Q_{gas}	gas flow rate normalised to atmospheric pressure	(m ³ /d)	170

Parameter	Description	Suggested Value
$f_{sl,xc}$	Soluble inerts from composites	0.1
$f_{xl,xc}$	Particulate inerts from composites	0.25
$f_{ch,xc}$	Carbohydrates from composites	0.20
$f_{pr,xc}$	Proteins from composites	0.20
$f_{li,xc}$	Lipids from composites	0.25
N_{xc}, N_l	Nitrogen content of composites and inerts	0.002
$f_{fa,li}$	Fatty acids from lipids	0.95
$f_{h2,su}$	Fatty acids from lipids	0.19
$f_{bu,su}$	Hydrogen from sugars	0.13
$f_{pro,su}$	Butyrate from sugars	0.27
$f_{ac,su}$	Propionate from sugars	0.41
$f_{h2,aa}$	Acetate from sugars	0.06
N_{aa}	Hydrogen in amino acids and proteins	0.007
$f_{va,su}$	Valerate from amino acids	0.23
$f_{bu,su}$	Butyrate from amino acids	0.26
$f_{pro,su}$	Propionate from amino acids	0.05
$f_{ac,su}$	Acetate from amino acids	0.40

9.8 Stoichiometric Matrix

Component →	i	1	2	3	4	5	6	7	8	9	10	11	12	13	14	15	Rate (r _i , kg COD m ⁻³ d ⁻¹)
Process ↓		S _{su}	S _{su}	S _{su}	S _{su}	S _{su}	S _{su}	S _{su}	S _{su}	S _{su}	S _{su}	S _{su}	S _{su}	S _{su}	S _{su}	S _{su}	
1 Disintegration																	$k_{dis} \cdot X_{su}$
2 Hydrolysis Carbohydrates		1															$k_{hyd,c} \cdot X_{su}$
3 Hydrolysis of Proteins			1														$k_{hyd,p} \cdot X_{su}$
4 Hydrolysis of Lipids		$1-f_{su,l}$		$f_{su,l}$													$k_{hyd,l} \cdot X_{su}$
5 Uptake of Sugars		-1						$(1-Y_{su}) \cdot f_{su,m}$		$(1-Y_{su}) \cdot f_{su,m}$		$(1-Y_{su}) \cdot f_{su,m}$	$(1-Y_{su}) \cdot f_{su,m}$				$-\sum_{i=1-13,16-30} C_i \cdot V_{i,5}$ $k_{u,su} \cdot \frac{S_{su}}{K_s + S_{su}} \cdot X_{su} \cdot I_1$
6 Uptake of Amino Acids			-1					$(1-Y_{su}) \cdot f_{su,m}$		$(1-Y_{su}) \cdot f_{su,m}$		$(1-Y_{su}) \cdot f_{su,m}$	$(1-Y_{su}) \cdot f_{su,m}$				$-\sum_{i=1-13,16-30} C_i \cdot V_{i,6}$ $k_{u,aa} \cdot \frac{S_{su}}{K_s + S_{su}} \cdot X_{su} \cdot I_1$
7 Uptake of LCFA				-1								$(1-Y_{su}) \cdot 0.7$	$(1-Y_{su}) \cdot 0.3$				$k_{u,lcfa} \cdot \frac{S_{su}}{K_s + S_{su}} \cdot X_{su} \cdot I_1$
8 Uptake of Valerate						-1						$(1-Y_{va}) \cdot 0.54$	$(1-Y_{va}) \cdot 0.31$	$(1-Y_{va}) \cdot 0.15$			$k_{u,va} \cdot \frac{(S_{su} + S_{va})}{K_s + (S_{su} + S_{va})} \cdot X_{su} \cdot \frac{1}{1 + (S_{su} + S_{va}) / (S_{su} + S_{va})} \cdot I_2$
9 Uptake of Butyrate										-1			$(1-Y_{bu}) \cdot 0.8$	$(1-Y_{bu}) \cdot 0.2$			$k_{u,bu} \cdot \frac{(S_{su} + S_{bu})}{K_s + (S_{su} + S_{bu})} \cdot X_{su} \cdot \frac{1}{1 + (S_{su} + S_{bu}) / (S_{su} + S_{bu})} \cdot I_2$
10 Uptake of Propionate											-1		$(1-Y_{pr}) \cdot 0.57$	$(1-Y_{pr}) \cdot 0.43$			$-\sum_{i=1-13,16-30} C_i \cdot V_{i,10}$ $k_{u,pr} \cdot \frac{(S_{su} + S_{pr})}{K_s + (S_{su} + S_{pr})} \cdot X_{su} \cdot I_2$
11 Uptake of Acetate												-1		$(1-Y_{ac})$			$-\sum_{i=1-13,16-30} C_i \cdot V_{i,11}$ $k_{u,ac} \cdot \frac{(S_{su} + S_{ac})}{K_s + (S_{su} + S_{ac})} \cdot X_{su} \cdot I_2$
12 Uptake of Hydrogen													-1	$(1-Y_{H_2})$			$-\sum_{i=1-13,16-30} C_i \cdot V_{i,12}$ $k_{u,H_2} \cdot \frac{S_{H_2}}{K_s + S_{H_2}} \cdot X_{su} \cdot I_1$
13 Decay of X _{su}																	$-\sum_{i=1-15} C_i \cdot r_{i,13}$ $k_{dec,su} \cdot X_{su}$
14 Decay of X _{su}																	$-\sum_{i=1-15} C_i \cdot r_{i,14}$ $k_{dec,su} \cdot X_{su}$
15 Decay of X _{su}																	$-\sum_{i=1-15} C_i \cdot r_{i,15}$ $k_{dec,su} \cdot X_{su}$
16 Decay of X _{su}																	$-\sum_{i=1-15} C_i \cdot r_{i,16}$ $k_{dec,su} \cdot X_{su}$
17 Decay of X _{su}																	$-\sum_{i=1-15} C_i \cdot r_{i,17}$ $k_{dec,su} \cdot X_{su}$
18 Decay of X _{su}																	$-\sum_{i=1-15} C_i \cdot r_{i,18}$ $k_{dec,su} \cdot X_{su}$
19 Decay of X _{su}																	$-\sum_{i=1-15} C_i \cdot r_{i,19}$ $k_{dec,su} \cdot X_{su}$
A4 Valerate Acid-Base					1	-1											$k_{A,1,004} (S_{su} \cdot S_{va} - K_{A,1,004} S_{su})$
A5 Butyrate Acid-Base							1	-1									$k_{A,2,004} (S_{su} \cdot S_{bu} - K_{A,2,004} S_{su})$
A6 Propionate Acid-Base									1	-1							$k_{A,3,004} (S_{su} \cdot S_{pr} - K_{A,3,004} S_{su})$
A7 Acetate Acid-Base											1	-1					$k_{A,4,004} (S_{su} \cdot S_{ac} - K_{A,4,004} S_{su})$
A10 Inorganic Carbon Acid-Base														1	-1		$k_{A,5,004} (S_{su} \cdot S_{CO_2} - K_{A,5,004} S_{su})$
A11 Inorganic Nitrogen Acid-Base																	$k_{A,6,004} (S_{su} \cdot S_{NH_4} - K_{A,6,004} S_{su})$
																	Inhibition factors: $I_1 = I_{pr, su} \cdot I_{pr, su}$ $I_2 = I_{pr, su} \cdot I_{pr, su} \cdot I_{pr, su} \cdot I_{pr, su} \cdot I_{pr, su}$ $I_3 = I_{pr, su} \cdot I_{pr, su} \cdot I_{pr, su} \cdot I_{pr, su}$ $I_4 = I_{pr, su} \cdot I_{pr, su}$

Component →	i	16	17	18	19	20	21	22	23	24	25	26	27	28	29	30	31	32	Rate (p _i , kg COD m ⁻³ d ⁻¹)
j Process ↓		S _{16,0}	S _{17,0}	S ₁₈	X ₁₉	X ₂₀	X ₂₁	X ₂₂	X ₂₃	X ₂₄	X ₂₅	X ₂₆	X ₂₇	X ₂₈	X ₂₉	X ₃₀	S _{CA1}	S _{AM}	
1 Disintegration				f _{dis}	-1	f _{dis,20}	f _{dis,21}	f _{dis,22}								f _{dis,30}			$k_{dis} \cdot X_{20}$
2 Hydrolysis Carbohydrates						-1													$k_{hyd,cb} \cdot X_{20}$
3 Hydrolysis of Proteins							-1												$k_{hyd,pr} \cdot X_{21}$
4 Hydrolysis of Lipids								-1											$k_{hyd,l} \cdot X_{22}$
5 Uptake of Sugars		-(Y _{su})N _{su}						Y _{su}											$k_{m,20} \cdot \frac{S_{20}}{K_S + S_{20}} \cdot X_{20} \cdot I_1$
6 Uptake of Amino Acids		N _{su} - (Y _{su})N _{su}							Y _{su}										$k_{m,21} \cdot \frac{S_{21}}{K_S + S_{21}} \cdot X_{21} \cdot I_1$
7 Uptake of LCFA		-(Y _{lc})N _{lc}								Y _{lc}									$k_{m,24} \cdot \frac{S_{24}}{K_S + S_{24}} \cdot X_{24} \cdot I_2$
8 Uptake of Valerate		-(Y _{va})N _{va}									Y _{va}								$k_{m,23} \cdot \frac{(S_{23} + S_{26})}{K_S + (S_{23} + S_{26})} \cdot X_{23} \cdot \frac{1}{1 + (S_{23} + S_{26}) / (S_{23} + S_{26})} \cdot I_2$
9 Uptake of Butyrate		-(Y _{bu})N _{bu}										Y _{bu}							$k_{m,24} \cdot \frac{(S_{24} + S_{26})}{K_S + (S_{24} + S_{26})} \cdot X_{24} \cdot \frac{1}{1 + (S_{24} + S_{26}) / (S_{24} + S_{26})} \cdot I_2$
10 Uptake of Propionate		-(Y _{pr})N _{pr}											Y _{pr}						$k_{m,27} \cdot \frac{(S_{27} + S_{29})}{K_S + (S_{27} + S_{29})} \cdot X_{27} \cdot I_2$
11 Uptake of Acetate		-(Y _{ac})N _{ac}												Y _{ac}					$k_{m,28} \cdot \frac{(S_{28} + S_{29})}{K_S + (S_{28} + S_{29})} \cdot X_{28} \cdot I_2$
12 Uptake of Hydrogen		-(Y _{h2})N _{h2}													Y _{h2}				$k_{m,h2} \cdot \frac{S_{h2}}{K_S + S_{h2}} \cdot X_{h2} \cdot I_4$
13 Decay of X ₂₀					1				-1										$k_{dec,20} \cdot X_{20}$
14 Decay of X ₂₁					1					-1									$k_{dec,21} \cdot X_{21}$
15 Decay of X ₂₄					1						-1								$k_{dec,24} \cdot X_{24}$
16 Decay of X ₂₃					1							-1							$k_{dec,23} \cdot X_{23}$
17 Decay of X ₂₇					1														$k_{dec,27} \cdot X_{27}$
18 Decay of X ₂₈					1														$k_{dec,28} \cdot X_{28}$
19 Decay of X ₂₂					1														$k_{dec,22} \cdot X_{22}$
A4 Valerate Acid-Base																			$k_{A/23} (S_{23} \cdot S_{26} - K_{A/23} S_{26})$
A5 Butyrate Acid-Base																			$k_{A/24} (S_{24} \cdot S_{26} - K_{A/24} S_{26})$
A6 Propionate Acid-Base																			$k_{A/27} (S_{27} \cdot S_{29} - K_{A/27} S_{29})$
A7 Acetate Acid-Base																			$k_{A/28} (S_{28} \cdot S_{29} - K_{A/28} S_{29})$
A10 Inorganic Carbon Acid-Base																			$k_{A/30} (S_{30} \cdot S_{CA1} - K_{A/30} S_{CA1})$
A11 Inorganic Nitrogen Acid-Base		1	-1																$k_{A/32} (S_{32} \cdot S_{AM} - K_{A/32} S_{AM})$
		Ammonium (kg-mole N m ⁻³)	Ammonia (kg-mole N m ⁻³)	Soluble lients (kg COD m ⁻³)	Composites (kg COD m ⁻³)	Carbohydrates (kg COD m ⁻³)	Proteins (kg COD m ⁻³)	Lipids (kg COD m ⁻³)	Sugar degraders (kg COD m ⁻³)	Amino acid degraders (kg COD m ⁻³)	LCFA degraders (kg COD m ⁻³)	Valerate and butyrate degraders (kg COD m ⁻³)	Propionate degraders (kg COD m ⁻³)	Acetate degraders (kg COD m ⁻³)	Hydrogen degraders (kg COD m ⁻³)	Particulate lients (kg COD m ⁻³)	Cations (kg-mole m ⁻³)	Anions (kg-mole m ⁻³)	Inhibition factors: I ₁ = I _{ph,20} · I _{ph,21} I ₂ = I _{ph,24} · I_{ph,23} · I_{ph,24} · I_{ph,27} · I_{ph,28}} I₃ = I_{ph,23} · I_{ph,24} · I_{ph,27} · I_{ph,28}} I₄ = I_{ph,h2}} · I_{ph,28}}}}}}}}}

10.1 CURRICULUM VITAE

EDUCATION

Doctor of Philosophy in Chemical and Biochemical Engineering, (2010)

University of Western Ontario, London, Canada

Master of Mathematics Degree, (2005)

University of Waterloo, Waterloo, Canada

**Master of Science Degree in Statistics, University of Baghdad, Baghdad, Iraq. (1995)
(Evaluated by University of Toronto and World Education Services US as
comparable to a Canadian/US Master of Science Degree specializing in Statistics)**

**Bachelor of Science Degree in Statistics, University of Baghdad, Baghdad, Iraq. (1990)
(Evaluated by University of Toronto and World Education Services US as
comparable to a Canadian/US four year Bachelor of Science Degree specializing in
Statistics)**

UNIVERSITY THESES

The Effect of Particle Size on Hydrolysis and the Modeling of Anaerobic Digestion:

Submitted to the university council to fulfill the thesis requirement for the degree of Doctor of Philosophy in Chemical and Biochemical Engineering, University of Western Ontario, Canada

Models of Wastewater Disinfection by Ultraviolet Light: Submitted to the university council to fulfill the thesis requirement for the degree of Master of Mathematics, University of Waterloo, Canada

Evaluation Study of Order Determination Methods of Autoregressive: Submitted to the university council to fulfill the thesis requirement for the degree of Master of Science in Statistics, University of Baghdad, Iraq

PROFESSIONAL EXPERIENCE

Business Manager, London Health Sciences Center, London, Ontario (2010)

Research Scientist, Trojan Technologies, London, Ontario (2002 – 2006)

Quality Engineer, Trojan Technologies, London, Ontario (2000 – 2002)

Assistant Professor and Researcher, University of Tripoli, Tripoli, Libya (1995 – 1999)

Consultant and Lecturer, International Centre for Languages, Tripoli, Libya (1995 – 1999)

Consultant and Adviser, Shams Al-Rabee, Baghdad, Iraq (1990 – 1995)

SOFTWARE

Anaerobic Digestion Model Software (ADM1-UWO) 2010
University of Western Ontario, Canada

Disinfection Guarantees 2006
Trojan Technologies, Canada

Ultraviolet Sizing Optimization Tool 2006
Trojan Technologies, Canada

Lagrangian Dose Model (LDM) 2005
Trojan Technologies, Canada

REFEREED AND SUBMITTED JOURNAL PAPERS

Modeling the Effect of Sonication on Biosolids Anaerobic Digestion 2010
Fuel and Energy, 2010, 24 (9), pp 4703–4711

Impact of Ultrasonication of Hog Manure on Anaerobic Digestibility 2010
Ultrasonics Sonochemistry, 2010, 18, pp 164-171.

Simulating the Degradation of Odors Precursors in Primary and Waste Activated Sludge during Anaerobic Digestion 2010
Journal of Hazardous Materials, Submitted

Modeling the Influence of Particulate Protein Size on Hydrolysis in Anaerobic Digestion 2010
Bioresource Technology, Submitted

Some Statistical Analysis with Application on Chemical Pollution 1998
College of Administration and Economics the Magazine, Iraq

Simulation Study to Compare Methods of Determining the Order of Autoregressive Model 1998
College of Administration and Economics the Magazine, Iraq

REFEREED CONFERENCE PROCEEDINGS

- Pre-treatment of Hog Manure Prior to Anaerobic Digestion** 2009
American Institute of Chemical Engineers (AIChE), Annual Meeting 2009
- Viability of Ultrasonication for Pre-Treatment of Biosolids** 2009
Water Environment Federation Technical Exhibition and Conference (WEFTEC)
- The Effect of Ultrasonic on Primary and Secondary Sludge Prior to Anaerobic Digestion** 2009
8th World Congress of Chemical Engineering
- Pre-treatment of Primary Sludge Prior to Anaerobic Digestion** 2008
American Institute of Chemical Engineers (AIChE), Annual Meeting 2008
- Sizing UV Reactors for Poor Quality Wastewater** 2006
International Water Association (IWA), Crete, Athens
- Using UV to Disinfect Low Quality Wastewater** 2006
Water Environment Federation Technical Exhibition and Conference (WEFTEC), Texas, USA
- UV Disinfection of Wastewater – The First Barrier in a Multiple Barrier Strategy for Drinking Water Protection** 2005
IWUWQ, Tianjin, China
- UV Reactor Sizing for Advanced Treatment of Wastewater Effluent** 2005
Water Environment Association of Ontario (WEAO), Canada
- Applying UV Disinfection for Combined Sewer Overflows** 2004
The Chartered Institution of Water and Environmental Management, United Kingdom
- Sizing UV Reactors for Wet Weather Flows** 2004
Water Environment Association of Ontario, Canada

ADDITIONAL TRAINING

- Management Information System**, Ministry of Health, Canada
- Crystal Reports, Advanced Level**, Polar Bear, Canada
- Crystal Reports, Intermediate Level**, Polar Bear, Canada
- Tools and Techniques for Managing Small Projects**, Strategic Project Management Ltd., Canada

Time Management Workshop, University of Waterloo, Canada

High Performance Computing, Cornell University, USA

Microbiology for Wastewater, Water Environment Federation, USA

Writing in Scientific and Engineering Fields Course, WISEonline, Canada

The Geometry of Very Large Data Sets, University of Ottawa, Canada

Consultation Principles, University of Tripoli, Libya

PROFESSIONAL EXPERIENCE

- Condensed, optimized and streamlined models and code fundamental to the sizing and electrical control of Drinking Water systems. The systems using these algorithms are providing drinking water for millions of people
- Analyzed water microbiology lab analysis data, for samples collected from over 500 wastewater plants throughout North America producing an understanding of the water quality parameters, resulting in more efficiently and competitively product sizing
- Simplified very complex electrical controls algorithm through the development of much simpler and more robust modelling, allowing for faster implementation of real-time process control implemented on a smaller PLC (computer)- significant time and capital equipment savings resulted
- Designed and analyzed experiments to determine the fundamental nature of the variables required for input into the control algorithm mentioned above, and for regulatory compliance
- Developed applications that efficiently retrieved historical data and used it to develop performance models
- Applied statistical theory and rules to conduct data analyses including data modelling, time series analysis, regression analysis, simulation, sampling, testing and forecasting
- Derived, identified and calculated probability distribution of certain components to recommend necessary design changes and design calculation simplifications
- Developed, designed, and programmed several Quality Assurance databases such as the non-conformance report database, scrap database, special inspection database, and field part return. Analyzed the accumulated data and generated reports for the executive level to assess performances of products, vendors, and parts
- As a member of the Quality Assurance team, developed the non-conformance report flowchart and set-up corrective action procedures
- Managed and analysed the clinical trials data for one of the biggest hospitals in North Africa, as a member of the University consulting team

- Provided statistical consulting; analyzed projects for medical research, insurance companies, banks, factories, import and export companies
- Supervised diploma dissertations that included software preparation for medical analysis laboratories and for a student registration system using FoxPro and Visual Basic
- Taught university level courses such as: Mathematical Statistics, Quality Control, Bio-Statistics, Experimental Design, Survival Analysis, Probability, and Principles of Statistics
- Supervised more than twelve graduate projects for senior students in the Faculty of Science, University of Tripoli. Projects included conducting surveys, collecting and analyzing data, and applying various statistical methods and techniques.

